Overcoming Anaerobic Digestion Toxicity of Aqueous Liquid from Wastewater Solids Pyrolysis

Seyedehfatemeh Seyedi
Marquette University

OVERCOMING ANAEROBIC DIGESTION TOXICITY OF AQUEOUS LIQUID FROM WASTEWATER SOLIDS PYROLYSIS

by

Seyedehfatemeh Seyedi

A Dissertation submitted to the Faculty of the Graduate School, Marquette University,
in Partial Fulfillment of the Requirements for the Degree of Doctor of Philosophy

Milwaukee, Wisconsin

December 2020

ABSTRACT

OVERCOMING ANAEROBIC DIGESTION TOXICITY OF AQUEOUS LIQUID FROM WASTEWATER SOLIDS PYROLYSIS

Seyedehfatemeh Seyedi

Marquette University, 2020

Pyrolysis treats and potentially recovers energy from wastewater solids (WWS). Aqueous pyrolysis liquid (APL), however, is produced and its management is a bottleneck to pyrolysis full-scale application. To overcome this bottleneck, anaerobic digestion (AD) may be a possible method to manage APL, but APL digestion has not been conclusively demonstrated. In AD, a select group of microorganisms convert organic chemicals to biogas containing methane that can be used as a fuel. In this dissertation work, APL derived from WWS pyrolysis was successfully converted into methane as the sole substrate and as a co-digestate with synthetic primary sludge in long-term, continuous anaerobic digesters for the first time. Methane production from APL that was previously hindered by APL recalcitrance and toxicity, increased by applying a low organic loading rate (OLR), high solids retention time (SRT), ozone pretreatment, and selecting appropriate microorganisms that were more proficient at APL biodegradation. APLs' anaerobic degradability produced at 500 and 700 °C pyrolysis temperatures was evaluated in anaerobic toxicity assays using four different anaerobic inocula. Higher pyrolysis temperature resulted in APL with higher toxicity. Pre-ozonation of APL for 2 h or less improved the methane production rate from 700°C APL. In contrast, ozonation did not have a substantial impact on the methane production rate from 500 °C APL. In long-term, continuous digestion studies, quasi steady state methanogenesis from 700 °C APL was accomplished by employing an appropriate, low APL OLR (0.03 gCOD/L APL) and a sufficiently long SRT (210 days), whereas shorter SRT and higher OLR values inhibited or stopped methane production. Employing a specific anaerobic inoculum from an industrial waste digester that was acclimated to constituents similar to those in APL resulted in more complete and more rapid methane production, compared to municipal anaerobic digester biomass. Microbial communities in digesters inoculated with the industrial biomass were dominated by hydrogenotrophic *Methanobacterium*, accompanied by an increased relative abundance of syntrophic bacteria belonging to phylum Synergistes and class Clostridia. Bacterial taxa capable of degrading N-heterocyclic compounds, *Enterococcus*, *Eubacterium*, and Bacillales, were also enriched. The results demonstrate that long-term methanogenesis from APL as the sole substrate in AD is possible. Anaerobic co-digestion of APL with primary sludge at municipal water resource recovery facilities is also a viable approach at facilities that already have digesters treating sludge. In this scenario, APL from pyrolyzed WWS can be added to digesters for increased biogas production, but care must be taken to control the OLR, SRT and biomass inventory to ensure APL digestion success.

ACKNOWLEDGMENT

Seyedehfatemeh Seyedi

I would like to extend my sincere gratitude to my dissertation advisor, Dr. Daniel H. Zitomer, for his unwavering support, guidance, and mentorship. His encouragement and confidence in me pushed me to find new limits in myself. He taught me how to become a researcher and a critical thinker. Pursuing my doctoral degree was an ambition that I could have not achieved without his help, and it will be an experience that I will cherish forever.

Next, I would like to thank my dissertation committee members, Dr. McNamara, Dr. Mayer, and Dr. Maki for their insight and feedback to improve this dissertation work. I learned many valuable lessons from you, and I appreciate it.

My achievement would have not been possible without the support and guidance from many individuals who I am so very grateful. I am thankful to Dr. Venkiteshwaran for helping me in every step of the way, answering all my questions with patience, and being a great mentor. Nicholas Benn, who always offered help and shared his knowledge with me. Also, Bethany Oceguera, my dedicated undergraduate research assistant. Your contribution to my work during this unprecedented time in this extraordinary year due to the COVID-19 outbreak and pandemic, was invaluable. This project would not have been completed without your gracious assistance.

Special thanks go to Mike Dollhopf, the lab manager at Water Quality Center, for his help and constant effort to keep the lab safe and operational. Acknowledgements are extended to the past and present members of the research team. Paige Peters for her input for the ozonation experimental design, Dr. Emily Gorsalitz, Dr. Joseph Heffron, Dr. Anthony Kappell, Dr. Yiran Tong, Dr. Zhongzhe Liu, Dr. Tonghui Xie, Faten Hussein, Donald Ryan, Lee Kimbell, Synthia Mallick, Eileen Kennedy, and Will Lynn.

I owe my deepest gratitude to my parents and my brother, Soroosh, for supporting me spiritually, believing in me, and providing me with the work ethics to achieve what I have so far in my life. I would like to thank my mother-in-law for her constant encouragement. I appreciate my friends, for always being there for me. I am also very grateful to Sarah and Adel Nasiri for their support.

Most importantly, I want to thank my husband, Bahram, for his unwavering love and constant support during my studies. You inspired me to follow my dreams and helped me to reach my goal. I could not have done this without you.

DEDICATION

This dissertation is dedicated to my husband, parents, and my brother for their endless love and support.

TABLE OF CONTENTS

ACKNOWLEDGMENT ..... **i**

LIST OF TABLES ..... **vi**

LIST OF FIGURES ..... **vii**

1 Introduction **1**

1.1. Renewable energy and sustainability 2
1.2. Pyrolysis for wastewater solids valorization 2
1.3. APL and its properties 4
1.4. APL treatment and valorization through anaerobic digestion 4
1.5. Research goal and objectives 6
1.6. References 7

2 Literature review **10**

2.1. Introduction 11
2.2. Pyrolysis 14
2.3. Hydrothermal liquefaction (HTL) 16
2.4. AD of APL and HTL-AP for energy recovery 18
2.5. APL and HTL-AP toxicity to methanogenesis 23
2.5.1. Effect of thermochemical process feedstock on APL degradability 23
2.5.2. Toxicity of organic constituents 24
2.5.3. Toxicity of inorganic constituents 27
2.5.4. Effect of thermochemical process temperature and condition and aqueous liquid organic loading on methane production 28
2.6. Pretreatment and co-treatment to compliment AD 31
2.7. Microbes and acclimation to improve AD 35
2.7.1. Bacterial community 37
2.7.2. Archaeal community 38
2.8. Outlook and conclusions 39
2.9. References 43

3 Inoculum microbiome and pre-ozonation affect methanogenesis from aqueous pyrolysis liquid **50**

3.1. Introduction 51
3.2. Materials and methods 55
3.2.1. APL production and pre-ozonation 55
3.2.2. ATA testing 56
3.2.3. Analytical methods 57
3.2.4. Statistical analysis 58

3.3. Results and discussion 59
3.3.1. Pyrolysis temperature affects APL composition 59
3.3.2. Pre-ozonation altered APL composition 60
3.3.3. GC-MS analysis of APL before and after ozonation 63
3.3.4. ATA results 67
3.3.5. Positive effect of ozonation and inocula selection on ATA methane production rate and initial lag phase 69
3.3.5.1. ATA methane production rate 69
3.3.5.2. ATA lag phase 72
3.4. Conclusion 77
3.5. References 79

4 Pre-ozonation and inocula selection increased quasi steady state methanogenesis using aqueous phase from sludge pyrolysis 83

4.1. Introduction 84
4.2. Materials and methods 88
4.2.1. APL production and ozonation 88
4.2.2. Anaerobic digesters 89
4.2.2.1. 15-d SRT digestion 90
4.2.2.2. 210-d SRT digestion 91
4.2.3. Synthetic primary sludge 91
4.2.4. Abiotic controls 92
4.2.5. Analytical methods and digester performance 92
4.2.6. DNA extraction and sequencing 93
4.2.7. Statistical analysis 94
4.3. Results and discussion 95
4.3.1. Raw and ozonated APL composition 95
4.4. Long-term digestion 97
4.4.1. 15-d SRT digestion performance 97
4.4.2. 210-d SRT digestion performance 98
4.4.2.1. Co-digesters performance 99
4.4.2.2. Mono-digesters performance 103
4.4.3. APL removal determined by GC-MS analysis 104
4.4.4. Microbial community analysis 106
4.4.4.1. Co-digesters 106
4.4.4.1.1 Archaea community in co-digesters 107
4.4.4.1.2 Bacteria community in co-digesters 110
4.4.4.2. Mono-digesters 117
4.4.4.2.1 Archaea community in mono-digesters 118
4.4.4.2.2 Bacteria community in mono-digesters 120
4.5. Conclusion 124
4.6. References 127

5 Overall conclusions and recommendations 132

5.1. Key findings 133

5.2. Future outlook....137

6 Appendices A....139

6.1. Supporting information 1....139
6.2. Supporting information 2....144

7 Appendices B....153

7.1. Introduction....154
7.2. Materials and methods....158
7.2.1. APL production and APL NH_3-N air stripping....158
7.2.2. Short-term semi-continuous anaerobic digestion....159
7.2.3. Long-term semi-continuous anaerobic digestion....160
7.2.4. Synthetic primary sludge....160
7.2.5. Analytical methods....161
7.2.6. DNA extraction and sequencing....161
7.2.7. Statistical analysis....162
7.3. Results and discussion....163
7.3.1. APL composition....163
7.3.2. Short-term semi-continuous anaerobic digestion....164
7.3.3. Short-term digestion microbial community analysis....168
7.3.3.1. Archaea community....169
7.3.3.2. Bacteria community....171
7.3.4. Long-term semi-continuous anaerobic digestion....175
7.4. Inhibition by APL and future considerations....178
7.5. Conclusions....180
7.6. Supplementary materials....181
7.7. References....186

LIST OF TABLES

Table 2.1. Methane yields from AD of APL under different conditions 21

Table 2.2. Methane yields from AD of HTL-AP under different conditions 22

Table 2.3. Inhibitory concentrations of some toxicants in APL or HTL-AP expressed in terms of IC_{50} 25

Table 3.1. APL characteristics at different pyrolysis temperatures[1]. 59

Table 4.1. Description of mono-digesters and co-digesters [1] 90

Table 4.2. APL composition before and after ozonation..... 96

Table 4.3. Alpha diversity indices in IB and MB inocula and in control digesters and co-digesters receiving ozonated and non-ozonated APL on day 215 of digestion. Average and standard deviations are from triplicate values. 107

Table 4.4. Alpha diversity indices in IB inoculum and in mono-digesters receiving ozonated and non-ozonated APL on day 215 of digestion. Average and standard deviations are from triplicate values. 117

Table 7.1. Aqueous pyrolysis liquid (APL) composition [a] 164

Table 7.2. Digester effluent characterization on day 45 [a]. 167

LIST OF FIGURES

Figure 2.1. Pyrolysis process schematics and its products. Carbon mass balance was adapted from Pokorna et al. (2009) performed on pyrolysis of dewatered sewage sludge..... 16

Figure 2.2. HTL process schematic and its products. Carbon fractions were adapted from Zhu et al. (2014) performed on HTL of woody biomass..... 18

Figure 2.3. Methane yield after 30 days from HTL-AP at 200 °C – 0.5 h and 320 °C – 0.5 h from rice straw before and after 1 kDa ultrafiltration. Adapted from Chen et al. (2017). 20

Figure 2.4. Biomethane production decrease during AD of HTL-AP with increasing temperatures using different feedstocks. AD of HTL-AP from rice straw under 170 – 320 °C (Chen et al., 2017). AD of HTL-AP of dewatered sewage sludge under 140 – 320 °C (Chen et al., 2019). AD of HTL-AP from a mixture of different model feedstocks at 200 – 350 °C (carbohydrate (Ch), protein (Pr), and lipid (Li)) (Posmanik et al., 2017)..... 30

Figure 3.1. Composition of 500 °C and 700 °C APL before and after 10 min and 2 h ozonation. (A) NH_3-N and total VFA, (B) SUVA and TP reduction, (C) COD and DOC. Error bars represent one standard deviation for triplicate systems. Some error bars are small and not visible..... 62

Figure 3.2. GC-MS analysis on APL composition before and after ozonation. The compounds with 10 highest peak area in non-ozonated,10 min and 2 h ozonated APLs are shown. These compounds contributed to >60% of the total organic compounds detected in all APLs. Undetected peaks were below detection of the GC-MS instrument ($<0.1\times10^8$). Compounds are sorted in increasing order of the molecular weight on the x axis. (A) 500 °C APL, (B) 700 °C APL. 66

Figure 3.3. ATA results on non-ozonated APL derived at 700 °C using IB1 at different APL COD concentrations. (A) Cumulative methane production, (B) Dose response curve on COD basis. Error bars represent standard deviation from triplicate experiments. Some error bars are small and not visible..... 69

Figure 3.4. Average IC_{50} values for non-ozonated, 10 min ozonated, and 2 h ozonated APLs using different inocula. Error bars represent standard deviation from triplicate bottles. Some error bars are small and not visible. IC_{50} values above 4 gCOD/L of APL are indicated by “>4”. (A) 500 °C APL, (B) 700 °C APL..... 72

Figure 3.5. Average lag phase time for non-ozonated, 10 min ozonated and 2 h ozonated APLs at highest loading (4 gCOD/L of APL) using different inocula. Error bars represent standard deviation from triplicate bottles. Some error bars are small and not visible. (A) 500 °C APL, (B) 700 °C APL. 74

Figure 3.6. Final cumulative methane production from ATAs on non-ozonated, 10 min ozonated and 2 h ozonated APL produced at 500 °C and 700 °C at different concentrations employing different inocula. The black bars show the theoretical stoichiometric methane production (395 mL CH_4 produced per gCOD removed at 35 °C and 1 atm) for comparison to the actual methane produced from APL COD at each concentration. Error bars represent standard deviation from triplicate bottles. Some error bars are small and not visible. 75

Figure 4.1. Quasi steady state methane production at 15-d SRT. Maximum stoichiometric methane from APL and synthetic primary sludge COD is shown in black bars. Error bars represent standard deviation from triplicate systems. 98

Figure 4.2. Quasi steady state methane production at 210-d SRT. (A) Methane production in co-digesters inoculated with IB and MB. Maximum stoichiometric methane from APL and synthetic primary sludge COD is shown in black bars. (B) Percent of maximum stoichiometric methane that is produced from APL COD in co-digesters inoculated with IB and MB. Error bars represent standard deviation from triplicate systems. 101

Figure 4.3. Quasi steady state methane production at 210-d SRT in mono-digesters. Percent of maximum stoichiometric methane that is produced from APL COD is shown. Error bars represent standard deviation from triplicate systems. 104

Figure 4.4. Organic compounds detected in abiotic controls and in co-digesters and mono-digesters receiving non-ozonated APL indicating complete biodegradation of APL compounds. Undetected peaks were below detection (BD) of the GC-MS instrument ($<0.05\times10^6$). The average and standard deviations are from triplicate sets. (A) No peaks were detected in co-digester digestate, whereas twelve peaks were identified in the abiotic control effluent sample, (B) More than twenty peaks were identified in abiotic control effluent sample, whereas no peaks were detected in mono-digesters digestate. 105

Figure 4.5. PCoA plot of archaeal community of IB and MB inocula (day 0) and co-digesters fed 2 h ozonated APL (day 215) based on Bray-Curtis distance. Ellipses represent 95% confidence intervals for the three points (each group represents the three triplicate digesters). IB and MB have distinctly different archaeal communities. APL co-digestion altered the archaeal community in both IB and MB inocula. 108

Figure 4.6. Dual hierarchical clustering of the 20 most abundant archaeal OTUs. These OTUs represent 87 ± 12% of total archaeal community relative abundance in all co-digesters. Taxonomic classification level of the OTUs is based on percent homology; <77% unknown, 77–80% unclassified phylum, 80–85% unclassified class, 85–90% unclassified order, 90–95% unclassified Family, 95–97% unclassified Genus. IB-inoculated co-digesters community was dominated by *Methanobacterium* (OTU 1). Whereas communities in MB-inoculated co-digesters

had *Methanosaeta* (OTU 29), *Methanoculleus* (OTU 111) and *Methanobacterium* (OTU 178) as dominant OTUs, also *Methanosaeta* (OTU 345) relative abundance increased in co-digesters fed ozonated and non-ozonated APL only. 110

Figure 4.7. PCoA plot on bacterial community of IB and MB inocula (day 0) and co-digesters fed 2 h ozonated APL (day 215) based on Bray-Curtis distance. Ellipses represent 95% confidence intervals for the three points (each group represents the three triplicate digesters). IB and MB have different bacterial communities. APL co-digestion transformed the bacterial community in both IB and MB inocula. 112

Figure 4.8. Dual hierarchical clustering of the 35 most abundant bacterial OTUs. These OTUs represent 50 ± 15% of the total bacterial community abundance in all co-digesters. Taxonomic classification of the OTUs is based on percent homology. Communities in IB clustered separately from MB. APL-fed IB-inoculated co-digesters community was dominated by *Enterococcus* (OTU 6), *Symbiobacterium* (OTU 22), and Ignavibacteriaceae (OTU 2). Communities in MB-inoculated co-digesters had *Bellilinea* (OTU 3) in control digesters and co-digesters receiving ozonated APL, while phenol-degrading Bacteroidales (OTU 8, 12, and 13) was dominant in co-digesters fed non-ozonated APL. 114

Figure 4.9. PCoA plot on archaeal community of mono-digesters inoculum (day 0) and digesters fed non-ozonated and 2 h ozonated APL (day 215) based on Bray-Curtis distance. Ellipses represent 95% confidence intervals for the three points (each group represents the three triplicate digesters). APL digestion shifted the archaeal community composition in inoculum as observed by distinct archaeal community clusters. Ozonated and non-ozonated APL digestion did not affect the archaeal community composition. 119

Figure 4.10. Dual hierarchical clustering of the 20 most abundant archaeal OTUs. These OTUs represent 93 ± 1.1% of total archaeal community relative abundance in mono-digesters. Taxonomic classification of the OTUs is based on percent homology. *Methanobacterium* (OTU 1) dominated in mono-digesters receiving ozonated and non-ozonated APL. 120

Figure 4.11. PCoA plot on bacterial community of mono-digesters inoculum (day 0) and digesters fed non-ozonated and 2 h ozonated APL (day 215) based on Bray-Curtis distance. Ellipses represent 95% confidence intervals for the three points (each group represents the three triplicate digesters). APL digestion shifted the bacterial community composition in inoculum as observed by distinct clusters. Ozonated and non-ozonated APL digestion did not affect the bacterial community composition significantly. 121

Figure 4.12. Dual hierarchical clustering of the 30 most abundant archaeal OTUs. These OTUs represent 75 ± 6% of the total bacterial community abundance in mono-digesters. Taxonomic classification of the OTUs is based on percent homology. SAOB *Symbiobacterium* (OTU 15), *Clostridiisalibacter* (OTU 17), and

Clostridiaceae (OTU 21) increased in relative abundance after APL digestion. Also, relative abundance of Ignavibacteriaceae (OTU 2) and *Desulfomonile* (OTU 5) increased. 123

Figure 7.1. Short-term digester functional data. Average and standard deviation values are from triplicate systems. (A) Methane production, (B) Digestate COD concentration, (C) Digestate SCOD concentration. The whiskers represent one standard deviation above and below the mean. Some whiskers are small and not visible. 166

Figure 7.2. Dual hierarchical clustering of the seven most abundant archaeal OTUs. These OTUs represent 94 2.6% of the total archaeal abundance in all digesters. Taxonomic classification in bold font represents the valid level based on percent homology, with the homology percentage ranges in parentheses. Digester communities on day 15 were dominated by Methanosaeta (OTU 56). However, communities in digesters co-fed catalyzed APL shifted by day 45 and were dominated by an unknown archaea (OTU 127). 170

Figure 7.3. Dual hierarchal clustering of the 50 most abundant bacteria. These OTUs represented 63.1 ± 2.3 % of total microbial community abundance in all the digesters. Taxonomic classification in bold font represent the valid level based on percent homology with the homology percentage ranges in parentheses. Communities on day 45 clustered separately from communities on day 15. On day 45, bacterial communities in the digesters fed catalyzed APL clustered separately from all other communities. *Clostridiaceae* (OTU 96) and *Ruminococcaceae* (OTU 97) were dominant in all digesters on days 15 and 45. In inhibited digesters, *Bacteroidales* (OTU 2), *Enterococcus* (OTU 15), *Erysipelotrichales* (OTU 22), *Campylobacter* (OTU 30), and *Tissierrella* (OTU 36) were dominant, but not in other digesters. 172

Figure 7.4. Methane production results from the long-term acclimation study. Control digesters received synthetic primary sludge and no APL, whereas non-catalyzed APL digesters were co-fed synthetic primary sludge and non-catalyzed APL. (A) Daily methane volume produced; the red lines show the time at which the APL OLR was changed. (B) Comparison between theoretical stoichiometric maximum daily expected methane from APL COD (blue bars) and the observed methane produced from APL (compared to controls) at each organic loading rate (red bars). Whiskers represent one standard deviation above and below the mean. Some whiskers are small and not visible. 176

Figure S7.1 Archaea nMDS plot. Ellipses represent 95% confidence intervals for the three points (each group represents the three triplicate digesters). On day 15, all digester Archaeal communities were similar. Exposure to catalyzed APL for 45 days altered the Archaeal community compared to control digester communities, whereas the *Archaeal* communities in digesters fed non-catalyzed APL were more similar 181

Figure S7.2 Bacteria nMDS plot. Ellipses represent 95% confidence intervals for triplicate digesters (each group represents the three triplicate digesters). Some ellipses are small and not visible. On day 15, all digester bacterial communities were similar. On day 45, Bacterial communities in digesters fed catalyzed APL was significantly different from Bacterial communities control digesters and digesters fed non-catalyzed APL. The points representing catalyzed digesters on day 15 and non-catalyzed digesters on day 15 overlap. Also, the points representing control digesters on day 45 and non-catalyzed digesters on day 45 overlap. 182

Figure S7.3 DESeq2 results to identify statistically different ($p<0.001$) OTUs between control digesters and digesters fed catalyzed APL. OTUs with greater/less than ±2 fold changes are shown. OTUs greater than 2-fold change are more abundant in digesters fed catalyzed APL compared to control digesters. 183

1 Introduction

1.1. Renewable energy and sustainability

Research to develop an alternative form of energy to fossil fuel has risen in the last decades (Acharya et al., 2015; Li and Feng, 2018a). One of the important and attractive renewable energy options is energy recovery from biomass and organic waste that simultaneously contributes to minimization of harmful environmental impacts (Cao and Pawłowski, 2012; Fonts et al., 2012). Wastewater solids are often composed of primary sludge and waste activated sludge generated at water resource recovery facilities (WRRFs). Wastewater solids have energy content and are potential energy resources (Liu et al., 2018). They can be used as a renewable energy source to supply some or all required energy at conventional WRRFs and even provide additional energy for other applications (Li and Feng, 2018a; Liu et al., 2018). They are produced constantly and continue to increase as the urban population grows and more strict effluent requirements are implemented (Seiple et al., 2017). However, conventional solids management approaches including landfilling and biosolids land application for agriculture do not retrieve most energy from the organic matter in wastewater solids (Agrafioti et al., 2013; McNamara et al., 2016). Furthermore, some of these conventional methods have raised health and environmental concerns due to potentially adding to the land pathogens, micropollutants, and other contaminants such as antibiotic resistance genes (Kimbell et al., 2018; Liu et al., 2018; Ross et al., 2016a).

1.2. Pyrolysis for wastewater solids valorization

One technology that can be implemented to extract energy from wastewater

solids while reducing the potential harmful impacts to the environment is pyrolysis (McNamara et al., 2016; Ross et al., 2016a). Pyrolysis offers multiple benefits including waste volume reduction, organic matter stabilization, pathogens and micropollutants removal, and fuel as well as possibly chemicals production (Syed-Hassan et al. 2017). In pyrolysis, wastewater solids are heated at 400 – 900 °C in the absence of oxygen, decomposing the organic matter and yielding the following products: (1) biochar, (2) pyrolysis gas (py-gas), and (3) pyrolysis liquid (Fabbri and Torri, 2016a; Liu et al., 2020; Torri et al., 2020). Biochar is the solid product that has good sorption properties and can be used as a soil amendment for plant growth because of its high capacity to hold moisture and nutrients for plants (Liu et al., 2018; McNamara et al., 2016). Other potential applications include using biochar as a catalyst, energy source, or a sorbent (Liu et al., 2018). The gaseous product, pyrolysis gas or py-gas, is a mixture of methane (CH_4), carbon dioxide (CO_2), hydrogen (H_2), carbon monoxide (CO) and other constituents (Pecchi and Baratieri, 2019a). Py-gas is a relatively clean energy source and can be used on-site at WRRFs for renewable energy generation (Liu et al., 2020). The pyrolysis liquid can be comprised of two phases, bio-oil and aqueous pyrolysis liquid (APL) (Fonts et al., 2012; Pecchi and Baratieri, 2019a). Crude bio-oil, which is a mixture of numerous organic compounds, has undesirable properties such as high viscosity, high water and ash content and high corrosiveness; therefore, it requires upgrading to be useable and cannot be directly used as a fuel (Seyedi, 2018). Upon upgrading, bio-oil is processed to become a renewable liquid fuel that can be employed for heat and energy generation (Chen et al., 2014; McNamara et al.,

2016).

1.3. APL and its properties

APL is a water-based solution with high chemical oxygen demand (COD) (30 to 500 gCOD/L) that has no known practical use (Fabbri and Torri, 2016a; Hübner and Mumme, 2015; Seyedi et al., 2019). It is generated from initial moisture in the feedstock and water produced during pyrolysis reactions (Mohan et al., 2006). Due to its low heating value, it cannot be ignited or used directly as fuel (Torri and Fabbri 2014). APL is comprised of numerous complex organics including carboxylic acids, aldehydes, phenols, alcohols, ketones, and nitrogenous organics such as pyridine, pyridinol, pyrrole, pyrazine, and aminophenol (Fabbri and Torri, 2016a; Hübner and Mumme, 2015; Seyedi et al., 2020). Many of the APL constituents such as nitrogenous organics are toxic to mammalian cells and microorganisms (Zhou et al. 2015; Tommaso et al. 2015). APL yield during some pyrolysis conditions can be high, contributing 70 – 100% of the total weight of the pyrolysis liquids and it has been shown to contain >45% of the feedstock biomass carbon (Liu et al., 2017; Lü et al., 2018; Mukarakate et al., 2017; Torri and Fabbri, 2014). Therefore, there is a need to carefully manage the large quantities of this hazardous liquid waste.

1.4. APL treatment and valorization through anaerobic digestion

One potential method to recover APL energy is through anaerobic digestion (AD) that is a common technology to obtain energy from organic waste in the form

of energy-rich biogas. AD involves biological conversion of organic chemicals into biogas containing CH_4 in the absence of oxygen by a community of anaerobic microorganisms through four main steps of hydrolysis, acidogenesis, acetogenesis and methanogenesis (Venkiteshwaran, 2016). APL derived from pyrolysis of organic matter is a good candidate to consider for AD since it has a high COD concentration (Torri et al., 2020; Wen et al., 2020; Zhou et al., 2019). Specifically, APL produced from pyrolysis of wastewater solids could be used as the sole substrate (mono-digestion) or as a co-digestate since it contains high concentrations of organics such as acetic acid (approximately 25 g/L) that are easily converted to biogas (Seyedi et al., 2019). However, a challenge to digest APL exists since it contains some problematic organic compounds that are known to inhibit methane-producing microbes such as phenols and nitrogenous organics that can reduce or stop methane production. Using APL as the sole substrate may be challenging due to its toxicity and may require high dilutions. Using APL as a co-digestate along with a primary substrate could be a viable approach to reduce its toxicity because APL will be blended with another waste. Anaerobic co-digestion is used to digest a combination of two or more wastes, to produce more biogas and utilize the maximum capacity of the digester (Zitomer et al., 2008). Furthermore, it would be beneficial if APL from wastewater solids pyrolyzed at WRRFs that already have digesters treating sludge could be added as a co-digestate.

1.5. Research goal and objectives

The overall goal of this research was to recover energy in APL through AD using different strategies to overcome inhibition and enhance methane production. A review of relevant literature is presented in Chapter 2. The overall approach involved the following research objectives:

1. Understand the impact of pyrolysis temperature on APL degradability (Chapter 3),
2. Investigate ozone pretreatment to reduce APL recalcitrance to biodegradation (Chapter 3),
3. Examine ozonated and non-ozonated APL anaerobic toxicity and inhibitory concentrations (Chapter 3),
4. Employ four different anaerobic inocula to identify different microbial communities capabilities for APL conversion to methane for ozonated and non-ozonated APL (Chapter 3),
5. Determine appropriate organic loading rates (OLR) and solids retention time (SRT) for anaerobic co-digestion or mono-digestion of ozonated and non-ozonated APL for improved methane production employing different inocula (Chapter 4),
6. Investigate the microbial community compositions in different digesters before and after APL digestion (Chapter 4).

Finally, the overall conclusions of this study and future recommendations are provided in Chapter 5.

1.6. References

Acharya B, Dutta A, Minaret J (2015) Review on comparative study of dry and wet torrefaction. Sustain. Energy Technol. Assessments 12:26–37

Agrafioti E, Bouras G, Kalderis D, Diamadopoulos E (2013) Biochar production by sewage sludge pyrolysis. J Anal Appl Pyrolysis 101:72–78. https://doi.org/10.1016/j.jaap.2013.02.010

Cao Y, Pawłowski A (2012) Sewage sludge-to-energy approaches based on anaerobic digestion and pyrolysis: Brief overview and energy efficiency assessment. Renew Sustain Energy Rev 16:1657–1665. https://doi.org/10.1016/j.rser.2011.12.014

Chen H, Zhai Y, Xu B, et al (2014) Characterization of bio-oil and biochar from high-temperature pyrolysis of sewage sludge. Environ Technol 36:470–478. https://doi.org/10.1080/09593330.2014.952343

Fabbri D, Torri C (2016) Linking pyrolysis and anaerobic digestion (Py-AD) for the conversion of lignocellulosic biomass. Curr Opin Biotechnol 38:167–173. https://doi.org/10.1016/j.copbio.2016.02.004

Fonts I, Gea G, Azuara M, et al (2012) Sewage sludge pyrolysis for liquid production: A review. Renew Sustain Energy Rev 16:2781–2805. https://doi.org/10.1016/j.rser.2012.02.070

Hübner T, Mumme J (2015) Integration of pyrolysis and anaerobic digestion – Use of aqueous liquor from digestate pyrolysis for biogas production. Bioresour Technol 183:86–92. https://doi.org/10.1016/j.biortech.2015.02.037

Kimbell LK, Kappell AD, McNamara PJ (2018) Effect of pyrolysis on the removal of antibiotic resistance genes and class I integrons from municipal wastewater biosolids. Environ Sci Water Res Technol 4:1807–1818. https://doi.org/10.1039/c8ew00141c

Li H, Feng K (2018) Life cycle assessment of the environmental impacts and energy efficiency of an integration of sludge anaerobic digestion and pyrolysis. J Clean Prod 195:476–485. https://doi.org/10.1016/j.jclepro.2018.05.259

Liu Z, Mayer BK, Venkiteshwaran K, et al (2020) The state of technologies and research for energy recovery from municipal wastewater sludge and biosolids. Curr. Opin. Environ. Sci. Heal. 14:31–36

Liu Z, McNamara P, Zitomer D (2017) Autocatalytic Pyrolysis of Wastewater Biosolids for Product Upgrading. Environ Sci Technol 51:9808–9816. https://doi.org/10.1021/acs.est.7b02913

Liu Z, Singer S, Tong Y, et al (2018) Characteristics and applications of biochars derived from wastewater solids. Renew Sustain Energy Rev 90:650–664. https://doi.org/10.1016/j.rser.2018.02.040

Lü F, Hua Z, Shao L, He P (2018) Loop bioenergy production and carbon sequestration of polymeric waste by integrating biochemical and thermochemical conversion processes: A conceptual framework and recent advances. Renew. Energy 124:202–211

McNamara PJ, Koch JD, Liu Z, Zitomer DH (2016) Pyrolysis of Dried Wastewater Biosolids Can Be Energy Positive. Water Environ Res 88:804–810. https://doi.org/10.2175/106143016X14609975747441

Mohan D, Pittman CU, Steele PH (2006) Pyrolysis of wood/biomass for bio-oil: A critical review. Energy and Fuels 20:848–889. https://doi.org/10.1021/ef0502397

Mukarakate C, Evans RJ, Deutch S, et al (2017) Reforming Biomass Derived Pyrolysis Bio-oil Aqueous Phase to Fuels. Energy and Fuels 31:1600–1607. https://doi.org/10.1021/acs.energyfuels.6b02463

Pecchi M, Baratieri M (2019) Coupling anaerobic digestion with gasification, pyrolysis or hydrothermal carbonization: A review. Renew. Sustain. Energy Rev. 105:462–475

Ross JJ, Zitomer DH, Miller TR, et al (2016) Emerging investigators series: Pyrolysis removes common microconstituents triclocarban, triclosan, and nonylphenol from biosolids. Environ Sci Water Res Technol 2:282–289. https://doi.org/10.1039/c5ew00229j

Seiple TE, Coleman AM, Skaggs RL (2017) Municipal wastewater sludge as a sustainable bioresource in the United States. J Environ Manage 197:673–680. https://doi.org/10.1016/j.jenvman.2017.04.032

Seyedi S (2018) Anaerobic Co-digestion of Aqueous Liquid from Biosolids Pyrolysis. Master's Thesis. Marquette University. Milwaukee, WI. USA

Seyedi S, Venkiteshwaran K, Benn N, Zitomer D (2020) Inhibition during Anaerobic Co-Digestion of Aqueous Pyrolysis Liquid from Wastewater Solids and Synthetic Primary Sludge. Sustainability 12:3441. https://doi.org/10.3390/su12083441

Seyedi S, Venkiteshwaran K, Zitomer D (2019) Toxicity of Various Pyrolysis Liquids From Biosolids on Methane Production Yield. Front Energy Res 7:1–12. https://doi.org/10.3389/fenrg.2019.00005

Torri C, Fabbri D (2014) Biochar enables anaerobic digestion of aqueous phase from intermediate pyrolysis of biomass. Bioresour Technol 172:335–341. https://doi.org/10.1016/j.biortech.2014.09.021

Torri C, Pambieri G, Gualandi C, et al (2020) Evaluation of the potential performance of hyphenated pyrolysis-anaerobic digestion (Py-AD) process for carbon negative fuels from woody biomass. Renew Energy 148:1190–1199. https://doi.org/10.1016/j.renene.2019.10.025

Venkiteshwaran K (2016) Bioaugmentation and Correlating Anaerobic Digester

Microbial Community to Process Function

Wen C, Moreira CM, Rehmann L, Berruti F (2020) Feasibility of anaerobic digestion as a treatment for the aqueous pyrolysis condensate (APC) of birch bark. Bioresour Technol 307:123199. https://doi.org/10.1016/j.biortech.2020.123199

Zhou H, Brown RC, Wen Z (2019) Anaerobic digestion of aqueous phase from pyrolysis of biomass: Reducing toxicity and improving microbial tolerance. Bioresour Technol 292:. https://doi.org/10.1016/j.biortech.2019.121976

Zitomer DH, Adhikari P, Heisel C, Dineen D (2008) Municipal anaerobic digesters for codigestion, energy recovery, and greenhouse gas reductions. Water Environ Res 80:229–237. https://doi.org/10.2175/106143007X221201

2 Literature review

This chapter is accepted for publication in *Reviews in Environmental Science and Bio/Technology:*

Seyedi, S., Veniteshwaran, K., Zitomer, D., (2020). Current status of biomethane production using aqueous liquid from pyrolysis and hydrothermal liquefaction of sewage sludge and similar biomass. Reviews in *Environmental Science and Bio/Technology*.

2.1. Introduction

The global interest in an alternative form of energy to fossil fuel that is renewable, sustainable, and poses minimal detrimental environmental consequences has risen in the last decades (Acharya et al. 2015; Li and Feng 2018a). Organic material such as lignocellulosic biomass in agricultural residues is one type of feedstock for energy production (Monlau et al. 2015). Alternatively, sewage sludge or solids from water resource recovery facilities (WRRFs) treating municipal wastewater are promising for energy recovery since they are continuously produced, organically rich and can supply the energy typically required at conventional WRRFs, and possibly yield additional energy for other uses (Li and Feng 2018b; Liu et al. 2018). Sludge generation continues to increase as the urban population grows and more strict effluent requirements are implemented (Seiple et al. 2017). More than 13 million U.S. tonnes per year of total sludge dry solids with approximately 80% w/w organic content are generated in the U.S. and could be utilized for biofuel production (Skaggs et al. 2017; Seiple et al. 2017).

Thermochemical technologies to recover energy from organic biomass have been investigated extensively in the last few decades (Cao and Pawłowski 2012; Syed-Hassan et al. 2017). Combustion does not typically produce an aqueous waste stream, whereas pyrolysis, gasification, hydrothermal liquefaction (HTL), and hydrothermal carbonization typically produce an aqueous waste with significant organic content (Pecchi and Baratieri 2019). Among these, most research pertaining to liquid fuel production from sludge involves pyrolysis (Fonts

et al. 2012), which has the potential to reduce waste volume by 50%, stabilize organic matter, and generate fuel and possibly chemicals (Syed-Hassan et al. 2017). HTL is also reported to be an appropriate process for wet biomass such as sewage sludge because it does not require the costly drying step of pyrolysis. Therefore, the number of studies investigating HTL to generate liquid fuel has increased substantially over the past decade (López Barreiro et al. 2013; Gollakota et al. 2018). HTL is synonymous with hydrous pyrolysis, but it is carried out at lower temperatures than pyrolysis (López Barreiro et al. 2013; Kumar et al. 2018).

Aqueous liquid containing high concentrations of organic and inorganic constituents is among the various products of both pyrolysis and HTL. During thermochemical conversions, organic matter is decomposed under high temperatures and/or pressure, resulting in liquid as well as solid and gaseous byproducts (Fabbri and Torri 2016). Liquid products of pyrolysis include an organic phase, referred to as bio-oil, and an aqueous phase, referred to as aqueous pyrolysis liquid (APL) (Pecchi and Baratieri 2019; Yang et al. 2020). During HTL, wet biomass is thermochemically converted into biocrude oil, and an aqueous phase liquid product (HTL-AP) is also produced (Watson et al. 2020).

Currently, there are no known beneficial uses for the aqueous liquids, APL or HTL-AP (Watson et al. 2020; Liu et al. 2020). In contrast, bio-oil and bio-crude oil can be used as renewable fuels after upgrading (Ul Islam et al. 2015; Maddi et al. 2017; Liu et al. 2020). Insufficient attention has been paid to beneficial use of the aqueous liquids and they are considered waste streams that must be carefully managed to preclude environmental damage (Fabbri and Torri 2016; Watson et al.

2020). APL and HTL-AP share comparable constituents and are produced from both the initial moisture of the feedstock during thermal conversion as well as thermochemical reactions such as dehydration of feedstock components (Seyedi 2018; Watson et al. 2020). They have low heating value and are not ignitable, so cannot be used directly as fuel (Torri and Fabbri 2014). APL and HTL-AP have high chemical oxygen demand (COD) with organic compounds such as carboxylic acids, aldehydes, phenols, alcohols, ketones, and nitrogenous organics that can be environmentally harmful (Tommaso et al. 2015; Seyedi et al. 2020). Many of the constituents such as nitrogenous organics are toxic to mammalians cells and microorganisms (Zhou et al. 2015; Tommaso et al. 2015).

One possible beneficial use for APL and HTL-AP is to recover energy from the organic-rich aqueous liquids via anaerobic digestion (AD). Both APL and HTL-AP contain high concentrations of organics such as acetic acid that can serve as a substrate for AD (Leng and Zhou 2018; Seyedi 2018; Si et al. 2018). However, the presence of some constituents that may be biodegradable but are toxic to anaerobic microbes makes AD of these aqueous liquids currently very challenging.

The aim of this review is to present advances made in the last five years to recover energy through AD of aqueous liquid generated during pyrolysis and HTL of wastewater sewage sludge. AD of aqueous streams obtained from other lignocellulosic feedstocks is also reported to complement results of studies regarding AD of thermochemical aqueous liquids from sewage sludge. A comparison of different toxicity effects to AD microbial communities and potential methods to overcome the toxicity is discussed.

2.2. Pyrolysis

Wastewater solids contain potential energy in the form of organic matter (Cao and Pawłowski 2012). Pyrolysis can recover energy from organic matter thermochemically, as well as reduce the sludge volume, and minimize or remove contaminants such as antibiotic resistance genes, micropollutants, and pathogens (Ross et al. 2016; Kappell et al. 2018). Lignocellulosic biomass such as corn stover, birch bark, wood pellets, and other agricultural biomass are also among the commonly used feedstock for pyrolysis (Monlau et al. 2015). Figure 2.1 illustrates the pyrolysis process and its products with their potential use. In pyrolysis, the organic substances are decomposed in the absence of oxygen under high temperatures (400 – 900°C) and converted into biochar, py-gas, and pyrolysis liquids (Li and Feng 2018; Liu et al. 2020). Biochar derived from wastewater solids has been shown to have good sorption characteristics as well as contain less contaminants of concern than wastewater solids and can be used as soil amendment to improve plant growth (Carey et al. 2015; Liu et al. 2018). Py-gas is a fuel primarily comprised of methane (CH_4), hydrogen gas (H_2), carbon monoxide (CO), carbon dioxide (CO_2) and other minor constituents that can be burned alone or mixed with anaerobic digester biogas or natural gas (Pecchi and Baratieri 2019; Seyedi et al. 2019).

The pyrolysis liquid partitions into two distinct phases: bio-oil and APL. Bio-oil is a complex mix of organic compounds including anhydrosugars, carboxylic acids, alcohols, ketones, phenols, and aldehydes that can be used as a renewable fuel in boilers or diesel engines for heat and power generation after upgrading (Ul

Islam et al. 2015; Feng and Lin 2017). Upgrading is typically required due to undesirable properties of raw bio-oil including instability, acidity, and corrosiveness. Upgrading can be relatively costly and, therefore, limits the commercial application of bio-oil at WRRFs (Liu et al. 2020). Biological conversion of bio-oil has also been investigated with the goal of producing valuable chemicals; however, microbial inhibitors present in raw bio-oil pose some challenges (Jarboe et al. 2011).

APL is a water-based solution containing numerous organic compounds with a high COD concentration ranging from 30 to 500 gCOD/L (Seyedi et al. 2019; Zhou et al. 2019; Wen et al. 2020). During some pyrolysis conditions, the yield of APL can be high, representing about 70 to 100% of the total weight of the pyrolysis liquids and up to 60% of the original biomass carbon, creating the need to carefully manage the large quantities of this liquid waste (Torri and Fabbri 2014; Liu et al. 2017; Mukarakate et al. 2017; Lü et al. 2018). The carbon fractions, mass balance, energy balance, and product yields during pyrolysis can vary considerably depending on feedstock, pyrolysis temperatures and extraction procedures. Pokorna et al. (2009) investigated the carbon percentages and product yields during flash pyrolysis of dewatered digested sludge at 500 °C. Product yields for biochar, py-gas, bio-oil and APL were 56, 17, 14, and 12% (mass of total products), respectively (Figure 2.1). The highest carbon fraction of pyrolyzed sludge was in APL. In addition, 69 wt% of the APL was comprised of carbon (Pokorna et al. 2009).

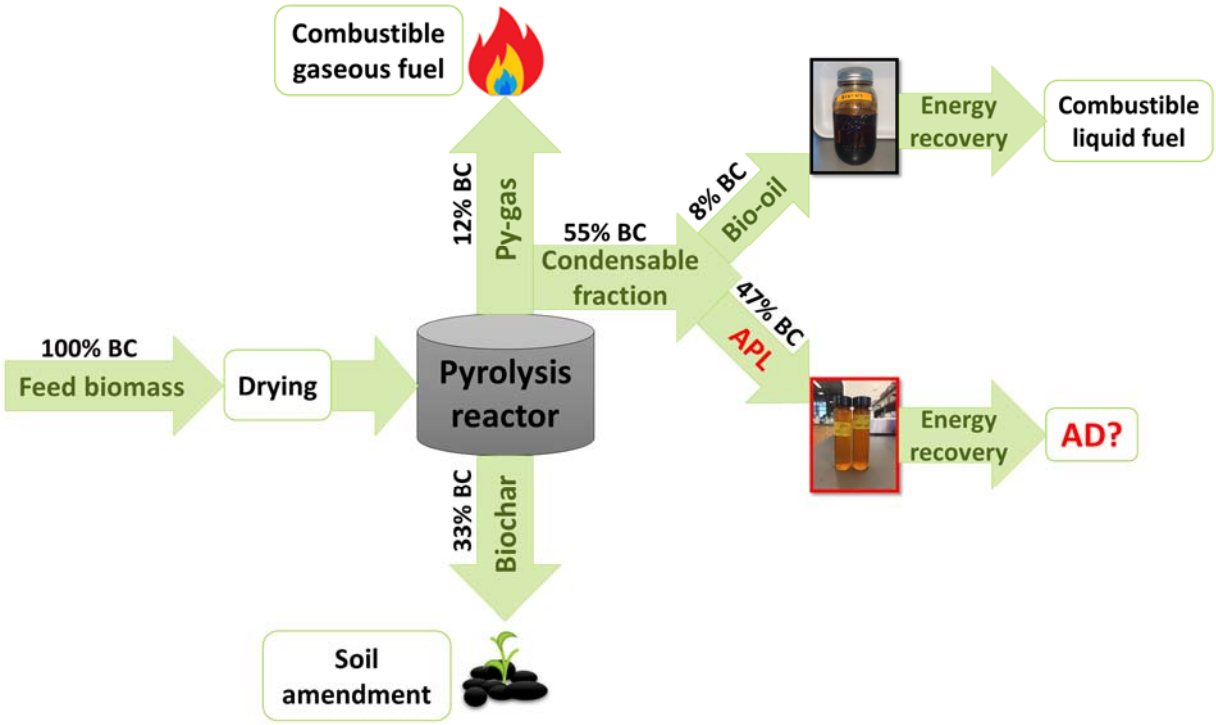

Figure 2.1. Pyrolysis process schematics and its products. Carbon mass balance was adapted from Pokorna et al. (2009) performed on pyrolysis of dewatered sewage sludge.

2.3. Hydrothermal liquefaction (HTL)

HTL is a thermochemical process that occurs at medium temperature and high pressure. Carbonaceous wet feedstock undergoes thermochemical conversion during HTL at 250 to 400 °C and 4 to 22 MPa, a pressure which is close to the critical point of water (374.2 °C and 22.1 MPa), and generates bio-crude oil as well as solid residue, a CO_2-rich gas and HTL-AP (Zhou et al. 2015; Chen et al. 2016; Maddi et al. 2017; Posmanik et al. 2017; Watson et al. 2020). An illustration of an HTL process along with its products is presented in Figure 2.2. Various feedstocks have been investigated for HTL, including sewage sludge, livestock manure, algae, rice straw, and woody biomass (Maddi et al. 2017; Si et

al. 2019). HTL bio-crude oil has a comparable heating value to petroleum oil and, like bio-oil, can be upgraded to liquid fuel (Maddi et al. 2017; Posmanik et al. 2017). The solid product can be burned to produce heat and electricity or possibly employed for recovery of nutrients for soil amendment (Cantero-Tubilla et al. 2018), although the presence of toxic constituents may preclude this as a safe option. HTL-AP contains organics such as alcohols, acids, ketones, aromatic compounds, and N-heterocyclic compounds and is comparable in composition to pyrolysis APL (Si et al. 2018). Similar to APL, feedstock composition along with reaction conditions (temperature, retention time, etc.) considerably affect the HTL products mass balance, elemental balance, product yields, and energy recovery. Xu et al. (2018) evaluated product distributions from sewage sludge HTL at different temperatures. At 340 °C, product yields for solid residue, bio crude oil, HTL-AP, and CO_2-rich gas accounted for 42, 22, 18, and 5 wt% of total products, respectively (Figure 2.2). The carbon content of different HTL products reported by Zhu et al. (2014) from woody biomass showed a high carbon fraction was transferred to HTL-AP (Figure 2.2). Despite the high organic content of HTL-AP (52 – 104 gCOD/L), research to recover HTL-AP organics for reuse has been limited (Gai et al. 2015; Zheng et al. 2017; Watson et al. 2018). Some valorization routes for HTL-AP have been examined. For example, in a recent study, Cordova et al. (2020) utilized HTL-AP in yeast fermentation for improved co-production of valuable chemicals employing different strains of *Y. lipolytica*. HTL-AP addition enhanced itanoic acid and triacetic acid lactone production, as well as other co-products such as lipids and citric acid.

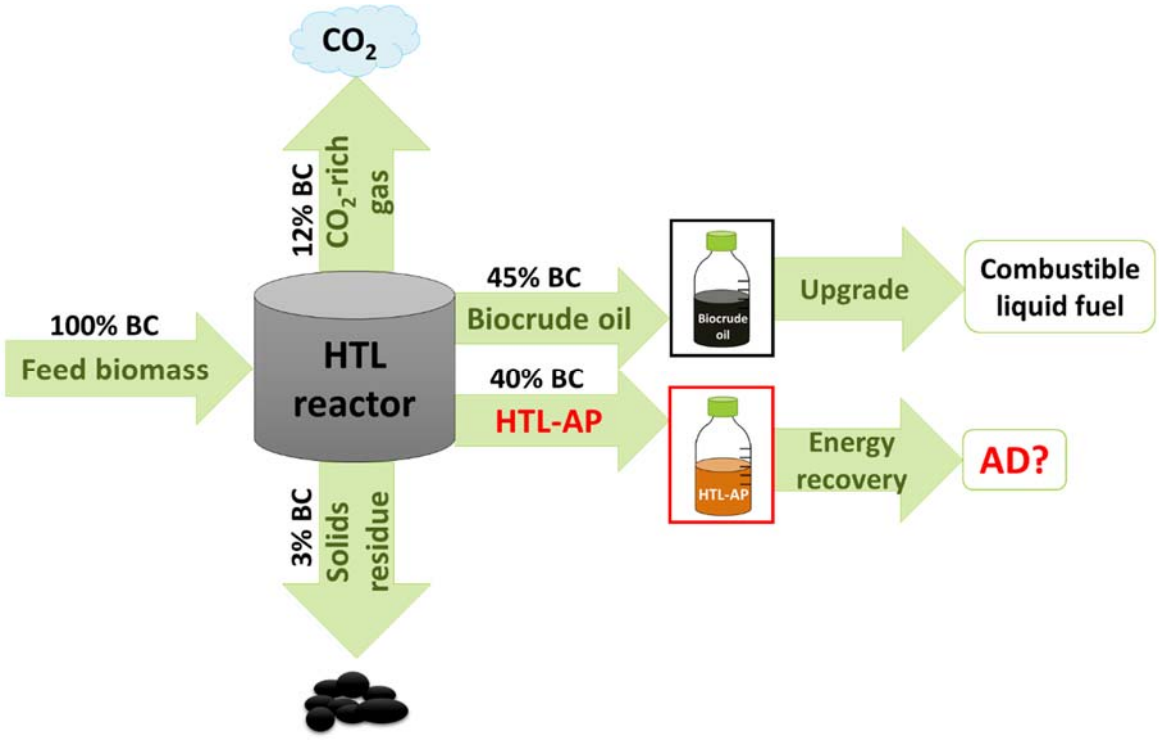

Figure 2.2. HTL process schematic and its products. Carbon fractions were adapted from Zhu et al. (2014) performed on HTL of woody biomass.

2.4. AD of APL and HTL-AP for energy recovery

AD is the biological transformation of biodegradable substrates into biogas containing CH_4 using a consortium of microorganisms under an oxygen-free environment (Venkiteshwaran et al. 2016). Syntrophic interactions within the complex microbial community take place in four biological stages of hydrolysis, acidogenesis (fermentation), acetogenesis, and methanogenesis (Venkiteshwaran et al. 2016). AD is one of the most common technologies to extract energy from organic waste in the form of energy-rich biogas. Aqueous liquids with high COD concentrations, such as APL and HTL-AP, are frequently reported as good candidates to consider for AD (Torri and Fabbri 2014; Hübner

and Mumme 2015; Chen et al. 2017; Si et al. 2019). The COD concentrations of various APLs and HTL-APs derived under different conditions are reported in Tables 1 and 2, respectively. The COD is exerted by organics such as acetic acid that are easily biodegradable, as well as other organics that are more difficult to degrade (Leng and Zhou 2018; Seyedi 2018). For example, APLs derived from a mixture of cow manure and maize digestate, fast pyrolysis of birch bark, and from coconut shell were reported to contain 25, 104, and 166 g/L of acetic acid, respectively (Torri and Fabbri 2014; Cheng et al. 2016; Wen et al. 2020). Similarly, the acetic acid concentrations of HTL-AP generated from cornstalk and swine manure were approximately 22 and 8 g/L, respectively (Si et al. 2018, 2019).

Some fraction of the recalcitrant organics may be high molecular weight (MW) compounds that are notoriously difficult to biodegrade. For example, the majority of the high MW organics (MW > 1000 g/mol) identified by gel filtration chromatography in HTL-AP derived from rice straw were not appreciably degraded and were detected in AD effluent (Chen et al. 2016). Chen et al. (2017) performed size distribution analyses of organics in HTL-AP derived from rice straw using ultrafiltration and determined the methane yield from the filtered and unfiltered samples. It was observed that compounds < 1 kDa were more biodegradable than larger molecules (> 1 kDa) (Figure 2.3).

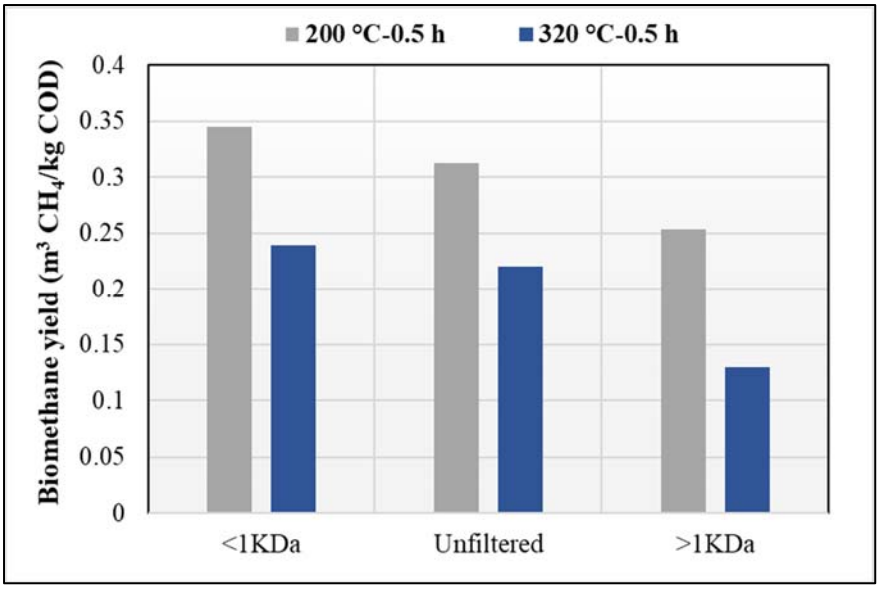

Figure 2.3. Methane yield after 30 days from HTL-AP at 200 °C – 0.5 h and 320 °C – 0.5 h from rice straw before and after 1 kDa ultrafiltration. Adapted from Chen et al. (2017).

A summary of methane yields reported from AD of APL and HTL-AP produced under different conditions and from different feedstock along with pretreatments used is presented in Tables 2.1 and 2.2. Typically, 30 to 65% of the aqueous liquid COD is converted to methane (Tables 2.1 and 2.2). This is in contrast to AD of food waste and other easily degraded substrates in which more than 85% of the feedstock COD is converted to methane (Speece 2008). Research to identify the origin of recalcitrance to biodegradation would assist in identifying appropriate AD strategies. Strategies that may be advantageous include altering the operational parameters in the pyrolysis and HTL processes, pretreatments prior to or concurrent with AD, reducing the digester organic loading rate (OLR), increasing the digester solids retention time and appropriate microbial acclimation or selection of the most effective seed microbes (Yang et al. 2018; Si et al. 2019; Watson et al. 2020; Seyedi et al. 2020).

Table 2.1. Methane yields from AD of APL under different conditions

Pyrolysis feedstock	Pyrolysis temperature	APL COD	AD operation mode	AD loading	Co-treatment or pretreatment	Acclimation	Cause of toxicity	Highest methane yield observed	Reference
-	°C	g/L	-	gCOD/L for batch, gCOD/L_r-d for continuous/semi-continuous	-	-	-	Percent of stoichiometric theoretical methane [a]	-
Milorganite	800	202	Semi-continuous	0.05 – 0.5	Co-digestion with synthetic primary sludge	Yes	Phenols, nitrogenous organics	100% at ≤0.1 gCOD/L_r-d	(Seyedi et al. 2020)
Birch bark	500	499	Batch	1.3 g/L acetic acid equivalent of APL	Biochar and nutrient addition	Yes	Phenols	100% of acetic acid equivalent	(Wen et al. 2020)
Corn stalk pellets	400	ThOD [b] = 0.7	Batch, Semi-continuous	35, 5 – 140	Biochar addition	No, Yes	Phenols	60%, 65%	(Torri and Fabbri 2014)
Mixture of cow manure and maize digestate	330, 430, 530	74, 76, 48	Batch	3, 6, 12, 30	-	No	Phenols, PAHs [c]	63% at 330 °C and 12 gCOD/L	(Hübner and Mumme 2015)
Organic fraction of municipal solid waste	450 – 850	20 – 275	Batch	Inoculum:substrate ratio 4:1, 8:1, 16:1, 32:1	-	No	NA [d]	57% at 450 °C and 16:1	(Yang et al. 2018)
Pine wood pellets	400	NA	Continuous	0.25 – 2.5	Biochar addition	No	Substituted phenol (catechol)	34%	(Torri et al. 2020)
Milorganite	800	32 (catalyzed), >200 (non-catalyzed)	Batch	0.06 – 4	NH_3-N stripping	No	High NH_3-N concentration, phenol, ethylbenzene, styrene, xylene, nitrogenous organics	NA	(Seyedi et al. 2019)
Corn stover	500	486	Batch, Step-wise fed-batch	4.9 – 49, 4.9 – 68 [e]	Overliming	No, Yes	Phenol, furan, furfural, creosol	NA	(Zhou et al. 2019)
Swine manure	NA	NA	Batch	NA	Co-digestion with swine manure	No	Phenols	NA	(Yu et al. 2020)
Douglas fir wood	500	NA	Batch	0.01 –0.1 g/L of APL	Pyrolysis feedstock acid-wash	No	Phenol, HAA [f]	NA	(Liaw et al. 2020)

[a] Stoichiometric theoretical methane: 395 mL CH_4 per g COD (1 atm, 35 °C); [b] ThOD: Theoretical oxygen demand (g ThOD/g); [c] PAH: Polycyclic aromatic hydrocarbon
[d] NA: not available; [e] Calculated based on 3% v/v APL equal to 14.58 gCOD/L; [f] HAA: hydroxyacetaldehyde

Table 2.2. Methane yields from AD of HTL-AP under different conditions

HTL feedstock	HTL temperature	HTL-AP COD	AD Operation mode	AD Loading	Co-treatment or Pretreatment	Acclimation	Cause of toxicity	Highest methane yield observed	Reference
-	°C	g/L	-	gCOD/L for batch, gCOD/L_r-d for continuous/semi-continuous	-	-	-	Percent of stoichiometric theoretical methane [a]	-
Rice straw	170 – 320	11 – 29	Batch	0.75	-	No	Furan, ketone, phenol, 5-HMF	90% at 200 °C	(Chen et al. 2017)
Chlorella 1067	300	76	Batch	2 – 5	Zeolite adsorption prior to AD	No	N-heterocyclic compounds, phenols, ketones, alcohols	84% at 4 g/L	(Li et al. 2019)
Dewatered sewage sludge	140 – 320	NA [b]	Batch	0.75	-	No	Humic acid-like, N-heterocyclic and phenols	82% at 170 °C	(Chen et al. 2019)
Algae *Chlorella* and *Tetraselmis*	NA [a]	75 and 85	Semi-continuous	0.8 – 1.5 gVS/L-d (20 – 80% v/v)	Co-digestion with clarified manure	Yes	Pyridine, pyrrolidine, and chloride salts	69% at 26% v/v *Chlorella*, 89% at 22% v/v *Tetraselmis*	(Fernandez et al. 2018)
Rice straw	280	21	Batch, Semi-continuous	0.75, NA	Petroleum ether organic solvent extraction	No	Furan, ketone, phenol	67%, 64%	(Chen et al. 2016)
Swine manure	270	40	Batch	0, 5, 10, 20	GAC [c] addition, ozone pretreatment and combination of GAC and ozone	No	N-heterocyclic and aromatic compounds such as benzoic acid and phenol	62% at 20 gCOD/L with GAC addition	(Si et al. 2019)
Swine manure	NA	104	Batch	3.3 – 66.7% (v/v)	PAC [d] addition	Yes	High NH_3-N concentration, low pH, phenol, nitrophenol, benzene, nitrobenzene, pyridine	53% at 3.3 and 6.7% loading	(Zhou et al. 2015)
Spirulina	300	89	Batch (two rounds of feeding)	7 (SCOD)	GAC, zeolite, polyurethane matrix addition	Yes	Phenol, benzene, N and O heterocyclic organics, straight amides	48% with GAC and polyurethane matrix	(Zheng et al. 2017)
Nannochloropsis	320	97	Batch	1	GAC adsorption prior to AD	No	Nitrogenous organics such as acridine and aromatic amides	24%	(Shanmugam et al. 2017)
Cornstalk	260	76	Continuous	8	-	No	Phenol, 4-ethyl-phenol, N-heterocyclic compounds, 3-hydroxypyridin, and furans	NA (67 – 70% COD removal rate)	(Si et al. 2018)
Mixed-culture algal biomass	260 – 320	30 – 70	Batch	0.04	-	Yes	Cyclic carbohydrates and amines, phenol, ketone, octahydro-1H-indene	NA	(Tommaso et al. 2015)

[a] Stoichiometric theoretical methane: 395 mL CH_4 per g COD (1 atm, 35 °C); [b] NA: not available; [c] Granulated activated carbon; [d] Powdered activated carbon

Analysis to determine the identity and concentration of most or all the constituents in APL and HTL-LP is difficult due to the large number of different complex chemicals that can be present. Si et al. (2019) showed that only a fraction (40 – 70%) of the total organic carbon in HTL-AP was accounted for when employing gas chromatography-mass spectrometry (GC-MS). Seyedi et al. (2019) employed two different GC-MS systems, and two different GC instruments using flame ionization detector (GC-FID), each with different columns to analyze APLs. The total organics identified by GC-MS in different APLs accounted for 55 – 85% of the total COD. When using common GC methods to analyze thermochemical liquids, results may be limited to volatile or semi-volatile compounds, resulting in incomplete identification of non-volatile organics. To obtain a more comprehensive analysis of chemical constituents in aqueous liquids, Black et al. (2016) employed a suite of techniques including aqueous-based gel chromatography, liquid chromatography-mass spectrometry, GC-MS, and elemental analysis to characterize between 75 – 100% of the organics in APL from hardwood biomass (Black et al. 2016). Therefore, more research and better techniques are needed to fully characterize the chemical composition of APL and HTL-AP produced under different conditions.

2.5. APL and HTL-AP toxicity to methanogenesis

2.5.1. Effect of thermochemical process feedstock on APL degradability

Changing the material fed to thermochemical processes significantly changes the aqueous liquid constituents and anaerobic toxicity. Most notably,

nitrogen in feedstocks such as sewage sludge, manure, or algae results in higher concentrations of ammonia-nitrogen (NH_3-N) and nitrogen-containing organics such as pyridine, pyridinol, pyrrole, pyrazine, and aminophenol that are toxic or difficult to degrade in anaerobic digesters (Zhou et al. 2015; Fernandez et al. 2018; Chen et al. 2019; Watson et al. 2020). In contrast, typical lignocellulosic biomass such as corn stalk or rice straw have significantly less nitrogen and result in aqueous liquids with low concentrations of NH_3-N and nitrogenous organics (Si et al. 2019; Watson et al. 2020).

Nitrogen-containing organics such as pyridine and pyrrolidine were reported to cause methane production inhibition or cessation in anaerobic co-digesters fed a mixture of algae-derived HTL-AP and manure (Fernandez et al. 2018). Methane production decreased or stopped when digester feed contained more than approximately 22% (v/v) of nitrogen-rich, algae-derived HTL-AP mixed with manure. Similarly, N-heterocyclic organics along with aromatic compounds such as phenols were reported to inhibit acetogenesis and methane production during AD of HTL-AP from swine manure (Si et al. 2019). Zhou et al. (2015) postulated that no methane was produced in a batch test of HTL-AP since toxic nitrogen-containing organics as well as cyclic hydrocarbons were present. Several organic compounds in APL and HTL-AP such as pyridine and its derivatives have been shown to degrade anaerobically, but at very low rates (Li et al. 2001; Si et al. 2018).

2.5.2. Toxicity of organic constituents

Many organic constituents in the aqueous liquids can be toxic and inhibit anaerobic microorganism activity, including hydrocarbons such as xylene and

ethylbenzene, oxygenated organics such as phenol, acetophenone, catechol, cresol, furan, hydroxymethylfurfural (HMF) and hydroxyacetaldehyde (HAA), and nitrogen-containing compounds such as pyridine, pyrrolidine, 3-hydroxypyridine, pyridinol, and pyrazine (Hübner and Mumme 2015; Black et al. 2016; Seyedi et al. 2019; Yu et al. 2020). Table 2.3 presents the inhibitory concentration of some toxicants to methanogens in terms of IC_{50} (the concentration of a toxicant that inhibits the methane production rate by 50%). Phenolic compounds are toxic to microbial cells by damaging membrane proteins, inactivating cell enzymatic systems and destroying intracellular components (Madigou et al. 2016). Aldehydes exert toxicity by denaturing the polynucleotides and damaging proteins, while furfural and HMF cause mutations in cell DNA (Jayakody et al. 2018; Wen et al. 2020). Nitrogenous compounds from thermochemical feedstocks with high protein content have been reported to adversely affect cell metabolism (Donlon et al. 1995).

Table 2.3. Inhibitory concentrations of some toxicants in APL or HTL-AP expressed in terms of IC_{50}

Compound	**IC_{50} value (mg/L)**
Phenol	2100 [a]
Ethylbenzene	160 [a]
Styrene	150 [b]
m-Xylene	250 [a]
Furfural (2-Furaldehyde)	180 [a]
m,p-Cresol	890 [a], 91 [a]

[a] (Blum and Speece 1991), [b] (Araya et al. 2000)

Typically, constituents are toxic at high concentrations, but not at lower concentrations. For example, Hübner and Mumme (2015) observed methane

production inhibition in batch AD tests using APL derived from pyrolysis of a mix of cow manure and maize digestate. Toxicity of the APL was attributed to phenolics and polycyclic aromatic hydrocarbons (PAHs). Except for cresol, the majority of APL organic compounds were reported to be degraded at digester COD loadings of 3 to 12 gCOD/L. At the very high COD loading of 30 gCOD/L, however, only furfural and 5-HMF were significantly degraded, whereas the remaining constituent removal was less than 30% (Hübner and Mumme 2015). Similarly, Wen et al. (2020) used APL derived from pyrolysis of birch bark at 500 °C as a substrate for AD. At a high APL loading, no methane production was observed, whereas at a loading that was an order of magnitude lower, biogas contained 24% methane. Inhibition at higher loadings was ascribed to the high concentration of total phenolics present in the APL (24 g/kg). In addition to phenolics, HAA was reported as a toxicant in APL derived from pyrolysis of wood biomass at 500 °C (Liaw et al. 2020). Methane production during batch AD tests of APL derived from Douglas Fir wood was reported to be inhibited by the high concentration of HAA. HAA content in APL decreased by 50% (0.24 to 0.12 wt%) when Douglas Fir wood was acid-washed prior to pyrolysis, resulting in higher methane production compared to APL from untreated feedstock. Toxicity may also originate from compounds present in the APL that are undetected by current methods or identified compounds for which anaerobic toxicity has not yet been measured.

Some toxic organic APL and HTL-AP constituents are partially or completely converted to methane when digested at lower, non-toxic concentrations. For example, methane production was 40 to 50% lower in upflow

anaerobic sludge blanket (UASB) and packed bed reactor (PBR) fed HTL-AP from corn stalk pyrolysis when compared to similar systems fed glucose (Si et al. 2018). While vanillin, furan and 5-HMF were reported to be fully degraded, 3-hydroxypyridine, phenol, and 4-ethyl-phenol were partially degraded (54 – 75%). The toxicity of constituents such as phenolic compounds can be reduced as biomass is exposed to the chemicals over a long period to acclimate, increasing microbial tolerance (Madigou et al. 2016).

2.5.3. Toxicity of inorganic constituents

APL and HTL-AP constituents including NH_3-N, and hydrogen (H^+) or hydroxide (OH^-) can inhibit methane production. NH_3-N concentrations higher than about 3 to 5 g/L NH_3-N (at neutral pH and 35 °C) results in reduced methanogenic activity of unacclimated microbes (Speece 1996). High NH_3-N concentrations result from pyrolysis feedstocks with a high concentration of nitrogenous compounds such as proteins and amino acids. For example, APL from pyrolysis of wastewater solids contained a high NH_3-N concentration (>60 g/L), which was toxic (Seyedi et al. 2019, 2020). Zhou et al. (2015) observed total cessation of methane production at high loadings of 33.3 and 66.7% (v/v) HTL-AP that may have been due to high NH_3-N (1.9 and 2.7 g/L in the reactor).

H^+ or OH^- ion (i.e., pH) toxicity to anaerobic microbes results from extremely acidic or alkaline aqueous liquids. AD typically requires pH values between 6.5 and 8.3 for biological activity (Speece 2008). Yang et al. (2018) showed that the higher the pyrolysis temperature and feedstock moisture, the higher the pH of the resulting APL, because the production of basic chemicals is promoted. In contrast,

some APLs have very low pH values due to high concentrations of volatile fatty acids (VFA) and other organic acids. APL derived from corn stover pyrolysis at less than 500 °C had pH of 2 and total VFA concentration of 46 g/L (Zhou et al. 2019). The authors mentioned that the high concentration of VFAs can inhibit methanogenesis and cause AD failure (Zhou et al. 2019).

2.5.4. Effect of thermochemical process temperature and condition and aqueous liquid organic loading on methane production

Yang et al. (2018) described pyrolysis temperature and APL loading as the dominant factors governing APL toxicity in AD. The APL toxicity typically increases with increased process temperature. The IC_{50} concentration decreased from 5.4 to 0.5 gCOD/L of the APL when the pyrolysis temperature of the organic fraction of municipal solid waste increased from 450 °C to 850 °C (Yang et al. 2018). In another study, Hübner and Mumme (2015) observed that methane production from APL derived from a mixture of cow manure and maize digestate decreased as pyrolysis temperature increased from 330 C (200 mL CH_4/gCOD) to 530°C (130 mL CH_4/gCOD). Toxicity also increases with increased toxicant concentration or a related increased AD OLR. Torri et al. (2020) investigated AD of APL produced from pyrolysis of commercial pine wood pellets at 400 °C in a UASB with biochar addition in an attempt to reduce the toxic effect of APL. At 0.25 gCOD/L_r-day, complete conversion of APL to methane was observed. However, when the OLR was increased to 1.25 gCOD/L_r-day, conversion of APL to methane declined by 30 to 70%. Some compounds (1,6-anhydro-b-glucopyranose) were completely removed, but some recalcitrant compounds were not degraded efficiently (e.g., catechol removal was 11%). Under the conditions studied, approximately 45% of

the APL carbon was reported to be undegradable (Torri et al. 2020). Yu et al. (2020) evaluated batch anaerobic co-digestion of swine manure mixed with APL diluted in water (5, 50, and 100 times dilution). Methane production was inhibited when the more concentrated APL was added (5 times diluted), producing only 23% of the methane produced in control digesters fed swine manure alone. In contrast, co-digesters receiving 50 and 100 times diluted APL generated about 22 and 13% more methane compared to control digesters.

Similar trends were observed during HTL-AP digestion in different studies using various feedstocks and process conditions, as shown in Figure 2.4. Posmanik et al. (2017) showed that while higher HTL temperature leads to more biocrude oil production from different model feedstocks (carbohydrate, protein, lipid), the HTL-AP resulting at higher temperatures exhibited significantly lower methane yield from AD. The authors attributed the lower methane yield to the increased formation of refractory compounds at higher temperature. Chen et al. (2017) reported 62% and 89% conversion to methane in batch tests using HTL-AP from rice straw at 320 °C – 0.5 h (217 mL CH_4/gCOD) and 200 °C - 0.5 h (314 mL CH_4/gCOD), respectively, signifying that as HTL temperature increased, lower methane yield was obtained.

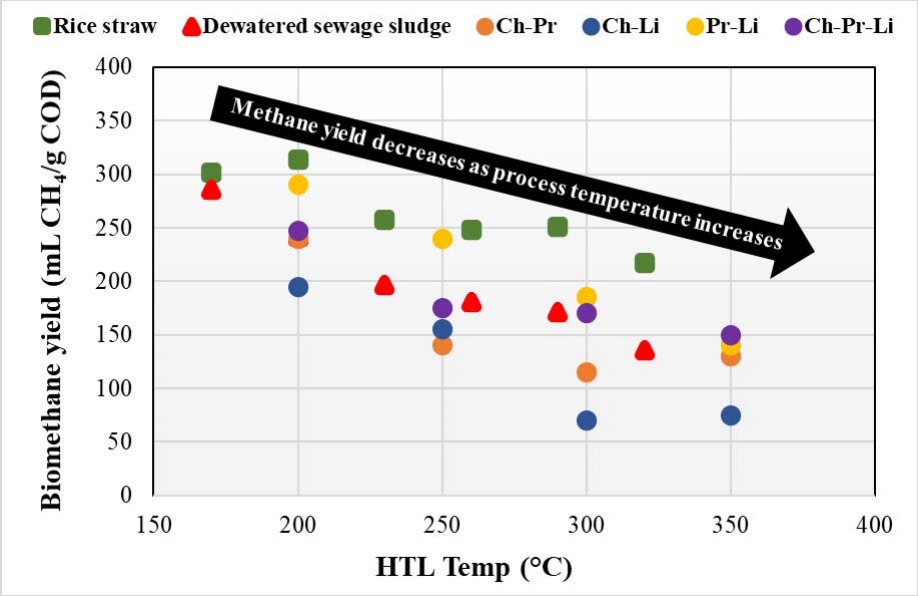

Figure 2.4. Biomethane production decrease during AD of HTL-AP with increasing temperatures using different feedstocks. AD of HTL-AP from rice straw under 170 – 320 °C (Chen et al., 2017). AD of HTL-AP of dewatered sewage sludge under 140 – 320 °C (Chen et al., 2019). AD of HTL-AP from a mixture of different model feedstocks at 200 – 350 °C (carbohydrate (Ch), protein (Pr), and lipid (Li)) (Posmanik et al., 2017).

Si et al. (2019) investigated the effect of different HTL-AP COD loadings on methane production in anaerobic batch tests; the HTL-AP was from swine manure processed at 270 °C. Increased COD loading from 5 to 20 gCOD/L reduced methane production substantially, from approximately 216 to 50 mL CH_4/gCOD. In another study, batch anaerobic experiments were performed at 0.75 gCOD/L using HTL-AP derived from dewatered sewage sludge processed under a range of temperatures and residence times of 140 – 320 °C and 0.5 – 6 h, respectively (Chen et al. 2019). Increased temperature and residence time led to decreased methane production from 286 to 136 mL CH_4/g COD with HTL-AP at 170 °C and 320 °C, respectively, and from 242 to 161 mL CH_4/g COD when residence time increased from 0.5 – 6 h (using 200 °C HTL-AP) (Chen et al. 2019). NH_3-N

concentration and pH of HTL-AP increased with increased temperature. Elevated content of constituents that can be toxic to methanogenic organisms, including phenols and nitrogenous organics such as pyridine and pyrazines, were detected in HTL-AP by GC-MS analysis at higher temperature. Methane production during AD of HTL-AP derived from wastewater commenced immediately when the HTL-AP temperature was lower (260 and 280 °C), whereas a 4.6-d lag time occurred when digesting ATL-AP produced at a higher temperature (360°C) (Tommaso et al. 2015).

The conditions under which pyrolysis of a given biomass is achieved can also significantly influence the anaerobic toxicity of the resulting APL. For example, Seyedi et al. (2019) compared AD of APL produced from conventional and autocatalytic pyrolysis of the same wastewater solids at 800 °C. Methane production was sustained in anaerobic systems fed conventional APL at COD loadings up to 0.5 gCOD/L, whereas no production was observed in anaerobic systems fed catalyzed APL at organic loadings of only 0.10 gCOD/L. Therefore, pyrolysis conditions (conventional or catalyzed) influenced subsequent APL anaerobic digestibility.

2.6. Pretreatment and co-treatment to compliment AD

Pretreatments or co-treatments have been investigated to remove toxic constituents and enhance APL and HTL-AP anaerobic degradability. Treatments studied include air stripping, solvent extraction, adsorption (activated carbon, biochar and zeolite), partial chemical oxidation (ozone, Fenton’s reagent, and

chlorine), overliming and acid pre-treatment of woody thermochemical feedstock. Air stripping reduced high NH_3-N concentrations in APLs produced from wastewater solids (Seyedi et al. 2019). An NH_3-N concentration decrease of 80% resulted in a 200% decrease in APL toxicity measured by IC_{50} value (from 0.3 to 0.9 gCOD/L); however, inhibition was still observed, indicating NH_3-N was not the only inhibitory constituent. Solvent extraction using petroleum ether was applied to HTL-AP from rice straw at 280 °C and 12 MPa and resulted in >20% increase in methane production (184 to 235 mLCH_4/gCOD) (Chen et al. 2016). The higher methane yield was assumed to be due to extraction of compounds that were toxic such as furans, ketones, and phenols.

Adsorbents such as granular activated carbon (GAC), powdered activated carbon (PAC) and zeolite have been contacted either with APL or HTL-AP prior to AD (i.e., pretreatment) or have been added directly to the anaerobic digesters (i.e., co-treatment). Results using pretreatment have varied, but most reports demonstrate improved digestion. Shanmugam et al. (2017) pretreated HTL-AP from algae by GAC adsorption at different levels (3 – 30% w/w GAC addition) prior to AD. Phenolics concentration decreased by 97% when treated with 30% (w/w) GAC for 1 h, whereas, using 3, 10, and 20% (w/w) GAC, phenolics decreased 24, 58, and 84%, respectively. Methane production in batch AD tests increased with increasing GAC addition; with 30% (w/w) GAC pretreatment, methane production was more than 160% greater (84 mL CH_4/gCOD) than that in non-treated controls (32 mL CH_4/gCOD). In a similar study, pretreatment using zeolite sorption mitigated toxicity exerted by nitrogenous organics and NH_3-N during batch AD of

HTL-AP from microalgae *Chlorella 1067* at 300 °C and 2 MPa (Li et al. 2019). Using zeolite-pretreated HTL-AP increased methane yield by 32 – 117% compared to raw HTL-AP. In contrast, when others contacted APL with activated carbon to remove phenolic content, methane production did not increase (Liaw et al. 2020).

In addition to pretreatment, co-treatment with sorbents that are added directly to the anaerobic digester has also been investigated. PAC was employed to co-treat HTL-AP from swine manure. When PAC was added directly to batch anaerobic digesters, methane production increased (Zhou et al. 2015). In a similar study, GAC and zeolite added directly to anaerobic digesters processing HTL-AP from *Spirulina* at 300 °C and 8 – 9 MPa increased methane production by 37% (169 mL CH_4/gCOD) and 11% (136 mL CH_4/gCOD) compared to untreated controls (122 mL CH_4/gCOD), respectively (Zheng et al. 2017).

Besides activated carbon, others have added biochar to anaerobic digesters to adsorb toxic constituents or otherwise increase biogas production. Torri and Fabbri (2014) added biochar during AD of APL from corn stalk pyrolysis at 400°C. Biochar addition (biochar:substrate ratio of 1:1) resulted in a doubling of the methane yield, which increased to 60% of the maximum theoretical amount. In addition, semi-continuous digestion of APL with biochar addition increased methane production to 65% of the maximum theoretical value (Torri and Fabbri 2014). Wen et al. (2020) also observed that biochar addition increased methane production in batch AD tests of APL from birch bark pyrolysis at 500 °C.

Pretreatment using chemical oxidation has been investigated to oxidize or partially oxidize APL and HTL-AP constituents in an attempt to reduce the

concentration of chemicals toxic to methanogenic organisms or to render the remaining organics more amenable to anaerobic biodegradation. For example, both ozone pretreatment and GAC pretreatment were incorporated as possible methods to increase anaerobic conversion efficiency in batch digestion tests of HTL-AP from swine manure under 270 °C (Si et al. 2019). Both ozone and GAC resulted in increased methane production, with methane yield increases of approximately 100% (approximately 110 mL CH_4/gCOD) and 300% (212 mL CH_4/gCOD), respectively. However, combined ozone/GAC treatment was no more effective than GAC treatment alone. Zhou et al. (2019) studied different APL pretreatments including partial oxidation with Fenton's reagent or sodium hypochlorite as well as overliming and activated carbon adsorption to reduce the toxicity of APL derived from pyrolysis of corn stover at 500 °C. Overliming, involving addition of $Ca(OH)_2$ powder (11 g) to 100 mL of the APL to reach a pH of 10, was most effective and increased biogas production. Semi-continuous digestion using the overlimed APL resulted in a 70% increase in biogas production rate when APL loading was increased from 6% to 18%, but biogas yield decreased and eventually stopped at higher organic loadings (>18%).

Others have investigated pretreatment of the thermochemical feedstock instead of the APL and HTL-AP products. Pretreatment of wood biomass with 10% acetic acid at 90 °C for 10 min prior to pyrolysis with the intent to remove the alkaline content from the wood biomass resulted in lower concentrations of inhibitory HAA in the resulting APL (Liaw et al. 2020). Methane production from APL derived from acetic acid-treated biomass was 2.8 times higher than that

derived from untreated feedstock.

2.7. Microbes and acclimation to improve AD

Pure cultures of facultative microbes have been investigated for their ability to tolerate and degrade toxic organic compounds in thermochemical aqueous liquids. Jayakody et al. (2018) engineered a soil bacterium, *Pseudomonas putida KT2440*, to partially overcome APL toxicity and produce value-added chemicals. Nelson et al. (2013) investigated the use of HTL-AP in growth media for three different microorganisms; *Escherichia coli, Pseudomonas putida, and Saccharomyces cerevisiae.* The highest growth for *E. coli* and *P. putida* was observed using 20% vol HTL-AP as the sole C, N, and P source in the media. However, glucose addition was necessary in case of *S. cerevisiae*.

In mixed cultures such as in AD, microorganisms involved in degrading common fermentation inhibitors present in APL and HTL-AP such as furfural, phenol, and pyridine, as well as their anaerobic biodegradation routes have been reported previously. Furfural is initially converted to furfuryl alcohol which can be oxidized further to furoic acid (Rivard and Grohmann 1991; Ran et al. 2014). Furoic acid is fermented to acetate that is converted to methane by acetoclastic methanogens. *Pseudomonas sp.* and *Desulfovibrio sp*. are capable of degrading furfural under anaerobic conditions (Wierckx et al. 2011; Si et al. 2018). Phenol degradation by *Geobacter sp.* was proposed to be initiated by production of benzoyl-coenzyme A from phenol, which is an intermediate from anaerobic biodegradation of phenol (Fuchs et al. 2011). Subsequently, the β-oxidation ring

opening and the aromatic ring reduction are performed through either ATP-independent or ATP-dependent pathways. Finally, three molecules of acetyl-CoA are generated which can be converted to methane by methanogens (Fuchs et al. 2011). Another bacterium reported to be responsible for phenol conversion is *Syntrophorhabdus*, which was detected in AD of HTL-AP (Chen et al. 2017). Pyridine degradation involving *Bacillus sp.* is thought to start with ring cleavage through a 1,4-dihydropyridine intermediate (Watson and Caint 1975). This step results in release of formamide and succinic semialdehyde, and eventually formic and succinic acid generation. Methane production from succinic acid is carried out by acetogens and methanogens. *Methanobacterium* can also convert formic acid directly to methane (Watson and Caint 1975). A deeper understanding of microbes able to ferment compounds in APL and HTL-AP is needed to adopt specific microbial strategies such as bioaugmentation with specific strains, or to select the most appropriate anaerobic seed biomass.

One approach to ameliorate aqueous liquid toxicity in AD is to enhance microbial robustness by acclimating microorganisms to the existing constituents. Anaerobic digesters have a complex consortium of microorganisms that has been shown to acclimate to toxic compounds such as phenols when exposed to the chemicals over a long time (Madigou et al. 2016). Acclimation to APL constituents has also been reported previously in continuous or semi-continuous digestion studies (Zhou et al. 2019; Seyedi et al. 2020). Seyedi et al. (2020) reported doubling of biomass tolerance to APL due to acclimation in a long-term co-digestion study (>500 days) (See Appendix B). Zhou et al. (2019) performed

stepwise AD referred to as “directed evolution” to increase the tolerance of the microbial community by gradually increasing loading rates of overlimed APL. Acclimation increased the microbes’ tolerance to APL when increasing the overlimed APL loading from 5% to 14% (v/v) of APL.

Acclimation has also been observed in batch AD experiments. In a batch study, after an initial lag phase, the methane production increased by 57% percent compared to inhibited systems during AD of HTL-AP from algae (Tommaso et al. 2015). Zhou et al. (2015) also observed a long lag phase during batch AD of HTL-AP from swine manure at loadings 13.3 and 26.7% (v/v), followed by increased biogas production, indicating acclimation of the microbial culture.

Investigating and monitoring shifts in microbial communities is helpful to recognize microbes associated with degrading the inhibitory compounds and to identify the taxa that are enriched for during digestion of aqueous liquids. However, not many studies have conducted microbial community analysis of digesters receiving APL and HTL-AP. Also, due to the varying composition of aqueous liquids from different sources, the enriched AD microbial community structures could vary. Since archaea are less diverse than bacteria in AD, the presence of toxicants in the majority of thermochemical aqueous streams may affect archaeal communities more significantly than bacterial community.

2.7.1. Bacterial community

Bacterial populations in methanogenic systems fed APL or HTL-AP have been shown to contain taxa that degrade phenols and other aromatics as well as furfural and N-heterocyclic compounds. For example, *Syntrophohabdus* was more

abundant in digesters fed APL rich in phenols, whereas *Proteobacteria* were observed as the dominant taxa in digesters fed APL containing high sugar content. Similarly, the relative abundance of *Syntrophorhabdus* capable of phenol degradation and *Geobacter* and *Desulfovibrio* capable of aromatics and phenols degradation increased during continuous digestion of HTL-AP from corn stalks produced at 260 °C (Si et al. 2018). Increased relative abundance values of families *Anaerolineaceae*, *Burkholderiaceae* and *Peptococcaceae*, which are associated with phenolics degradation and crude oil remediation, were observed during AD of HTL-AP from corn stalk (Si et al. 2019). The relative abundance of *Pseudomonas* that can degrade furfural and N-heterocyclic compounds increased in methanogenic systems fed HTL-AP derived from dewatered sewage sludge (Chen et al. 2019).

2.7.2. Archaeal community

Regarding methanogens, AD of APL and HTL-AP typically results in increased hydrogenotrophic methanogen abundance with a concomitant decrease in acetoclastic methanogen abundance. For example, archaeal shifts during AD of the aqueous liquids showed enrichment for the hydrogenotrophic population, probably because hydrogenotrophic methanogens are more tolerant under extreme conditions compared to acetoclastic methanogens (Demirel and Scherer 2008). A concomitant increase in relative abundance of syntrophic bacteria was also observed. Similarly, hydrogenotrophic *Methanobrevibacter and Methanoculleus* were dominant over the acetoclastic methanogens during batch AD of HTL-AP from rice straw (Chen et al. 2017). Microbial community analysis of

anaerobic digesters fed overlimed-APL after acclimation also indicated that the hydrogenotrophic methanogenesis pathway was selected for over the acetoclastic pathway (Zhou et al. 2019). Si et al. (2019) observed increased hydrogenotrophic methanogen relative abundance along with syntrophic bacteria, while acetoclastic *Methanosaeta* decreased in abundance in GAC-assisted batch AD tests degrading HTL-AP from swine manure. Co-digestion of APL with synthetic primary sludge led to reduction in acetoclastic *Methanosaeta*, whereas an unknown archaea assumed to be a hydrogenotrophic methanogen was observed concurrently with syntrophic bacteria belonging to *Syntrophomonadaceae* and *Synergistaceae* (Seyedi et al. 2020) (See Appendix B).

When considering the acetoclastic methanogens alone, *Methanosarcina* were more abundant when degrading APL and HTL-AP than *Methanosaeta* probably since *Methanosarcina* are more tolerant of toxicants and metabolically versatile, able to perform both acetoclastic and hydrogenotrophic methanogenesis (Chen et al. 2017; Fernandez et al. 2018).

2.8. Outlook and conclusions

Currently, APL and HTL-AP are considered waste streams and can restrict the feasible implementation of pyrolysis and HTL of wastewater sludge. AD may be an attractive pathway to recover the energy in APL and HTL-AP since it produces energy-rich biogas. However, knowledge of the exact composition of APL and HTL-AP produced under different conditions is lacking. Research to identify and measure the majority of constituents in thermochemical liquids is

warranted to better characterize these liquids for valorization. Complete anaerobic degradation of APL and HTL-AP in their raw forms is not easily accomplished and successful anaerobic degradation may require pretreatment before adding APL or HTL-AP to anaerobic digesters.

Integrating AD and thermochemical processes may be a feasible approach that could promote a circular economy by developing resource recovery, reducing environmental pollution, and improving sustainable development. While APL and HTL-AP encompass high energy potential to be recovered, toxic organics present in them inhibit anaerobic microorganisms and make AD challenging. When integrating AD and thermochemical processes, the thermochemical operating conditions greatly influence the anaerobic biodegradability of the resulting aqueous liquids. For example, thermochemical processes at lower temperatures and shorter retention times typically produce liquids with lower toxicity for AD (Chen et al. 2017, 2019). However, higher temperatures produce more py-gas and bio-crude oil for fuel. When wastewater management scenarios are considered at water reclamation facilities it may be beneficial to balance pyrolysis conditions with product toxicity if all processing is to be conducted at the facility. However, if maximizing bio-oil production is the overarching goal, then this balance may not be as critical.

The identity of the feedstock used in pyrolysis and HTL is also an important factor to consider since the compounds formed in the aqueous liquids are dependent upon the feedstock composition. Notably, feedstocks high in nitrogen, such as some sewage sludges, result in more toxic aqueous liquids due to the

presence of NH_3-N and nitrogenated organics. It may be prudent to consider pyrolysis or HTL of a mix of sewage sludge along with cellulosic material to reduce the concentration of NH_3-N and nitrogenated organics while increasing overall fuel production. Alternatively, pretreatment to remove NH_3-N from APL and HTL-AP prior to AD may be warranted.

In the future, full-scale approaches to mitigate or reduce the toxicity of APL and HTL-AP and enhance methane production from AD may also include utilizing adsorbents such as activated carbon or biochar in the digester to adsorb toxicants, pretreatment prior to AD such as ozonation or overliming, as well as feedstock pretreatment. More research is warranted to develop adsorption and pretreatment methods to enhance methane production. Co-digesting APL and HTL-AP with other organic feedstock is another option to consider. An extensive techno-economic analysis on feasibility of APL and HTL-AP anaerobic digestion and the surveyed toxicity reduction strategies is required and should be performed in the future to provide guidance for decision making regarding the best options for commercial-scale implementation.

Enhancing the AD microbial tolerance by acclimating the microorganisms to the APL and HTL-AP constituents or using suitable seed biomass is another approach that requires more research. Preliminary studies have shown that when the microbial consortium is adapted, APL and HTL-AP digestion is possible (Righi et al. 2016; Zhou et al. 2019; Seyedi et al. 2020). Not many studies have examined the microbial community composition and shifts in the composition when thermochemical aqueous liquids are continuously digested. Future research is

required to identify the appropriate microorganisms capable of tolerating and degrading the complex compounds in thermochemical liquids. Bioaugmentation or use of specific seed culture may be an appropriate method to increase methane production.

2.9. References

Araya P, Chamy R, Mota M, Alves M (2000) Biodegradability and toxicity of styrene in the anaerobic digestion process. Biotechnol Lett 22:1477–1481. https://doi.org/10.1023/A:1005636030693

Arturi KR, Kucheryavskiy S, Søgaard EG (2016) Performance of hydrothermal liquefaction (HTL) of biomass by multivariate data analysis. Fuel Process Technol 150:94–103. https://doi.org/10.1016/j.fuproc.2016.05.007

Black BA, Michener WE, Ramirez KJ, et al (2016) Aqueous Stream Characterization from Biomass Fast Pyrolysis and Catalytic Fast Pyrolysis. https://doi.org/10.1021/acssuschemeng.6b01766

Blum DJW, Speece RE (1991) A database environmental interspecies of chemical bacteria to toxicity in and its use and correlations comparisons. Water Environ Fed 63:198–207

Cantero-Tubilla B, Cantero DA, Martinez CM, et al (2018) Characterization of the solid products from hydrothermal liquefaction of waste feedstocks from food and agricultural industries. J Supercrit Fluids 133:665–673. https://doi.org/10.1016/j.supflu.2017.07.009

Cao Y, Pawłowski A (2012) Sewage sludge-to-energy approaches based on anaerobic digestion and pyrolysis: Brief overview and energy efficiency assessment. Renew Sustain Energy Rev 16:1657–1665. https://doi.org/10.1016/j.rser.2011.12.014

Carey DE, McNamara PJ, Zitomer DH (2015) Biochar from Pyrolysis of Biosolids for Nutrient Adsorption and Turfgrass Cultivation. Water Environ Res 87:2098–2106. https://doi.org/10.2175/106143015x14362865227391

Chen H, Rao Y, Cao L, et al (2019) Hydrothermal conversion of sewage sludge: Focusing on the characterization of liquid products and their methane yields. Chem Eng J 357:367–375. https://doi.org/10.1016/j.cej.2018.09.180

Chen H, Wan J, Chen K, et al (2016) Biogas production from hydrothermal liquefaction wastewater (HTLWW): Focusing on the microbial communities as revealed by high-throughput sequencing of full-length 16S rRNA genes. Water Res 106:98–107. https://doi.org/10.1016/j.watres.2016.09.052

Chen H, Zhang C, Rao Y, et al (2017) Methane potentials of wastewater generated from hydrothermal liquefaction of rice straw: Focusing on the wastewater characteristics and microbial community compositions. Biotechnol Biofuels 10:1–16. https://doi.org/10.1186/s13068-017-0830-0

Cheng J-R, Liu X-M, Chen Z-Y, et al (2016) A novel mesophilic anaerobic digestion system for biogas production and in situ methane enrichment from coconut shell pyroligneous. Appl Biochem Biotechnol 178:1303–1314

Cordova LT, Lad BC, Ali SA, et al (2020) Valorizing a hydrothermal liquefaction

aqueous phase through co-production of chemicals and lipids using the oleaginous yeast Yarrowia lipolytica. Bioresour Technol 313:123639. https://doi.org/10.1016/j.biortech.2020.123639

Demirel B, Scherer P (2008) The roles of acetotrophic and hydrogenotrophic methanogens during anaerobic conversion of biomass to methane: A review. Rev. Environ. Sci. Biotechnol. 7:173–190

Donlon BA, Eli´ E, Razo-Flores E, et al (1995) Toxicity of N-Substituted Aromatics to Acetoclastic Methanogenic Activity in Granular Sludge

Fabbri D, Torri C (2016) Linking pyrolysis and anaerobic digestion (Py-AD) for the conversion of lignocellulosic biomass. Curr Opin Biotechnol 38:167–173. https://doi.org/10.1016/j.copbio.2016.02.004

Feng Q, Lin Y (2017) Integrated processes of anaerobic digestion and pyrolysis for higher bioenergy recovery from lignocellulosic biomass: A brief review. Renew Sustain Energy Rev 77:1272–1287. https://doi.org/10.1016/j.rser.2017.03.022

Fernandez S, Srinivas K, Schmidt AJ, et al (2018) Anaerobic digestion of organic fraction from hydrothermal liquefied algae wastewater byproduct. Bioresour Technol 247:250–258. https://doi.org/10.1016/j.biortech.2017.09.030

Fonts I, Gea G, Azuara M, et al (2012) Sewage sludge pyrolysis for liquid production: A review. Renew Sustain Energy Rev 16:2781–2805. https://doi.org/10.1016/j.rser.2012.02.070

Fuchs G, Boll M, Heider J (2011) Microbial degradation of aromatic compounds-From one strategy to four. Nat Rev Microbiol 9:803–816. https://doi.org/10.1038/nrmicro2652

Gai C, Zhang Y, Chen WT, et al (2015) Characterization of aqueous phase from the hydrothermal liquefaction of Chlorella pyrenoidosa. Bioresour Technol 184:328–335. https://doi.org/10.1016/j.biortech.2014.10.118

Gollakota ARK, Kishore N, Gu S (2018) A review on hydrothermal liquefaction of biomass. Renew. Sustain. Energy Rev. 81:1378–1392

Hübner T, Mumme J (2015) Integration of pyrolysis and anaerobic digestion – Use of aqueous liquor from digestate pyrolysis for biogas production. Bioresour Technol 183:86–92. https://doi.org/10.1016/j.biortech.2015.02.037

Jarboe LR, Wen Z, Choi D, Brown RC (2011) Hybrid thermochemical processing: Fermentation of pyrolysis-derived bio-oil. Appl Microbiol Biotechnol 91:1519–1523. https://doi.org/10.1007/s00253-011-3495-9

Jayakody LN, Johnson CW, Whitham JM, et al (2018) Thermochemical wastewater valorization: Via enhanced microbial toxicity tolerance. Energy Environ Sci 11:1625–1638. https://doi.org/10.1039/c8ee00460a

Kappell AD, Kimbell LK, Seib MD, et al (2018) Removal of antibiotic resistance genes in an anaerobic membrane bioreactor treating primary clarifier effluent at 20 °C. Environ Sci Water Res Technol 4:1783–1793.

https://doi.org/10.1039/c8ew00270c

Kumar M, Olajire Oyedun A, Kumar A (2018) A review on the current status of various hydrothermal technologies on biomass feedstock. Renew. Sustain. Energy Rev. 81:1742–1770

Leng L, Zhou W (2018) Chemical compositions and wastewater properties of aqueous phase (wastewater) produced from the hydrothermal treatment of wet biomass: A review. ENERGY SOURCES, PART A Recover Util Environ Eff 40:2648–2659

Li H, Feng K (2018) Life cycle assessment of the environmental impacts and energy efficiency of an integration of sludge anaerobic digestion and pyrolysis. J Clean Prod 195:476–485. https://doi.org/10.1016/j.jclepro.2018.05.259

Li R, Liu D, Zhang Y, et al (2019) Improved methane production and energy recovery of post-hydrothermal liquefaction waste water via integration of zeolite adsorption and anaerobic digestion. Sci Total Environ 651:61–69. https://doi.org/10.1016/j.scitotenv.2018.09.175

Li Y, Gu G, Zhao J, Yu H (2001) Anoxic degradation of nitrogenous heterocyclic compounds by acclimated activated sludge. Process Biochem 37:81–86. https://doi.org/10.1016/S0032-9592(01)00176-5

Liaw S-S, Perez VH, Westerhof R, et al (2020) Biomethane Production from Pyrolytic Aqueous Phase: Biomass Acid Washing and Condensation Temperature Effect on the Bio-oil and Aqueous Phase Composition. BioEnergy Res

Liu Z, Mayer BK, Venkiteshwaran K, et al (2020) The state of technologies and research for energy recovery from municipal wastewater sludge and biosolids. Curr. Opin. Environ. Sci. Heal. 14:31–36

Liu Z, McNamara P, Zitomer D (2017) Autocatalytic Pyrolysis of Wastewater Biosolids for Product Upgrading. Environ Sci Technol 51:9808–9816. https://doi.org/10.1021/acs.est.7b02913

Liu Z, Singer S, Tong Y, et al (2018) Characteristics and applications of biochars derived from wastewater solids. Renew Sustain Energy Rev 90:650–664. https://doi.org/10.1016/j.rser.2018.02.040

López Barreiro D, Prins W, Ronsse F, Brilman W (2013) Hydrothermal liquefaction (HTL) of microalgae for biofuel production: State of the art review and future prospects. Biomass and Bioenergy 53:113–127. https://doi.org/10.1016/j.biombioe.2012.12.029

Lü F, Hua Z, Shao L, He P (2018) Loop bioenergy production and carbon sequestration of polymeric waste by integrating biochemical and thermochemical conversion processes: A conceptual framework and recent advances. Renew. Energy 124:202–211

Maddi B, Panisko E, Wietsma T, et al (2017) Quantitative Characterization of Aqueous Byproducts from Hydrothermal Liquefaction of Municipal Wastes,

Food Industry Wastes, and Biomass Grown on Waste. https://doi.org/10.1021/acssuschemeng.6b02367

Madigou C, Poirier S, Bureau C, Chapleur O (2016) Acclimation strategy to increase phenol tolerance of an anaerobic microbiota. Bioresour Technol 216:77–86. https://doi.org/10.1016/j.biortech.2016.05.045

Monlau F, Sambusiti C, Antoniou N, et al (2015) A new concept for enhancing energy recovery from agricultural residues by coupling anaerobic digestion and pyrolysis process. Appl Energy 148:32–38. https://doi.org/10.1016/j.apenergy.2015.03.024

Mukarakate C, Evans RJ, Deutch S, et al (2017) Reforming Biomass Derived Pyrolysis Bio-oil Aqueous Phase to Fuels. Energy and Fuels 31:1600–1607. https://doi.org/10.1021/acs.energyfuels.6b02463

Nelson M, Zhu L, Thiel A, et al (2013) Microbial utilization of aqueous co-products from hydrothermal liquefaction of microalgae Nannochloropsis oculata. Bioresour Technol 136:522–528. https://doi.org/10.1016/j.biortech.2013.03.074

Pecchi M, Baratieri M (2019) Coupling anaerobic digestion with gasification, pyrolysis or hydrothermal carbonization: A review. Renew Sustain Energy Rev 105:462–475. https://doi.org/10.1016/j.rser.2019.02.003

Pokorna E, Postelmans N, Jenicek P, et al (2009) Study of bio-oils and solids from flash pyrolysis of sewage sludges. Fuel 88:1344–1350. https://doi.org/10.1016/j.fuel.2009.02.020

Posmanik R, Labatut RA, Kim AH, et al (2017) Coupling hydrothermal liquefaction and anaerobic digestion for energy valorization from model biomass feedstocks. Bioresour Technol 233:134–143. https://doi.org/10.1016/j.biortech.2017.02.095

Righi S, Bandini V, Marazza D, et al (2016) Life Cycle Assessment of high ligno-cellulosic biomass pyrolysis coupled with anaerobic digestion. Bioresour Technol 212:245–253. https://doi.org/10.1016/j.biortech.2016.04.052

Rivard C j., Grohmann karel (1991) Degradation of furfural (2- furaldehyde) to methane and carbon dioxide by an anaerobic consortium. Appl Biochem Biotechnol 28–29:285–295. https://doi.org/10.1007/BF02922608

Ross JJ, Zitomer DH, Miller TR, et al (2016) Emerging investigators series: Pyrolysis removes common microconstituents triclocarban, triclosan, and nonylphenol from biosolids. Environ Sci Water Res Technol 2:282–289. https://doi.org/10.1039/c5ew00229j

Seiple TE, Coleman AM, Skaggs RL (2017) Municipal wastewater sludge as a sustainable bioresource in the United States. J Environ Manage 197:673–680. https://doi.org/10.1016/j.jenvman.2017.04.032

Seyedi S (2018) Anaerobic Co-digestion of Aqueous Liquid from Biosolids Pyrolysis. Master's Thesis. Marquette University. Milwaukee, WI. USA

Seyedi S, Venkiteshwaran K, Benn N, Zitomer D (2020) Inhibition during Anaerobic Co-Digestion of Aqueous Pyrolysis Liquid from Wastewater Solids and Synthetic Primary Sludge. Sustainability 12:3441. https://doi.org/10.3390/su12083441

Seyedi S, Venkiteshwaran K, Zitomer D (2019) Toxicity of Various Pyrolysis Liquids From Biosolids on Methane Production Yield. Front Energy Res 7:1–12. https://doi.org/10.3389/fenrg.2019.00005

Shanmugam SR, Adhikari S, Wang Z, Shakya R (2017) Treatment of aqueous phase of bio-oil by granular activated carbon and evaluation of biogas production. Bioresour Technol 223:115–120. https://doi.org/10.1016/j.biortech.2016.10.008

Si B, Li J, Zhu Z, et al (2018) Inhibitors degradation and microbial response during continuous anaerobic conversion of hydrothermal liquefaction wastewater. Sci Total Environ 630:1124–1132. https://doi.org/10.1016/j.scitotenv.2018.02.310

Si B, Yang L, Zhou X, et al (2019) Anaerobic conversion of the hydrothermal liquefaction aqueous phase: Fate of organics and intensification with granule activated carbon/ozone pretreatment. Green Chem 21:1305–1318. https://doi.org/10.1039/c8gc02907e

Skaggs RL, Coleman AM, Seiple TE, Milbrandt AR (2017) Waste-to-Energy biofuel production potential for selected feedstocks in the conterminous United States. Renew Sustain Energy Rev 82:2640–2651. https://doi.org/10.1016/j.rser.2017.09.107

Speece RE (2008) Anaerobic Biotechnology and Odor/Corrosion Control for Municipalities and Industries. Archae Press, Nashville, TN

Speece RE (1996) Anaerobic Biotechnology for Industrial Wastewaters. Archae Press, Nashville, TN

Syed-Hassan SSA, Wang Y, Hu S, et al (2017) Thermochemical processing of sewage sludge to energy and fuel: Fundamentals, challenges and considerations. Renew. Sustain. Energy Rev. 80:888–913

Tommaso G, Chen WT, Li P, et al (2015) Chemical characterization and anaerobic biodegradability of hydrothermal liquefaction aqueous products from mixed-culture wastewater algae. Bioresour Technol 178:139–146. https://doi.org/10.1016/j.biortech.2014.10.011

Torri C, Fabbri D (2014) Biochar enables anaerobic digestion of aqueous phase from intermediate pyrolysis of biomass. Bioresour Technol 172:335–341. https://doi.org/10.1016/j.biortech.2014.09.021

Torri C, Pambieri G, Gualandi C, et al (2020) Evaluation of the potential performance of hyphenated pyrolysis-anaerobic digestion (Py-AD) process for carbon negative fuels from woody biomass. Renew Energy 148:1190–1199. https://doi.org/10.1016/j.renene.2019.10.025

Ul Islam Z, Barbary Hassan E, Zhisheng Y, et al (2015) Microbial conversion of

pyrolytic products to biofuels: a novel and sustainable approach toward second-generation biofuels. Artic J Ind Microbiol 42:1557–1579. https://doi.org/10.1007/s10295-015-1687-5

Venkiteshwaran K, Bocher B, Maki J, Zitomer D (2016) Relating Anaerobic Digestion Microbial Community and Process Function. Microbiol Insights 8:37. https://doi.org/10.4137/MBI.S33593

Watson GK, Caint RB (1975) Microbial Metabolism ofthe Pyridine Ring METABOLIC PATHWAYS OF PYRIDINE BIODEGRADATION BY SOIL BACTERIA

Watson J, Wang T, Si B, et al (2020) Valorization of hydrothermal liquefaction aqueous phase: pathways towards commercial viability. Prog. Energy Combust. Sci. 77:100819

Watson J, Zhang Y, Si B, et al (2018) Gasification of biowaste: A critical review and outlooks. Renew. Sustain. Energy Rev. 83:1–17

Wen C, Moreira CM, Rehmann L, Berruti F (2020) Feasibility of anaerobic digestion as a treatment for the aqueous pyrolysis condensate (APC) of birch bark. Bioresour Technol 307:123199. https://doi.org/10.1016/j.biortech.2020.123199

Wierckx N, Koopman F, Ruijssenaars HJ, De Winde JH (2011) Microbial degradation of furanic compounds: Biochemistry, genetics, and impact. Appl Microbiol Biotechnol 92:1095–1105. https://doi.org/10.1007/s00253-011-3632-5

Xu D, Lin G, Liu L, et al (2018) Comprehensive evaluation on product characteristics of fast hydrothermal liquefaction of sewage sludge at different temperatures. Energy 159:686–695. https://doi.org/10.1016/j.energy.2018.06.191

Yang Y, Heaven S, Venetsaneas N, et al (2018) Slow pyrolysis of organic fraction of municipal solid waste (OFMSW): Characterisation of products and screening of the aqueous liquid product for anaerobic digestion. Appl Energy 213:158–168. https://doi.org/10.1016/j.apenergy.2018.01.018

Yang Z, Liu Y, Zhang J, et al (2020) Improvement of biofuel recovery from food waste by integration of anaerobic digestion, digestate pyrolysis and syngas biomethanation under mesophilic and thermophilic conditions. J Clean Prod 256:120594. https://doi.org/10.1016/j.jclepro.2020.120594

Yu X, Zhang C, Qiu L, et al (2020) Anaerobic digestion of swine manure using aqueous pyrolysis liquid as an additive. Renew Energy 147:2484–2493. https://doi.org/10.1016/j.renene.2019.10.096

Zheng M, Schideman LC, Tommaso G, et al (2017) Anaerobic digestion of wastewater generated from the hydrothermal liquefaction of Spirulina: Toxicity assessment and minimization. Energy Convers Manag 141:420–428. https://doi.org/10.1016/j.enconman.2016.10.034

Zhou H, Brown RC, Wen Z (2019) Anaerobic digestion of aqueous phase from pyrolysis of biomass: Reducing toxicity and improving microbial tolerance. Bioresour Technol 292:. https://doi.org/10.1016/j.biortech.2019.121976

Zhou Y, Schideman L, Zheng M, et al (2015) Anaerobic digestion of post-hydrothermal liquefaction wastewater for improved energy efficiency of hydrothermal bioenergy processes. https://doi.org/10.2166/wst.2015.435

Zhu Y, Biddy MJ, Jones SB, et al (2014) Techno-economic analysis of liquid fuel production from woody biomass via hydrothermal liquefaction (HTL) and upgrading. Appl Energy 129:384–394. https://doi.org/10.1016/j.apenergy.2014.03.053

3 Inoculum microbiome and pre-ozonation affect methanogenesis from aqueous pyrolysis liquid

This chapter will be submitted to the journal *Applied Energy:*

Seyedi, S., Veniteshwaran, K., Zitomer, D., (2020). Inoculum microbiome and pre-ozonation affect methanogenesis from aqueous pyrolysis liquid. *Applied Energy*.

3.1. Introduction

Eight million tonnes of wastewater primary and waste activated sludge solids are generated annually by United States water resource recovery facilities (WRRFs) (Liu et al., 2018; USEPA, 1999). Wastewater solids are potentially valuable resources that have energy content due to organic matter that can be recovered through processes such as pyrolysis. In addition to energy recovery, pyrolysis offers advantages including reducing solids volume and eliminating contaminants such as antibiotic resistance genes, pathogens, and micropollutants that can enter the environment through wastewater solids land application, or landfilling (Kimbell et al., 2018; Liu et al., 2018; Ross et al., 2016a).

During pyrolysis, organic material is heated to 400 – 900 °C with no or little oxygen, yielding biochar, pyrolysis gas (py-gas), and pyrolysis liquid (Fonts et al., 2012; McNamara et al., 2016). Biochar can be used as a soil amendment, sorbent, or catalyst (Liu et al., 2018). Py-gas, which is comprised of methane (CH_4), carbon dioxide (CO_2), hydrogen (H_2) and carbon monoxide (CO), can be burned for heat and energy (Liu et al., 2020). Pyrolysis liquid often consists of two fractions: an organic phase known as bio-oil that can be upgraded to liquid fuel for energy generation (Feng and Lin, 2017), and an aqueous pyrolysis liquid (APL) containing water from thermochemical reactions as well as initial feedstock moisture. The APL has a low heating value and cannot be used as a fuel and its composition is highly dependent on pyrolysis feedstock and temperature (Torri & Fabbri, 2014; Seyedi et al., 2020). APL management is a bottleneck to implementation of pyrolysis because it has no current beneficial use (Liu et al., 2020; Seyedi et al., 2018). APL

has a high chemical oxygen demand (COD) (30 – 500 gCOD/L) and contains various organic compounds including carboxylic acids, alcohols, aldehydes, ketones, phenols, and nitrogen-containing organics such as pyridine, pyridinol, pyrazine, and 3-pyridinamine (Seyedi et al., 2019; Wen et al., 2020; Zhou et al., 2019). If APL is defined as a waste, then it may be a hazardous waste due to the presence of toxic organics, such as pyridine, and can result in environmental pollution upon discharge. Furthermore, the energy from APL organic compounds is lost if not captured and can have high associated disposal costs (Yang et al., 2018). Therefore, new ways to manage APL as well as recover energy would be beneficial.

Anaerobic digestion (AD) to transform APL organic constituents into biogas containing methane may be an APL management approach (Fabbri and Torri, 2016a; Zhou et al., 2019; Zitomer et al., 2008). The presence of organic compounds such as acetic acid makes APL an appealing substrate for energy recovery in the form of biomethane from AD (Cheng et al., 2016; Seyedi, 2018; Wen et al., 2020). However, constituents such as phenols and nitrogenous organics are toxic to anaerobic microorganisms and make APL AD challenging. Others have reported methane production inhibition during AD of APL. Torri and Fabbri (2014) observed AD batch tests loaded with 35 gCOD/L APL from corn stalk pyrolysis at 400°C were inhibited (Torri and Fabbri, 2014). Zhou et al. (2019) observed that APL derived from pyrolysis of corn stover at 500 °C inhibited methane production at 14.6 gCOD/L (3% v/v) of APL during short-term, batch biochemical methane potential (BMP) tests. APL degradability is greatly

dependent on pyrolysis process temperature, affecting its recalcitrance and toxicity to anaerobic microorganisms. Yang et al. (2018) described pyrolysis temperature as the main factor influencing toxicity of APLs generated from the organic fraction of municipal solid waste. Higher pyrolysis temperature resulted in lower APL COD content, but higher toxicity to AD. In this study, APLs produced from wastewater solids pyrolysis at 500 and 700 °C were investigated for their anerobic degradability with the hypothesis that APL derived from higher pyrolysis temperature would result in higher anaerobic toxicity.

Ozone pretreatment may be one method to reduce APL toxicity for subsequent AD. Ozone oxidation of biorefractory compounds can either occur indirectly by hydroxyl radicals (●OH) that can attack a wide range of organic compounds (Eggen and Vogelsang 2015), or by direct ozone molecules that target electron-rich functional groups such as phenols, amines and unsaturated organics (double bonds) (Eggen and Vogelsang 2015), that are common compounds detected in the APL (Seyedi et al. 2019). Therefore, ozone is hypothesized to be able to partially oxidize APL constituents to more biodegradable, less toxic products that could be anaerobically digested. Ozone pretreatment was used successfully to reduce the toxicity of bio-oil as well as olive oil mill wastewater and hydrothermal liquefaction aqueous phase (HTL-AP) (Benitez et al., 1997; Xu et al., 2011; L. Yang et al., 2018a). Ozonation of bio-oil from rice husk pyrolysis converted aldehydes to carboxylic acids (Xu et al., 2011). Ozonation of olive mill wastewater for 8 h reduced the total phenolics (TP) concentration by more than 94% and increased subsequent methane yield by 37% (Benitez et al., 1997).

Ozone pretreatment was employed to convert recalcitrant compounds in HTL-AP derived from swine manure at 270 °C into more easily degradable products (Yang et al., 2018a). Consequently, biodegradability was enhanced as shown by a BOD_5:COD ratio increase from 0.31 to 0.41 after 200 min of ozonation (Yang et al., 2018a). APL ozonation decreased the APL TP concentration as indicated by a color change from dark to light brown and decreased the average molecular weight of APL constituents (Liaw et al., 2016).

Employing appropriate AD inoculum may be another approach to overcome APL toxicity. Microbe acclimation can improve APL biodegradability; however, it requires a long time, which can limit its practicality. Seyedi et al. (2020) investigated the long-term (>500 d) acclimation of anaerobic biomass to APL derived from pyrolysis of wastewater solids at 800 °C and found that acclimation resulted in a doubling of biomass tolerance to APL toxicity (See Appendix B). Using inoculum already acclimated to some or all APL constituents may shorten start-up time. Therefore, it is hypothesized that using an acclimated anaerobic inocula may be more efficient in degrading the APL organics.

In this study, the objectives were (1) to use APLs derived from wastewater solids pyrolyzed at different temperatures to evaluate pyrolysis temperature effects on APL degradability, since pyrolysis temperature is one of the major factors affecting the degradability of the resulting APL, (2) to investigate different ozone pretreatment contact times to partially oxidize APL organics and convert them to more biodegradable products for subsequent AD, and (3) to employ four different methanogenic inocula in anaerobic toxicity assays (ATAs) with ozonated and non-

ozonated APLs to assess different microbial communities capabilities in degrading APL. The inocula were obtained from both municipal anaerobic digesters treating waste different from APL as well as industrial anaerobic digesters treating wastes containing one or more APL constituents. The hypotheses were that (1) APL produced at higher pyrolysis temperature will be more toxic in AD, (2) pretreating APL by partial oxidation using ozone and (3) employing inocula acclimated to one or more toxic APL constituents will result in increased methane production rates.

3.2. Materials and methods

3.2.1. APL production and pre-ozonation

APLs were produced by pyrolyzing a mix of dried, anaerobically digested primary sludge and raw waste activated sludge (Milorganite, Milwaukee Metropolitan Sewerage District, Milwaukee, WI, USA). Pyrolysis was conducted at either 500 °C or 700 °C, as described elsewhere (Liu et al., 2017).

Pre-ozonation of APL was performed using ozone-enriched oxygen gas. Ozone was generated using a lab-scale corona discharge ozone generator (LAB2B, Ozonia, Leonia, NJ) at a dry oxygen flow rate of 4 L/min (1 atm, 20 °C), resulting in a gas ozone concentration of 20 ± 2 mg/L. A diluted APL sample (50 mL of APL in 200 mL of deionized water) was used in a 500 mL bubble column reactor (see Figure S3.1). Prior to ozonation, APL pH was increased to 11 using 6 N NaOH to help increase hydroxyl radical formation for advanced oxidation. Ozone contact times of either 10 min or 2 h were employed. Preliminary results showed that the majority of TP removal occurred in the first 10 min of ozonation. A 2 h

ozonation time was used to determine if changes other than TP removal occurred that influenced subsequent AD. Ozone concentrations in ozone-enriched oxygen gas and off gas were measured using a UV-ozone analyzer (Model 106-H, 2B Technologies, Boulder, CO, USA).

3.2.2. ATA testing

ATA testing was conducted using 160 mL glass serum bottles with 50 mL working volume in triplicate according to a standard protocol (Owen et al., 1979). Each triplicate set received a different concentration (0.3, 0.8, 1.6, 2.3, and 4 gCOD/L) of ozonated or non-ozonated APL along with 10 g/L calcium acetate. COD loadings were selected based on preliminary data with the intent to provide concentrations ranging from non-inhibitory to inhibitory concentrations to evaluate APL toxic effects. A control set received only calcium acetate and no APL. Inhibitory effects were quantified based on the concentration of APL that caused a 50% decrease in methane production rate (i.e., the IC_{50} concentration) and a dose-response relationship between APL dose and methane production rate was developed.

ATA testing was performed using 24 possible combinations of three independent variables (four inocula, three pre-treatment conditions and two pyrolysis temperatures) in triplicate. Two inocula were from municipal anaerobic digesters at the South Shore Water Reclamation Facility in Oak Creek, WI, USA (MB1) and the Fox River Water Reclamation Facility in Brookfield, WI, USA (MB2) stabilizing primary and waste activated sludge. Two other inocula were from industrial up-flow anaerobic sludge blanket (UASB) reactors treating organic acids

including polyphenols and carboxylic acids in the USA (IB1) and treating wastewater containing acetate, benzoate and phenolic compounds in Western Europe (IB2). Inoculum IB2 was not used for all ATA combinations investigated due to shipping volume limitations. The APL pretreatment conditions included no pretreatment, 10 min ozonation and 2 h ozonation. In addition, APLs produced at 500 and 700 °C were tested.

3.2.3. Analytical methods

Biogas volume was measured using a 100 mL wetted-barrel glass syringe by inserting the needle through serum bottle septa. Biogas methane content was determined by gas chromatography (GC System 7890A, Agilent Technologies, Irving, TX, USA) using a thermal conductivity detector (TCD). Volatile fatty acids (VFA) concentrations were measured by gas chromatography (GC System 7890A, Agilent Technologies, Irving, TX, USA) using a flame ionization detector (FID). COD and soluble COD (SCOD) concentrations were measured according to standard methods (American Public Health Association, 1998). For SCOD, the sample was filtered through a 0.45 μm pore size membrane syringe filter and the filtrate COD was determined. Total and volatile suspended solids (TSS and VSS) concentrations were determined by standard methods (American Public Health Association, 1998). The pH was monitored using a pH probe and meter (Orion 4 Star, Thermo, Waltham, MA, USA).

Dissolved organic carbon (DOC) was measured using a total organic carbon (TOC) analyzer (TOC-V, Shimadzu, Japan) by filtering and acidifying the samples (American Public Health Association 1998). TP concentration was

determined using the micro-scale Folin–Ciocalteu method (Folin and Ciocalteu, 1927; Rover & Brown, 2013). For specific ultraviolet absorbance (SUVA) determination, the absorbance at 254 nm (UV_{254}) was measured using a spectrophotometer (Genesys 10S UV-Vis spectrophotometer, Thermo Scientific, USA). SUVA was calculated as the ratio of UV_{254} absorbance and DOC concentration (Chaparro et al., 2010).

APL constituent concentrations were measured using a gas chromatography-mass spectrophotometry system (GC-MS, Thermo Scientific Trace DSQII) with a DB wax column with 30m × 0.53mm ID × 1.0μm film thickness (DB-Wax column, Agilent Technologies). The injection volume was 1 μL and the split ratio was 40:1. The GC oven was programmed with an initial temperature of 40 °C for 1 min, temperature ramp of 5 °C/min and a final temperature of 240 °C for 20 min. Helium carrier gas flow rate was constant at 1.0 mL/min. All samples were dissolved in acetone at a ratio of 1:10.

3.2.4. Statistical analysis

Statistical analyses including average, standard deviation, normality test, and two-sample student's t-test calculations were performed using Microsoft Excel 2015. One-way analysis of variance (ANOVA) with post-hoc Tukey's multiple comparisons test was performed using R software. Cumulative methane production curves were analyzed by fitting the modified Gompertz model (Equation 1) using non-linear regression (Si et al., 2019; Zhou et al., 2019) in IBM SPSS Statistics version 26:

$$P(t) = P_{max} \exp\left[-\exp\left(R_{max} \times e/P_{max}\right) \times (\lambda - t) + 1\right] \qquad \text{Equation 1}$$

where P is the specific cumulative methane produced at time t (days) in mL CH_4/gVSS; P_{max} is the maximum cumulative methane volume (mL CH_4/gVSS); R_{max} is the maximum methane production rate (mL CH_4/gVSS-d); λ is the lag length in days, t is the digestion time in days, and e is exp (1) = 2.71828.

3.3. Results and discussion

3.3.1. Pyrolysis temperature affects APL composition

As pyrolysis temperature increased, the resulting APL had lower COD, NH_3-N, and total VFA concentrations. APL generated at 500 °C had higher COD, NH_3-N, and total VFA concentrations compared to APL produced at 700 °C (Table 3.1). This is consistent with other studies that demonstrated with rise in pyrolysis temperature, the resulting APL has lower COD concentration and higher pH (Yang et al., 2018). Elevated NH_3-N concentration in APL is primarily due to deamination of amino acids resulting in production of NH_3-N from protein-rich feedstock such as manure and sewage sludge (Watson et al., 2018). Analogous to APL, HTL-AP generated from sewage sludge contained a high NH_3-N concentration and increase in the thermochemical process temperature (170 to 320 °C) doubled the NH_3-N concentration (54 to 115 mg NH_3-N/gCOD) (Chen et al., 2019).

Table 3.1. APL characteristics at different pyrolysis temperatures[1].

APL	COD (g/L)	NH_3-N (g/L)	Total VFA concentration (expressed as g/L of acetic acid)	pH
500 °C	350 ± 11	100 ± 4.9	38 ± 4.1	9.3
700 °C	190 ± 3.7	50 ± 2.0	20 ± 5.9	9.4

[1] Results are expressed in average ± standard deviation from triplicate measurements.

3.3.2. Pre-ozonation altered APL composition

Ozonation resulted in decreased NH_3-N concentration as well as TP and SUVA values, indicating the pretreatment may result in lower toxicity, more readily degradable products, and more complete methane production from the ozonated product. In addition, ozonation reduced the APL COD and DOC concentrations, but only by less than 20%. Therefore, the ozonated product may be more amenable to anaerobic biodegradation but still contains a significant concentration of organic carbon for potential conversion to methane.

Ozonation for 10 min reduced the NH_3-N concentration by 70 ± 1.5% for APL produced at 500°C, but no additional NH_3-N removal was observed after 2 h ozonation (Figure 3.1A). In contrast, ozonation for 10 min did not reduce NH_3-N concentration in APL produced at 700°C, but 52 ± 0.8% of the NH_3-N was removed after 2 h. The NH_3-N removal may have been due to gas stripping of the NH_3-N to the atmosphere (Figure 3.1A).

Regarding TP, it decreased more than 60% in the first 10 min of ozonation in both APLs (Figure 3.1B). After 2 h, TP decreased by 79 ± 0.01% and 83 ± 0.01% for 500 °C and 700 °C APL, respectively. Also, SUVA decreased more than 35% in both 500 °C and 700 °C APLs after 10 min, and it decreased more than 60% in both APLs after 2 h ozonation (Figure 3.1B). Reduction in SUVA indicates a decrease in aromaticity and molecular weight, which are both favorable for AD (Chaparro et al., 2010; Li et al., 2015).

The VFA concentration in 500 °C APL did not change significantly after ozonation ($p=0.12$, $n=9$) (Figure 3.1A). The non-ozonated 700 °C APL contained

20 ± 5.9 g/L VFAs. After 10 min ozonation, the VFAs concentration was reduced to 15 ± 1.1 g/L VFA, and in 2 h ozonated samples, the VFA remained the same as non-ozonated APL (16 ± 1.4 g/L VFA) ($p=0.09$, $n=4$).

Ozonation for 2 h decreased the COD concentration by 8.9 ± 2.8% ($p=0.01$, $n=6$) and 17 ± 0.1% ($p=0.00$, $n=6$) in APL produced at 500 and 700 °C, respectively (Figure 3.1C). However, no COD reduction was observed after only 10 min ozonation in either 500 or 700 °C APLs ($p=0.36$, $n=6$) (Figure 3.1C). The COD removal may have been due to COD oxidation and/or gas stripping of volatile organics to the atmosphere. The DOC concentration in 500 °C APL decreased by 16 ± 0.8% after 10 min ozonation and did not change after 2 h ozonation (Figure 3.1C). In 700 °C APL, the DOC concentration decreased by 11 ± 0.3% and 16 ± 1% after 10 min and 2 h of ozonation, respectively (Figure 3.1C). The DOC decrease may have been due to DOC oxidation to CO_2 or gas stripping of volatile organics to the atmosphere.

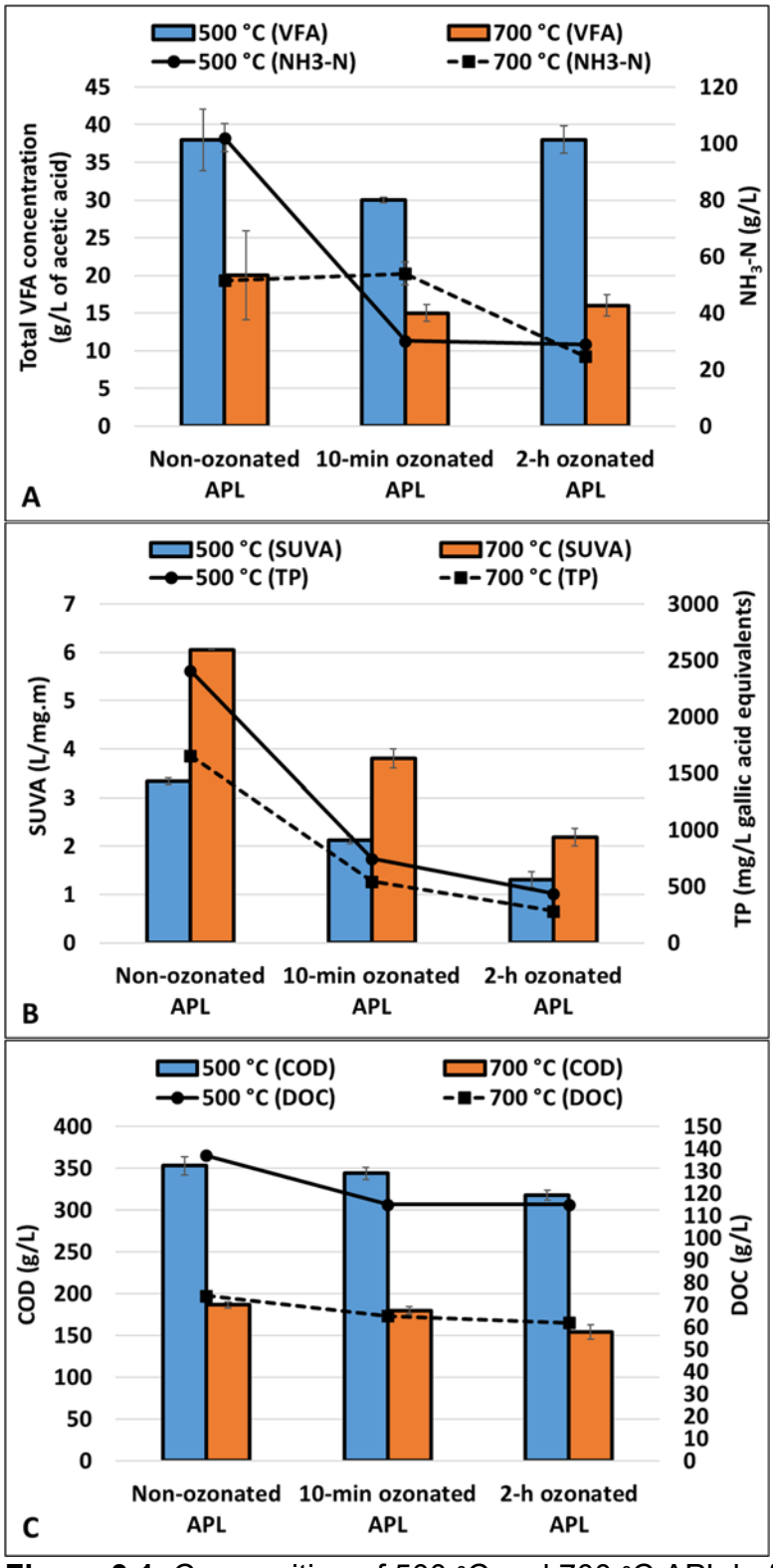

Figure 3.1. Composition of 500 °C and 700 °C APL before and after 10 min and 2 h ozonation. (A) NH_3-N and total VFA, (B) SUVA and TP reduction, (C) COD and DOC. Error bars represent one standard deviation for triplicate systems. Some error bars are small and not visible.

3.3.3. GC-MS analysis of APL before and after ozonation

Partial or complete removal of some of the APL organic constituents occurred after 10 min and 2 h ozonation that could lead to less toxic APL in subsequent AD. The majority of compounds detected by GC-MS in the APLs were N-heterocyclic organics including acetamide, 2-pyrrolidinone, 2-pyridinol, 4-pyridinemethanol, pyrrole, pyridine, and 3-aminopyridine (Table S3.1. and Figure 3.2A and 3.2B). The pyrolysis feedstock was sewage sludge, which can have significant nitrogen content compared to lignocellulosic feedstocks (wood, corn stover, etc.) and lead to high nitrogen content of the resulting APL (Chen et al., 2019; Seyedi et al., 2019). N-heterocyclic compounds can be produced during Maillard reaction when amino acids react with reducing sugars from hydrolysis of hydrocarbons and form nitrogenous organics including pyrrole, pyrrolidinone, pyridine and their derivatives (Gai et al., 2015). Organic compounds with functional groups such as amines and amides have also been reported to form during breakdown of proteins in the pyrolysis process (Chen et al., 2019). HTL-AP from sewage sludge was previously reported to contain high concentrations of nitrogen-containing organics, including amides and N-heterocyclic compounds such as pyrazine, 2-pyrrolidinone, and 2-piperidinone (Watson et al., 2020). It was also found that nitrogen-containing compounds tend to accumulate in the HTL-AP using a protein-rich feedstock such as manure or sewage sludge. Some of these compounds such as pyrazine, pyridine, and pyrrolidinone can be anaerobically degraded; however, they require high dilution to preclude toxicity and a long acclimation time (Watson et al., 2020). These compounds can inhibit acetogenesis

and result in accumulation of propionate, butyrate, and valerate in the system (Watson et al., 2020).

Many N-heterocyclic compounds were removed below detection limit of the GC-MS instrument after APL 10 min or 2 h ozonation. In 500 °C APL, compounds such as acetonitrile, 3-pyridinol, 4-pyridinemethanol, 5,5-dimethyl-2,4-imidazolidinedione, dl-5-Ethyl-5-methyl-2,4-imidazolidinedione, and 5-Isopropyl-2,4-imidazolidinedione were removed >95% after 2 h ozonation (Figure 3.2A). In 700 °C APL, acetonitrile, pyrrole, pyridine, 1H-imidazole-4-methyl, 3-aminopyridine and phenol were also removed >95% after 2 h ozonation (Figure 3.2A). More compounds were removed to below detection concentrations after 2 h ozonation compared to 10 min ozonation (Figure 3.2A and 3.2B). Yang et al. (2018) also observed reduction in percent relative peak area of phenolics and N-heterocyclic compounds after 200 min ozonation of HTL-AP from swine manure. Peak area in straight and branched amides such as acetamide and propenamide increased in 700 °C APL after ozonation, indicating oxidation of N-heterocyclic compounds during ozonation which is consistent with reduced SUVA values after ozonation (Figure 3.2B). Acetamide has been shown to be degradable under anaerobic conditions in a UASB through breakdown into acetate and NH_3-N, and finally into methane by methanogens (Guyot et al., 1995; Ramirez et al., 1998).

Overall, ozonation removed more than 70% of the compounds partially or completely after 2 h ozonation in both 500 and 700 °C APL based on percent peak area. However, only about 30% of the compounds were removed after 10 min ozonation. It was previously reported that intermediates produced during the first

10 min of ozonation of biologically pretreated coal gasification wastewater could lead to increased toxicity, but continuous ozonation for longer periods decreases toxicity (Zhu et al., 2018). Partial oxidation after 10 min ozonation in this study could possibly have resulted in generation of more toxic ozonation intermediates which could be more detrimental to AD than the original non-ozonated APL, leading to decreased methane production rate or increased lag time in ATAs. Some compounds that were generated after 10 min ozonation in 500 and 700 °C APLs include 1-butanol, pyridine, butane 1-isothiocyanato-3-methyl, pyrazine-methyl, and 2(1H)-pyridinone.

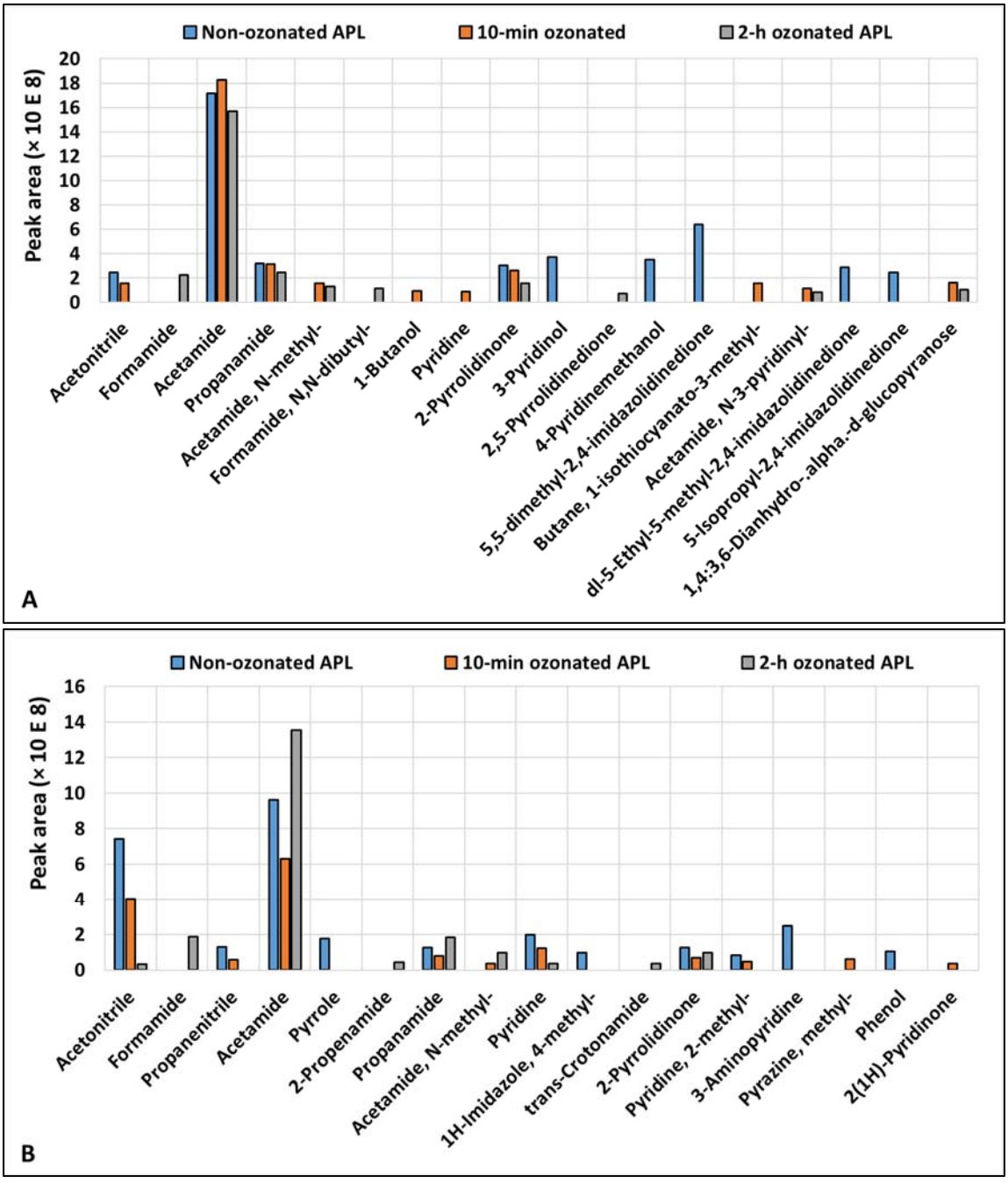

Figure 3.2. GC-MS analysis on APL composition before and after ozonation. The compounds with 10 highest peak area in non-ozonated,10 min and 2 h ozonated APLs are shown. These compounds contributed to >60% of the total organic compounds detected in all APLs. Undetected peaks were below detection of the GC-MS instrument (<0.1×10^8). Compounds are sorted in increasing order of the molecular weight on the x axis. (A) 500 °C APL, (B) 700 °C APL.

3.3.4. ATA results

ATA testing was performed on non-ozonated, 10 min and 2 h ozonated APLs to evaluate the effect of ozonation on improving or reducing APL degradability. Four different inocula (MB1, MB2, IB1, IB2) were employed to assess the capability of different inocula microbial communities in degrading APL. Figure 3.3A shows the results for an ATA test employing IB1 along with the dose response curve for the non-ozonated 700 °C APL at different concentrations. ATA plots for all other conditions are presented in Figure S3.2.

APL digestion at the relatively low organic loadings tested was achievable, but at high loadings the toxicity inhibited the initial methane production rate, which was followed by acclimation. Methane production rate decreased as the APL concentration increased ($p<0.05$, $n=9$) above a 1.6 gCOD/L dose compared to the control bottles which did not receive APL (Figure 3.3A). At lower concentrations of 0.3 to 1.6 gCOD/L, no significant inhibition was observed, and the methane production rates were similar to those of the control bottles ($p>0.05$, $n=12$). At 4 gCOD/L APL, significant inhibition was observed with a relatively long, 13 ± 1.4 day lag phase before methane production started. After the lag phase, methane production occurred at a lower rate compared to the control systems, demonstrating acclimation of the microorganisms to the APL constituents. The acclimation resulted in 82 ± 29% of the stoichiometric maximum theoretical methane production (395 mL CH_4 per gCOD removed at 35 °C and 1 atm) by the end of the test. This shows that APL digestion is feasible at relatively low organic loadings, and at high loadings the toxicity can inhibit the initial methane production

rate, but acclimation can occur. The inhibition could be attributed to the presence of N-heterocyclic and phenolic compounds that are known to adversely affect methanogenic cultures at high concentrations by damaging membrane proteins, inactivating cell enzymatic systems and adversely affecting cell metabolism (Donlon et al., 1995; Hübner and Mumme, 2015; Madigou et al., 2016; Si et al., 2019; Torri and Fabbri, 2014; Watson et al., 2020). A similar pattern was observed with the other three inocula using non-ozonated 700 °C APL, demonstrating an inverse relationship between APL concentration and methane production rate at concentrations greater than 1.6 gCOD/L (Figure S3.2B). The extent of inhibition was lower in APL produced at 500 °C (Figure S3.2A), which is consistent with other studies that demonstrated that APL generated at lower temperatures is less toxic to methanogenic cultures (Hübner and Mumme, 2015; Y. Yang et al., 2018).

Methane production data were evaluated to determine the concentration of APL that inhibited the methane production rate by 50% (i.e., the IC_{50} value) by plotting the dose response curves (Figure 3.3B). The IC_{50} value was 2.2 gCOD/L for non-ozonated 700 °C APL, and the highest APL COD loading that demonstrated no inhibition was 1.6 gCOD/L.

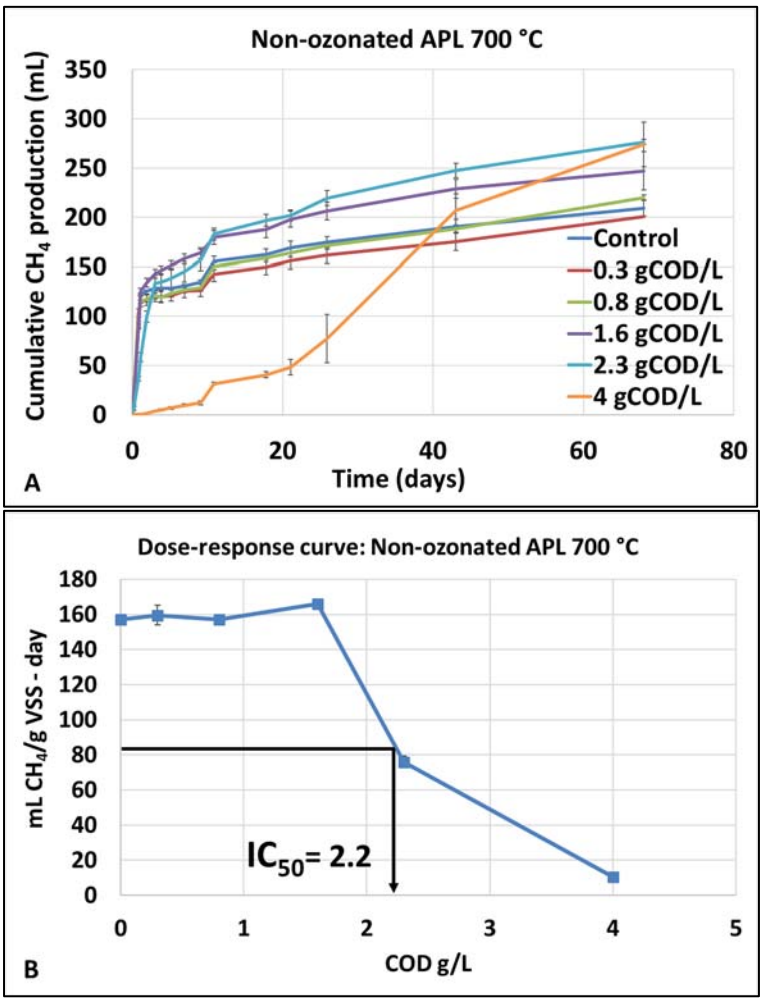

Figure 3.3. ATA results on non-ozonated APL derived at 700 °C using IB1 at different APL COD concentrations. (A) Cumulative methane production, (B) Dose response curve on COD basis. Error bars represent standard deviation from triplicate experiments. Some error bars are small and not visible.

3.3.5. Positive effect of ozonation and inocula selection on ATA methane production rate and initial lag phase

3.3.5.1. ATA methane production rate

Pre-ozonation resulted in increased methane production rate from 700 °C APL, specifically at the highest loading (4 gCOD/L of APL), indicating ozonation reduced the APL toxicity (Figure 3.4B). IC_{50} values increased as the ozonation time

increased for 700 °C APL (Figure 3.4B). In systems inoculated with MB1, the IC_{50} increased from 1.5 ± 0.09 gCOD/L to 2.3 ± 0.1 and 2.2 ± 6E-3 gCOD/L (p=0.001, n=6), corresponding to 55 ± 9% and 47 ± 8% increase in 10 min and 2 h ozonated 700 °C APL compared to non-ozonated APL, respectively. With IB1, the IC_{50} enhanced from 2.2 ± 0.02 in digesters receiving non-ozonated APL to 2.75 ± 0.06 (24 ± 4%) and 3.1 ± 0.14 (40 ± 6%) in systems fed 10 min and 2 h ozonated APL, respectively ($p<0.05$, n=6). In MB2, the IC_{50} value in bottles receiving 10 min ozonated APL did not change compared to using non-ozonated APL (p=0.5, n=6), whereas, using 2 h ozonated APL increased the IC_{50} to >4 gCOD/L (>10%) (p=0.02, n=3) (Figure 3.4B). Similarly, employing IB2, the IC_{50} value in 2 h ozonated APL compared to non-ozonated APL increased to >4 gCOD/L (>35%) (p=0.006, n=6). This shows that no inhibition was observed at any concentration tested when 2 h ozonated APL was used with MB2 and IB2.

For non-ozonated 500 °C APL, almost no inhibition was observed at the concentrations tested using all inocula and ozonation did not have a considerable impact on methane production rate (Figure 3.4A). All IC_{50} values were ≥4 gCOD/L of APL, signifying no inhibition was observed until 4 gCOD/L APL (IC_{50} for 10 min ozonated APL using MB1 was 3.8 ± 0.2 gCOD/L APL which was statistically similar to 4 gCOD/L APL (p=0.36, n=6)). These results demonstrate that the APL generated at lower temperature (500 °C) was less toxic to methanogenic cultures compared to the 700 °C APL, which is consistent with results of other studies (Hübner and Mumme, 2015; Y. Yang et al., 2018). The higher degradability of the 500 °C APL could also be associated with higher VFAs concentration such as

acetic acid in the 500 °C APL compared to 700 °C APL. Decrease in IC_{50} in 10 min ozonated APL in MB1 could be due to the production of more toxic ozonation intermediates.

Different inocula showed different capabilities to degrade the more toxic 700 °C APL (Figure 3.4B). MB2 demonstrated the highest tolerance for APL as indicated by the highest IC_{50} values regardless of ozonated or non-ozonated APL being used. Following that, the IB2 showed robustness in APL degradation and tolerating toxicity. MB1 and IB1 were more sensitive to APL toxicity and were more inhibited.

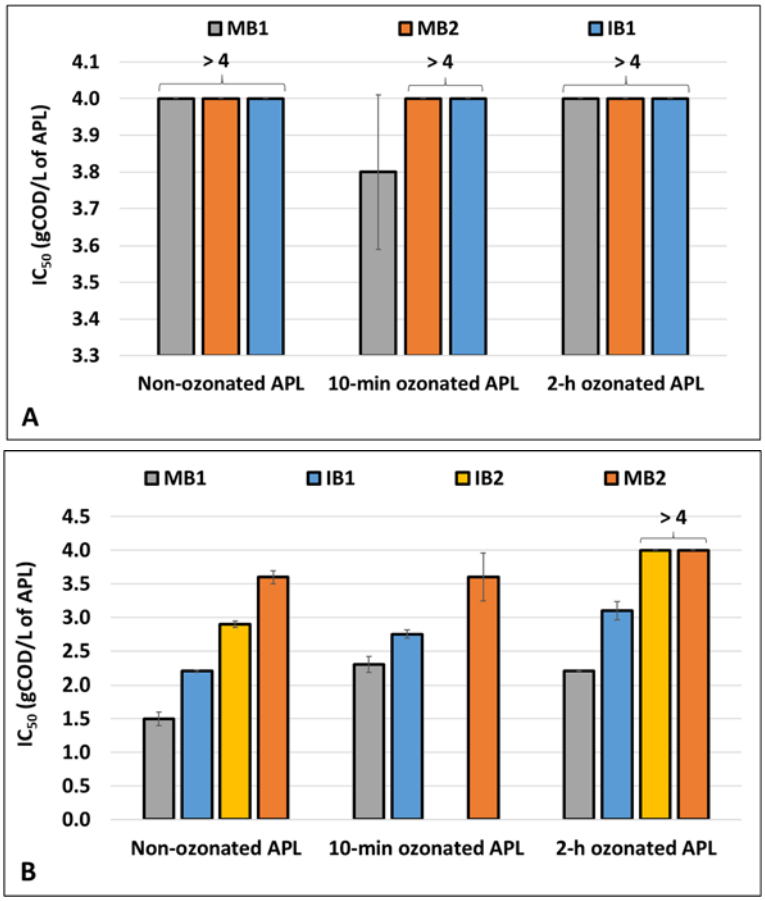

Figure 3.4. Average IC_{50} values for non-ozonated, 10 min ozonated, and 2 h ozonated APLs using different inocula. Error bars represent standard deviation from triplicate bottles. Some error bars are small and not visible. IC_{50} values above 4 gCOD/L of APL are indicated by ">4". (A) 500 °C APL, (B) 700 °C APL.

3.3.5.2. ATA lag phase

APL ozonation for 2 h also reduced the initial lag phase before methane production began in 4 gCOD/L systems, but 10 min ozonation increased the lag phase. As estimated by the Gompertz model, the lag phase in 4 gCOD/L systems inoculated with IB1 decreased from 13 ± 1.4 days in non-ozonated 700 °C APL, to 0.95 ± 0.34 days (>90%) when 2 h ozonated APL was used. However, ozonation for 10 min resulted in an increased lag to 40 ± 0.04 days (Figure 3.5B). This could

be attributed to the generation of more toxic ozonation intermediates during 10 min ozonation. A similar pattern was observed in ATA tests with other inocula performed on 700 °C APL at 4 gCOD/L, when employing 10 min ozonated APL caused an increase in the lag phase, whereas 2 h ozonation decreased the lag phase time compared to when non-ozonated APL was used (Figure 3.5B).

In contrast, using ozonated APL did not affect the lag phase in digesters inoculated with MB2 as they demonstrated statistically similar lag phase to non-ozonated APL ($p=0.1$, $n=6$). Using MB1, the lowest lag phase was observed employing the non-ozonated (2.0 days) and 10 min ozonated (1.6 days) 500 °C APL ($p=0.07$, $n=6$), while 2 h ozonated APL exhibited slightly longer lag phase (2.7 days) compared to non-ozonated APL ($p=0.008$, $n=6$). The IB1 displayed no lag phase using either ozonated or non-ozonated APL (Figure 3.5A).

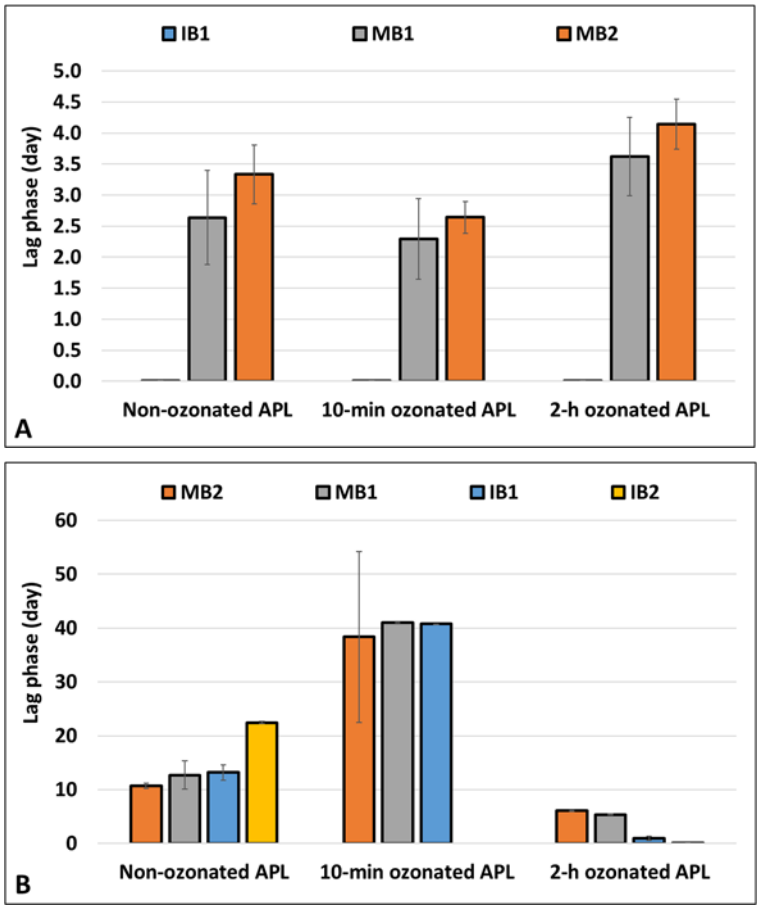

Figure 3.5. Average lag phase time for non-ozonated, 10 min ozonated and 2 h ozonated APLs at highest loading (4 gCOD/L of APL) using different inocula. Error bars represent standard deviation from triplicate bottles. Some error bars are small and not visible. (A) 500 °C APL, (B) 700 °C APL.

Final cumulative methane produced from APL COD based on stoichiometric maximum theoretical methane production was calculated (Figure 3.6). Using IB1 inoculum, the highest final cumulative methane production from both ozonated or non-ozonated 500 °C and 700 °C APLs was achieved (Figure 3.6). In 500 °C APL, more than 90% of the maximum theoretical methane from non-ozonated and about 80% of the 10 min and 2 h ozonated APL at every concentration was generated when employing IB1 inoculum. In digesters inoculated with IB1 fed 700 °C APL,

more than 80% of the maximum theoretical methane from non-ozonated and 2 h ozonated APL at all concentrations was produced.

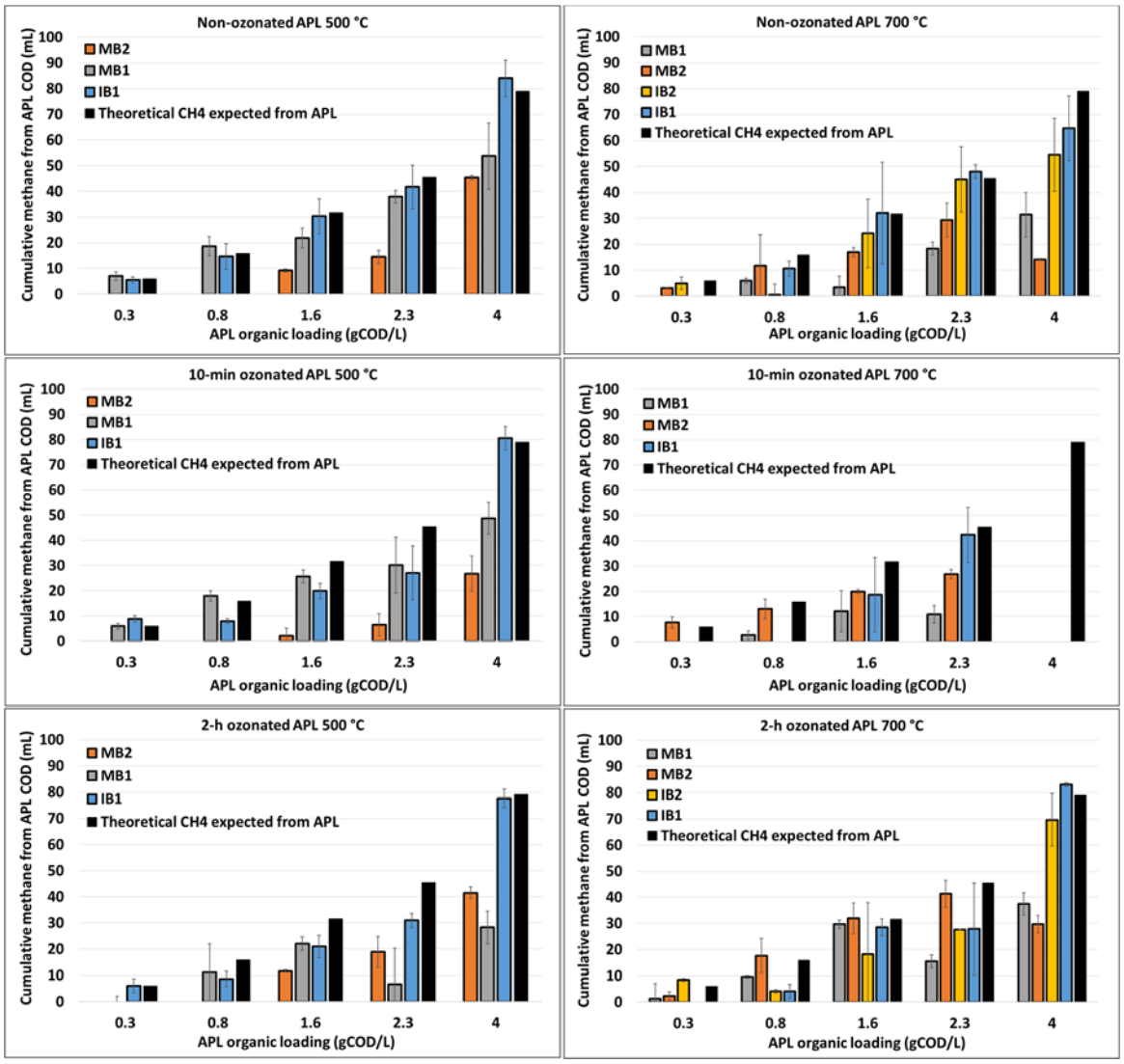

Figure 3.6. Final cumulative methane production from ATAs on non-ozonated, 10 min ozonated and 2 h ozonated APL produced at 500 °C and 700 °C at different concentrations employing different inocula. The black bars show the theoretical stoichiometric methane production (395 mL CH_4 produced per gCOD removed at 35 °C and 1 atm) for comparison to the actual methane produced from APL COD at each concentration. Error bars represent standard deviation from triplicate bottles. Some error bars are small and not visible.

Overall, ATA results demonstrated that increased methane production rate (higher IC_{50}) and decreased lag time was achieved employing 2 h ozonated 700 °C APL. Feeding 10 min ozonated APL also resulted in increased IC_{50} in 700 °C APL using MB1 and IB1, but IC_{50} did not change when MB2 was used. On the other hand, employing 10 min ozonated APL increased the lag time significantly in all systems. Regarding 500 °C APL, ozonation did not have a considerable influence on methane production rate as observed by IC_{50}≥4 gCOD/L at all cases. However, when 10 min and 2 h ozonated APLs were used, lag time increased in digesters inoculated with MB1. Longer lag phase could be attributed to production of toxic ozonation intermediates after 10 min or 2 h of ozonation (Zhu et al., 2018) that could lead to more toxicity as compared to non-ozonated APL, therefore requiring more time to acclimate to the toxic compounds. Yang et al. (2018) also observed methane production increase in anaerobic digesters receiving ozone-pretreated HTL-AP by 68% compared to systems receiving raw HTL-AP; however, the initial methane production lag phase increased from 12.6 days in raw HTL-AP to 21.3 days in ozonated HTL-AP, which was related to generation of some toxic chemicals during ozonation.

ATA results using different inocula also revealed varying capabilities of inocula in degrading APL. Employing MB2 and IB2 resulted in the highest IC_{50} value while degrading 700 °C APL amongst other inocula, indicating they were less sensitive to APL toxicity. The IB1 inoculum generated the highest final cumulative methane production from APL COD with both 500 and 700 °C APL. No significant inhibition was observed degrading 500 °C APL among the different inocula.

3.4. Conclusion

Anaerobic degradability of APLs derived from wastewater solids pyrolyzed at 500 and 700 °C under different pre-ozonation conditions using different inocula were evaluated. Ozone pretreatment was hypothesized to reduce APL toxicity, and it was observed that ozonation for 10 min and 2 h removed some of the potential inhibitory compounds and rendered APL less toxic and more amenable to AD in some cases. Different inocula demonstrated different capabilities to degrade the more toxic APL (700 °C), such that employing MB2 resulted in the highest IC_{50} value amongst all inocula, followed by IB2, suggesting their robustness towards APL toxicity. It was originally hypothesized that acclimated inocula would result in more efficient APL conversion to methane, but it was observed that municipal inocula was also capable in degrading APL.

APL toxicity increased with increased pyrolysis temperature. APL produced at 500 °C contained higher COD concentration but exhibited no toxicity during ATA (IC_{50} >4 gCOD/L APL) under the conditions studied, compared to APL produced at 700 °C APL which had lower COD concentration but was more toxic to anaerobic microorganisms (1.5 gCOD/L APL< IC_{50} <3.6 gCOD/L APL).

The majority of APL constituents identified were nitrogen-containing organics. The concentration of problematic compounds such as aromatics and phenolics decreased due to ozonation as indicated by SUVA and TP results. However, some ozonation intermediates were also generated that could have led

to more toxicity or increased lag time in some cases compared to non-ozonated APL.

APL ozonation for 2 h and using MB inoculum demonstrated the highest methane production rate and lowest lag phase in the case of 700 °C APL. In general, IC_{50} values increased as the ozonation time increased for 700 °C APL such that no inhibition was observed at any concentration when 2 h ozonated APL was used with MB2 and IB2. Employing APL ozonated for 2 h also decreased initial lag phase before methane production started in 700 °C APL employing all inocula. However, using 10 min ozonated APL increased the lag time in 700 °C APL. Feeding ozonated 500 °C APL did not have a substantial impact on methane production rate from APL using either inocula. However, digesters inoculated with MB1 demonstrated decreased IC_{50} and increased lag time when 10 min and 2 h APLs were used, respectively. Results of this study demonstrated that both APL ozonation and type of inocula affected the anaerobic toxicity response to APL.

3.5. References

American Public Health Association (1998) Standard Methods for the Examination of Water and Wastewater.

Benitez FJ, Beltran-Heredia J, Torregrosa J, Acero JL (1997) Improvement of the anaerobic biodegradation of olive mill wastewaters by prior ozonation pretreatment. Bioprocess Eng 17:169–175. https://doi.org/10.1007/s004490050371

Chaparro TR, Botta CM, Pires EC (2010) Toxicity and recalcitrant compound removal from bleaching pulp plant effluents by an integrated system: Anaerobic packed-bed bioreactor and ozone. Water Sci Technol 61:199–205. https://doi.org/10.2166/wst.2010.794

Chen H, Rao Y, Cao L, et al (2019) Hydrothermal conversion of sewage sludge: Focusing on the characterization of liquid products and their methane yields. Chem Eng J 357:367–375. https://doi.org/10.1016/j.cej.2018.09.180

Cheng J-R, Liu X-M, Chen Z-Y, et al (2016) A novel mesophilic anaerobic digestion system for biogas production and in situ methane enrichment from coconut shell pyroligneous. Appl Biochem Biotechnol 178:1303–1314

Donlon BA, Eli´ E, Razo-Flores E, et al (1995) Toxicity of N-Substituted Aromatics to Acetoclastic Methanogenic Activity in Granular Sludge

Eggen T, Vogelsang C (2015) Occurrence and Fate of Pharmaceuticals and Personal Care Products in Wastewater. In: Comprehensive Analytical Chemistry. Elsevier B.V., pp 245–294

Fabbri D, Torri C (2016) Linking pyrolysis and anaerobic digestion (Py-AD) for the conversion of lignocellulosic biomass. Curr Opin Biotechnol 38:167–173. https://doi.org/10.1016/j.copbio.2016.02.004

Feng Q, Lin Y (2017) Integrated processes of anaerobic digestion and pyrolysis for higher bioenergy recovery from lignocellulosic biomass: A brief review. Renew Sustain Energy Rev 77:1272–1287. https://doi.org/10.1016/j.rser.2017.03.022

Fonts I, Gea G, Azuara M, et al (2012) Sewage sludge pyrolysis for liquid production: A review. Renew Sustain Energy Rev 16:2781–2805. https://doi.org/10.1016/j.rser.2012.02.070

Gai C, Zhang Y, Chen WT, et al (2015) Characterization of aqueous phase from the hydrothermal liquefaction of Chlorella pyrenoidosa. Bioresour Technol 184:328–335. https://doi.org/10.1016/j.biortech.2014.10.118

Guyot JP, Ferrer H, Florina R (1995) Methane production from acetamide in an upflow anaerobic sludge-blanket reactor based on a synergistic association between an aerobic rod and methanogens. Appl Microbiol Biotechnol

43:1107–1111. https://doi.org/10.1007/BF00166933

Hübner T, Mumme J (2015) Integration of pyrolysis and anaerobic digestion – Use of aqueous liquor from digestate pyrolysis for biogas production. Bioresour Technol 183:86–92. https://doi.org/10.1016/j.biortech.2015.02.037

Kimbell LK, Kappell AD, McNamara PJ (2018) Effect of pyrolysis on the removal of antibiotic resistance genes and class I integrons from municipal wastewater biosolids. Environ Sci Water Res Technol 4:1807–1818. https://doi.org/10.1039/c8ew00141c

Li P, Ailijiang N, Cao X, et al (2015) Pretreatment of coal gasification wastewater by adsorption using activated carbons and activated coke. Colloids Surfaces A Physicochem Eng Asp 482:177–183. https://doi.org/10.1016/j.colsurfa.2015.05.006

Liaw S-S, Justo O, Perez V, et al (2016) Ozonation of Pyrolytic Aqueous Phase: Changes in the Content of Phenolic Compounds and Color. Chem Eng Technol 39:1828–1834. https://doi.org/10.1002/ceat.201500420

Liu Z, Mayer BK, Venkiteshwaran K, et al (2020) The state of technologies and research for energy recovery from municipal wastewater sludge and biosolids. Curr. Opin. Environ. Sci. Heal. 14:31–36

Liu Z, McNamara P, Zitomer D (2017) Autocatalytic Pyrolysis of Wastewater Biosolids for Product Upgrading. Environ Sci Technol 51:9808–9816. https://doi.org/10.1021/acs.est.7b02913

Liu Z, Singer S, Tong Y, et al (2018) Characteristics and applications of biochars derived from wastewater solids. Renew Sustain Energy Rev 90:650–664. https://doi.org/10.1016/j.rser.2018.02.040

Madigou C, Poirier S, Bureau C, Chapleur O (2016) Acclimation strategy to increase phenol tolerance of an anaerobic microbiota. Bioresour Technol 216:77–86. https://doi.org/10.1016/j.biortech.2016.05.045

McNamara PJ, Koch JD, Liu Z, Zitomer DH (2016) Pyrolysis of Dried Wastewater Biosolids Can Be Energy Positive. Water Environ Res 88:804–810. https://doi.org/10.2175/106143016X14609975747441

Owen WF, Stuckey DC, Healy JB, et al (1979) Bioassay for monitoring biochemical methane potential and anaerobic toxicity. Water Res 13:485–492. https://doi.org/10.1016/0043-1354(79)90043-5

Ramirez F, Monroy O, Favela E, et al (1998) Acetamide Degradation by a Continuous-Fed Batch Culture of Bacillus sphaericus. In: Biotechnology for Fuels and Chemicals. Humana Press, pp 215–223

Ross JJ, Zitomer DH, Miller TR, et al (2016) Emerging investigators series: Pyrolysis removes common microconstituents triclocarban, triclosan, and nonylphenol from biosolids. Environ Sci Water Res Technol 2:282–289. https://doi.org/10.1039/c5ew00229j

Rover MR, Brown RC (2013) Quantification of total phenols in bio-oil using the Folin – Ciocalteu method. J Anal Appl Pyrolysis 104:366–371. https://doi.org/10.1016/j.jaap.2013.06.011

Seyedi S (2018) Anaerobic Co-digestion of Aqueous Liquid from Biosolids Pyrolysis. Master's Thesis. Marquette University. Milwaukee, WI. USA

Seyedi S, Venkiteshwaran K, Benn N, Zitomer D (2020) Inhibition during Anaerobic Co-Digestion of Aqueous Pyrolysis Liquid from Wastewater Solids and Synthetic Primary Sludge. Sustainability 12:3441. https://doi.org/10.3390/su12083441

Seyedi S, Venkiteshwaran K, Zitomer D (2018) Anaerobic Co-Digestion of Condensate from Biosolids Pyrolysis. In: WEF Residuals and Biosolids Conference 2018

Seyedi S, Venkiteshwaran K, Zitomer D (2019) Toxicity of Various Pyrolysis Liquids From Biosolids on Methane Production Yield. Front Energy Res 7:1–12. https://doi.org/10.3389/fenrg.2019.00005

Si B, Yang L, Zhou X, et al (2019) Anaerobic conversion of the hydrothermal liquefaction aqueous phase: Fate of organics and intensification with granule activated carbon/ozone pretreatment. Green Chem 21:1305–1318. https://doi.org/10.1039/c8gc02907e

Torri C, Fabbri D (2014) Biochar enables anaerobic digestion of aqueous phase from intermediate pyrolysis of biomass. Bioresour Technol 172:335–341. https://doi.org/10.1016/j.biortech.2014.09.021

USEPA (1999) Biosolids Generation, Use, and Disposal in The United States

Watson J, Wang T, Si B, et al (2020) Valorization of hydrothermal liquefaction aqueous phase: pathways towards commercial viability. Prog. Energy Combust. Sci. 77:100819

Watson J, Zhang Y, Si B, et al (2018) Gasification of biowaste: A critical review and outlooks. Renew. Sustain. Energy Rev. 83:1–17

Wen C, Moreira CM, Rehmann L, Berruti F (2020) Feasibility of anaerobic digestion as a treatment for the aqueous pyrolysis condensate (APC) of birch bark. Bioresour Technol 307:123199. https://doi.org/10.1016/j.biortech.2020.123199

Xu J, Jiang J, Dai W, et al (2011) Bio-oil upgrading by means of ozone oxidation and esterification to remove water and to improve fuel characteristics. Energy and Fuels 25:1798–1801. https://doi.org/10.1021/ef101726g

Yang L, Si B, Martins MA, et al (2018a) Improve the biodegradability of post-hydrothermal liquefaction wastewater with ozone: Conversion of phenols and N-heterocyclic compounds. Water Sci Technol 248–255. https://doi.org/10.2166/wst.2018.108

Yang L, Si B, Tan X, et al (2018b) Integrated anaerobic digestion and algae cultivation for energy recovery and nutrient supply from post-hydrothermal liquefaction wastewater. Bioresour Technol 266:349–356. https://doi.org/10.1016/j.biortech.2018.06.083

Yang Y, Heaven S, Venetsaneas N, et al (2018c) Slow pyrolysis of organic fraction of municipal solid waste (OFMSW): Characterisation of products and screening of the aqueous liquid product for anaerobic digestion. Appl Energy 213:158–168. https://doi.org/10.1016/j.apenergy.2018.01.018

Yao Y, Xie Y, Zhao B, et al (2020) N-dependent ozonation efficiency over nitrogen-containing heterocyclic contaminants: A combined density functional theory study on reaction kinetics and degradation pathways. Chem Eng J 382:122708. https://doi.org/10.1016/j.cej.2019.122708

Zhou H, Brown RC, Wen Z (2019) Anaerobic digestion of aqueous phase from pyrolysis of biomass: Reducing toxicity and improving microbial tolerance. Bioresour Technol 292:. https://doi.org/10.1016/j.biortech.2019.121976

Zhu H, Ma W, Han H, et al (2018) Degradation characteristics of two typical N-heterocycles in ozone process: Efficacy, kinetics, pathways, toxicity and its application to real biologically pretreated coal gasification wastewater. Chemosphere 209:319–327. https://doi.org/10.1016/j.chemosphere.2018.06.067

Zitomer DH, Adhikari P, Heisel C, Dineen D (2008) Municipal anaerobic digesters for codigestion, energy recovery, and greenhouse gas reductions. Water Environ Res 80:229–237. https://doi.org/10.2175/106143007X221201

4 Pre-ozonation and inocula selection increased quasi steady state methanogenesis using aqueous phase from sludge pyrolysis

This chapter will be submitted to the journal *Water Research:*

Seyedi, S., Venkiteshwaran, K., Ocequera, B., Zitomer, D., (2020). Pre-ozonation and inocula selection increased quasi steady state methanogenesis using aqueous phase from sludge pyrolysis. *Water Research*.

4.1. Introduction

Continuous sludge production, with over 13 million tonnes/year of dry solids in the U.S. containing 80% w/w organic content, creates the need for sustainable and efficient sludge management strategies (Seiple et al., 2017; Skaggs et al., 2017). Conventionally, sludge is incinerated, landfilled or land applied (Tyagi and Lo, 2013). However, potential introduction of contaminants to the environment raises concerns about conventional solids management methods (Tyagi and Lo, 2013). Wastewater solids pyrolysis involves heating to 400 – 900 °C in the absence of oxygen and offers several benefits including reduction of solids volume, removal of contaminants such as micropollutants, antibiotic resistance genes as well as pathogens, and possible energy recovery (Liu et al., 2018; Ross et al., 2016b). Wastewater solids pyrolysis products include: biochar, py-gas, and pyrolysis liquid (Liu et al., 2018, 2017; McNamara et al., 2016). The biochar can be used as a soil amendment and an absorbent (Carey et al., 2015; Hoffman et al., 2016; Liu et al., 2018; McNamara et al., 2016). Py-gas is an energy source consisting of methane (CH_4), carbon monoxide (CO), carbon dioxide (CO_2), hydrogen gas (H_2) and other constituents that can be combusted on-site at water resource recovery facilities (WRRFs) (Domínguez et al., 2006; McNamara et al., 2016).

Pyrolysis liquid often contains two phases: bio-oil, which is a light non-aqueous organic phase, and an aqueous phase referred to as aqueous pyrolysis liquid (APL) (Liu et al., 2020). Bio-oil can be utilized as a renewable fuel for heat and power generation in boilers or diesel engines. However, raw bio-oil requires upgrading due to undesirable properties including instability and corrosiveness

(Feng and Lin, 2017; Ul Islam et al., 2015). As opposed to bio-oil, there are no beneficial uses for APL. APL has a high chemical oxygen demand (COD) (30 to 500 gCOD/L) and contains organic compounds including carboxylic acids, aldehydes, phenols, and nitrogenous organics that can be environmentally detrimental (Seyedi et al., 2020; Wen et al., 2020; Zhou et al., 2019). APL yield can be 70 to 100% of the total weight of the pyrolysis liquids and up to 60% of the original carbon in the solids, thus requiring careful management of large quantities of this potentially hazardous liquid (Liu et al., 2017; Lü et al., 2018; Mukarakate et al., 2017; Torri and Fabbri, 2014).

One potential method to recover energy in APL is anaerobic digestion (AD). AD is the biochemical conversion of organic material into biogas containing methane and is carried out by anaerobic microorganisms (Venkiteshwaran et al., 2016a). APL from wastewater solids could be used as a substrate in AD because it often contains a high concentration of acetic acid (approximately 25 g/L) that is easily converted to methane (Seyedi et al., 2019, 2018). However, APL also contains some problematic organic compounds such as phenolics and nitrogenous organics that are known to inhibit methane-producing microbes and reduce or stop methane generation (Hübner and Mumme, 2015; Seyedi et al., 2019; Si et al., 2019; Yu et al., 2020b). Due to its toxicity, using APL as the sole substrate (mono-digestion) may be challenging and not practical and it may require high dilutions to preclude toxicity. Therefore, APL could be used as a co-digestate along with a primary substrate. Anaerobic co-digestion involves treating a mixture of two or more organic wastes, commonly high-organic-strength wastes, to produce more

biogas and utilize the maximum capacity of an existing digester (Zitomer et al., 2008). In fact, APL co-digestion can be a potential method to overcome its toxicity since APL toxicity will be reduced when blended with the primary substrate. Furthermore, it would be beneficial if APL from wastewater solids pyrolyzed at WRRFs that already have digesters treating sludge could be added as a co-digestate.

Previous studies have investigated using APL in AD for methane production and have described the associated challenges due to toxicity (Chen et al., 2019, 2017; Seyedi et al., 2020; Torri and Fabbri, 2014; Zhou et al., 2019). Yu et al. (2020) observed that co-digestion of dilute APL (1:4 v/v APL:digester liquid) with swine manure reduced methane production by 77%. When biochar was added to help reduce toxicity, APL from pine wood pyrolyzed at 400 °C was degraded at 0.25 gCOD/L-day in an upflow anaerobic sludge blanket (UASB) (Torri et al., 2020). However, increasing the organic loading rate (OLR) to 1.25 gCOD/L-day reduced APL conversion to methane by up to 70%. Approximately 45% of the APL carbon was reported to be nondegradable under the conditions studied (Torri et al., 2020). Methane production was also inhibited at an OLR of 0.05 gCOD/L-d in continuous co-digestion of APL derived from wastewater solids at 800 °C with synthetic primary sludge using an unacclimated anaerobic biomass (Seyedi et al. 2020) (See Appendix B).

Pretreatment of APL organics by ozone may be an option to reduce APL toxicity by oxidizing organics to more biodegradable, less toxic products for subsequent AD. Biorefractory compounds such as phenols, amines, and

unsaturated organics that are commonly detected in the APL have been shown to be oxidized through direct or indirect ozone oxidation (Eggen and Vogelsang 2015; Seyedi et al. 2019; Yao et al. 2020) and converted into more easily degradable compounds (Alvares et al. 2001). Therefore, APL ozonation is hypothesized to transform APL constituents to more biodegradable compounds that could be anaerobically digested. APL pretreatment using ozone has shown promising results in batch anaerobic toxicity assays (ATAs) as shown in Chapter 3. However, long-term digestion of ozonated APL derived from wastewater solids has not yet been reported. Others have used pretreatment by overliming APL produced from corn stover pyrolysis at 500 °C and observed a 70% increase in biogas production when APL loading was increased from 6% to 18%, but biogas production decreased and eventually stopped at higher organic loadings.

The use of appropriate inocula may be another method to manage APL toxicity and increase methane production. Utilizing inocula that is exposed to constituents similar to those in APL could decrease start-up time and increase methane production. For example, long term acclimation of a microbiome (over 500 days) to APL resulted in increased methane production and doubling the microbial tolerance (Seyedi et al., 2020). Hence, it was hypothesized that a methanogenic culture already acclimated to one or more APL constituents would enhance methane production from APL.

In this study, the first objective was to ozonate APL prior to AD in an effort to partially oxidize the recalcitrant APL organics and reduce the toxicity exerted on anaerobic microbes. Subsequently, long-term, quasi steady state anaerobic mono-

digestion of ozonated and non-ozonated APL alone, as well as co-digestion using ozonated and non-ozonated APL with synthetic primary sludge were evaluated in the second objective. Inocula from full-scale anaerobic digesters treating both municipal and industrial wastewater were employed to assess the capability of different microbial communities to degrade APL constituents. It was hypothesized that ozone would convert the biorefractory constituents such as N-heterocyclic and phenolic compounds in the APL into more easily degradable compounds, therefore, ozonated APL would be converted to methane more completely than non-ozonated APL. Additionally, the acclimated microbiome could contain appropriate taxa that can degrade some APL organics, therefore, be more appropriate than a municipal inocula not acclimated to the specific compounds. Hence, it was hypothesized that using an inoculum that was previously exposed to constituents similar to those in APL (industrial inoculum) would result in more complete APL conversion to methane in the timeframe of the study (7 months).

4.2. Materials and methods

4.2.1. APL production and ozonation

APL was generated at 700°C by pyrolysis of a commercially available soil amendment, Milorganite ®, composed of dried anaerobically digested primary and raw waste activated sludge from municipal wastewater (Liu et al., 2017).

APL ozonation was carried out following methods described in Chapter 3. Briefly, ozonation was performed employing a 500 mL lab-scale bubble column reactor containing a diluted APL sample at a pH adjusted to 11 using 6 N NaOH in

order to increase hydroxyl radical formation for advanced oxidation. A pure oxygen flow rate of 4 L/min (1 atm, 20 °C) was supplied to an ozone generator (LAB2B, Ozonia, Leonia, NJ) and the resulting gas ozone concentration was 20 ± 2 mg/L. The ozonated gas was sparged through APL for either 10 min or 2 h. Ozone concentration in feed gas and off gas from the bubble column reactor was measured using a UV-ozone analyzer (Model 106-H, 2B Technologies, Boulder, CO, USA).

4.2.2. Anaerobic digesters

Thirteen sets of triplicate anaerobic digesters were operated using two different anaerobic inocula (Table 4.1). Digesters were 160 mL serum bottles capped with butyl rubber stoppers and incubated at 35 °C on a shaker table at 150 rpm. Five digester sets were inoculated with municipal anaerobic digester biomass (municipal biomass; MB) from South Shore Water Reclamation Facility (Oak Creek, WI). The remaining digester sets were inoculated with biomass from a UASB in the southeast US treating petrochemical wastewaters containing organic acids including phenolic/aromatic and carboxylic acids (industrial biomass; IB). Control digesters received only synthetic primary sludge (see Table 4.1). Ozonation for 2 h removed some NH_3-N from the APL, ostensibly by gas stripping (non-ozonated APL NH_3-N = 52 ± 2 g/L, ozonated APL NH_3-N = 25 ± 0.4 g/L). In order to distinguish the influence of lower NH_3-N concentration from other ozonation effects, some digesters received 2 h ozonated APL to which ammonium chloride was added to return the NH_3-N to the concentration observed before ozone was applied (Table 4.1).

Table 4.1. Description of mono-digesters and co-digesters [1]

Digester set	Inocula	APL co-digestate 1	Co-digestate 2
1-1	Industrial	Non-ozonated	None
1-2	Industrial	10 min ozonated	None
1-3	Industrial	2 h ozonated	None
1-4	Industrial	2 h ozonated + NH_3-N	None
2-1 (Control 1)	Municipal	None	Synthetic sludge
2-2	Municipal	Non-ozonated	Synthetic sludge
2-3	Municipal	10 min ozonated	Synthetic sludge
2-4	Municipal	2 h ozonated	Synthetic sludge
2-5	Municipal	2 h ozonated + NH_3-N	Synthetic sludge
3-1 (Control 2)	Industrial	None	Synthetic sludge
3-2	Industrial	Non-ozonated	Synthetic sludge
3-3	Industrial	10 min ozonated	Synthetic sludge
3-4	Industrial	2 h ozonated	Synthetic sludge
3-5	Industrial	2 h ozonated + NH_3-N	Synthetic sludge

[1] All digester systems were operated in triplicate.

4.2.2.1. 15-d SRT digestion

The digestion study was carried out at two different SRTs and OLRs. First, digesters were operated at a 15-d SRT by feeding either (1) 0.2 gCOD/L-d of ozonated and non-ozonated APLs as the sole substrate (digester sets 1-1 to 1-4), (2) 2.5 gCOD/L-d of synthetic primary sludge (digester sets 2-1 and 3-1, i.e. control 1 and control 2), or (3) both APL and synthetic primary sludge together (co-digester sets 2-2 to 2-5 and 3-2 to 3-5). These digesters were operated for 3 SRTs (45 days) under consistent conditions to reach quasi steady state operation when digester performance such as daily methane production rate variations are less than 10%. All digesters were then continued for 15 more days to monitor the

digester performance during quasi steady state. APL pH was typically high (~10); Therefore, feed pH was adjusted to ~7 with NaOH addition.

4.2.2.2. 210-d SRT digestion

In the long-term trial, digesters were operated at a 210-d SRT by feeding either (1) 0.03 gCOD/L-d of the various APLs (digester sets 1-1 to 1-4), (2) 0.18 gCOD/L-d of synthetic primary sludge (control 1 and control 2), or (3) both co-digestates together (co-digester sets 2-2 to 2-5 and 3-2 to 3-5). These digesters were run for 1 SRT (210 days) to reach quasi steady state. All digesters were continued for 15 more days to monitor the digester performance during quasi steady state. APL pH was also adjusted to ~7 with NaOH addition.

4.2.3. Synthetic primary sludge

Synthetic primary sludge was ground, dry dog food (Nutro Natural Choice, Franklin, TN, USA) sieved to 150 μm <particle size< 250 μm and mixed with basal nutrients with the following concentrations [mg/L]: NH_4Cl [400]; $MgSO_4 \cdot 7H_2O$ [400]; KCl [400]; $Na_2S \cdot 9H_2O$ [300]; $CaCl_2 \cdot 2H_2O$ [50]; $(NH_4)_2HPO_4$ [80]; $FeCl_3 \cdot 4H_2O$ [10]; $CoCl_2 \cdot 6H_2O$ [1.0]; $ZnCl_2$ [1.0]; KI [10]; $(NaPO_6)_6$ [10]; the trace metal salts: $MnCl_2 \cdot 4H_2O$, NH_4VO_3, $CuCl_2 \cdot 2H_2O$, $AlCl_3 \cdot 6H_2O$, $Na_2MoO_4 \cdot 2H_2O$, H_3BO_3, $NaWO_4 \cdot 2H_2O$, and Na_2SeO_3 [each at 0.5]; cysteine [10] and yeast extract [100]. Synthetic primary sludge was employed according to previous studies as a consistent substrate to avoid inconsistencies inherent when using real primary sludge (Benn and Zitomer, 2018; Carey, 2016; Inaba et al., 2020).

4.2.4. Abiotic controls

Abiotic controls were prepared in triplicate by adding 50 mL of digester feed to 160 mL serum bottles capped with butyl rubber stoppers and incubated at 35 °C on a shaker table at 150 rpm. To stop biological activity, 3 g/L of NaN_3 was added as described by others (Prandini et al., 2016). Digester sets 2 and 3 abiotic controls also contained MB solids, whereas abiotic controls for set 1 contained IB solids at the same volatile suspended solids (VSS) concentrations as the active digesters. Abiotic control effluents were analyzed by gas chromatography-mass spectrophotometry (GC-MS) after one week of incubation and were compared to active digester effluents at quasi steady state.

4.2.5. Analytical methods and digester performance

Biogas volume was measured using a 100 mL wetted-barrel glass syringe by inserting a needle through the respective serum bottle butyl rubber stopper. Biogas methane concentration was measured by gas chromatography (GC System 7890A, Agilent Technologies, Irving, TX, USA) with a thermal conductivity detector (GC-TCD). The pH was measured using a pH probe (Orion 4 Star, Thermo, Waltham, MA, USA). Total suspended solids (TSS), VSS and COD concentrations were measured using standard methods (American Public Health Association, 1998). The soluble COD (SCOD) concentration was measured by filtering the digestate through a 0.45 µm pore size syringe filter and measuring filtrate COD. Volatile fatty acids (VFAs) concentration in the filtrate was measured using gas chromatography (GC System 7890A, Agilent Technologies, Irving, TX, USA) with a flame ionization detector (FID). Dissolved organic carbon (DOC)

concentration before and after ozonation was assessed using a total organic carbon (TOC) analyzer after filtering and acidifying the samples (American Public Health Association 1998) (TOC-V, Shimadzu, Japan). The aromaticity of APL constituents before and after ozonation were measured through SUVA by measuring the UV absorbance at 254 nm (UV_{254}) using a spectrophotometer (Genesys 10S UV-Vis spectrophotometer, Thermo Scientific, USA) and normalizing it by DOC concentration (Chaparro et al., 2010). Total phenolics (TP) was determined according to the micro-scale Folin–Ciocalteu method (Folin and Ciocalteu, 1927; Rover & Brown, 2013).

The APL constituents were characterized by peak areas using a GC-MS system (HP-7890A GC with a 5975A mass selective detector) equipped with an HP-5MS column with 30m × 0.25mm ID × 1.0μm film thickness (HP5-MS column, Agilent Technologies). The injection volume was 0.5 μL with a split ratio of 5:1. The oven was programmed with an initial temperature of 50 °C for 1 min, ramped at 10 °C/min and a final temperature of 250 °C and 4 min final hold time. The flow rate was constant at 1.2 mL/min of the helium carrier gas.

4.2.6. DNA extraction and sequencing

Biomass samples were collected to investigate microbiome composition in the digesters. Approximately 1.8 mL of inocula biomass (before digestion) and biomass samples from digesters fed non-ozonated and 2 h ozonated APL on day 215 were taken and stored at −20 °C. DNA extractions were carried out using a commercial kit (DNeasy PowerLyzer PowerSoil Kit, Qiagen, USA) following the manufacturer’s procedures.

Forward and reverse primers (515F and 806R) were used to amplify the V4 region of bacterial and archaeal 16S rRNA genes (Fujimoto et al. 2019) and the PCR products were purified. Sequencing was done using the Illumina MiSeq sequencing platform with methods based on the bTEFAP® process (Dowd et al., 2008). Briefly, sequences were joined and those with <150 bp and ambiguous base calls were removed. Sequences were quality filtered and denoised and depleted from barcodes and primers. Unique sequences with sequencing and/or PCR point errors were deleted, followed by chimera removal. Exact sequence variant or zero-radius operational taxonomic units (zOTUs) were provided based on 100% sequence similarity (Porter and Hajibabaei, 2018) and final zOTUs were classified into taxonomic categories employing BLASTn against a curated database derived from NCBI (www.ncbi.nlm.nih.gov).

4.2.7. Statistical analysis

Statistical analyses including average, standard deviation, normality test, two-sample student's t-test calculations were performed using Microsoft Excel 2015. Analysis of variance (ANOVA) with post-hoc Tukey's multiple comparisons test were performed using R software. For microbial community analysis, dual hierarchical clustering (using R command hclust and heatmap) and principal coordinate analysis (PCoA) based on Bray-Curtis distance (using R command ordinate) employing the VEGAN package were performed using custom R scripts (Venkiteshwaran et al., 2016b). The PCoA clustering was performed based on a 95% confidence interval. Dual hierarchical clustering and heatmap construction were performed using the 20 dominant archaeal and 30 to 35 dominant bacterial

OTUs for digesters based on relative abundance values. The dominant OTUs were selected based on OTUs with >1% relative abundance in at least five co-digesters/one mono-digester. Alpha diversity indices (observed OTUs, Shannon and Chao1) were determined based on Illumina sequence results as described by Falk et al. (2009) using the R command estimate_richness.

4.3. Results and discussion

4.3.1. Raw and ozonated APL composition

Ozonation significantly altered APL composition. TP concentration and SUVA, both of which are positively correlated to anaerobic microorganism inhibition decreased considerably (Table 4.2). More than 60% of the TP reduction was achieved in the first 10 min of ozonation. SUVA was also reduced in APLs after ozonation by more than 35% and 60% in 10 min and 2 h ozonated APL, respectively, signifying a decrease in aromaticity and molecular weight of the organics which are favorable for AD (Chaparro et al., 2010; Li et al., 2015).

Other APL constituent concentrations were also changed by ozonation. The NH_3-N concentration after 10 min ozonation did not change (p=0.4, n=6), but after 2 h ozonation, more than 50% of the NH_3-N was removed that could be due to gas stripping (Table 4.2). APL ozonation for 10 min resulted in no COD reduction (p=0.07, n=6), whereas 2 h ozonation reduced COD by 17 ± 0.1% (p=0.00, n=6) (Table 4.2). COD removal could be due to oxidation or gas stripping of volatile organics into the atmosphere. DOC concentration decreased 11 ± 0.3% and 16 ± 1% in 10 min and 2 h ozonated APLs, respectively. Decreased DOC indicates

mineralization or gas stripping of APL organics occurred. The APL VFA concentration after 10 min ozonation decreased by more than 20%, but after 2 h ozonation, it was statistically similar to non-ozonated APL VFA concentration ($p=0.09$, $n=4$). The APL pH was raised to 11 prior to ozonation to increase hydroxyl radical generation and it did not change after 10 min ozonation. However, the pH decreased to 10.0 ± 0.01 after 2 h ozonation, indicating possible production of acids.

Table 4.2. APL composition before and after ozonation

APL	TP (mg/L gallic acid equivalent)	SUVA (L/mg-m)	COD (g/L)	NH_3-N (g/L)	Total VFA concentration (expressed as g/L of acetic acid)	DOC (g/L)
Non-ozonated	1650 ± 0.00	6.1 ± 0.0	186 ± 3.7	52 ± 2.0	20 ± 5.9	74 ± 0.5
10 min ozonated	544 ± 7.7	3.8 ± 0.2	180 ± 3.0	54 ± 4.0	15 ± 1.1	65 ± 0.2
2 h ozonated	281 ± 1.5	2.2 ± 0.2	155 ± 3.1	25 ± 0.4	16 ± 1.4	62 ± 0.8
2 h ozonated + NH_3-N	281 ± 1.5	2.2 ± 0.2	155 ± 3.1	52 ± 2.0	16 ± 1.4	62 ± 0.8

Ozonation removed some APL organic compounds partially or completely after 10 min and 2 h that could result in lower APL toxicity in subsequent AD. The majority of APL constituents identified by GC-MS analysis were N-heterocyclic organics such as acetamide, pyrrole, 2-pyrrolidinone, pyridine, 2-aminopyridin, and 3-pyridinol (Figure S4.1). Sewage sludge as the pyrolysis feedstock can have high protein content and, therefore, result in high nitrogen content of resulting APL. N-heterocyclic compounds can be produced during Maillard reaction in which amino acids, the products of protein hydrolysis, react with reducing sugars from

hydrolysis of hydrocarbons and form nitrogenous organics including pyrrole, pyrrolidinone, pyridine, and their derivatives (Gai et al., 2015).

After 2 h ozonation, many compounds including pyrrole, pyridine, pyridine 2-methyl, 2-aminopyridine, 3-pyridinol, nitroacetamide, 2-pyridinamine 5-methyl-acetamide, and L-valine methyl ester were below GC-MS detection (Figure S4.1). However, three compounds that were not present in the non-ozonated APL (guanidine N,N-dimethyl, propanamide 2-hydroxy, and 1H-Imidazole 1-methyl-4-nitro) were detected after 2 h ozonation. In addition, the amount of some constituents such as fampridine and butanamide 3-methyl increased after 10 min ozonation but decreased after 2 h ozonation. Removal of these potential inhibitory compounds could ostensibly result in improved methane production in subsequent digestion.

4.4. Long-term digestion

4.4.1. 15-d SRT digestion performance

The co-digesters operated at a 15-d SRT did not perform well, as demonstrated by their operational parameters such as methane production and digestate COD and VFA concentrations (Table S4.1). The poor performance could be due to the short SRT and high OLR not providing the microorganisms sufficient time to degrade the complex toxic organics. Methane production was extremely inhibited in all digesters (Figure 4.1). While daily methane production in control digesters (digester set 2-1 and 3-1 receiving only synthetic primary sludge and no APL) was >80% of the stoichiometric theoretical maximum amount (395 mL CH_4

per gCOD removed at 35 °C and 1 atm) for both inocula, co-digesters receiving ozonated or non-ozonated APL were inhibited (Figure 4.1). Corresponding to methane production results, digestate COD, SCOD and VFA concentrations in digestate increased in inhibited co-digesters (Table S4.1). Mono-digesters stopped producing biogas after about 20 days of operation (data not shown).

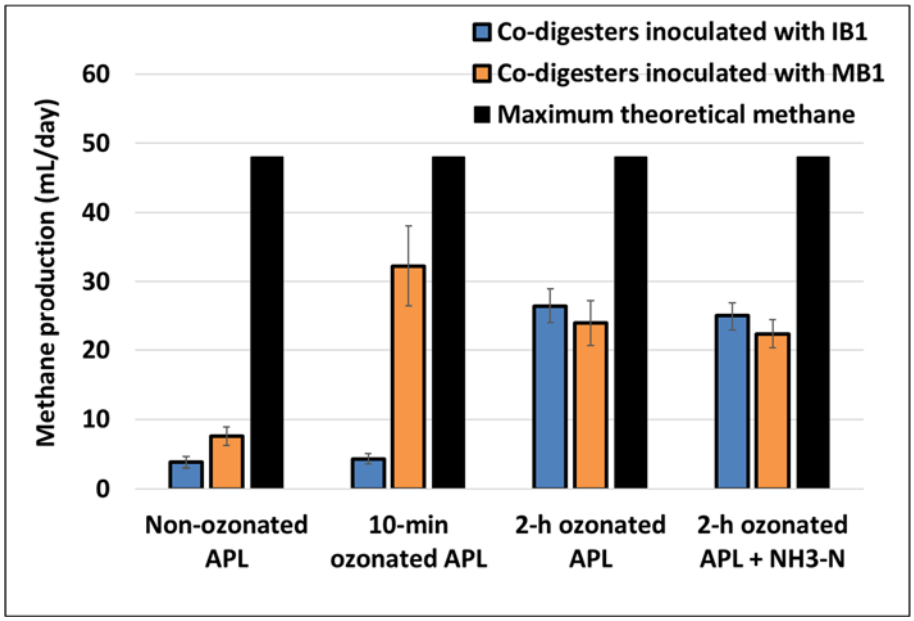

Figure 4.1. Quasi steady state methane production at 15-d SRT. Maximum stoichiometric methane from APL and synthetic primary sludge COD is shown in black bars. Error bars represent standard deviation from triplicate systems.

4.4.2. 210-d SRT digestion performance

In an attempt to increase APL conversion to methane, the SRT was increased to 210 days and the OLR was decreased to 0.03 gCOD/L of APL in all digesters. After the change, APL was anaerobically digested under the new conditions. With the longer SRT and lower OLR, methane production in mono-digesters and co-digesters receiving different APLs was not inhibited. In fact, APL

organics were converted into methane during mono-digestion and co-digestion, producing almost all of the stoichiometric maximum methane anticipated from APL COD loading.

4.4.2.1. Co-digesters performance

Co-digesters reached quasi steady state, indicated by <10% variation in methane production rate over time in about 160 days (day 163 – 226). During quasi steady state (day 163 – 226), all co-digesters receiving synthetic primary sludge and all types of APL produced statistically more methane ($p<0.05$, $n=24$) than corresponding control digesters receiving synthetic primary sludge alone (Figure S4.2A and S4.2B). Co-digesters inoculated with IB receiving non-ozonated (3-2), 10 min ozonated (3-3), and 2 h ozonated APL (3-4), produced 60 ± 32%, 79 ± 32%, and 98 ± 29 of the maximum stoichiometric theoretical methane that was expected from the APL COD during quasi steady state, respectively (Figure 4.2A and B). These results indicate that co-digesters receiving 2 h ozonated APL (3-4) exhibited the highest methane production ($p=0.03$, $n=6$), followed by 10 min ozonated (3-3) and non-ozonated APL (3-2) which were statistically similar ($p=0.68$, $n=6$). Co-digesters inoculated with MB receiving non-ozonated (2-2), 10 min ozonated (2-3), and 2 h ozonated APL (2-4) generated 48 ± 28%, 55 ± 24%, and 64 ± 28%, respectively, of the maximum stoichiometric theoretical methane expected from the APL COD during quasi steady state, which were statistically similar to each other ($p=0.5$, $n=9$) (Figure 4.2A and B). Therefore, ozonation did not have a substantial effect on methane production from co-digesters inoculated with MB.

Ozonation resulted in destruction of APL constituents and was the primary cause in reducing APL toxicity, and NH_3-N reduction due to ozonation was not the reason for APL toxicity reduction. Co-digesters receiving 2 h ozonated APL + NH_3-N inoculated with MB (2-5) and IB (3-5) generated 83 ± 20% and 57 ± 26% of the stoichiometric theoretical methane expected from the APL COD, respectively, which were statistically similar to that of the corresponding co-digesters fed 2 h ozonated APL (2-4 and 3-4) ($p=0.09$ and 0.6, $n=8$), indicating ozonation of APL constituents was the main reason in reducing APL toxicity, and not NH_3-N.

The IB inoculum was more capable of converting APL organics to methane, whereas MB was more sensitive yet degraded some of the APL. The co-digesters inoculated with IB produced more methane from APL (60 – 98% of the expected theoretical maximum methane) than co-digesters inoculated with MB (48 – 64% of the expected theoretical maximum methane) (Figure 4.2A and B).

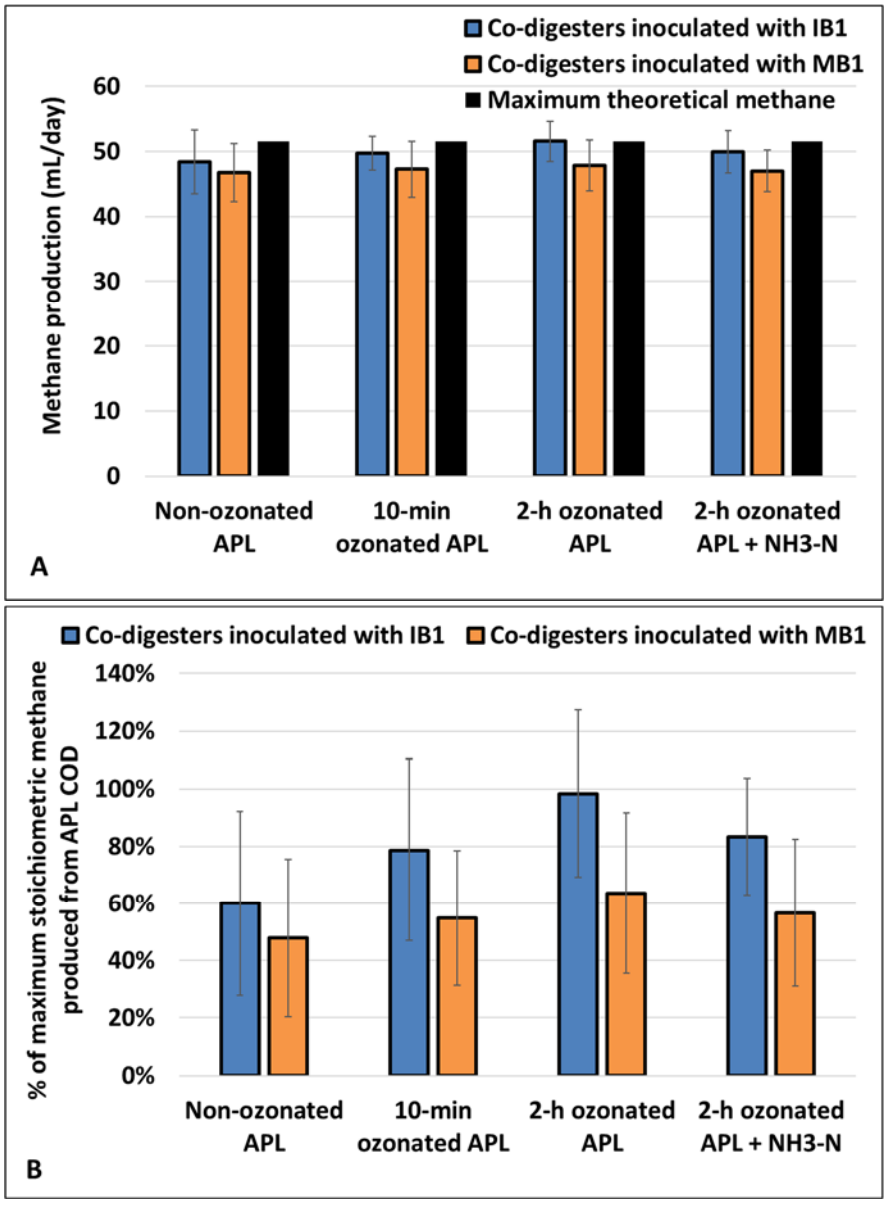

Figure 4.2. Quasi steady state methane production at 210-d SRT. (A) Methane production in co-digesters inoculated with IB and MB. Maximum stoichiometric methane from APL and synthetic primary sludge COD is shown in black bars. (B) Percent of maximum stoichiometric methane that is produced from APL COD in co-digesters inoculated with IB and MB. Error bars represent standard deviation from triplicate systems.

COD removals in co-digesters inoculated with IB receiving different ozonated or non-ozonated APL was statistically similar ($p>0.05$, $n=8$) to that of control digesters during quasi steady state (>35%) (Figure S4.3A). COD removal

in co-digesters inoculated with MB fed ozonated or non-ozonated APL ranged between 69 – 72%, while it was higher in control digesters (74 ± 5%) ($p<0.05$, n=8) (Figure S4.3A). VSS reduction in control digesters and co-digesters receiving different ozonated or non-ozonated APLs were statistically similar ranging between 70 – 75% in co-digesters inoculated with IB (Figure S4.4B). MB-inoculated co-digesters demonstrated 88 – 90% VSS reduction (Figure S4.4B). All co-digesters contained VFAs concentration below detection limit (<50 mg/L) during quasi steady state, except for the co-digester inoculated with MB fed non-ozonated APL which contained 125 ± 22 mg/L of acetic acid which is also low (Figure S4.7A).

Overall, continuous co-digestion results demonstrate that increased SRT and decreased OLR increased APL conversion to methane. Inocula selection was an important factor, with IB exhibiting better performance to degrade APL. In addition, ozonation enhanced APL degradability and consequently, increased methane production was observed from co-digesters receiving ozonated APL inoculated with IB. APL ozonated for 2 h resulted in highest methane production during co-digestion (98 ± 29%), followed by 10 min ozonated (79 ± 32%) and non-ozonated APL (60 ± 32%), but the latter two were not statistically different. On the other hand, no significant difference was observed among MB-inoculated co-digesters receiving ozonated or non-ozonated APL. The non-ozonated APL was observed to be degradable under the conditions provided (longer SRT and lower OLR), showing the acclimation capacity of the biomass to non-ozonated APL compounds and enhanced microbial tolerance. Co-digesting APL can improve biogas production at WRRFs that already have digesters treating sludge and

pyrolyze wastewater solids.

4.4.2.2. Mono-digesters performance

Mono-digesters also performed significantly better when the SRT was increased and OLR decreased such that more than 90% conversion of APL organics into methane was observed in all mono-digesters regardless of using ozonated or non-ozonated APL ($p>0.05$, $n=24$) (Figure 4.3 and S4.2C). Digesters receiving 2 h ozonated APL + NH_3-N (1-4) generated statistically similar methane to digesters receiving 2 h ozonated APL (1-3) ($p=0.89$, $n=6$), indicating that ozonation resulted in toxicity reduction of APL during digestion and NH_3-N reduction due to ozonation was not the main reason for APL toxicity reduction (Figure 4.3). During quasi steady state, digestate COD and SCOD concentrations were very low (<3 g/L) (Figure S4.5), and no VFAs were detected in the digestate (Figure S4.7B). VSS reduction of >80% was achieved in digesters (Figure S4.6B).

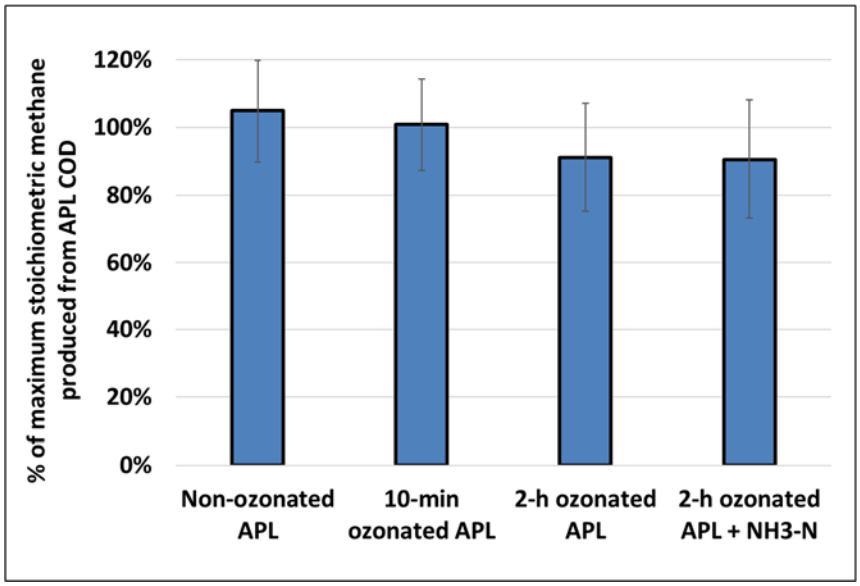

Figure 4.3. Quasi steady state methane production at 210-d SRT in mono-digesters. Percent of maximum stoichiometric methane that is produced from APL COD is shown. Error bars represent standard deviation from triplicate systems.

4.4.3. APL removal determined by GC-MS analysis

GC-MS results showed removal of the APL constituents occurred in both co-digesters and mono-digesters (Figure 4.4). While no constituents were detected in the digestate of co-digesters inoculated with either IB or MB (peaks were below detection limit of the GC-MS instrument ($<0.05\times10^6$)), twelve compounds were detected in the abiotic control effluent (Figure 4.4A). Similarly, no peaks were detected in mono-digesters digestate, but more than twenty peaks were identified in the abiotic control effluent (Figure 4.4B).

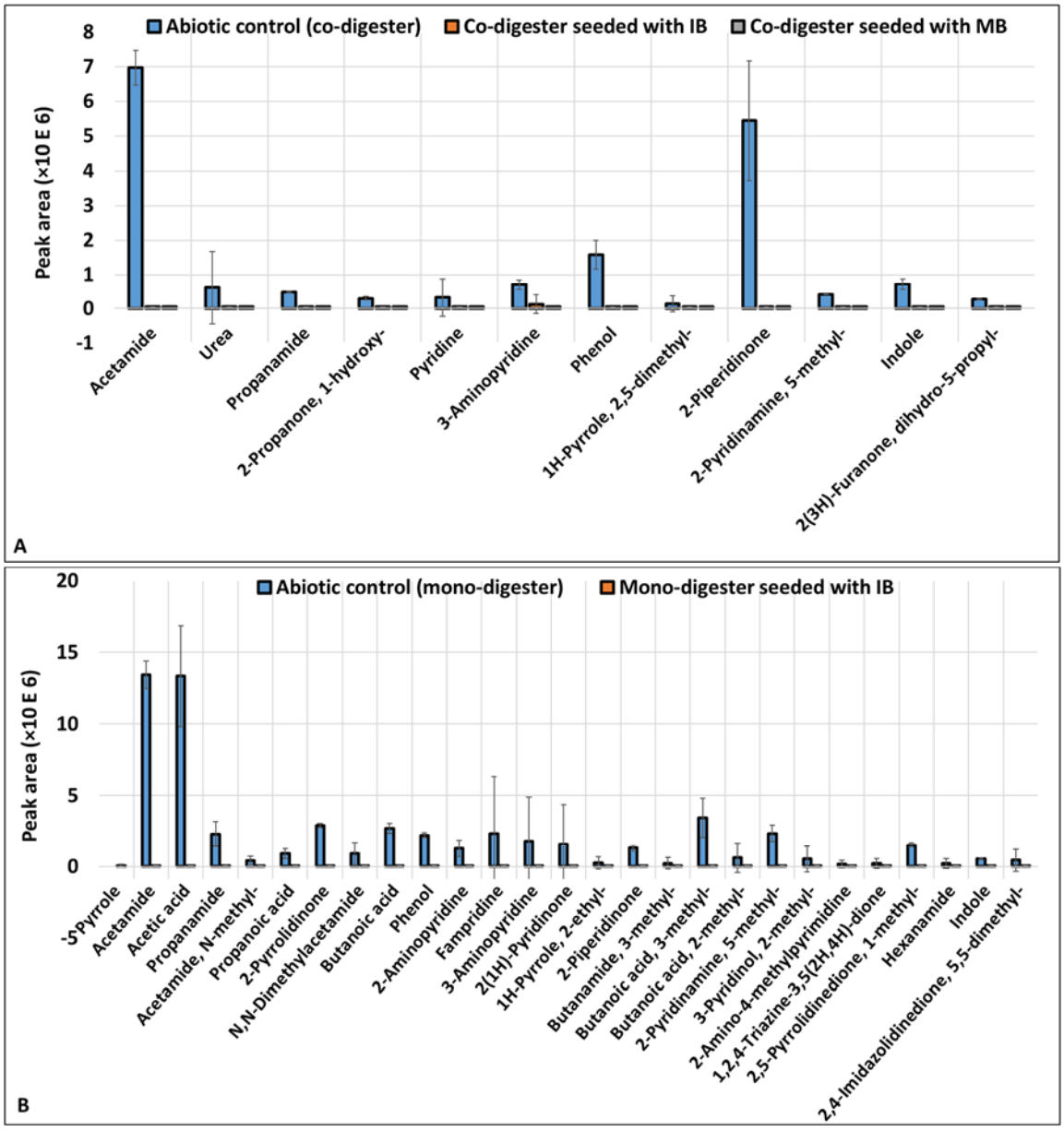

Figure 4.4. Organic compounds detected in abiotic controls and in co-digesters and mono-digesters receiving non-ozonated APL indicating complete biodegradation of APL compounds. Undetected peaks were below detection (BD) of the GC-MS instrument ($<0.05\times10^6$). The average and standard deviations are from triplicate sets. (A) No peaks were detected in co-digester digestate, whereas twelve peaks were identified in the abiotic control effluent sample, (B) More than twenty peaks were identified in abiotic control effluent sample, whereas no peaks were detected in mono-digesters digestate.

4.4.4. Microbial community analysis

4.4.4.1. Co-digesters

Illumina sequencing generated over 680,000 sequence reads in co-digesters with 29,030 ± 1152 reads per IB co-digester sample and 27,678 ± 970 reads per MB co-digester samples. Based on 97% similarity, a total of 1316 microbial OTUs were observed with an average of 526 ± 81 OTUs per IB co-digester and 495 ± 44 OTUs per MB co-digester. Microbial community compositions in MB and IB inocula were significantly different, clustering separately in both archaeal and bacterial PCoA plots (Figure 4.5 and 4.7).

After APL digestion, the archaeal and bacterial communities changed compared to the original inoculum communities (Table 4.3). Chao1 index increased in APL-fed co-digesters inoculated with IB compared to the IB original inocula, indicating a diversified community after APL digestion. Shannon index showed no statistical difference after digestion ($p>0.05$, $n=6$). In contrast, APL-fed co-digesters inoculated with MB exhibited lower (Shannon) or similar (Chao1) diversity compared to the MB original inoculum (Table 4.3). A highly diverse community is usually correlated with better digester performance and higher stability of the system (Carballa et al., 2015; Chen et al., 2020). Therefore, higher methane production in IB-inoculated digesters could be associated with higher microbial diversity. There were no statistical differences observed in Shannon and Chao1 index between the co-digesters receiving non-ozonated and ozonated APL in either IB or MB inoculated co-digesters ($p>0.05$, $n=6$).

Table 4.3. Alpha diversity indices in IB and MB inocula and in control digesters and co-digesters receiving ozonated and non-ozonated APL on day 215 of digestion. Average and standard deviations are from triplicate values.

	IB			MB		
Sample	**Observed OTUs**	**Chao1**	**Shannon**	**Observed OTUs**	**Chao1**	**Shannon**
Inocula	398 ± 2.3	437 ± 3.9	4.2 ± 0.06	543 ± 2.5	612 ± 8.9	4.7 ± 0.01
Control digester	553 ± 23	674 ± 36	3.7 ± 0.2	497 ± 13	589 ± 55	3.9 ± 0.06
Co-digester fed non-ozonated APL	553 ± 16	646 ± 46	3.9 ± 0.2	430 ± 22	547 ± 59	3.5 ± 0.13
Co-digester fed ozonated APL	602 ± 14	734 ± 21	4.1 ± 0.06	510 ± 4.2	614 ± 18	3.9 ± 0.11

4.4.4.1.1 Archaea community in co-digesters

An average of 66 ± 3 and 29 ± 7 archaeal OTUs in each digester with corresponding relative abundance of 29 ± 4.1% and 2.1 ± 1.1% of the total microbial community abundance were identified in co-digesters inoculated with IB and MB, respectively. Based on the pairwise Bray-Curtis dissimilarity distance, the archaeal community was altered after digestion in IB (76 ± 3% dissimilarity) and MB (64 ± 5% dissimilarity) digesters (Figure 4.5 and S4.8). Exposure to ozonated or non-ozonated APL shifted the archaeal community composition compared to control digester communities in IB (12 ± 0.2% dissimilarity) less than it shifted communities in MB co-digesters (31 ± 3.1% dissimilarity) (Figure S4.8). This indicates that feeding APL had a more significant effect on MB compared to IB co-digester archaeal community. In addition, archaeal communities in co-digesters fed non-ozonated and ozonated APL inoculated with IB were more similar to each other (4 ± 0.8% dissimilarity) than co-digesters fed non-ozonated and ozonated APL inoculated with MB (25 ± 4% dissimilarity) (Figure S4.8). So, APL ozonation

had a smaller impact on IB archaeal community compared to MB.

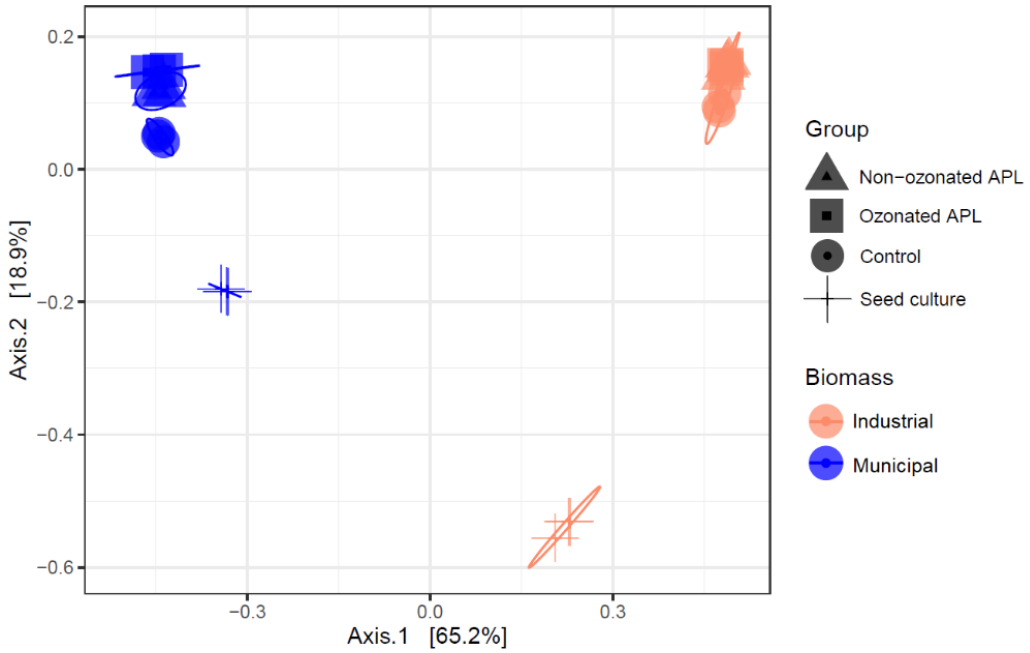

Figure 4.5. PCoA plot of archaeal community of IB and MB inocula (day 0) and co-digesters fed 2 h ozonated APL (day 215) based on Bray-Curtis distance. Ellipses represent 95% confidence intervals for the three points (each group represents the three triplicate digesters). IB and MB have distinctly different archaeal communities. APL co-digestion altered the archaeal community in both IB and MB inocula.

Methane production in IB-inoculated co-digesters was primarily through hydrogenotrophic archaea, whereas MB-inoculated co-digesters had both acetoclastic and hydrogenotrophic archaea active in methane production. There were 20 dominant archaeal OTUs that accounted for 87 ± 12% of total archaeal community relative abundance shown in the heatmap (Figure 4.6). Among them, the IB inoculum was dominated by genera *Methanospirillium* (OTU 23 and 11), *Methanolinea* (OTU 18), *Methanobacterium* (OTU 1) and family Methanotrichaceae (OTU 46) (Figure 4.6). After co-digestion, the IB digester communities were dominated by *Methanobacterium* (OTU 1) (80 ± 2% of total

archaeal community relative abundance) for which the relative abundance increased more than 400% compared to the inoculum, indicating that the hydrogenotrophic pathway of methane production was significant in all control and APL-fed co-digesters. On the other hand, the MB archaeal community was comprised of distinct *Methanolinea* (OTU 126) and *Methanosaeta* (OTU 29) genera, and the same *Methanospirillium* (OTU 23) genus as in IB (Figure 4.6). After co-digestion, *Methanosaeta* (OTU 29) was still dominant in the MB digester communities (22 ± 6% of total archaeal community relative abundance) in all co-digesters. *Methanosaeta* (OTU 345) relative abundance that was less than 0.04% in MB inoculum increased to more than 15% in co-digesters fed ozonated and non-ozonated APL (Figure 4.6). In addition, genera *Methanoculleus* (OTU 111) and *Methanobacterium* (OTU 178) that had <1% relative abundance, increased to more than 15% in relative abundance during co-digestion in all systems (Figure 4.6). This suggests that both acetoclastic and hydrogenotrophic pathways for methane production were utilized in MB-inoculated co-digesters.

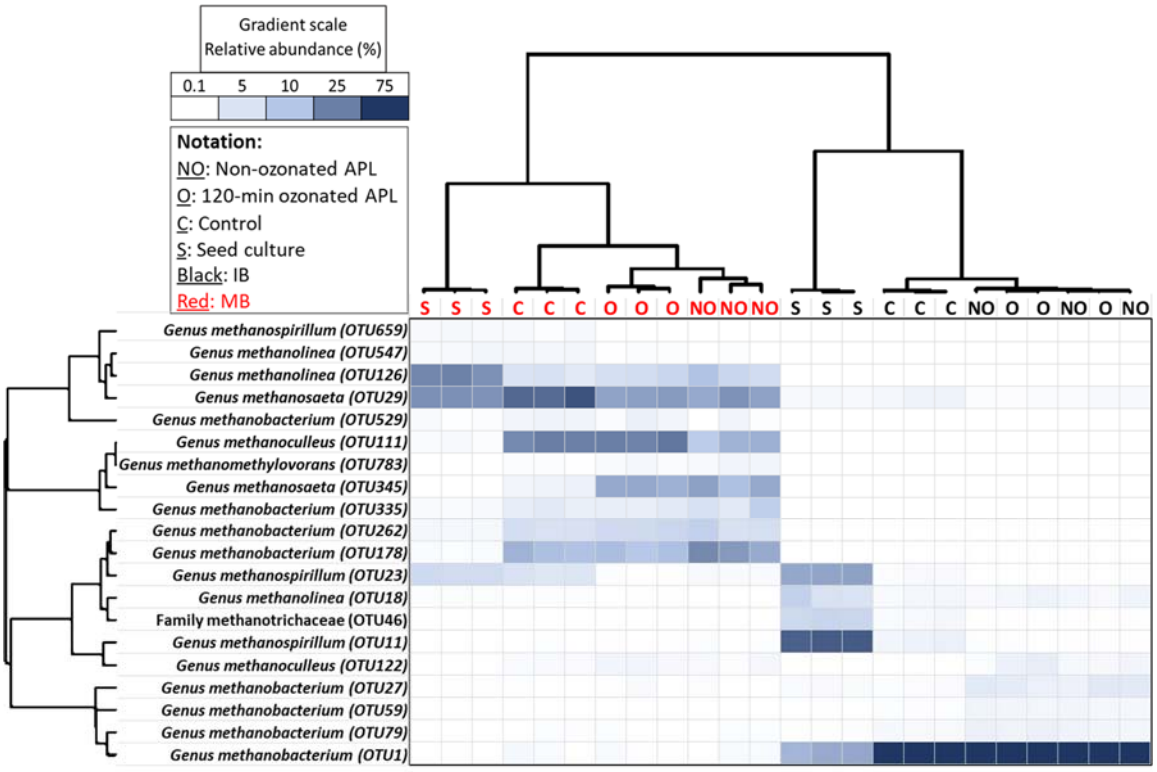

Figure 4.6. Dual hierarchical clustering of the 20 most abundant archaeal OTUs. These OTUs represent 87 ± 12% of total archaeal community relative abundance in all co-digesters. Taxonomic classification level of the OTUs is based on percent homology; <77% unknown, 77–80% unclassified phylum, 80–85% unclassified class, 85–90% unclassified order, 90–95% unclassified Family, 95–97% unclassified Genus. IB-inoculated co-digesters community was dominated by *Methanobacterium* (OTU 1). Whereas communities in MB-inoculated co-digesters had *Methanosaeta* (OTU 29), *Methanoculleus* (OTU 111) and *Methanobacterium* (OTU 178) as dominant OTUs, also *Methanosaeta* (OTU 345) relative abundance increased in co-digesters fed ozonated and non-ozonated APL only.

4.4.4.1.2 Bacteria community in co-digesters

Bacterial community in MB inoculum was affected by APL co-digestion more than IB inoculum. Also, feeding ozonated versus non-ozonated APL impacted MB bacterial community more than IB community, such that co-digesters fed ozonated APL had a more similar community to control digesters. An average of 460 ± 80 and 464 ± 40 bacterial OTUs in each digester with corresponding relative abundance of 71 ± 4.1% and 98 ± 1.1% of the total microbial community

abundance were identified in co-digesters inoculated with IB and MB, respectively. The bacterial community in IB co-digesters fed ozonated and non-ozonated APL were more similar to inoculum communities, whereas control digester communities were different from inoculum communities (Figure 4.7). The dissimilarity distance between IB inoculum and control digester communities (90 ± 0.5% dissimilarity) was statistically higher than the dissimilarity distance between inoculum and co-digesters fed ozonated (78 ± 1% dissimilarity) or non-ozonated APL communities (83 ± 0.6% dissimilarity) ($p=0.00$, $n=6$) (Figure S4.9A). This suggests that the IB inoculum bacterial community was more acclimated to compounds in the APL compared to compounds in the synthetic primary sludge; therefore, a smaller change in community composition occurred when APL was co-digested. In contrast, the MB inoculum was not exposed to similar constituents as in the APL; therefore, a significant shift in bacterial community in co-digesters fed ozonated (80 ± 0.9% dissimilarity) and non-ozonated (90 ± 2.5% dissimilarity) APL was observed, while control digester communities changed to a lesser extent (60 ± 1.5% dissimilarity) ($p=0.00$, $n=6$) (Figure 4.7 and S4.9B). The acclimated bacterial community in IB co-digesters could ostensibly have provided higher APL degradation, which subsequently resulted in higher methane production observed in IB co-digesters compared to the co-digesters inoculated with MB.

APL ozonation reduced its toxicity as observed from more similar bacterial community in co-digesters fed ozonated APL and control digesters. (Figure S4.9). Based on pairwise Bray-Curtis distance, co-digesters fed ozonated APL had more similar bacterial community to control digesters compared to co-digesters fed non-

ozonated APL in both IB (64 ± 2% versus 72 ± 2% dissimilarity in co-digesters fed ozonated and non-ozonated APL compared to control) and MB inoculum (56 ± 4% versus 84 ± 3% dissimilarity in co-digesters fed ozonated and non-ozonated APL compared to control), demonstrating that ozonation reduced APL toxicity (Figure S4.9).

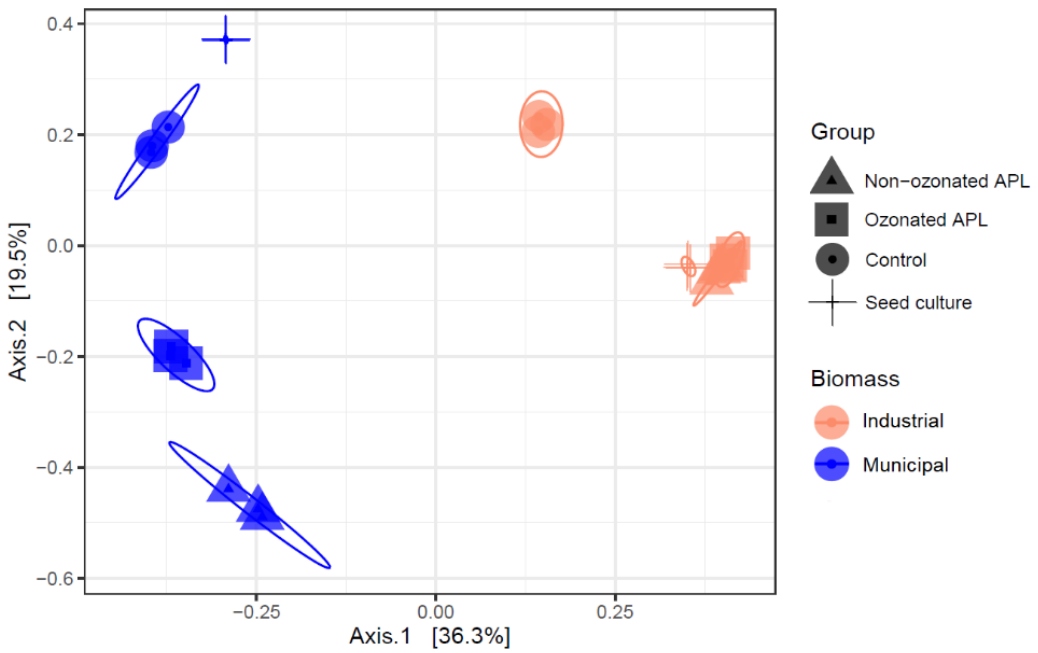

Figure 4.7. PCoA plot on bacterial community of IB and MB inocula (day 0) and co-digesters fed 2 h ozonated APL (day 215) based on Bray-Curtis distance. Ellipses represent 95% confidence intervals for the three points (each group represents the three triplicate digesters). IB and MB have different bacterial communities. APL co-digestion transformed the bacterial community in both IB and MB inocula.

There were 35 dominant bacterial OTUs having the highest relative abundance that represented 50 ± 15% of the total bacterial community abundance (Figure 4.8). Bacterial communities in IB and MB inocula changed when APL was co-digested. In the IB-inoculated co-digesters, feeding non-ozonated APL selected

for genus *Enterococcus* (OTU 6), contributing to more than 18% relative abundance of total bacterial community, whereas it was not selected for in control digesters (2-1) fed only synthetic sludge (Figure 4.8). *Enterococcus* is a facultative anaerobic bacterium that utilizes amino acids, purine and pyrimidine bases for growth (Vos et al., 2009). Genus *Symbiobacterium* (OTU 22) contributed to less than 0.001% of total bacterial community relative abundance in IB inoculum, increased to more than 7% and 5% in co-digesters fed non-ozonated and ozonated APL, respectively, whereas, it remained less than 0.02% in control digesters. *Symbiobacterium* belongs to family Symbiobacteriaceae that is described as moderately anaerobic, thermophilic and chemo-organotrophic bacteria involved in syntrophic acetate oxidation (SAO) (Shiratori-Takano et al., 2014). Family Ignavibacteriaceae (OTU 2) relative abundance in APL-fed co-digesters remained statistically similar to inoculum (7.8 ± 2%) ($p=0.4$, $n=9$); however, it decreased to 2.1 ± 0.3 in control digesters. Family Ignavibacteriaceae is strictly anaerobe heterotrophic bacteria that grow on a range of sugars (such as D-glucose) as one of its substrates in moderately thermophilic conditions (Iino et al., 2010).

In MB-inoculated co-digesters, different OTUs belonging to order Bacteroidales (OTU 8, 12, and 13) increased in relative abundance from less than 0.001% to 9 – 16% of the total bacterial community in co-digesters fed non-ozonated APL and remained less than 3% in co-digesters fed ozonated APL. Order Bacteroidales was previously enriched for during anaerobic digestion of phenol (Poirier et al., 2016). Phenol was detected in non-ozonated APL but was not detected in 2 h ozonated APL (Figure S4.1). In control digesters and co-digesters

receiving ozonated APL, the relative abundance of genus *Bellilinea* (OTU 3) increased more than 200% from the inoculum. *Bellilinea* has been found in methanogenic propionate-degrading constoria (Yamada et al., 2007).

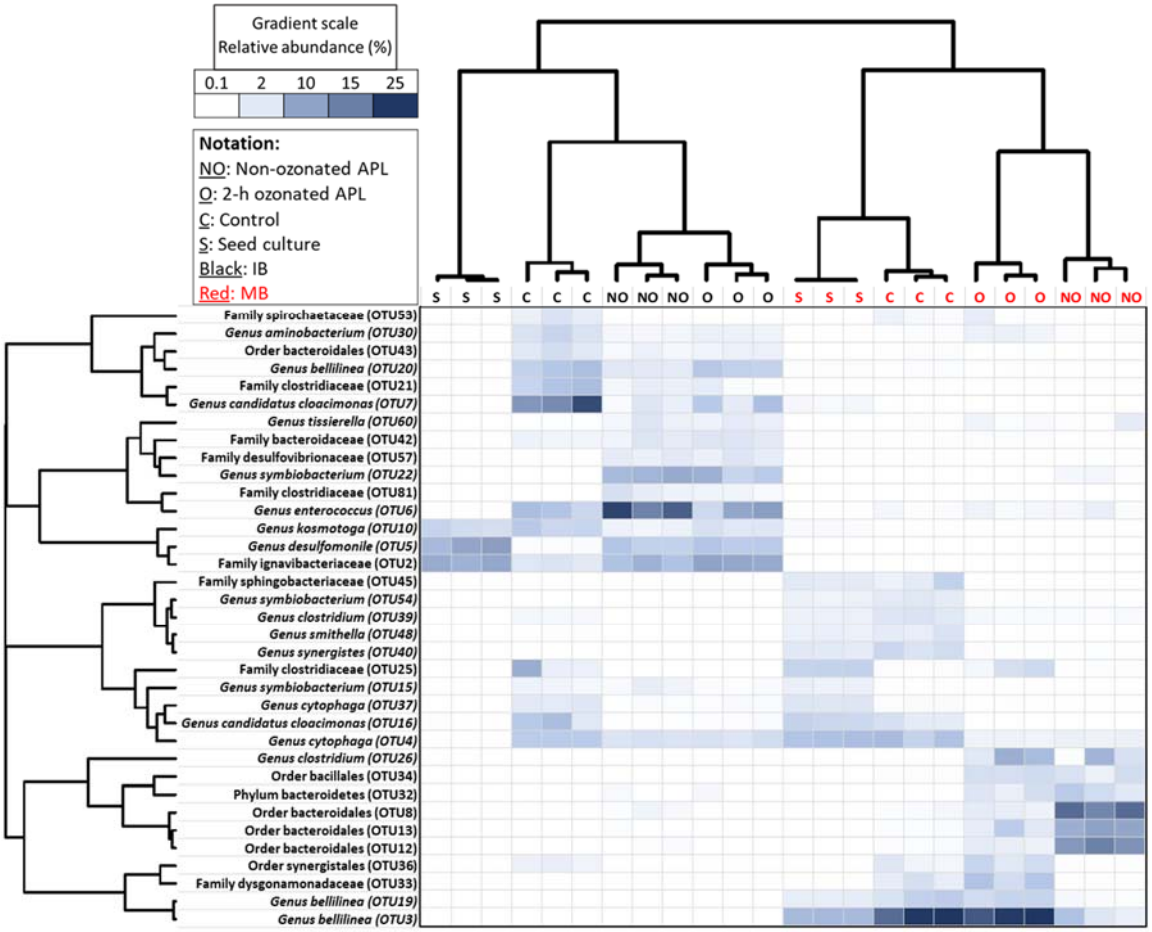

Figure 4.8. Dual hierarchical clustering of the 35 most abundant bacterial OTUs. These OTUs represent 50 ± 15% of the total bacterial community abundance in all co-digesters. Taxonomic classification of the OTUs is based on percent homology. Communities in IB clustered separately from MB. APL-fed IB-inoculated co-digesters community was dominated by *Enterococcus* (OTU 6), *Symbiobacterium* (OTU 22), and Ignavibacteriaceae (OTU 2). Communities in MB-inoculated co-digesters had *Bellilinea* (OTU 3) in control digesters and co-digesters receiving ozonated APL, while phenol-degrading Bacteroidales (OTU 8, 12, and 13) was dominant in co-digesters fed non-ozonated APL.

Relative abundance of many syntrophic bacteria belonging to phylum Synergistes increased concomitantly with hydrogenotrophic methanogen archaea. Within the syntrophic populations in IB, the relative abundance of genera *Aminobacterium* (OTU 30) and *Aminivibrio pyruvatiphilus* (OTU 371) belonging to family Synergistaceae contributed to less than 0.001% of total bacterial community relative abundance in the inoculum. After digestion, the relative abundance increased to 0.8 – 3% and 0.04 – 0.1% of the total bacterial community relative abundance, respectively, in all co-digesters. *Aminobacterium* and *Aminivibrio pyruvatiphilus* are strictly anaerobic amino-acid degrading bacteria that work in association with hydrogen-utilizing *Methanobacterium* (Baena et al., 2000, 1999; Honda et al., 2013). Similarly, in MB-inoculated digesters, relative abundance of *Aminobacterium* (OTU 30) increased from less than 0.002% in total bacterial community in the inoculum to 0.2 ± 0.01% in control and co-digesters fed non-ozonated APL, and 1.2 ± 0.2% in co-digesters fed ozonated APL. Genus *Anaerobaculum (OTU 106)* was selected for in MB-inoculated co-digesters fed non-ozonated APL (1.3 ± 0.01% relative abundance), while it was not selected for in control digesters (<0.04%). *Anaerobaculum* is an anaerobic bacterium from family Synergistaceae, isolated from production water of a petroleum reservoir, that ferments a range of organic acids and protein extracts (Rees et al., 1997). Genus *Aminomonas* (OTU 36) was also selected for in co-digesters fed ozonated APL (2.9 ± 0.8%), while its relative abundance remained less than 1.3% in control digesters inoculated with MB. *Aminomonas* is also an amino-acid degrading anaerobic bacteria working synergistically with hydrogen-utilizing

Methanobacterium (Baena et al., 2000, 1999; Honda et al., 2013).

Two known syntrophic acetate oxidizing bacteria (SAOB) species, namely thermotolerant *Tepidanaerobacter acetatoxydans* and mesophilic *Clostridium ultunense* belonging to class Clostridia (Westerholm et al., 2016), identified in the bacterial population in IB and MB inocula, both increased in relative abundance after digestion. In IB co-digesters, relative abundance of genus *Tepidanaerobacter acetatoxydans* (OTUs 691, 1197, and 998) in total bacterial community increased from less than 0.0001% in inocula to 0.01 – 0.04% in co-digesters fed with non-ozonated and ozonated APLs. Additionally, relative abundance of genus *Clostridium ultunense* (OTU 726, 718, and 1019) also increased from less than 0.0001% to 0.01 – 0.08% of total bacterial community in co-digesters receiving non-ozonated and ozonated APL. *Eubacterium* (OTU 75, 135), another genus from Clostridia class that is known for degrading N-heterocyclic compounds such as pyridine was enriched for in IB co-digesters fed ozonated and non-ozonated APL (0.6 – 1.9%) (Fekry et al., 2016). In MB-inoculated co-digesters, the relative abundance of genus *Tepidanaerobacter acetatoxydans* (OTUs 332 and 527) increased from less than 0.0001% in inocula to 0.03 – 0.17% in non-ozonated and ozonated APL.

Overall, these results indicate that methane production from APL in IB-inoculated co-digesters occurred primarily under hydrogenotrophic methanogenesis (*Methanobacterium*) in syntrophy with bacterial partners such as genera in phylum Synergistes and class Clostridia. Other important bacterial taxa that were enriched for during APL digestion include *Enterococcus*, *Eubacterium,*

Symbiobacterium, and Ignavibacteriaceae. In MB-inoculated co-digesters, methanogenesis took place by acetoclastic (*Methanosaeta*) and hydrogenotrophic (*Methanoculleus* and *Methanobacterium*) methanogenesis. Relative abundance of several SAOB belonging to phylum Synergistes and class Clostridia also increased in MB-inoculated co-digesters. Phenol degrading bacterial order, Bacteroidales was also selected for in MB-inoculated co-digesters.

4.4.4.2. Mono-digesters

Approximately 268,000 sequence reads were yielded in mono-digesters with 29,767 ± 577 reads per digester sample. Based on 97% similarity, total of 791 microbial OTUs were observed with an average of 463 ± 51 OTUs per digester. Chao1 index increased in digesters fed ozonated and non-ozonated APL compared to inoculum ($p<0.05$, $n=6$) showing a more diverse community after digestion that could be associated with better digester performance and increased methane production (Carballa et al. 2015; Chen et al. 2020) (Table 4.4). However, Shannon diversity index decreased ($p<0.05$, $n=6$). There were no differences observed in Shannon and Chao1 index between the digesters receiving non-ozonated and ozonated APL ($p>0.05$, $n=6$) (Table 4.4).

Table 4.4. Alpha diversity indices in IB inoculum and in mono-digesters receiving ozonated and non-ozonated APL on day 215 of digestion. Average and standard deviations are from triplicate values.

	IB		
Sample	**Observed OTUs**	**Chao1**	**Shannon**
Inocula	398 ± 2.3	437 ± 3.9	4.2 ± 0.06
Mono-digester fed non-ozonated APL	483 ± 15	586 ± 32	2.9 ± 0.1
Mono-digester fed ozonated APL	508 ± 11	621 ± 24	2.9 ± 0.04

4.4.4.2.1 Archaea community in mono-digesters

Feeding APL shifted the archaeal community in mono-digesters, however, feeding ozonated versus non-ozonated APL did not affect it. An average of 72 ± 6 archaeal OTUs in each digester with corresponding relative abundance of 44 ± 11% of the total microbial community abundance were identified in mono-digesters. As shown by 95% confidence ellipses in the PCoA plot, exposure to APLs altered the archaeal community composition after digestion (75 ± 2% dissimilarity) (Figure 4.9). However, feeding ozonated or non-ozonated APL did not impact the archaeal community composition significantly based on pairwise Bray-Curtis dissimilarity distance (3 ± 0.9% dissimilarity) (Figure 4.9).

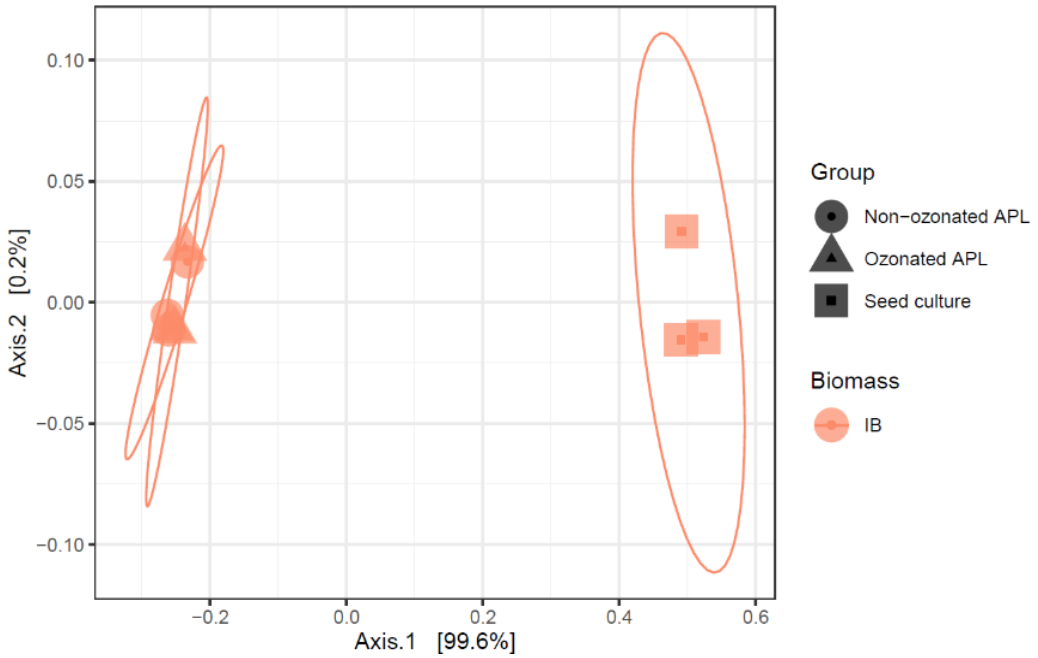

Figure 4.9. PCoA plot on archaeal community of mono-digesters inoculum (day 0) and digesters fed non-ozonated and 2 h ozonated APL (day 215) based on Bray-Curtis distance. Ellipses represent 95% confidence intervals for the three points (each group represents the three triplicate digesters). APL digestion shifted the archaeal community composition in inoculum as observed by distinct archaeal community clusters. Ozonated and non-ozonated APL digestion did not affect the archaeal community composition.

Methane production in mono-digesters was conducted by hydrogenotrophic archaea. The 20 dominant archaeal OTUs accounted for 93 ± 1.1% of total archaeal community relative abundance (Figure 4.10). Similar to IB co-digester results, mono-digesters were dominated by *Methanobacterium* (OTU 1), and its relative abundance increased by 400% in both mono-digesters fed ozonated and non-ozonated APL (Figure 4.10). Relative abundance of genera *Methanospirillium* (OTU 23 and 11), *Methanolinea* (OTU 18), and family Methanobacteriaceae (OTU 50) which were dominant in inoculum decreased significantly after APL digestion ($p<0.05$, $n=6$) (Figure 4.10). These results show that hydrogenotrophic methanogenesis was the primary pathway for methane production in mono-

digesters. Ozonation did not influence the archaeal community composition in mono-digesters which was similar to methane production results from mono-digesters that was statistically similar among mono-digesters fed ozonated and non-ozonated APL.

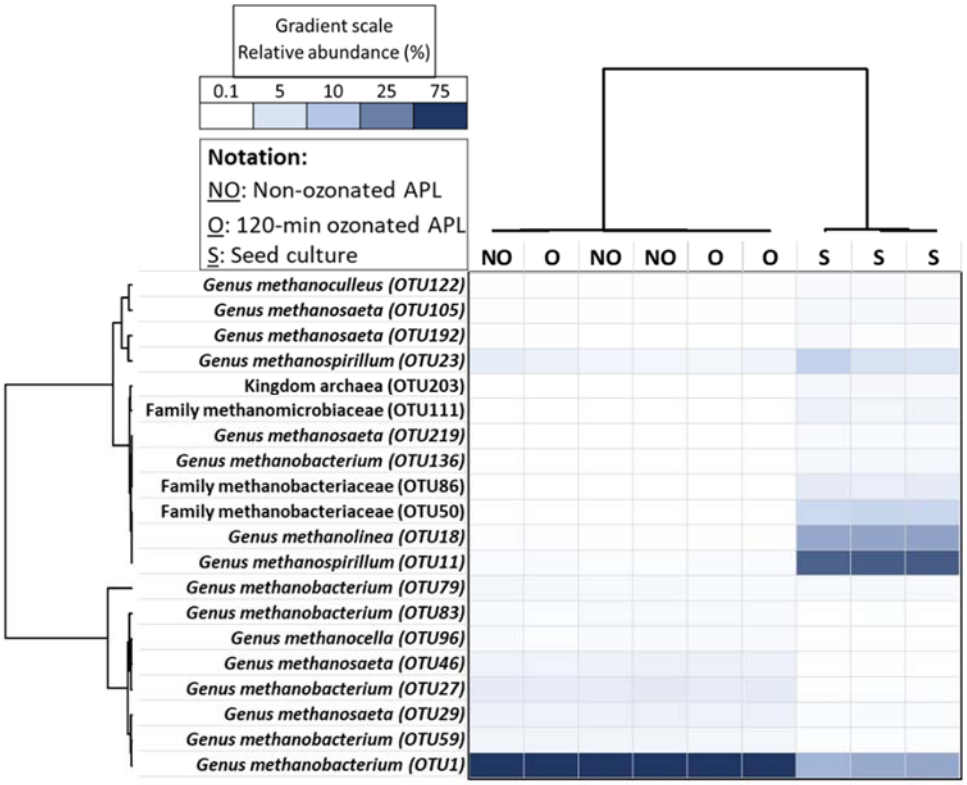

Figure 4.10. Dual hierarchical clustering of the 20 most abundant archaeal OTUs. These OTUs represent 93 ± 1.1% of total archaeal community relative abundance in mono-digesters. Taxonomic classification of the OTUs is based on percent homology. *Methanobacterium* (OTU 1) dominated in mono-digesters receiving ozonated and non-ozonated APL.

4.4.4.2.2 Bacteria community in mono-digesters

Similar to archaea, bacterial community was also altered after APL digestion and ozonation did not affect the bacterial composition. An average of 391 ± 45 bacterial OTUs in each digester with corresponding relative abundance of 56

± 11% of the total microbial community abundance were identified in mono-digesters. Bacterial community composition was altered after APL digestion (68 ± 0.6% dissimilarity) as shown by 95% confidence ellipses in the PCoA plot (Figure 4.11). Bacterial community composition between ozonated and non-ozonated APLs did not change substantially (14 ± 1% dissimilarity) based on pairwise Bray-Curtis dissimilarity distance, demonstrating feeding ozonated or non-ozonated APL did not affect the bacterial composition (Figure 4.11).

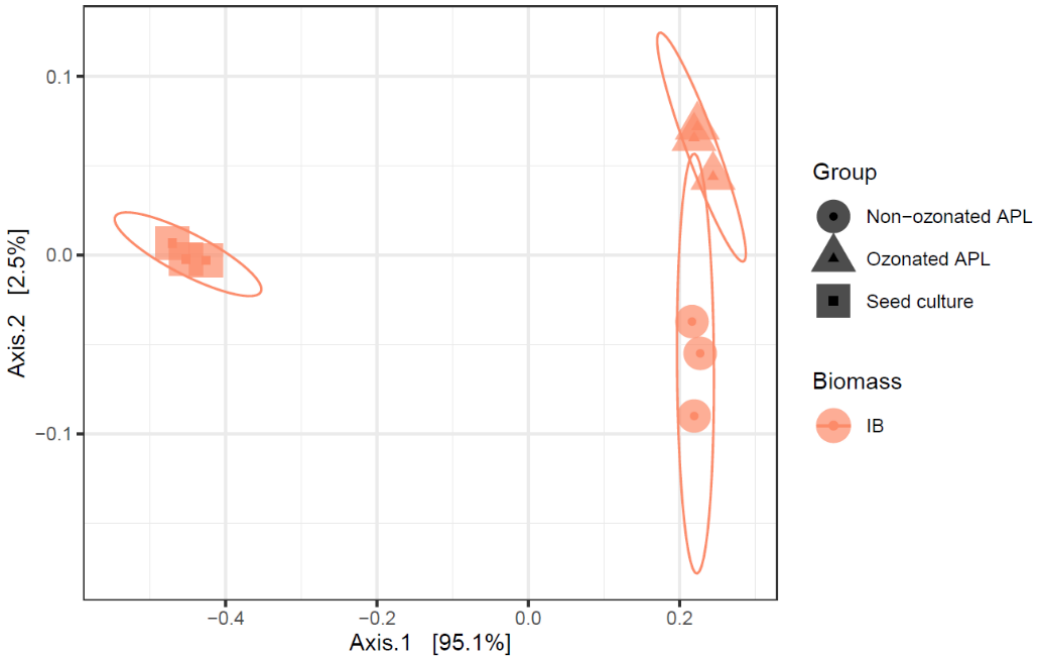

Figure 4.11. PCoA plot on bacterial community of mono-digesters inoculum (day 0) and digesters fed non-ozonated and 2 h ozonated APL (day 215) based on Bray-Curtis distance. Ellipses represent 95% confidence intervals for the three points (each group represents the three triplicate digesters). APL digestion shifted the bacterial community composition in inoculum as observed by distinct clusters. Ozonated and non-ozonated APL digestion did not affect the bacterial community composition significantly.

There were 30 dominant bacterial OTUs having the highest relative abundance values that represented 75 ± 6% of the total bacterial community

abundance (Figure 4.11). Bacterial communities altered when APL was digested. Relative abundance of family Ignavibacteriaceae (OTU 2) and genus *Desulfomonile* (OTU 5) increased from about 9% in the inoculum to 39 ± 0.4% and 14 ± 1.2%, respectively, in APL-fed mono-digesters (Figure 4.12). Genera *Symbiobacterium* (OTU 15) and *Clostridiisalibacter* (OTU 17), and family Clostridiaceae (OTU 21) contributed to less than 0.001% of total bacterial community relative abundance in inoculum and they increased to more than 5%, 3% and 2% of total bacterial community relative abundance, respectively (Figure 4.12). All these OTUs belong to order Clostridiales which is involved in SAO along with hydrogenotrophic methanogens. Additionally, order Bacillales (OTU 47) that can convert N-heterocyclic compounds into methane was selected for in co-digesters receiving APL (1.5 – 3.7% in bacterial community relative abundance) (Si et al., 2018).

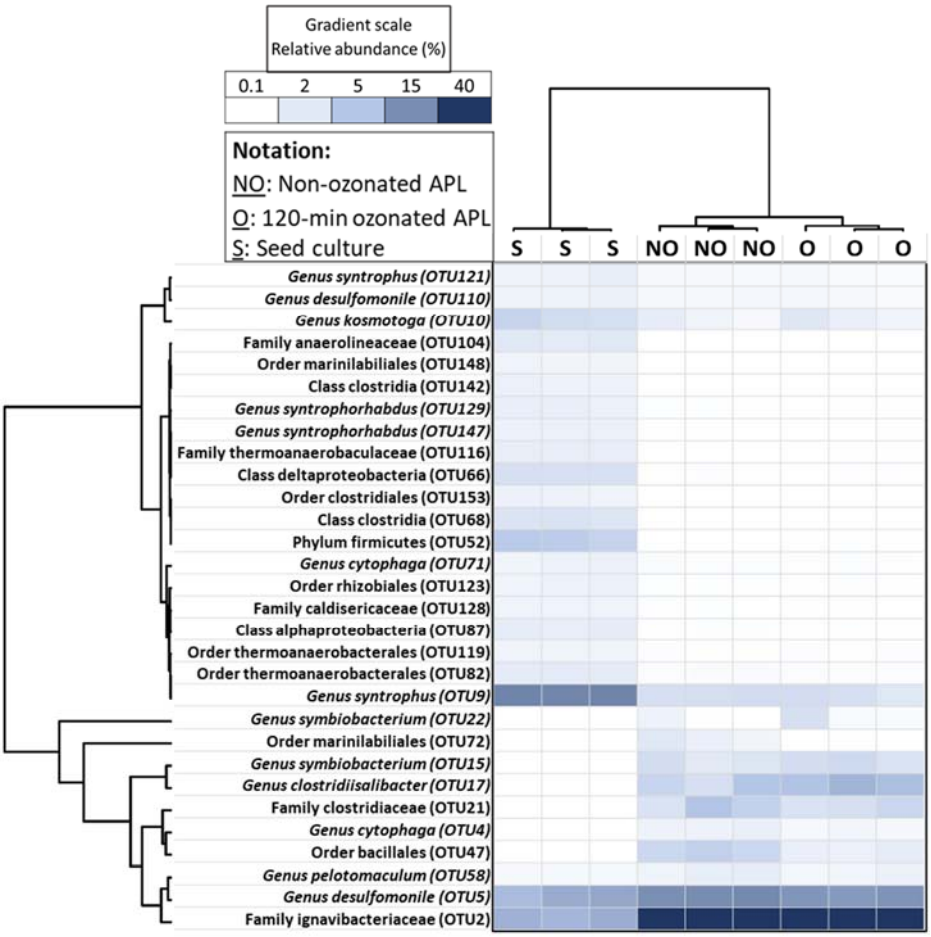

Figure 4.12. Dual hierarchical clustering of the 30 most abundant archaeal OTUs. These OTUs represent 75 ± 6% of the total bacterial community abundance in mono-digesters. Taxonomic classification of the OTUs is based on percent homology. SAOB *Symbiobacterium* (OTU 15), *Clostridiisalibacter* (OTU 17), and Clostridiaceae (OTU 21) increased in relative abundance after APL digestion. Also, relative abundance of Ignavibacteriaceae (OTU 2) and *Desulfomonile* (OTU 5) increased.

Generally, these results demonstrate the simultaneous increase in syntrophic bacteria with hydrogenotrophic methanogens (*Methanobacterium*) which was the primary route of methane production in mono-digesters. Simultaneous increase in relative abundance of OTUs belonging to order Clostridiales was observed.

4.5. Conclusion

APL derived from wastewater solids was anaerobically converted into methane as the sole substrate and as co-digestate with synthetic sludge. Results of this study demonstrate feasibility of mono-digesting APL which was previously reported to be challenging. Co-digesting APL was also successful, which is a viable approach at WRRFs that already have digesters treating sludge and pyrolyze wastewater solids for improved biogas production. Strategies applied that resulted in more complete APL conversion into methane included employing a low SRT and high OLR to overcome APL toxicity, selection of a proper inocula that is acclimated to compounds similar to APL constituents, and APL pre-ozonation.

Employing 210-d SRT and decreasing the OLR to 0.03 gCOD/L APL improved methane production considerably in all co-digesters and mono-digesters, whereas methane production was extremely inhibited in all co-digesters and mono-digesters operated at 15-d SRT and 0.2 gCOD/L APL. More than 90% conversion of APL organics into methane was observed in all mono-digesters operated at 210-d SRT. Likewise, co-digesters produced 48 – 98% of the stoichiometric maximum methane from APL when operated at 210-d SRT. APL degradation was also confirmed by analyzing the digestate using GC-MS analysis which showed removal of APL organics after digestion was due to biodegradation.

IB inoculum was more capable of degrading APL organics compared to MB. Co-digesters inoculated with IB produced 60 – 98% of the stoichiometric theoretical methane, but only 48 – 64% in MB was observed. Under the conditions

studied, the non-ozonated APL was also degraded in mono-digesters, and to some extent in both IB and MB inoculated co-digesters. APL ozonation removed some problematic APL constituents such as N-heterocyclic compounds, as well as reduced SUVA and TP concentrations which are associated with methane production inhibition were reduced after ozonation, resulting in more complete methane production from ozonated APL. The highest methane production (98% of the stoichiometric maximum methane) was observed from co-digesters receiving 2 h ozonated APL inoculated with IB. Ozonation did not have a significant impact on methane production from mono-digesters and MB-inoculated co-digesters.

Microbial community analysis revealed hydrogenotrophic methanogenesis (*Methanobacterium*) was the primary route in IB-inoculated co-digesters and mono-digesters with concurrent increase of syntrophic bacteria and SAOBs, whereas both acetoclastic (*Methanosaeta*) and hydrogenotrophic (*Methanoculleus* and *Methanobacterium*) pathways occurred in MB-inoculated co-digesters. Bacterial genera associated with N-heterocyclic degradation were enriched for in IB-inoculated co-digesters and mono-digesters, such as *Enterococcus*, *Euobacterium*, and order Bacillales. Phenol degrading bacterial order, Bacteroidales was selected for in MB-inoculated co-digesters. These results signify the impact of inoculum community in successful anaerobic degradation of APL. Microbial communities in the digesters inoculated with different biomass (IB and MB) were noticeably different after digestion, indicating that the inocula plays an important role and different inocula exhibit different functionality.

The findings of this study demonstrate the feasibility of mono-digesting and

co-digesting APL, which was previously reported as infeasible. Importance of employing appropriate SRT and OLR for APL degradation, selection of a proficient inocula, and the promising effect of APL ozonation in reducing APL toxicity and improving methane production was also observed. Future research focused on bioaugmenting MB-inoculated digesters with IB for improved performance of MB in APL conversion to methane is warranted.

4.6. References

Alvares ABC, Diaper C, Parsons SA (2001) Partial oxidation by ozone to remove recalcitrance from wastewaters - a review. Environ Technol (United Kingdom) 22:409–427. https://doi.org/10.1080/09593332208618273

American Public Health Association (1998) Standard Methods for the Examination of Water and Wastewater.

Baena S, Fardeau M-L, Labat M, et al (2000) Aminobacterium mobile sp. nov., a new anaerobic amino-acid-degrading bacterium

Baena S, Fardeau M-L, Ollivier B, et al (1999) Aminomonas paucivorans gen. nov., sp. nov., a mesophil ic, anaerobic, amino-acid-uti l izing bacterium

Benn N, Zitomer D (2018) Pretreatment and Anaerobic Co-digestion of Selected PHB and PLA Bioplastics. Front Environ Sci 5:1–9. https://doi.org/10.3389/fenvs.2017.00093

Carballa M, Regueiro L, Lema JM (2015) Microbial management of anaerobic digestion: Exploiting the microbiome-functionality nexus. Curr Opin Biotechnol 33:103–111. https://doi.org/10.1016/j.copbio.2015.01.008

Carey DE (2016) the Role of Household Antimicrobials in the Proliferation of Antibiotic Resistance During Anaerobic Digestion

Carey DE, McNamara PJ, Zitomer DH (2015) Biochar from Pyrolysis of Biosolids for Nutrient Adsorption and Turfgrass Cultivation. Water Environ Res 87:2098–2106. https://doi.org/10.2175/106143015x14362865227391

Chaparro TR, Botta CM, Pires EC (2010) Toxicity and recalcitrant compound removal from bleaching pulp plant effluents by an integrated system: Anaerobic packed-bed bioreactor and ozone. Water Sci Technol 61:199–205. https://doi.org/10.2166/wst.2010.794

Chen H, Hao S, Chen Z, et al (2020) Mesophilic and thermophilic anaerobic digestion of aqueous phase generated from hydrothermal liquefaction of cornstalk: Molecular and metabolic insights. Water Res 168:115199. https://doi.org/10.1016/j.watres.2019.115199

Chen H, Rao Y, Cao L, et al (2019) Hydrothermal conversion of sewage sludge: Focusing on the characterization of liquid products and their methane yields. Chem Eng J 357:367–375. https://doi.org/10.1016/j.cej.2018.09.180

Chen H, Zhang C, Rao Y, et al (2017) Methane potentials of wastewater generated from hydrothermal liquefaction of rice straw: Focusing on the wastewater characteristics and microbial community compositions. Biotechnol Biofuels 10:1–16. https://doi.org/10.1186/s13068-017-0830-0

Domínguez A, Menéndez JA, Inguanzo M, Pís JJ (2006) Production of bio-fuels by high temperature pyrolysis of sewage sludge using conventional and microwave heating. Bioresour Technol 97:1185–1193.

https://doi.org/10.1016/j.biortech.2005.05.011

Dowd SE, Sun Y, Wolcott RD, et al (2008) Bacterial tag-encoded FLX amplicon pyrosequencing (bTEFAP) for microbiome studies: Bacterial diversity in the ileum of newly weaned Salmonella-infected pigs. Foodborne Pathog Dis 5:459–472. https://doi.org/10.1089/fpd.2008.0107

Eggen T, Vogelsang C (2015) Occurrence and Fate of Pharmaceuticals and Personal Care Products in Wastewater. In: Comprehensive Analytical Chemistry. Elsevier B.V., pp 245–294

Falk MW, Song KG, Matiasek MG, Wuertz S (2009) Microbial community dynamics in replicate membrane bioreactors - Natural reproducible fluctuations. Water Res 43:842–852. https://doi.org/10.1016/j.watres.2008.11.021

Fekry MI, Engels C, Zhang J, et al (2016) The strict anaerobic gut microbe *Eubacterium hallii* transforms the carcinogenic dietary heterocyclic amine 2-amino-1-methyl-6-phenylimidazo[4,5-b]pyridine (PhIP). Environ Microbiol Rep 8:201–209. https://doi.org/10.1111/1758-2229.12369

Feng Q, Lin Y (2017) Integrated processes of anaerobic digestion and pyrolysis for higher bioenergy recovery from lignocellulosic biomass: A brief review. Renew Sustain Energy Rev 77:1272–1287. https://doi.org/10.1016/j.rser.2017.03.022

Fujimoto M, Carey DE, Zitomer DH (2019) Syntroph diversity and abundance in anaerobic digestion revealed through a comparative core microbiome approach

Gai C, Zhang Y, Chen WT, et al (2015) Characterization of aqueous phase from the hydrothermal liquefaction of Chlorella pyrenoidosa. Bioresour Technol 184:328–335. https://doi.org/10.1016/j.biortech.2014.10.118

Hoffman TC, Zitomer DH, McNamara PJ (2016) Pyrolysis of wastewater biosolids significantly reduces estrogenicity. J Hazard Mater 317:579–584. https://doi.org/10.1016/j.jhazmat.2016.05.088

Honda T, Fujita T, Tonouchi A (2013) Aminivibrio pyruvatiphilus gen. nov., sp. nov., an anaerobic, amino-acid-degrading bacterium from soil of a Japanese rice field. Int J Syst Evol Microbiol 63:3679–3686. https://doi.org/10.1099/ijs.0.052225-0

Hübner T, Mumme J (2015) Integration of pyrolysis and anaerobic digestion – Use of aqueous liquor from digestate pyrolysis for biogas production. Bioresour Technol 183:86–92. https://doi.org/10.1016/j.biortech.2015.02.037

Iino T, Mori K, Uchino Y, et al (2010) Ignavibacterium album gen. nov., sp. nov., a moderately thermophilic anaerobic bacterium isolated from microbial mats at a terrestrial hot spring and proposal of Ignavibacteria classis nov., for a novel lineage at the periphery of green sulfur bacteria. Int J Syst Evol Microbiol 60:1376–1382. https://doi.org/10.1099/ijs.0.012484-0

Inaba T, Aoyagi T, Hori T, et al (2020) Long-term acclimatization of sludge

microbiome for treatment of high-strength organic solid waste in anaerobic membrane bioreactor. Biochem Eng J 154:107461. https://doi.org/10.1016/j.bej.2019.107461

Li P, Ailijiang N, Cao X, et al (2015) Pretreatment of coal gasification wastewater by adsorption using activated carbons and activated coke. Colloids Surfaces A Physicochem Eng Asp 482:177–183. https://doi.org/10.1016/j.colsurfa.2015.05.006

Liu Z, Mayer BK, Venkiteshwaran K, et al (2020) The state of technologies and research for energy recovery from municipal wastewater sludge and biosolids. Curr. Opin. Environ. Sci. Heal. 14:31–36

Liu Z, McNamara P, Zitomer D (2017) Autocatalytic Pyrolysis of Wastewater Biosolids for Product Upgrading. Environ Sci Technol 51:9808–9816. https://doi.org/10.1021/acs.est.7b02913

Liu Z, Singer S, Tong Y, et al (2018) Characteristics and applications of biochars derived from wastewater solids. Renew Sustain Energy Rev 90:650–664. https://doi.org/10.1016/j.rser.2018.02.040

Lü F, Hua Z, Shao L, He P (2018) Loop bioenergy production and carbon sequestration of polymeric waste by integrating biochemical and thermochemical conversion processes: A conceptual framework and recent advances. Renew. Energy 124:202–211

McNamara PJ, Koch JD, Liu Z, Zitomer DH (2016) Pyrolysis of Dried Wastewater Biosolids Can Be Energy Positive. Water Environ Res 88:804–810. https://doi.org/10.2175/106143016X14609975747441

Mukarakate C, Evans RJ, Deutch S, et al (2017) Reforming Biomass Derived Pyrolysis Bio-oil Aqueous Phase to Fuels. Energy and Fuels 31:1600–1607. https://doi.org/10.1021/acs.energyfuels.6b02463

Poirier S, Bize A, Bureau C, et al (2016) Community shifts within anaerobic digestion microbiota facing phenol inhibition: Towards early warning microbial indicators? Water Res 100:296–305. https://doi.org/10.1016/j.watres.2016.05.041

Porter TM, Hajibabaei M (2018) Scaling up: A guide to high-throughput genomic approaches for biodiversity analysis. Mol Ecol 27:313–338. https://doi.org/10.1111/mec.14478

Prandini JM, da Silva MLB, Mezzari MP, et al (2016) Enhancement of nutrient removal from swine wastewater digestate coupled to biogas purification by microalgae Scenedesmus spp. Bioresour Technol 202:67–75. https://doi.org/10.1016/j.biortech.2015.11.082

Rees GN, Patel BKC, Grassia,' And S, Sheehy' AJ (1997) Anaerobaculum themoterrenum gen Bacterium Which Ferments Citrate. International Union of Microbiological Societies

Ross JJ, Zitomer DH, Miller TR, et al (2016) Emerging investigators series:

Pyrolysis removes common microconstituents triclocarban, triclosan, and nonylphenol from biosolids. Environ Sci Water Res Technol 2:282–289. https://doi.org/10.1039/c5ew00229j

Rover MR, Brown RC (2013) Quantification of total phenols in bio-oil using the Folin – Ciocalteu method. J Anal Appl Pyrolysis 104:366–371. https://doi.org/10.1016/j.jaap.2013.06.011

Seiple TE, Coleman AM, Skaggs RL (2017) Municipal wastewater sludge as a sustainable bioresource in the United States. J Environ Manage 197:673–680. https://doi.org/10.1016/j.jenvman.2017.04.032

Seyedi S, Venkiteshwaran K, Benn N, Zitomer D (2020) Inhibition during Anaerobic Co-Digestion of Aqueous Pyrolysis Liquid from Wastewater Solids and Synthetic Primary Sludge. Sustainability 12:3441. https://doi.org/10.3390/su12083441

Seyedi S, Venkiteshwaran K, Zitomer D (2018) Anaerobic Co-Digestion of Condensate from Biosolids Pyrolysis. In: WEF Residuals and Biosolids Conference 2018

Seyedi S, Venkiteshwaran K, Zitomer D (2019) Toxicity of Various Pyrolysis Liquids From Biosolids on Methane Production Yield. Front Energy Res 7:1–12. https://doi.org/10.3389/fenrg.2019.00005

Shiratori-Takano H, Akita K, Yamada K, et al (2014) Description of Symbiobacterium ostreiconchae sp. nov., Symbiobacterium turbinis sp. nov. and Symbiobacterium terraclitae sp. nov., isolated from shellfish, emended description of the genus Symbiobacterium and proposal of Symbiobacteriaceae fam. nov. Int J Syst Evol Microbiol 64:3375–3383. https://doi.org/10.1099/ijs.0.063750-0

Si B, Li J, Zhu Z, et al (2018) Inhibitors degradation and microbial response during continuous anaerobic conversion of hydrothermal liquefaction wastewater. Sci Total Environ 630:1124–1132. https://doi.org/10.1016/j.scitotenv.2018.02.310

Si B, Yang L, Zhou X, et al (2019) Anaerobic conversion of the hydrothermal liquefaction aqueous phase: Fate of organics and intensification with granule activated carbon/ozone pretreatment. Green Chem 21:1305–1318. https://doi.org/10.1039/c8gc02907e

Skaggs RL, Coleman AM, Seiple TE, Milbrandt AR (2017) Waste-to-Energy biofuel production potential for selected feedstocks in the conterminous United States. Renew Sustain Energy Rev 82:2640–2651. https://doi.org/10.1016/j.rser.2017.09.107

Torri C, Fabbri D (2014) Biochar enables anaerobic digestion of aqueous phase from intermediate pyrolysis of biomass. Bioresour Technol 172:335–341. https://doi.org/10.1016/j.biortech.2014.09.021

Torri C, Pambieri G, Gualandi C, et al (2020) Evaluation of the potential performance of hyphenated pyrolysis-anaerobic digestion (Py-AD) process for carbon negative fuels from woody biomass. Renew Energy 148:1190–1199.

https://doi.org/10.1016/j.renene.2019.10.025

Tyagi VK, Lo SL (2013) Sludge: A waste or renewable source for energy and resources recovery? Renew. Sustain. Energy Rev. 25:708–728

Ul Islam Z, Barbary Hassan E, Zhisheng Y, et al (2015) Microbial conversion of pyrolytic products to biofuels: a novel and sustainable approach toward second-generation biofuels. Artic J Ind Microbiol 42:1557–1579. https://doi.org/10.1007/s10295-015-1687-5

Venkiteshwaran K, Bocher B, Maki J, Zitomer D (2016a) Relating Anaerobic Digestion Microbial Community and Process Function. Microbiol Insights 8:37. https://doi.org/10.4137/MBI.S33593

Venkiteshwaran K, Milferstedt K, Hamelin J, Zitomer DH (2016b) Anaerobic digester bioaugmentation influences quasi steady state performance and microbial community. Water Res 104:128–136. https://doi.org/10.1016/j.watres.2016.08.012

Wen C, Moreira CM, Rehmann L, Berruti F (2020) Feasibility of anaerobic digestion as a treatment for the aqueous pyrolysis condensate (APC) of birch bark. Bioresour Technol 307:123199. https://doi.org/10.1016/j.biortech.2020.123199

Westerholm M, Moestedt J, Schnürer A (2016) Biogas production through syntrophic acetate oxidation and deliberate operating strategies for improved digester performance. Appl Energy 179:124–135. https://doi.org/10.1016/j.apenergy.2016.06.061

Yamada T, Imachi H, Ohashi A, et al (2007) Bellilinea caldifistulae gen. nov., sp. nov. and Longilinea arvoryzae gen. nov., sp. nov., strictly anaerobic, filamentous bacteria of the phylum Chloroflexi isolated from methanogenic propionate-degrading consortia. Int J Syst Evol Microbiol 57:2299–2306. https://doi.org/10.1099/ijs.0.65098-0

Yao Y, Xie Y, Zhao B, et al (2020) N-dependent ozonation efficiency over nitrogen-containing heterocyclic contaminants: A combined density functional theory study on reaction kinetics and degradation pathways. Chem Eng J 382:122708. https://doi.org/10.1016/j.cej.2019.122708

Yu X, Zhang C, Qiu L, et al (2020) Anaerobic digestion of swine manure using aqueous pyrolysis liquid as an additive. Renew Energy 147:2484–2493. https://doi.org/10.1016/j.renene.2019.10.096

Zhou H, Brown RC, Wen Z (2019) Anaerobic digestion of aqueous phase from pyrolysis of biomass: Reducing toxicity and improving microbial tolerance. Bioresour Technol 292:. https://doi.org/10.1016/j.biortech.2019.121976

Zitomer DH, Adhikari P, Heisel C, Dineen D (2008) Municipal anaerobic digesters for codigestion, energy recovery, and greenhouse gas reductions. Water Environ Res 80:229–237. https://doi.org/10.2175/106143007X221201

5 Overall conclusions and recommendations

Pyrolysis is a thermochemical technology to valorize and recover energy from wastewater solids and simultaneously minimize the potential detrimental impacts from wastewater solids land application or landfill. APL, however, requires suitable management methods to avoid environmental pollution, as well as recover its energy.

The overall objective of this dissertation work was to implement AD to recover APL energy derived from different pyrolysis temperatures in form of biogas containing methane and apply different approaches to overcome APL recalcitrance and toxicity to anaerobic microorganisms. For the first time, APL from wastewater solids pyrolysis was anaerobically digested and successfully converted into methane as the sole substrate and as co-digestate with synthetic sludge in long-term, continuous anaerobic digesters. APL digestion was previously hindered by APL recalcitrance to biodegradation and toxicity to anaerobic microorganisms. The strategies to overcome methane production inhibition include employing a low OLR and sufficiently high SRT, applying ozonation to reduce APL recalcitrance, and using suitable microorganisms that are proficient at APL biodegradation. The results from this research demonstrate that long-term methanogenesis from APL as the sole substrate is achievable. Anaerobic co-digestion of APL with primary sludge is also a viable approach to be conducted at WRRFs that already have digesters treating sludge, where APL from pyrolyzed wastewater solids can be added to digesters for increased biogas production. It is necessary to exercise caution to control for OLR, SRT and biomass inventory to

ensure APL digestion success. The specific goals in this study included:

1. Determining pyrolysis temperature impact on APL degradability (Chapter 3),
2. Evaluating APL ozone pretreatment to render APL less toxic and more easily degradable (Chapter 3),
3. Determining ozonated and non-ozonated APL composition and anaerobic toxicity (Chapter 3),
4. Employing four different anaerobic inocula to evaluate different microbial communities capabilities in converting ozonated and non-ozonated APL organics into methane (Chapter 3)
5. Finding appropriate OLR and SRT for improved methane production in anaerobic mono-digestion or co-digestion of ozonated and non-ozonated APL employing different inocula (Chapter 4),
6. Characterizing microbial community composition in the digesters (Chapter 4).

5.1. Key findings

The first objective of this study was to determine the anaerobic degradability of APLs generated under 500 and 700 °C pyrolysis temperatures. Pyrolysis temperature is one of the major factors affecting the degradability of the resulting APL; therefore, this study was performed on APL derived at two different pyrolysis temperatures. APL generated at 500 °C pyrolysis was degradable under the conditions studied and exhibited no toxicity during ATA (IC_{50} >4 gCOD/L APL).

However, 700 °C was more toxic to anaerobic microorganisms using all inocula (1.5 gCOD/L APL< IC_{50} <3.6 gCOD/L APL). This was consistent with other studies describing that APL toxicity increases with increased pyrolysis temperature. APL produced at 500 °C in this study contained higher COD, VFA and NH_3-N concentrations, compared to APL produced at 700 °C APL. The higher degradability of the 500 °C APL could also be correlated with higher VFA concentrations such as acetic acid in the 500 °C APL compared to 700 °C APL. The majority of 500 and 700 °C APLs constituents were N-heterocyclic organics.

For the second objective, APL ozonation for 10 min and 2 h was conducted. APL ozone pretreatment altered its composition such that problematic compounds like aromatics, N-heterocyclic organics and phenolics content decreased due to ozonation as indicated by GC-MS analysis as well as SUVA and TP measurements. The majority of TP concentrations was removed during the first 10 min of ozonation. Ozonation was also conducted for 2 h to assess if changes other than TP removal occurred that influenced subsequent AD. Less than 20% of APL COD and DOC concentrations were removed during ozonation due to oxidation of organics or gas stripping. Therefore, the ozonated product still contained significant concentrations of organic carbon for potential conversion to methane that was more amenable to anaerobic biodegradation.

Following objective two, the goal in the third and fourth objectives were to employ ATAs to determine the effect of ozonation and use of different inocula in APL degradation. ATAs were conducted at different concentrations of non-ozonated, 10 min ozonated and 2 h ozonated 500 and 700 °C APL to determine

inhibitory concentration (IC_{50}) employing two industrial inocula (IB1 and IB2) and two municipal inocula (MB1 and MB2). Different inocula demonstrated different capabilities to degrade the more toxic APL (700 °C), such that employing MB2 resulted in the highest IC_{50} value amongst all inocula, followed by IB2, suggesting their robustness towards APL toxicity, and IB1 achieving the highest final cumulative methane production. Ozone pretreatment removed some of the potential inhibitory compounds and rendered APL less toxic and more amenable to AD in some cases. Ozonation improved methane production rate from 700 °C APL such that IC_{50} values increased as the ozonation time increased and no inhibition was observed at any concentration when 2 h ozonated APL was used with MB2 and IB2. Ozonation for 2 h also significantly decreased initial lag phase in 700 °C APL in ATAs employing all inocula, whereas using 10 min ozonated APL increased the lag phase time compared to non-ozonated APL. Higher lag phase after ozonation could be due to production of more toxic ozonation intermediates that resulted in longer acclimation time. On the other hand, APL ozonation did not significantly influence methane production rate in ATAs using 500 °C APL. However, digesters inoculated with MB1 demonstrated increased lag time when 10 min ozonated and 2 h APLs were used.

The fifth objective was to operate lab-scale anaerobic mono-digesters and co-digesters for long-term APL digestion feasibility employing MB1 and IB1 as inocula and investigate the appropriate SRT and OLR for APL degradability. APL derived at 700 °C pyrolysis was used in this objective since it was more inhibitory than 500 °C APL. Results of this objective showed that APL was digested under

the conditions studied and the majority of the APL organics were converted to methane. Ozonated and non-ozonated APLs were used as the sole substrate or co-digestate with synthetic primary sludge at: (1) 0.2 gCOD/L APL at 15-d SRT and (2) 0.03 gCOD/L APL at 210-d SRT. Methane production was inhibited in all co-digesters and mono-digesters when employing shorter SRT and higher OLR but increasing the SRT and decreasing OLR significantly improved methane production. Mono-digesters operated at 210-d SRT demonstrated >90% conversion of APL organics into methane. Similarly, co-digesters produced 48 – 98% of the stoichiometric maximum methane from APL when operated at 210-d SRT. . IB inoculum performed better in degrading APL compared to MB, since it was acclimated to similar compounds as the APL constituents. Between 60 – 98% of the expected theoretical methane from APL COD was generated from IB-inoculated co-digesters, whereas MB-inoculated co-digesters produced 48 – 64% of the expected theoretical methane from APL COD. Under the conditions studied, the non-ozonated APL was also degraded in both IB and MB inoculated co-digesters to some extent. Ozonation for 2 h improved methane production in co-digesters inoculated with IB such that >95% of the theoretical stoichiometric methane from APL COD was observed, whereas co-digesters receiving non-ozonated and 10 min ozonated APLs were statistically lower (60 – 79% of stoichiometric maximum methane from APL COD). NH_3-N concentration reduction due to ozonation was not the reason in reducing APL toxicity, whereas ozonation of organics was found to be the primary factor in improving APL degradability. APL degradation was also confirmed by analyzing the digestate using GC-MS analysis,

which showed removal of APL organics after digestion was due to biodegradation.

In the last objective, microbial communities in the digesters were investigated. Microbial community analysis revealed hydrogenotrophic methanogenesis was the primary route in IB-inoculated co-digesters and mono-digesters, whereas MB-inoculated co-digesters employed both acetoclastic and hydrogenotrophic pathways for methane production. By the end of APL digestion, the archaeal community in IB-inoculated co-digesters was primarily dominated by genus *Methanobacterium*. The associated bacterial partners which were SAOBs such as genera in phylum Synergistes and class Clostridia also increased in relative abundance in bacterial community. Other important bacterial taxa capable of degrading N-heterocyclic compounds that were selected for in IB-inoculated co-digesters or mono-digesters receiving APL include genera *Enterococcus* and *Eubacterium*, and order Bacillales. In MB-inoculated co-digesters, the archaeal community was dominated by acetoclastic *Methanosaeta* and hydrogenotrophic *Methanoculleus* and *Methanobacterium*. Relative abundance of several SAOB belonging to phylum Synergistes and class Clostridia also increased in MB-inoculated co-digesters. The phenol degrading bacterial order, Bacteroidales was enriched for in MB-inoculated co-digesters.

5.2. Future outlook

The findings of this study demonstrate the importance of employing an appropriate OLR and SRT, selection of a proficient inocula, and pre-ozonation to reduce APL recalcitrance and toxicity during AD for improved methane production.

Further research is required to improve the overall efficiency of the process. For example, future work should consider exposing the microbes to increased OLR and decreased SRT to determine if the microbes can show tolerance and handle higher APL OLRs. APL was digested alone and co-digested with synthetic primary sludge using an industrial biomass (IB). Using municipal anaerobic digester biomass (MB) also resulted in APL degradation to some extent, but it was more sensitive to APL toxicity. Therefore, future research focused on bioaugmenting municipal digesters with IB to improve performance is warranted. In the co-digestion scenario, using real primary sludge should be considered to mimic the real-world AD.

The 2 h ozonation period or less was able to reduce APL toxicity generated at higher pyrolysis temperatures to enhance methane production during digestion. More research on APL ozonation kinetics is essential to understand removal and transformation mechanisms during ozonation and improve the process.

Pilot-scale testing is required to corroborate the results of this research in order to implement these strategies for full-scale applications. Additionally, an extensive techno-economic analysis on viability of APL AD and the toxicity reduction strategies is required to assist in decision making regarding commercial-scale implementation.

Finally, the overall outcome of this dissertation indicated that integration of pyrolysis and anaerobic digestion is a promising pathway for wastewater solids management, valorizing APL as a waste, and preventing a potentially hazardous material from entering the environment.

6 Appendices A

6.1. Supporting Information 1

Table S3.1. Percent of total organic compounds peak area detected in 500 °C and 700 °C APL by GC-MS. Compounds sorted in increasing order of the molar mass.

		% of total organic compound peak area detected	
Compounds	**Molar mass (g/mol)**	**Non-ozonated 500 °C APL**	**Non-ozonated 700 °C APL**
Acetonitrile	41.05	2.4	15
Propanenitrile	55.08	0.7	2.6
Acetamide	59.07	17	19
Acetic acid	60.06	15	-
Pyrrole	67.09	0.5	3.5
1H-Imidazole	68.08	-	1.3
2-Propenamide	71.08	-	0.8
Propanamide	73.09	3.2	2.5
Acetamide, N-methyl-	73.09	1.6	1.3
Propionic acid	74.08	1.7	-
1-Butanol	74.12	1.3	0.8
Pyridine	79.10	1.2	3.9
1,3-Diazine	80.09	-	0.6
1H-Pyrazole, 3-methyl-	82.10	0.6	-
1H-Imidazole, 4-methyl-	82.10	-	1.9
trans-Crotonamide	85.10	-	0.7
2-Pyrrolidinone	85.11	3.0	2.5
Acetamide, N,N-dimethyl-	87.12	0.8	0.6
Propanoic acid, 2-methyl-	88.11	1.0	-
Glycerin	92.09	1.3	-
Pyridine, 2-methyl-	93.13	-	1.7
Pyridine, 3-methyl-	93.13	-	0.9
2-Aminopyridine	94.11	0.5	-
3-Aminopyridine	94.11	2.0	4.9
Phenol	94.11	-	2.1
Pyrazine, methyl-	94.11	-	1.7
2-Aminopyridine	94.11	-	0.8
Pyrimidine, 2-methyl-	94.11	-	0.7
2(1H)-Pyridinone	95.10	0.5	1.4
3-Pyridinol	95.10	3.7	4.1
1H-Imidazole, 2,4-dimethyl-	96.13	-	1.4
3-Dimethylaminoacrylonitrile	96.13	-	0.6
2-Furanmethanol	98.10	-	1.3
2,5-Pyrrolidinedione	99.09	1.6	1.7
2-Piperidinone	99.13	1.2	-
Butanamide, 3-methyl-	101.2	1.0	0.6
Phenol, 4-methyl-	108.1	0.8	1.3
2-Pyridinamine, 5-methyl-	108.1	-	1.0
Pyrimidine, 4,6-dimethyl-	108.1	-	0.9
4-Pyridinemethanol	109.1	3.5	-
3-Pyridinol, 2-methyl-	109.1	0.6	1.0
3-Pyridinol, 6-methyl-	109.1	-	2.9
2-Amino-4-methylpyrimidine	109.1	-	0.4
2(1H)-Pyridinone, 3-methyl-	109.1	-	0.6

Table S3.1. Continued.

		% of total organic compound peak area detected	
Compounds	**Molar mass (g/mol)**	**Non-ozonated 500 °C APL**	**Non-ozonated 700 °C APL**
Pyrrole-2-carboxamide	110.1	0.8	-
2(1H)Pyrimidinone,1-methyl-	110.1	0.5	-
3,4-Dimethyl-3-pyrrolin-2-one	111.1	0.5	-
2,5-Pyrrolidinedione, 1-methyl-	113.1	0.5	1
2,4-Imidazolidinedione, 5-methyl-	114.1	0.6	-
Pentanoic acid, 3-methyl-	116.2	2.1	-
Pentanamide, 5-hydroxy-	117.2	0.6	-
Indolizine	117.2	-	0.6
Pyrazine, 2-ethyl-3-methyl-	122.2	-	0.7
2(1H)-Pyridinone, 3,6-dimethyl-	123.2	-	0.8
1-Propanone, 1-(2-furanyl)-	124.1	0.5	-
5,6-Dihydro-6-methyluracil	128.1	1.1	1.5
5,5-dimethyl-2,4-imidazolidinedione	128.1	6.4	1.8
Oxazolidine, 2-ethyl-2,3-dimethyl-	129.2	0.7	-
DL-Alanine, N-acetyl-	131.1	0.7	0.6
Quinoline, 5,6,7,8-tetrahydro-	133.2	-	0.9
Acetamide, N-3-pyridinyl-	136.2	1.7	0.8
dl-5-Ethyl-5-methyl-	142.2	2.9	0.9
5-Isopropyl-2,4-imidazolidinedione	142.2	2.4	-
6-Amino-1-methylpurine	150.2	1.0	0.6
Acetamide, N-(4-aminophenyl)-	150.2	0.6	-
Formamide, N,N-dibutyl-	157.3	1.9	-
Uric acid	168.1	1.6	-
Phosphonic acid, (p-hydroxyphenyl)-	174.1	1.0	-
D-Allose	180.2	0.9	-
Pyrrolo[1,2-a]pyrazine-1,4-dione, hexahydro-3-(2-methylpropyl)-	210.3	1.0	-
5,10-Diethoxy-2,3,7,8-tetrahydro-1H,6H-dipyrrolo[1,2-a;1',2'-d]pyrazine	250.3	1.2	-
Piperazine, 1-[(2,4-dichlorobenzoyl)methyl]-4-methyl-	287.2	-	0.5
Pyrimidine-2,4,6-trione, 1-cyclohexyl-5-[(2-piperazin-1-yl-ethylamino)methylene]-	349.4	-	0.5
Deoxyspergualin	387.5	-	0.4

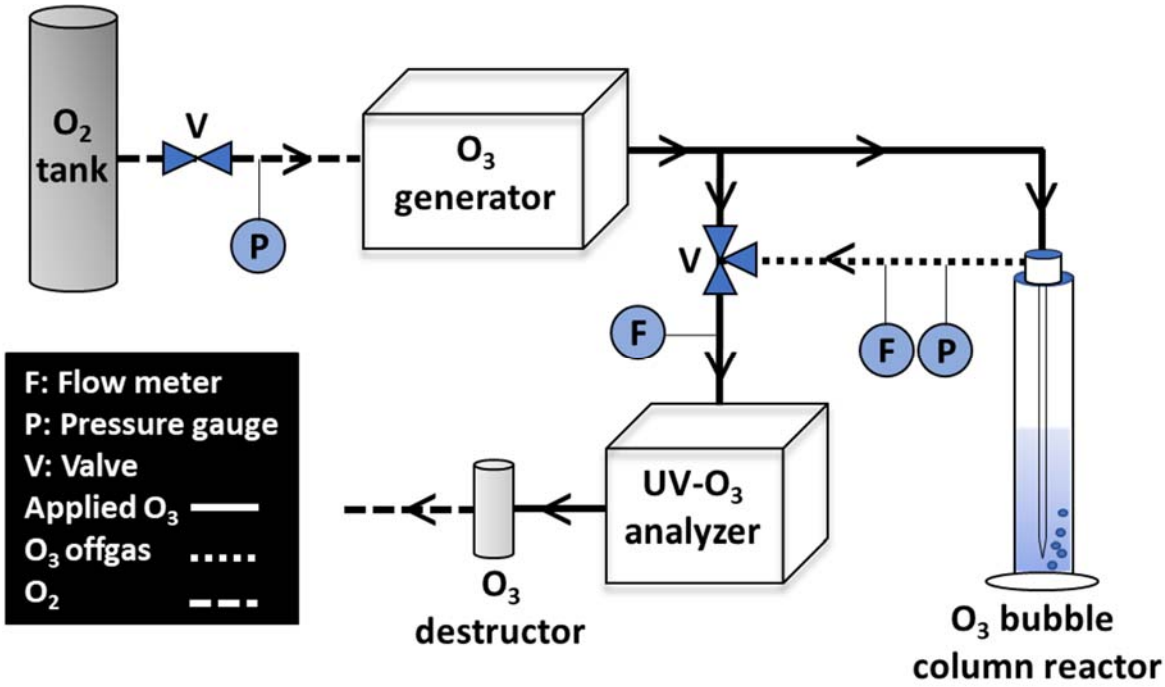

Figure S3.1. Pre-ozonation Schematic.

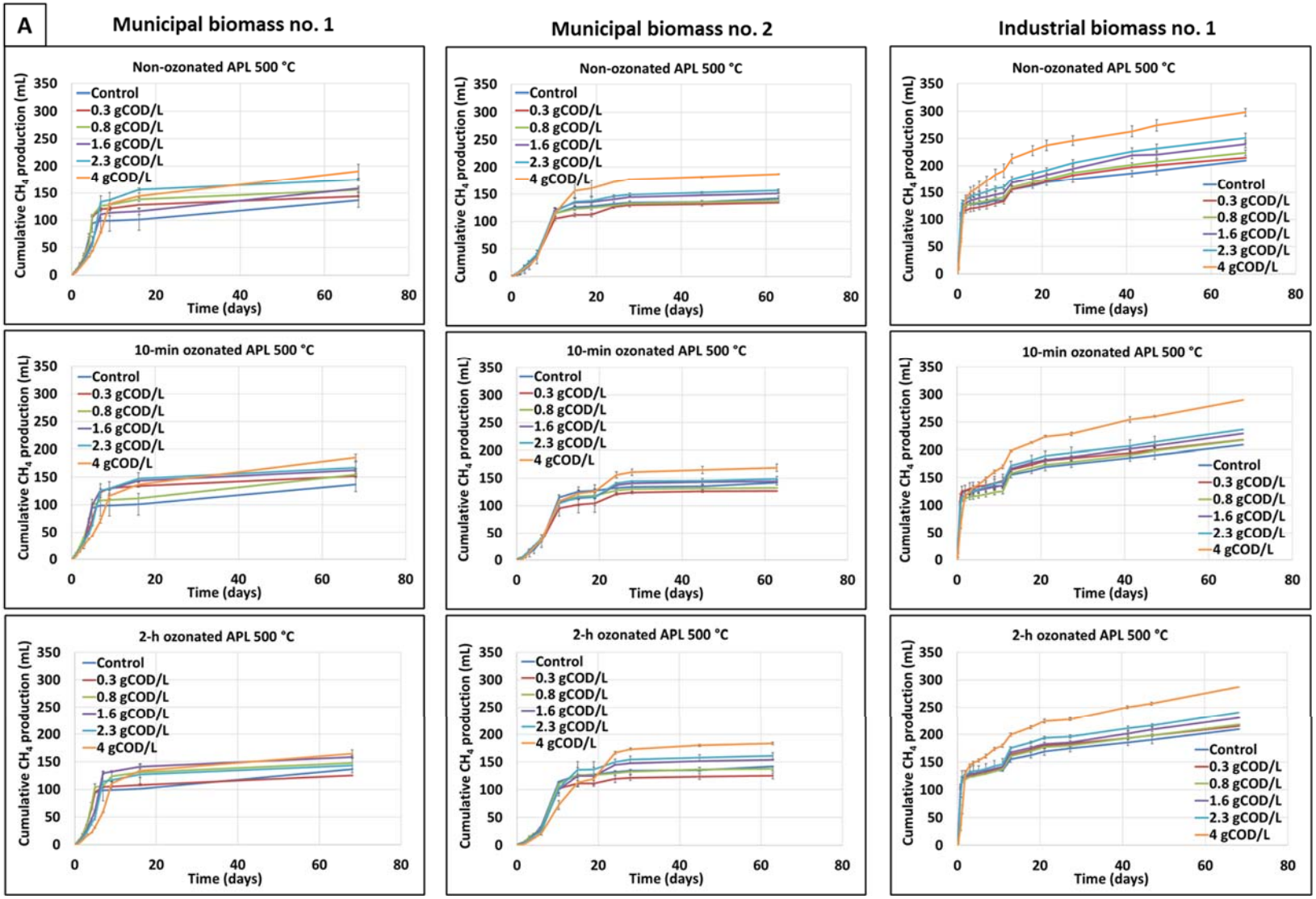
A
Municipal biomass no. 1
Municipal biomass no. 2
Industrial biomass no. 1
Non-ozonated APL 500 °C
10-min ozonated APL 500 °C
2-h ozonated APL 500 °C
Cumulative CH4 production (mL)
Time (days)
Control
0.3 gCOD/L
0.8 gCOD/L
1.6 gCOD/L
2.3 gCOD/L
4 gCOD/L

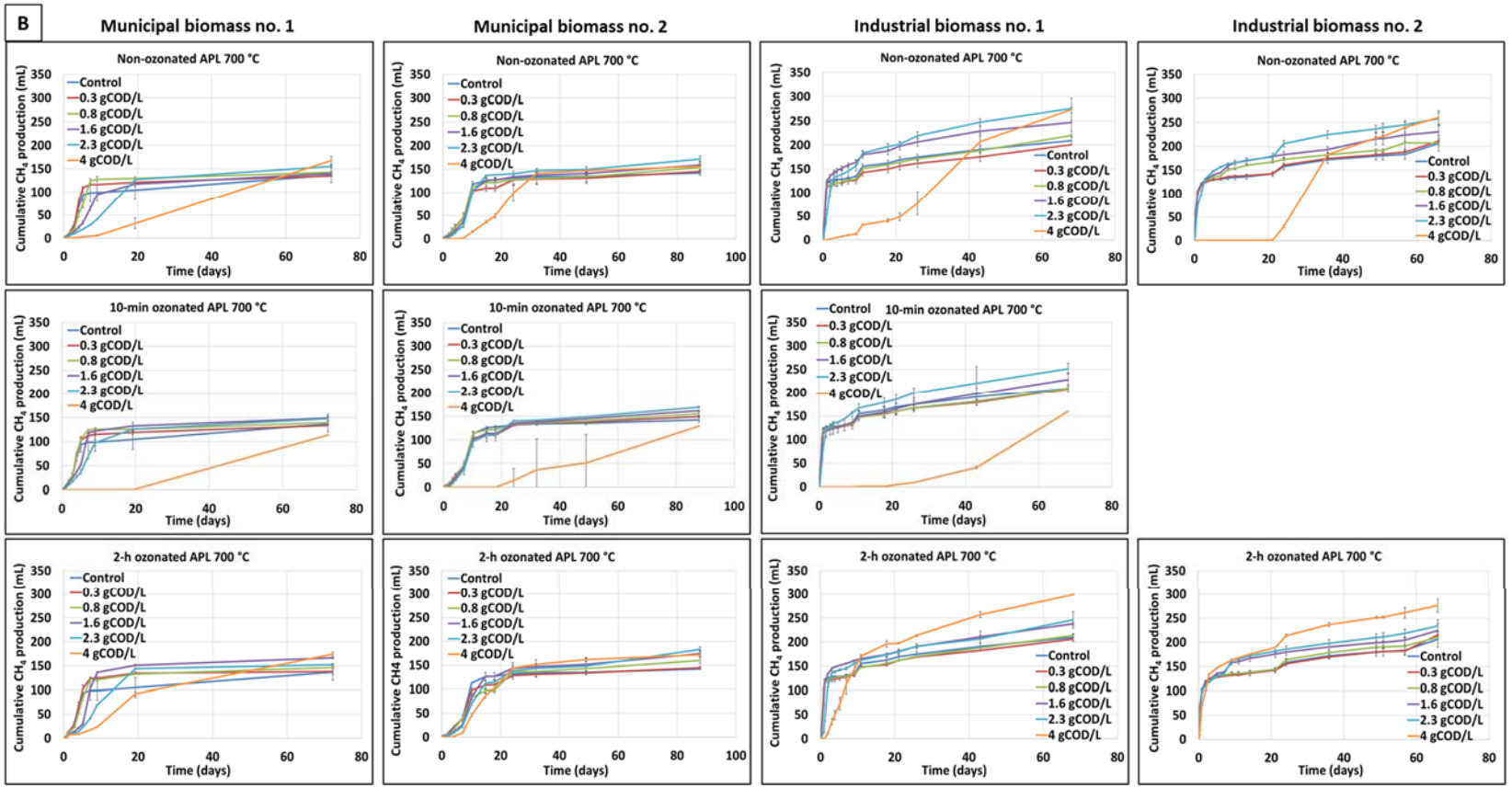

Figure S3.2. Cumulative methane production from ATA on non-ozonated, 10 min ozonated and 2 h ozonated APL using different inocula at different APL COD concentrations. Average values and standard deviations are from triplicates bottles. (A) 500 °C APL, (B) 700 °C APL.

6.2. Supporting information 2

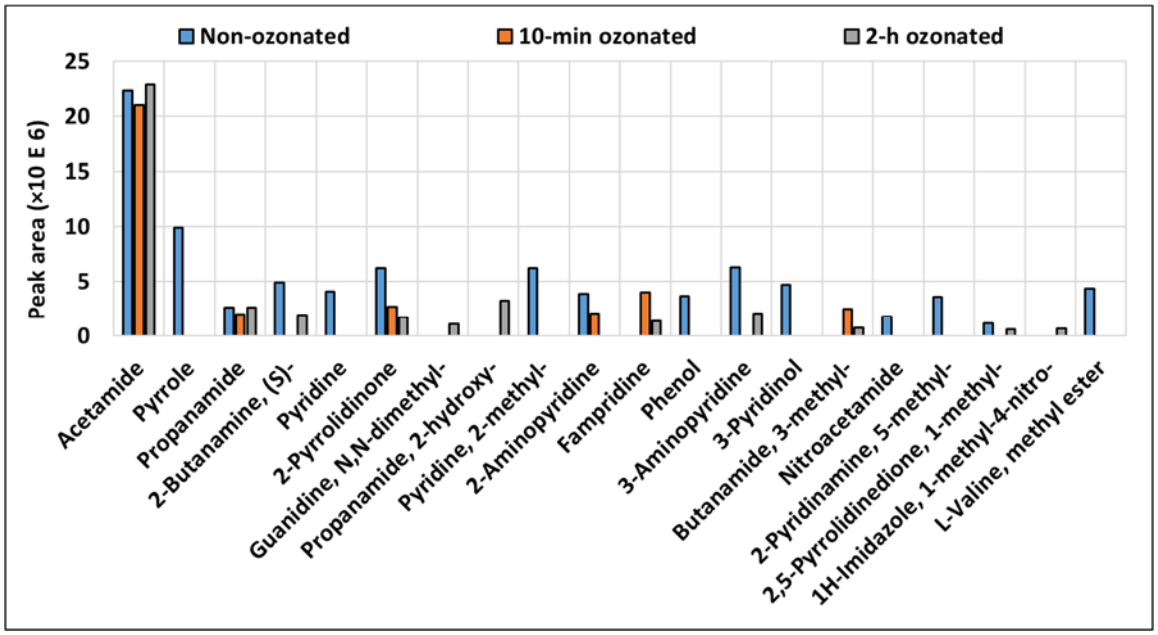

Figure S4.1. APL organic compounds peak area in non-ozonated, 10 min and 2 h ozonated APL detected by GC-MS analysis. Undetected peaks were below detection (BD) of the GC-MS instrument ($<0.05\times10^6$).

Table S4.1. Operational parameters during quasi steady state operation of the co-digesters run at 15-d SRT. Co-digester set 2 was inoculated with MB and co-digesters set 3 was inoculated with IB. Average and standard deviations are from four consecutive measurements of triplicate co-digesters during quasi steady state operation.

Digester set	CH_4 production rate	Biogas CH_4 content	Digestate COD	Digestate SCOD	Digestate VFA	Digestate TSS	Digestate VSS
-	mL/d	%	g/L	g/L	g/L as acetic acid	g/L	g/L
2-1 (Control 1)	36 ± 3.9	63 ± 5.6	11 ± 0.8	1.5 ± 0.1	0.2 ± 0.1	8.8 ± 0.4	6.2 ± 0.5
2-2	7.5 ± 1.4	41 ± 1.6	31 ± 2.1	17 ± 1.5	5.6 ± 1.8	11 ± 0.6	8.5 ± 0.2
2-3	32 ± 5.8	67 ± 8.6	23 ± 0.7	12 ± 0.9	4.8 ± 1.9	10 ± 0.3	7.4 ± 0.3
2-4	24 ± 3.3	58 ± 6.1	23 ± 1.4	13 ± 1.5	5.2 ± 1.8	11 ± 0.4	7.7 ± 0.5
2-5	22 ± 2.0	59 ± 4.1	23 ± 1.6	12 ± 0.4	4.5 ± 1.1	11 ± 0.7	7.7 ± 0.4
3-1 (Control 2)	38 ± 2.5	65 ± 2.6	13 ± 0.4	1.4 ± 0.1	0.2 ± 0.0	11 ± 1.0	7.3 ± 0.2
3-2	3.8 ± 0.8	29 ± 1.4	35 ± 1.5	20 ± 1.2	5.3 ± 1.4	12 ± 0.3	9.3 ± 0.4
3-3	4.2 ± 0.7	28 ± 0.4	33 ± 1.9	20 ± 1.9	8.1 ± 1.7	12 ± 0.5	9.0 ± 0.2
3-4	26 ± 2.5	50 ± 6.7	20 ± 0.4	7.8 ± 0.6	2.1 ± 0.2	12 ± 1.0	8.0 ± 0.3
3-5	25 ± 2.0	64 ± 2.5	23 ± 1.1	11 ± 0.5	2.5 ± 1.4	13 ± 1.7	9.0 ± 1.3

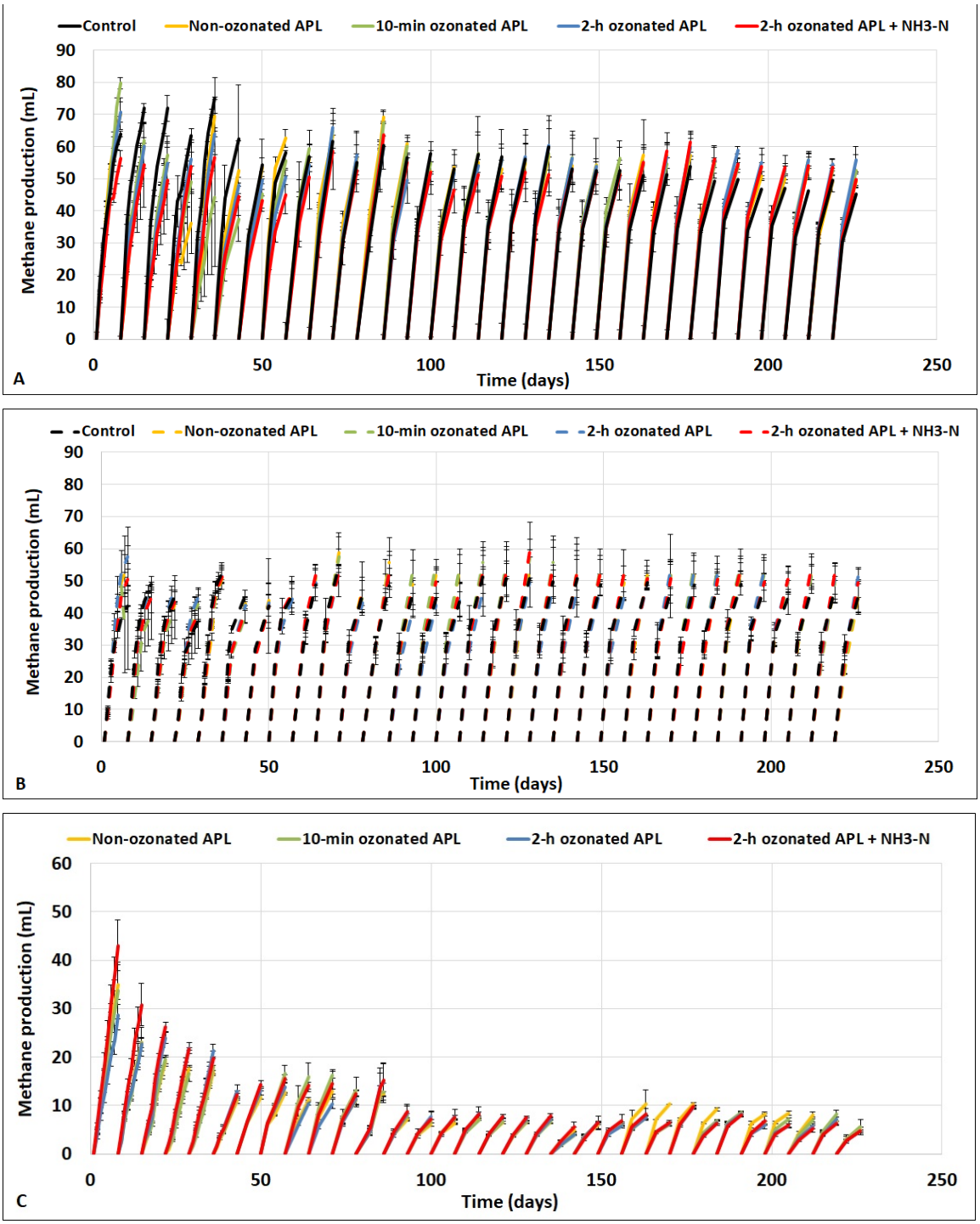

Figure S4.2. Methane production results of the 210-d SRT digestion. Weekly cumulative methane production in digesters and co-digesters receiving non-ozonated, 10 min, 2 h ozonated, and 2 h ozonated APL + NH_3-N in (A) co-digesters inoculated with IB, (B) co-digesters inoculated with MB, (C) mono-digesters. Control indicate digesters receiving only synthetic sludge. Error bars represent standard deviation from triplicate experiments during quasi steady state. Some error bars are small and not visible.

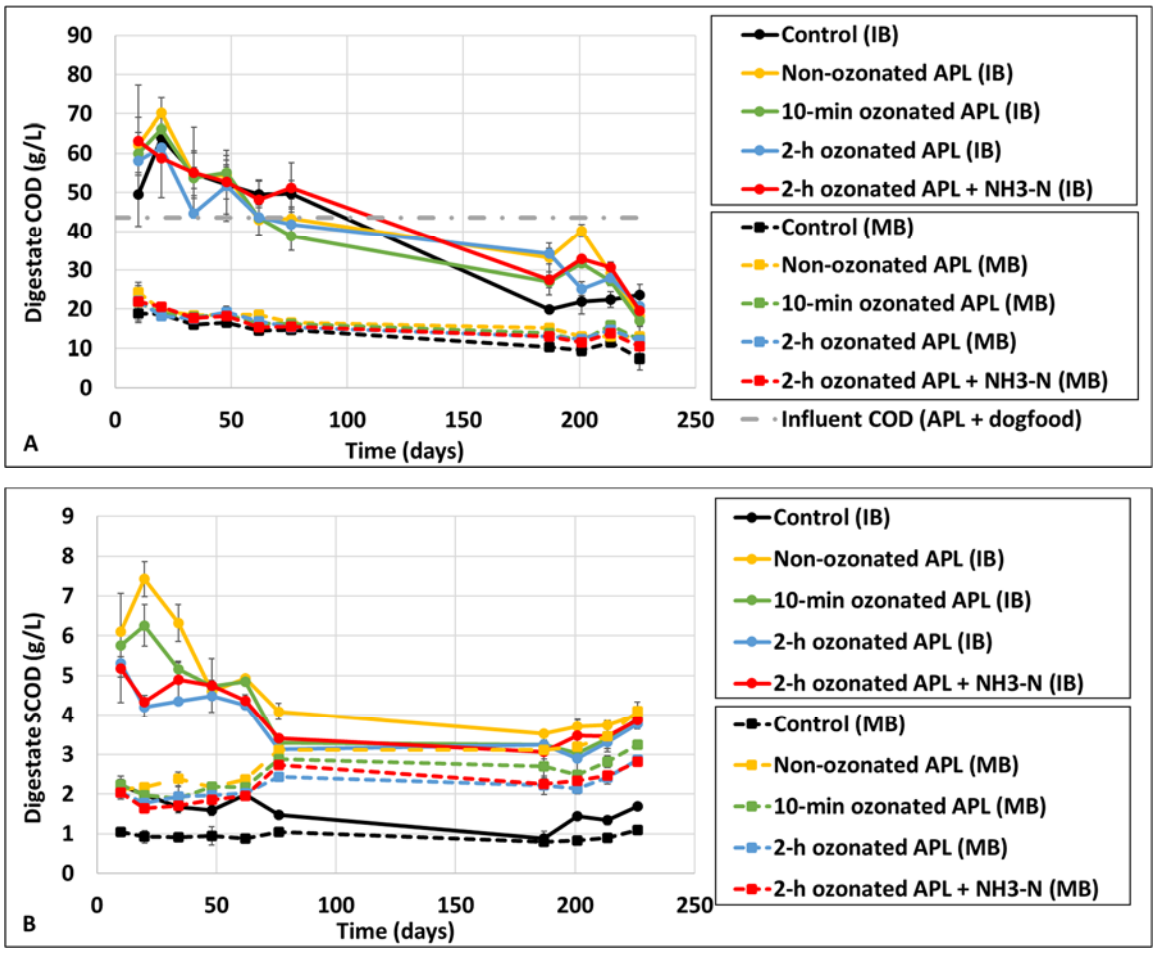

Figure S4.3. Digestate COD and SCOD concertation in co-digesters inoculated with MB or IB run at 210-d SRT receiving non-ozonated, 10 min ozonated, 2 h ozonated, and 2 h ozonated APL + NH_3-N. Control indicates digesters receiving only synthetic primary sludge. (A) COD concentration, (B) SCOD concentration. Error bars represent standard deviation from triplicate experiments during quasi steady state. Some error bars are small and not visible.

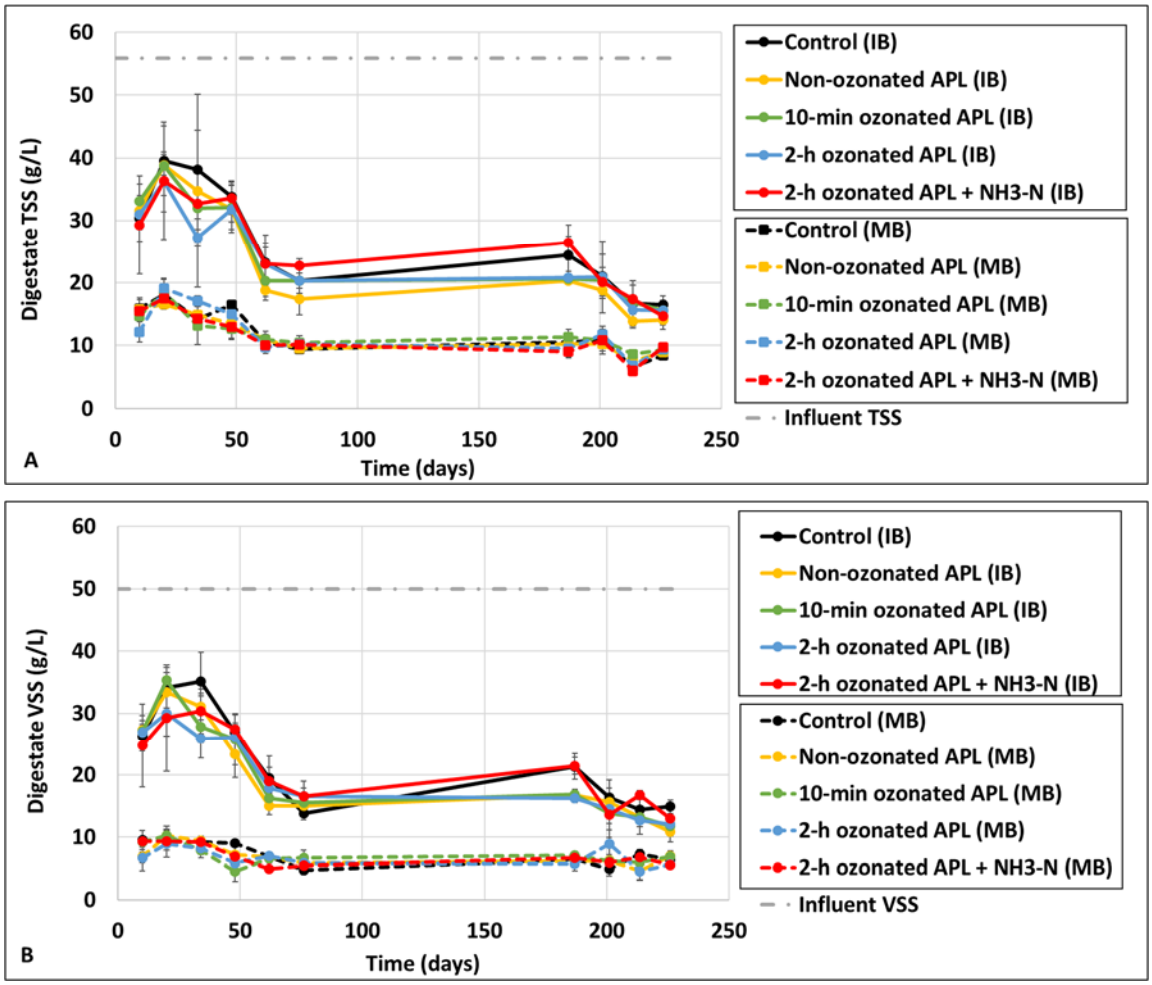

Figure S4.4. Digestate TSS and VSS concertation in co-digesters inoculated with MB or IB run at 210-d SRT receiving non-ozonated, 10 min ozonated, 2 h ozonated, and 2 h ozonated APL + NH_3-N. Control indicates digesters receiving only synthetic primary sludge. (A) TSS concentration, (B) VSS concentration. Error bars represent standard deviation from triplicate experiments during quasi steady state. Some error bars are small and not visible.

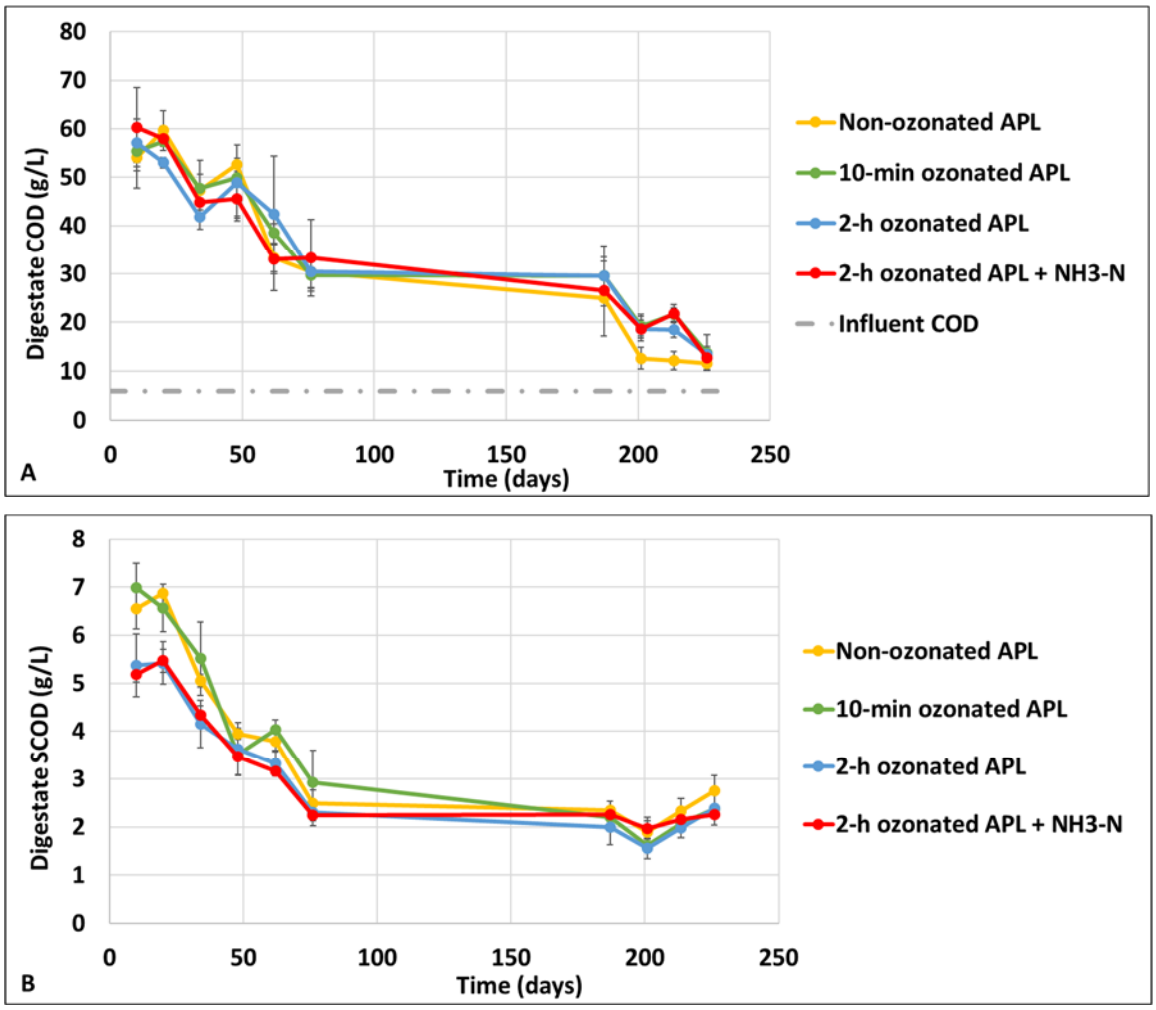

Figure S4.5. Digestate COD and SCOD concertation in mono-digesters inoculated with MB or IB run at 210-d SRT receiving non-ozonated, 10 min ozonated, 2 h ozonated, 2 h ozonated APL + NH_3-N. (A) COD concentration, (B) SCOD concentration. Error bars represent standard deviation from triplicate experiments during quasi steady state. Some error bars are small and not visible.

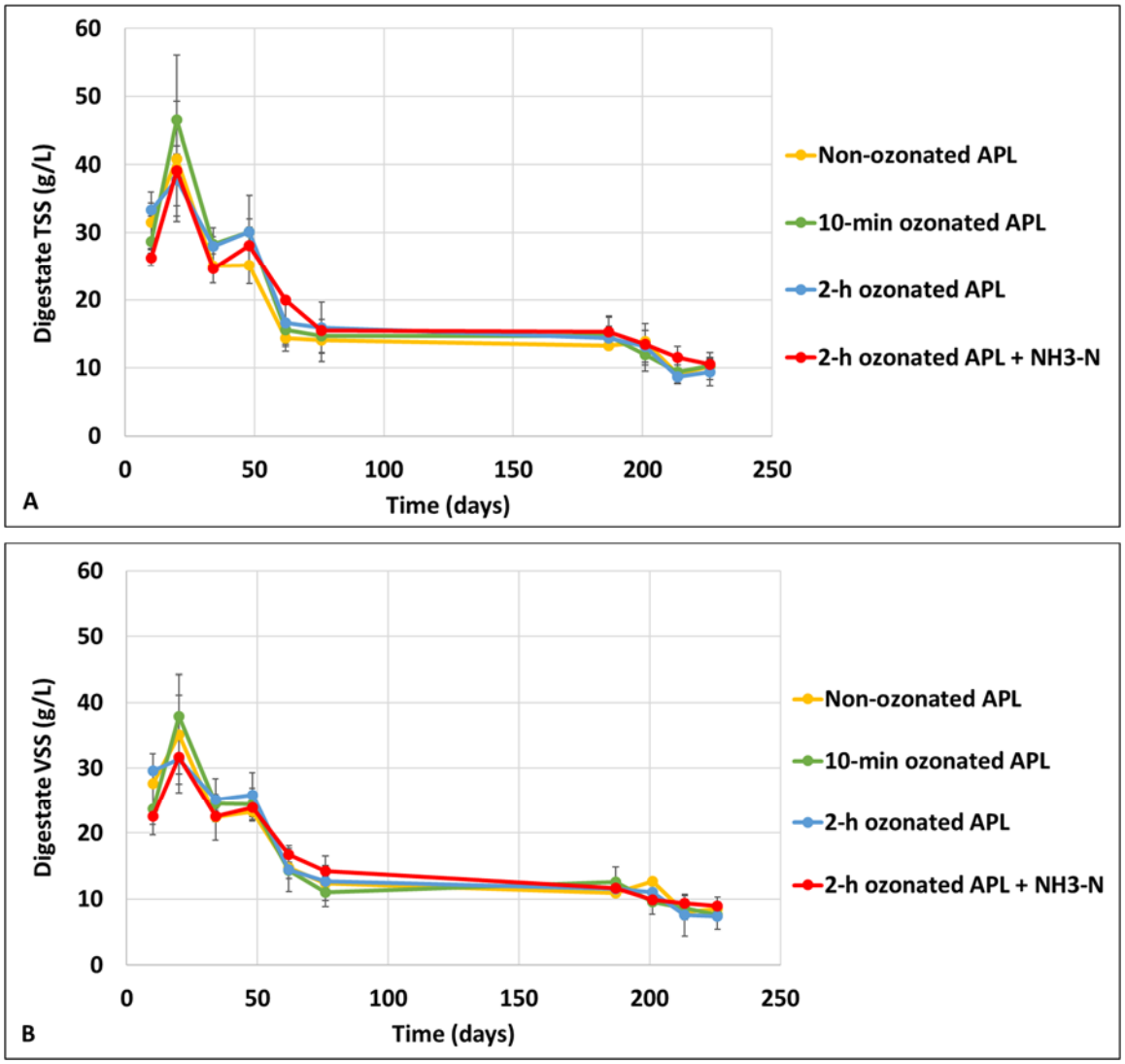

Figure S4.6. Digestate TSS and VSS concertation in mono-digesters inoculated with MB or IB run at 210-d SRT receiving non-ozonated, 10 min ozonated, 2 h ozonated, and 2 h ozonated APL + NH_3-N. (A) TSS concentration, (B) VSS concentration. Error bars represent standard deviation from triplicate experiments during quasi steady state. Some error bars are small and not visible.

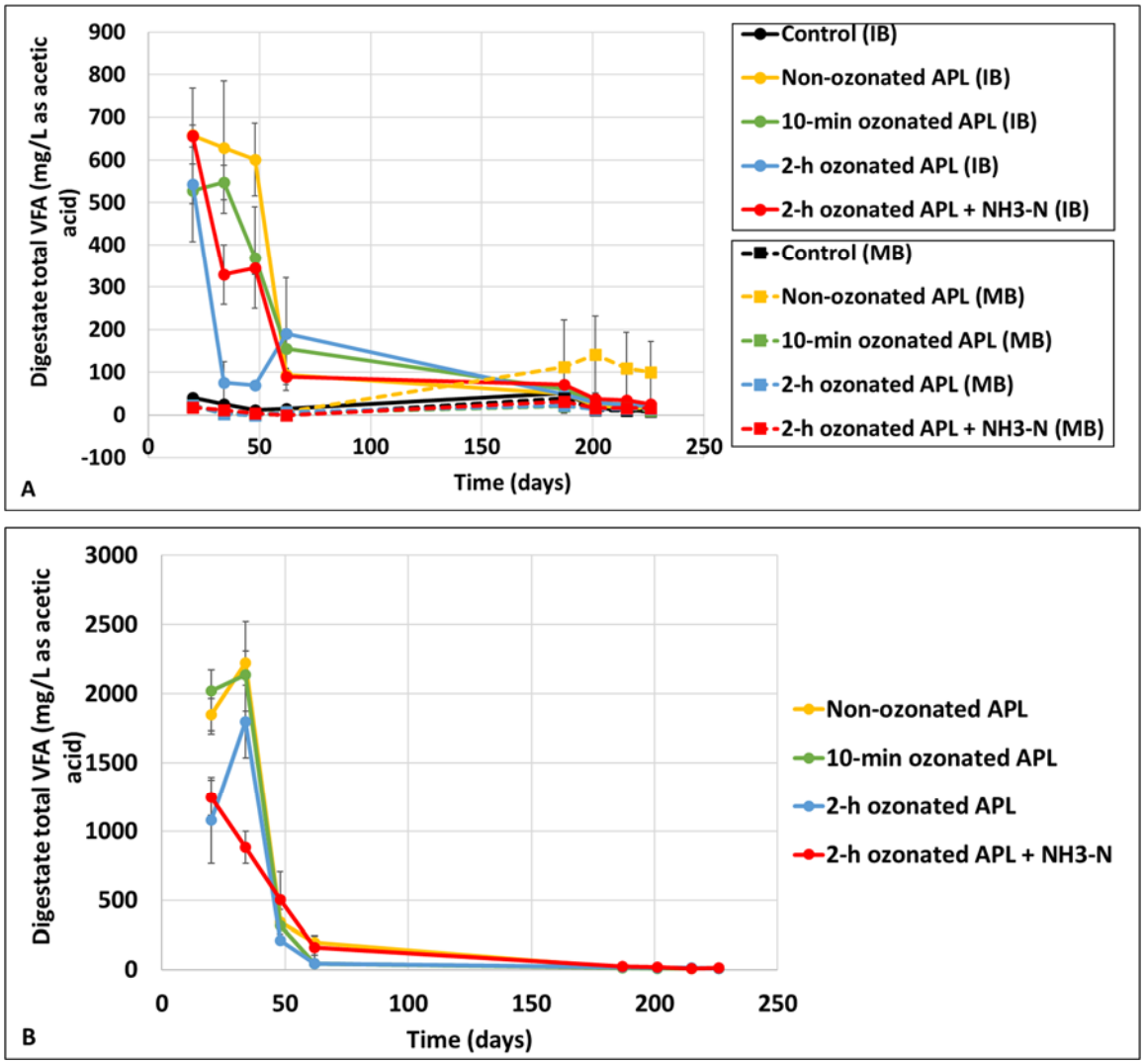

Figure S4.7. Digestate VFAs concertation in co-digesters and mono-digesters inoculated with MB or IB run at 210-d SRT receiving non-ozonated, 10 min ozonated, 2 h ozonated, and 2 h ozonated APL + NH_3-N. Control indicates digesters receiving only synthetic primary sludge. (A) Co-digesters, (B) mono-digesters. Error bars represent standard deviation from triplicate experiments during quasi steady state. Some error bars are small and not visible.

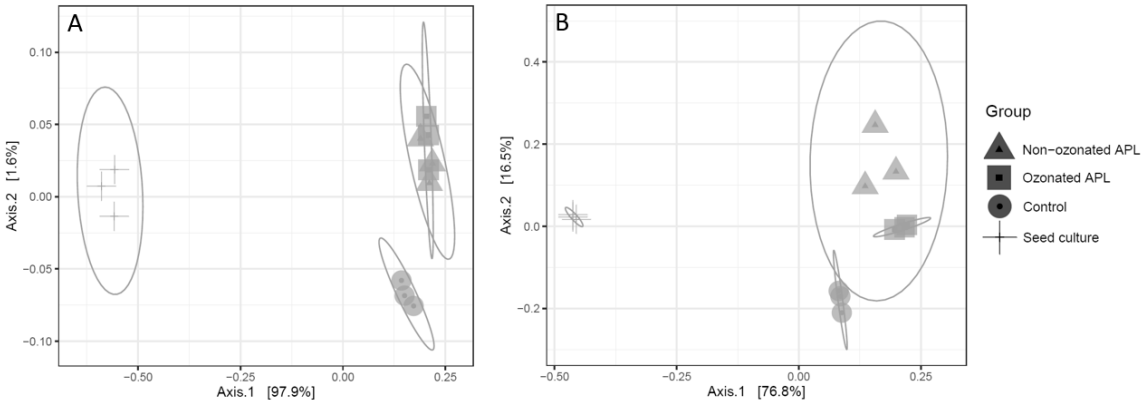

Figure S4.8. PCoA plots on archaeal community in (A) IB, and (B) MB, inocula (day 0) and co-digesters (day 215) based on Bray-Curtis distance. Ellipses represent 95% confidence intervals for the three points (each group represents the three triplicate digesters. Archaeal community in ozonated and non-ozonated APL co-digestion was shifted from inocula community in both IB and MB. The control digesters inoculated with MB was more similar to APL-fed co-digesters, whereas the control digesters se inoculated eded with MB was different from APL-fed co-digesters.

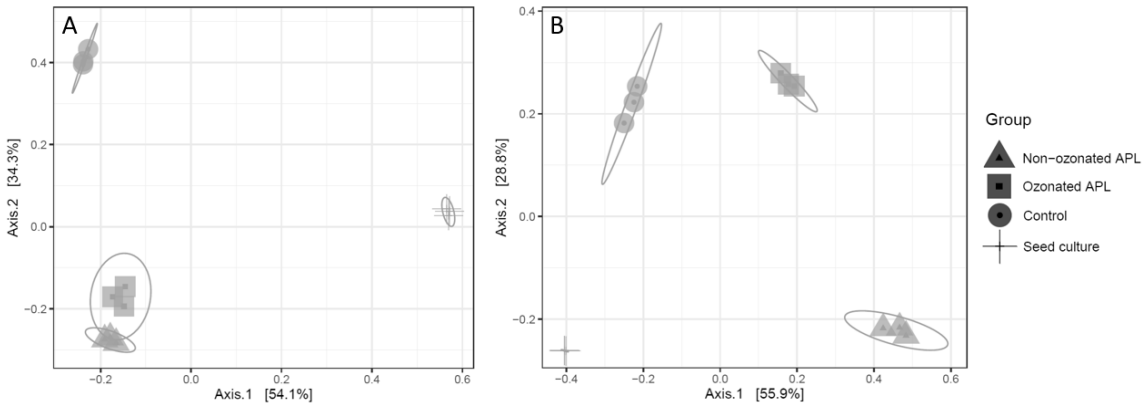

Figure S4.9. PCoA plots on bacterial community in (A) IB, and (B) MB, inocula (day 0) and co-digesters (day 215) based on Bray-Curtis distance. Ellipses represent 95% confidence intervals for the three points (each group represents the three triplicate digesters. Bacterial community in IB- inoculated ozonated and non-ozonated APL co-digesters were more similar to inocula compared to control digesters. In contrast, significant shift in bacterial community in MB- inoculated co-digesters fed ozonated and non-ozonated APL was observed, while control digesters had a smaller shift.

7 Appendices B

This chapter is published in the journal *Sustainability:*

Seyedi S, Venkiteshwaran K, Benn N, Zitomer D (2020) Inhibition during Anaerobic Co-Digestion of Aqueous Pyrolysis Liquid from Wastewater Solids and Synthetic Primary Sludge. *Sustainability* 12:3441.

7.1. Introduction

Contaminants such as antibiotic resistance genes, pathogens and other micropollutants can enter the environment when wastewater solids are land applied or landfilled(Tsai et al. 2009; Liu et al. 2018). Release of these constituents may be reduced if solids management technologies such as pyrolysis are employed to remove or destroy these contaminants and reduce the volume of biosolids (Ross et al. 2016; Kimbell et al. 2018; Liu et al. 2018). Pyrolysis involves the thermal conversion of wastewater solids in the absence of oxygen at temperatures between 400 and 1000 °C, and yields three products: biochar, pyrolysis gas (py-gas) and pyrolysis liquid (Fonts et al. 2012; McNamara et al. 2016; Seyedi 2018; Liu et al. 2020). Biochar can be used as a soil amendment to increase crop growth and an adsorbent to remove pollutants (McNamara et al. 2016; Ross et al. 2016; Seyedi 2018). Py-gas is a mixture of methane (CH_4), carbon monoxide (CO), hydrogen (H_2) and other gases that can be combusted directly for heat and power generation. Pyrolysis liquid is a complex mixture of organic compounds with water and often partitions into bio-oil (a light non-aqueous phase liquid) and aqueous pyrolysis liquid (APL) (Fonts et al. 2012; Torri and Fabbri 2014; Liu et al. 2020). Bio-oil can be used as a renewable fuel after conditioning to remove water, organic acids and other constituents that are corrosive during combustion. By contrast, APL is water-based, has a low heating value and currently has no known beneficial use (Li et al. 2009; Torri and Fabbri 2014; Hübner and Mumme 2015). APL can be environmentally harmful if not managed properly due to its high chemical oxygen demand (COD) concentration

and the presence of potentially toxic organic compounds such as cresol, ethylbenzene, phenol and xylene (Seyedi et al. 2019).

Autocatalytic pyrolysis is a recently-developed process that uses previously-produced biochar from biosolids pyrolysis as a catalyst to increase py-gas while decreasing bio-oil and APL production (McNamara et al. 2016; Liu et al. 2017, 2020). The novel autocatalytic process has been shown to increase py-gas energy by more than three times (from 2940 kJ/kg biosolids-pyrolyzed to 10,200 kJ/kg biosolids-pyrolyzed) (Liu et al. 2017). Additionally, as illustrated in the graphical abstract, autocatalytic pyrolysis of wastewater biosolids at 800 °C resulted in no bio-oil production, but APL was still produced (catalyzed APL) that had a lower organic content and fewer unsaturated hydrocarbons compared to non-catalyzed APL (Liu et al. 2017; Seyedi et al. 2019).

One possible APL management strategy involves anaerobic digestion, since APL contains a high concentration of organics (30–300 gCOD/L), including acetic acid (approximately 25 g/L) that possibly could be converted to biogas containing methane for renewable energy generation (Torri and Fabbri 2014; Seyedi et al. 2019). However, previous studies have shown anaerobic digestion is challenging since APL contains organic compounds that are known to inhibit methanogens and reduce or stop digester methane production (Torri and Fabbri 2014; Hübner and Mumme 2015; Zhou et al. 2019). In addition, high ammonia nitrogen (NH_3-N) concentration in APL may also cause digester inhibition (Yenigün and Demirel 2013; Seyedi et al. 2019). Both catalyzed and non-catalyzed APLs used in this study contained high NH_3-N concentrations. Therefore, air-stripping

pretreatment was employed to reduce NH_3-N content in APLs.

Anaerobic degradability of APL produced under different pyrolysis conditions has been previously investigated mostly in batch systems that do not mimic full-scale, continuously-fed systems. No reports were found regarding semi-continuous anaerobic co-digestion of APL derived from wastewater solids, biomass acclimation and the influence of APL feeding on the digester microbiome. Additionally, catalyzed APL derived from the novel autocatalytic pyrolysis process (Liu et al. 2017) has yet to be investigated as a viable co-digestate for anaerobic digestion. Parry et al. (2012) reported anaerobic co-digestion of APL obtained from pyrolysis of dried wastewater biosolids as well as thickened sludge; APL digestion resulted in 8% of the expected methane in a batch biochemical methane potential (BMP) test. The pyrolysis was performed at a low temperature (200 °C) and the APL generated was fed one time in a batch mode at 3.75 gCOD/L (Parry et al. 2012). In another batch study, APL from corn stalk pyrolysis at 400 °C inhibited methanogenic activity at organic loading of 35 $gCOD/L_r$ and nutrient supplement did not improve methane production, but biochar addition helped increase methane production in the batch and semi-continuous processes (Torri and Fabbri 2014). Hübner and Mumme (2015) also conducted a batch study using unacclimated biomass with APL derived at different temperatures (330, 430 and 530 °C) and demonstrated greater inhibition from APL derived at higher temperatures. In a recent study, Yu et al. (2020) added different dilutions of APL (5, 50 and 100 times dilution) diluted with pure water during anaerobic digestion of swine manure. Anaerobic digestion of swine manure with APL addition was

reported feasible in a batch test at low APL concentrations, whereas methane production ceased when the 5-time dilution was used. Phenolic compounds in the APL was described as a possible cause for the digester failure (Yu et al. 2020). In another recent study, anaerobic digestion of APL generated from birch bark at 500 °C resulted in poor methane production, probably due to the high phenolics concentration (24 g/kg total phenolics) (Wen et al. 2020). Biochar addition was reported to increase methane production by adsorbing some inhibitors (Wen et al. 2020). Zhou et al. (2019) used different APL pretreatments including overliming to reduce the toxicity of the APL derived from pyrolysis of corn stover under 500 °C. The overliming method removed a majority of the toxic compounds and increased biogas production. Subsequently, acclimation increased the microbial tolerance to APL after overliming.

The objective of this study was to elucidate co-digestion behavior for semi-continuously fed anaerobic digesters treating synthetic primary sludge along with APLs derived from wastewater biosolids pyrolysis. It was hypothesized that the catalyzed APL would exhibit toxicity different from that of conventional APL. Additionally, it was hypothesized that acclimation of microorganisms would increase methane production in the long-term semi-continuous co-digestion of APL with synthetic primary sludge. Synthetic primary sludge was co-fed to simulate co-digestion operations that could occur at municipal water resource reclamation facilities that currently have primary sludge digestion and may add solids pyrolysis in the future. Co-digesters treating synthetic primary sludge were separately co-fed with raw (non-air-stripped) and air-stripped catalyzed and non-catalyzed APLs.

APL air stripping was performed to reduce NH_3-N concentration in APL to prevent NH_3-N toxicity to anaerobic microorganisms. The effects of autocatalytic pyrolysis and air-stripping pretreatment on APL digestibility and anaerobic microbial community were investigated in this study. Additionally, a long-term (over 500 days) co-digestion study was conducted to investigate biomass acclimation to APL toxicity.

7.2. Materials and methods

7.2.1. APL production and APL NH_3-N air stripping

Catalyzed and non-catalyzed APLs were produced by pyrolysis at 800 °C of commercially available, dried biosolids, derived from anaerobically digested primary sludge and raw waste activated sludge (Milorganite) from the Jones Island Water Resource Recovery Facility (Milwaukee, Wisconsin) as described elsewhere (Liu et al. 2017). Milorganite a commercially available soil conditioner and has a nutrient composition of 6% nitrogen (N), 4% phosphorus (P) and 2.5% total iron (Fe) (“Specifications: Milorganite”,n.d; “Fertilizer Basics: Milorganite”, n.d). In an effort to remove NH_3-N that could inhibit methanogenesis, some catalyzed and non-catalyzed APL samples (30 mL) were aerated for 9 h at 2 L/min air flow (1 atm, 20 °C) to strip NH_3-N (Seyedi 2018). Volatile constituents such as ethylbenzene and styrene were also removed during air stripping (Table S7.1) (Seyedi et al. 2019).

7.2.2. Short-term semi-continuous anaerobic digestion

Anaerobic digesters were inoculated with anaerobic biomass from municipal digesters at the Fox River Water Pollution Control Center (Brookfield, WI). Digesters were 160 mL serum bottles with 50 mL working volume and were capped with butyl rubber stoppers. Five sets of triplicate digesters were operated at a 10-day solid retention time (SRT); each set was fed daily with synthetic primary sludge at a solids loading rate of 1.3 gVS/L_r-d (VS = volatile solids, L_r = liter of reactor) corresponding to an organic loading rate (OLR) of 2 gCOD/L_r-d. One digester set was a control receiving synthetic sludge and no APL. The remaining four digester sets were co-fed catalyzed APL, catalyzed air-stripped APL, non-catalyzed APL and non-catalyzed air-stripped APL, respectively, at an OLR of 0.05 gCOD/L_r-d along with synthetic primary sludge. The APL OLR of 0.05 gCOD/L_r-d was employed since it did not inhibit methanogenesis in a previous study which determined APL IC_{50} values (i.e., APL concentration that inhibited methane production rate by 50%) of 0.3–2.3 gCOD/L for the various APLs used in this study (Seyedi et al. 2019). Digesters were incubated at 35 °C and mixed on a shaker table at 150 rpm. All five digester sets were operated for 30 days to reach quasi steady state operation, which is determined as operation for at least 3 SRTs (i.e., 30 days) under consistent conditions when digester performance such as daily biogas production rate or effluent COD concentration variations are less than 10%. The digesters were then continued for 15 more days.

7.2.3. Long-term semi-continuous anaerobic digestion

A long-term co-digestion study was carried out for 523 days in 160 mL serum bottle digesters with 50 mL working volume capped with butyl rubber stoppers. Two sets of triplicate digesters were seeded with anaerobic biomass from municipal digesters at the Fox River Water Pollution Control Center (Brookfield, WI). Digesters were operated at 1.3 gVS/L_r-d (2 gCOD/L_r-d OLR) from the synthetic primary sludge and at a 10-day SRT. One set received synthetic primary sludge and no APL (control), whereas the other set was co-fed non-catalyzed APL and synthetic primary sludge. The initial APL OLR was 0.05 gCOD/L_r-d and was increased over time in a stepwise progression to 0.5 gCOD/L_r-d.

7.2.4. Synthetic primary sludge

Synthetic primary sludge was a mix of ground, dry dog food (Nutro Natural Choice, Franklin, TN, USA) and basal nutrient media with the following characteristics: 1.2 gCOD/L and 0.78 gVS/L and 0.94 gTS/L (TS = Total solids). The dry dog food has a mix of proteins (26%) and fats (12%) and previously has been used as consistent synthetic primary sludge in anaerobic digestion testing since the inherent variability of actual primary sludge causes inconsistent operations (Dang et al. 2016; Benn and Zitomer 2018; Venkiteshwaran et al. 2019). Basal nutrient media was a modified version of media described by Speece (2008). The nutrient media contained the following (mg/L): $MgSO_4.7H_2O$ (400); KCl (400); $CaCl_2.2H_2O$ (50); $(NH_4)_2.HPO_4$ (80); $FeCl_2.4H_2O$ (10); $CoCl_2.6H_2O$ (1); KI

(10); $(NaPO_3)_6$ (10); $Na_2S.9H_2O$ (300); the salts $MnCl_2.4H_2O$, NH_4VO_3, $CuCl_2.2H_2O$, $ZnCl_2$, $AlCl_3.6H_2O$, $Na_2MoO_4.2H_2O$, H_3BO_3, $NiCl_2.6H_2O$, $NaWO_4.2H_2O$, and Na_2SeO_3 (each at 0.5); yeast extract (10); Cysteine (10); and $NaHCO_3$ (6000).

7.2.5. Analytical methods

Biogas production was measured daily using a 150 mL wetted-barrel glass syringe. Biogas methane concentration was measured by gas chromatography (GC System 7890A, Agilent Technologies, Irving, TX, USA) using a thermal conductivity detector (TCD). Volatile fatty acids (VFA) concentrations were measured by gas chromatography (GC System 7890A, Agilent Technologies, Irving, TX, USA) using a flame ionization detector (FID). The APLs were analyzed by GC-FID using a 1701 capillary column to quantify hydrocarbons (Seyedi et al. 2019). The pH was measured using a pH probe and meter (Orion 4 Star, Thermo, Waltham, MA, USA). Soluble COD (SCOD) was measured by filtering the sample through a 0.45 m pore size membrane syringe filter and determining the filtrate COD by standard methods (American Public Health Association 1998). Total COD, TS, VS, total suspended solids (TSS) and volatile suspended solids (VSS) concentrations were determined by standard methods (American Public Health Association 1998).

7.2.6. DNA extraction and sequencing

Digester biomass samples were analyzed using Illumina sequencing. Approximately 1.8 mL of biomass was removed on day 15 before quasi steady state was achieved and on day 45 after quasi steady state was achieved. Samples

were stored at 20 C prior to DNA extraction. DNA was extracted using a commercial kit (DNeasy PowerLyzer PowerSoil Kit, Qiagen, USA) according to the manufacturer instructions. Sequencing was performed by a commercial company (Molecular Research, LP, Shallowater, TX, USA) using the Illumina MiSeq v3 300 base pair sequencing platform (Illumina, San Diego, CA, USA). Universal primers, 515F and 806R were used for PCR amplification to target the V4 variable region of the 16S rRNA gene as described elsewhere (Carey et al. 2016). Raw un-joined sequence data were quality filtered and sequences were depleted from barcodes and primers. Subsequently, sequences with ambiguous base reads, those with less than 200 base pairs, and those with homopolymer sequences of six base pairs or longer were removed. Sequences were denoised and clustered in operational taxonomic units (OTU) using 97% similarity. Each taxonomic unit was compiled into taxonomic counts and then classified using BLASTn against a curated database derived from GreenGenes, Ribosomal Database Project II (RDPII) and National Center for Biotechnology Information (NCBI).

7.2.7. Statistical analysis

Statistical analyses including average, standard deviation, normality test and two-sample student's t-test calculations were performed using Microsoft Excel 2015 and Minitab 18.1.0. For microbial community analysis, dual hierarchical clustering (using R command hclust and heatmap) and non-metric multidimensional scaling (nMDS) using the VEGAN package were performed using custom R scripts (Venkiteshwaran et al. 2016). The nMDS clustering was performed based on a 95% confidence interval. Dual hierarchical clustering and

heatmap construction were performed using the seven dominant archaeal and 50 dominant bacterial OTUs based on relative abundance values. Analysis was performed to identify OTU abundance value differences ($p < 0.001$) between control, catalyzed APL and non-catalyzed APL digesters using the negative binomial test as implemented in the DESeq2 package (Anders and Huber 2010; Kappell et al. 2018). The 223 major archaeal and bacterial OTUs with relative abundance >0.1% in at least three samples were used in DEseq2 analysis. Shannon diversity index values (H) and Evenness index (E) were determined based on Illumina sequence results as described by Falk et al. (2009).

7.3. Results and discussion

7.3.1. APL composition

APL from autocatalytic pyrolysis (catalyzed APL) contained 84% lower COD and significantly reduced VFA concentrations compared to non-catalytic APL before air stripping (Table 7.1). However, the NH_3-N concentration in APL after autocatalysis was 14% greater than that of non-catalytic APL (Table 7.1); the NH_3-N concentration increase was ostensibly due to the more complete reduction of nitrogenous compounds to NH_3-N during autocatalysis. Compounds detected by the GC-FID method in non-catalyzed APL included 23 hydrocarbons, phenols and methoxy-substituted aromatic constituents, whereas only four constituents were detected in the catalyzed APL (Table S7.1). Only 0.74% (w/w) of the total organic content in the catalyzed APL was detected, whereas about 5% (w/w) in non-catalyzed APLs was identified (Table S7.1). Therefore, there are other organics in

the APL that remained undetected. The majority of the compounds that were identified in non-catalyzed APL were aromatic and nitrogen-containing organics including substituted phenols and benzenes (Table S7.1).

Table 7.1. Aqueous pyrolysis liquid (APL) composition [a]

APL	COD (g/L)	NH_3-N (g/L)	VFA concentration as acetic acid (g/L)
Non-catalyzed	202 ± 4.3	63 ± 0.1	29 ± 1.6
Non-catalyzed, air-stripped	198 ± 7.8	13 ± 0.6	33 ± 1.1
Catalyzed	33 ± 1.1	72 ± 3.4	0.06 ± 0.009
Catalyzed, air-stripped	17 ± 0.7	25 ± 0.3	BD

[a] BD indicates the concentration was below the detection limit. COD: chemical oxygen demand; VFA: volatile fatty acids.

After air stripping, NH_3-N concentration was reduced by 79% in non-catalyzed APL and 67% in catalyzed APL (Table 7.1). Air stripping did not have a significant effect on the COD and VFA concentrations of non-catalyzed APL ($p>0.05$, $n=6$); however, COD concentration in catalyzed APL decreased by approximately 50% after air stripping (Table 7.1). Styrene and ethylbenzene were removed from catalyzed APL by air stripping (Table S7.1).

7.3.2. Short-term semi-continuous anaerobic digestion

During short-term digestion study (<50 days), catalyzed APL fed at the loadings employed substantially inhibited methane production regardless of whether or not the APL was pretreated by air stripping. During quasi steady state operation (days 30–45), COD removals in digesters fed catalyzed APL with and without air stripping were 47 ± 4% and 52 ± 7%, respectively, whereas COD

removal in control digesters was 76 ± 4%. COD removal in digesters fed non-catalyzed APL with and without air stripping was 73 ± 3%. The methane production was significantly lower in digesters that received catalyzed APL compared to all other digesters ($p<0.05$, $n=45$) (Figure 7.1A). Pretreatment of catalyzed and non-catalyzed APLs using air stripping did not influence the extent of inhibition, methane production, effluent COD or effluent SCOD concentrations of the co-digesters ($p>0.05$, $n=3$) (Table 7.2).

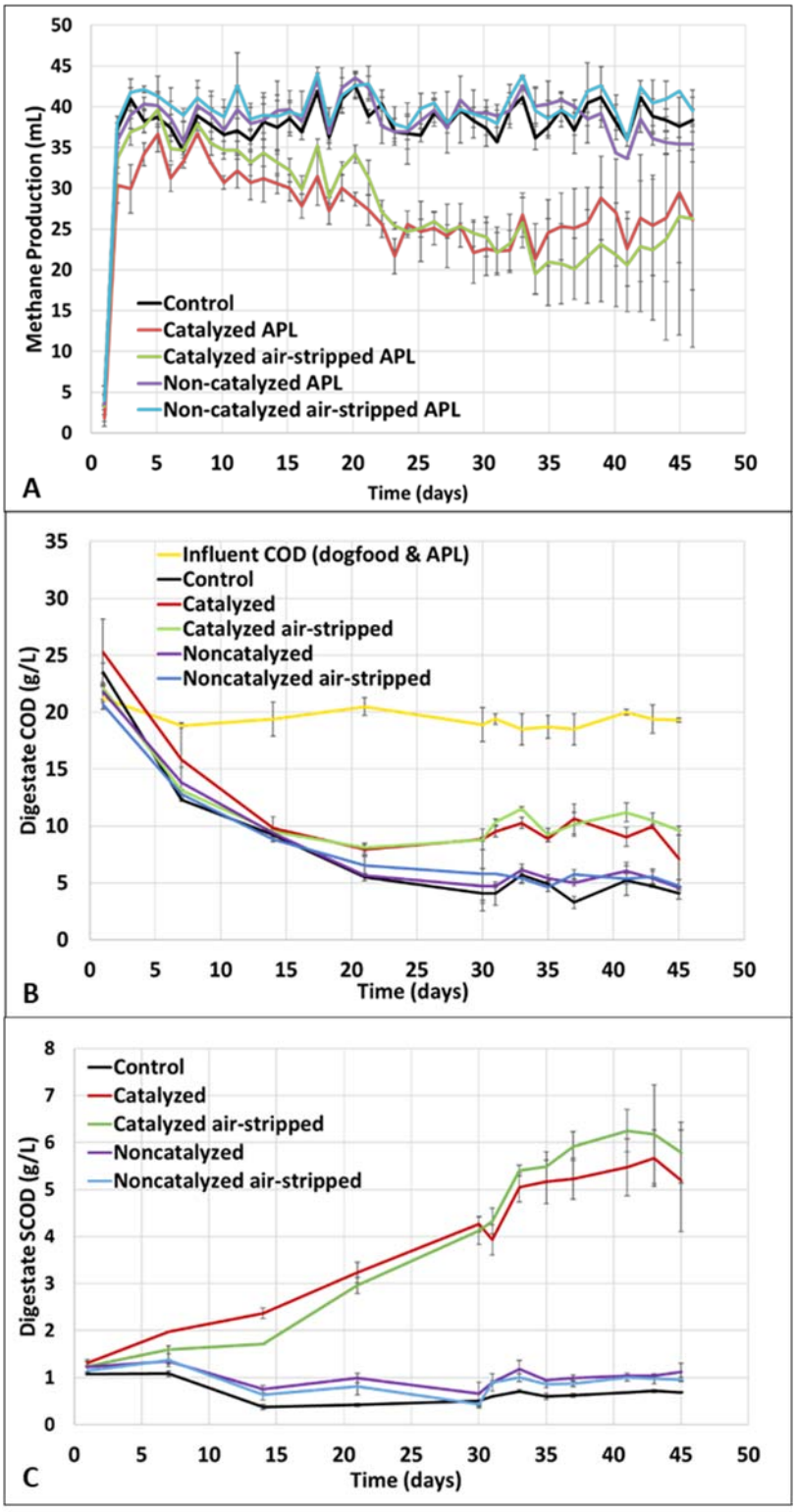

Figure 7.1. Short-term digester functional data. Average and standard deviation values are from triplicate systems. (A) Methane production, (B) Digestate COD concentration, (C) Digestate SCOD concentration. The whiskers represent one standard deviation above and below the mean. Some whiskers are small and not visible.

Table 7.2. Digester effluent characterization on day 45 [a].

Co-digestate Feed	Total VFA concentration as acetic acid (mg/L)	Acetic acid concentration (mg/L)	COD concentration (g/L)	SCOD concentration (g/L)	Methane production (mL/d)
None (Control)	BD	BD	4.1 ± 0.52	0.7 ± 0.02	38.8 ± 1.8
Catalyzed	2010 ± 43	1500 ± 164	7.1 ± 2.5	5.2 ± 1.1	28.0 ± 4.0
Catalyzed air-stripped	2070 ± 34	1530 ± 153	9.6 ± 0.4	5.8 ± 0.65	28.0 ± 5.9
Non-catalyzed	50.0 ± 16	BD	4.5 ± 0.16	0.9 ± 0.05	38.0 ± 2.7
Non-catalyzed air-stripped	BD	BD	4.7 ± 0.57	4.1 ± 0.2	4.4 ± 2.0

[a] BD indicates the concentration was below the detection limit. SCOD: soluble chemical oxygen demand.

Despite detecting fewer phenolic compounds in catalyzed APL compared to non-catalyzed APL, SCOD and VFAs accumulated in the digesters fed catalyzed APL and methane production was inhibited (Figure 7.1). It was apparent from digester methane production, COD, SCOD and VFA results that catalyzed APL exerted a higher toxicity to digester taxa than non-catalyzed APL. Both raw and air-stripped non-catalyzed APL did not inhibit methane production during co-digestion. However, only a maximum of 1 mL of methane per day was expected based on stoichiometry from the total conversion of the APL to methane at the loading rate employed. Therefore, the APL loading employed was too low to discern its conversion to methane but was necessary to preclude toxicity to the unacclimated anaerobic biomass. Despite the increased OLR due to APL addition, digester methane production from the digesters co-fed air-stripped and raw non-catalyzed APL was not discernably greater than that of the control digesters fed only synthetic primary sludge ($p>0.05$, $n=45$) (Figure 7.1A). During quasi steady

state operation from days 30 to 45, the control digesters produced 38.8 ± 1.8 mL methane per day (average standard deviation) and digesters fed non-catalyzed APL with and without air stripping produced 40.4 ± 2.0 and 38.0 ± 2.7 mL methane per day, respectively. The control digesters and digesters fed air-stripped and raw non-catalyzed APL also exhibited similar COD and SCOD reduction ($p>0.05$, $n=3$) (Figure 7.1B) (Table 7.2).

The observed digester pH ranged from 7.2 to 7.5 during the quasi steady state period in all digesters. The effluent total VFA concentrations in control digesters and digesters fed non-catalyzed APLs were below 60 mg/L as acetic acid (Table 7.2). However, the digesters that received air-stripped and raw catalyzed APL showed the highest quasi steady state effluent total VFA concentrations of >2 g/L, with a majority of VFAs produced as acetic acid (Table 7.2). Short-term co-digestion of catalyzed APL, regardless of NH_3-N reduction from air stripping pretreatment, substantially reduced methane production and COD removal compared to control digesters receiving no APL and co-digesters receiving non-catalyzed APL. Counter to the predicted reduction in inhibition, the catalyzed APL used in the current study was an inhibitory co-substrate. Therefore, investigating the microbial community composition shifts in these short-term co-digesters is vitally important for understanding anaerobic treatment of APL.

7.3.3. Short-term digestion microbial community analysis

Illumina sequencing yielded over 1 million sequence reads, with 58,730 ± 9924 reads per digester sample. Based on 97% similarity, 5073 microbial OTUs were observed with an average of 1853 ± 480 OTUs per digester. Previous studies

have described that higher microbial diversity and evenness are associated with digesters that perform well under transient conditions, whereas inhibited digesters have lower diversity and evenness (Xu et al. 2010; Carballa et al. 2015). However, this was not observed in this study as Shannon diversity (H) values were 4.7–5.2 and evenness (E) values were 0.7–0.8 among the inhibited and uninhibited digesters on days 15 and 45, demonstrating no statistical difference between inhibited and uninhibited digesters ($p>0.05$, $n=3$).

7.3.3.1. Archaea community

A total of 79 archaeal OTUs were identified among all digesters with an average relative abundance of 3.2 ± 1.5% of the total microbial community in each digester. Exposure to catalyzed APL for 45 days altered the archaeal community compared to control digester communities, whereas the archaeal communities in the uninhibited digesters that maintained >70% COD removal (control digesters and digesters fed non-catalyzed APL) were more similar (Figure S7.1).

The 7 dominant archaeal OTUs accounted for 94 ± 2.6% of total archaeal community relative abundance (Figure 7.2). Of the seven dominant archaeal OTUs, two were classified as the genus *Methanosaeta* (OTUs 56 and 71), one *Methanobacterium* (OTU 128), one *Thermogymnomonas* (OTU 125) and one as family Methanobrevibacter (OTU 124); the other two OTUs were unknown archaea (OTU 126 and 127) (Figure 7.2).

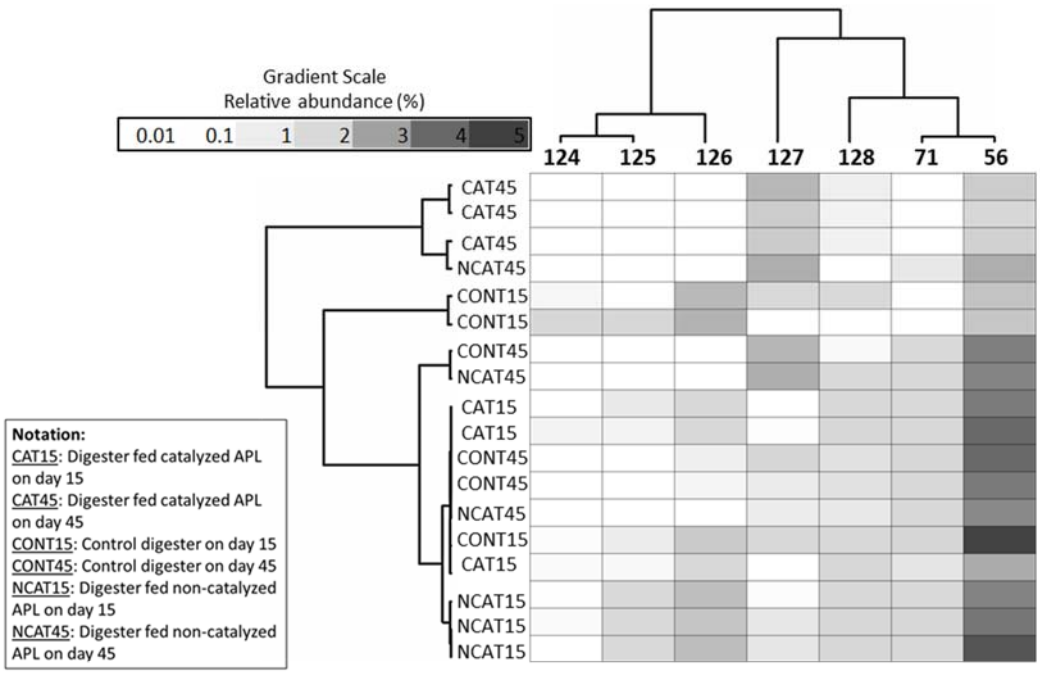

OTU	Phylum (> 77 %)	Class (80 - 85 %)	Order (85 - 90 %)	Family (90 - 95 %)	Genus (> 95 %)	Percent Homology
56	Euryarchaeota	Methanomicrobia	Methanosarcinales	Methanosaetaceae	**Methanosaeta**	99.6
71	Euryarchaeota	Methanomicrobia	Methanosarcinales	Methanosaetaceae	**Methanosaeta**	100
128	Euryarchaeota	Methanobacteria	Methanobacteriales	Methanobacteriaceae	**Methanobacterium**	99.6
127	Unknown Archaea	Unknown Archaea	Unknown Archaea	Unknown Archaea	Unknown Archaea	74.5
126	Unknown Archaea	Unknown Archaea	Unknown Archaea	Unknown Archaea	Unknown Archaea	70.6
125	Euryarchaeota	Thermoplasmata	Thermoplasmatales	Thermoplasmatales	**Thermogymnomonas**	98.2
124	Euryarchaeota	Methanobacteria	Methanobacteriales	**Methanobacteriaceae**	Methanobrevibacter	93.0

Figure 7.2. Dual hierarchical clustering of the seven most abundant archaeal OTUs. These OTUs represent 94 2.6% of the total archaeal abundance in all digesters. Taxonomic classification in bold font represents the valid level based on percent homology, with the homology percentage ranges in parentheses. Digester communities on day 15 were dominated by Methanosaeta (OTU 56). However, communities in digesters co-fed catalyzed APL shifted by day 45 and were dominated by an unknown archaea (OTU 127).

The conventional and autocatalytic pyrolysis conditions under which APL was produced affected the archaeal communities during anaerobic co-digestion. All digesters on day 15 had Methanosaeta (OTU 56) as the dominant archaeal OTU with more than 70% of total archaeal community relative abundance (Figure 7.2). On day 45, Methanosaeta (OTU 56) was still dominant in the uninhibited

digesters. The effluent acetic acid concentrations in the uninhibited digesters were very low (<2 mg/L after day 30), ostensibly due to the activity of the dominant acetoclastic Methanosaeta (OTU 56 and 71) (Table 7.2). However, its relative abundance decreased to less than 30% after day 15 in digesters fed catalyzed APL (Figure 7.2). This was also indicated by DESeq2 analysis that showed decreased abundance ($p < 0.001$) of two *Methanosaeta* genera (OTU 56 and 71) in digesters fed catalyzed APL compared to control digesters on day 45 (Figure S7.3). Additionally, abundance of an unknown archaeal OTU (127) increased in the inhibited digesters (Figure 7.2).

7.3.3.2. Bacteria community

A total of 4994 bacterial OTUs were observed across all digesters, with an average of 1823 ± 469 bacterial OTUs in each digester. There were 50 dominant bacterial OTUs having the highest relative abundance values that together represented 63.1 ± 2.3% of the total microbial community abundance. Among these dominant OTUs, *Clostridiaceae* (OTU 96) and *Ruminococcaceae* (OTU 97) were most dominant in all digesters on both days 15 and 45 (Figure 7.3). Both are strictly anaerobic, fermentative bacteria; Clostridiaceae produces organic acids and alcohols from carbohydrates or peptones and Ruminococcaceae generates organic acids and H_2 as end products (Vos et al. 2009; Shkoporov et al. 2016).

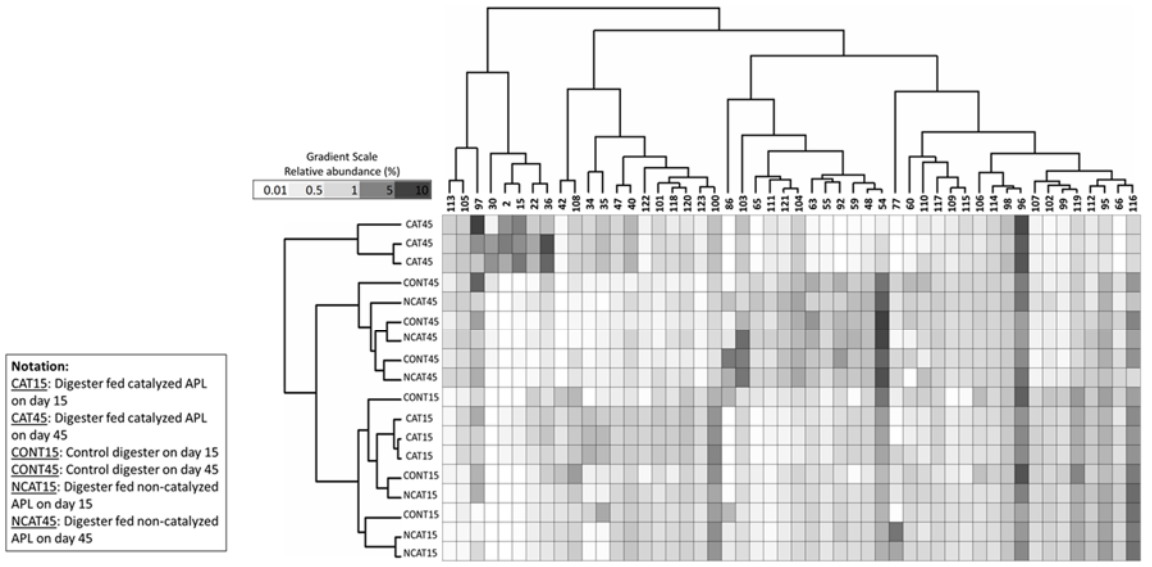

OTU 4	Phylum (> 77 %)	Class (80 - 85 %)	Order (85 - 90 %)	Family (90 - 95 %)	Genus (> 95 %)	Percent Homology
2	Bacteroidetes	Bacteroidia	**Bacteroidales**	Rikenellaceae	Rikenella	86.1
15	Firmicutes	Bacilli	Lactobacillales	Enterococcaceae	**Enterococcus**	99.3
22	Firmicutes	Erysipelotrichia	**Erysipelotrichales**	Erysipelotrichaceae	Turicibacter	87.5
30	Proteobacteria	Epsilonproteobacteria	Campylobacterales	Campylobacteraceae	**Campylobacter**	99.3
34	Verrucomicrobia	Verrucomicrobiae	**Verrucomicrobiales**	Verrucomicrobiaceae	Verrucomicrobium	87.1
35	Bacteroidetes	Bacteroidia	Bacteroidales	Bacteroidaceae	**Bacteroides**	99.6
36	Firmicutes	Clostridia	Clostridiales	Clostridiales Xi.	**Tissierella**	97.8
40	Chloroflexi	Anaerolineae	Anaerolineales	Anaerolineaceae	**Bellilinea**	96.3
42	Firmicutes	Clostridia	Clostridiales	Clostridiales Xi.	**Sedimentibacter**	97.8
47	Synergistetes	Synergistia	Synergistales	**Synergistaceae**	Synergistes	94.9
48	Bacteroidetes	Bacteroidia	Bacteroidales	**Rikenellaceae**	Rikenella	90.1
54	Bacteroidetes	Bacteroidia	**Bacteroidales**	Rikenellaceae	Rikenella	89.0
55	Deferribacteres	Deferribacteres	Deferribacterales	Deferribacteraceae	**Deferribacter**	99.6
59	Bacteroidetes	Bacteroidia	**Bacteroidales**	Rikenellaceae	Rikenella	89.3
60	Proteobacteria	Deltaproteobacteria	Desulfuromonadales	Geobacteraceae	**Geobacter**	98.9
63	Thermotogae	Thermotogae	Thermotogales	Thermotogaceae	**Kosmotoga**	99.6
65	Firmicutes	Clostridia	**Clostridiales**	Eubacteriaceae	Acetobacterium	89.4
66	Verrucomicrobia	Verrucomicrobiae	**Verrucomicrobiales**	Verrucomicrobiaceae	Verrucomicrobium	87.5
77	Firmicutes	Clostridia	Clostridiales	Ruminococcaceae	**Ruminococcus**	97.1
86	Firmicutes	Clostridia	Clostridiales	Clostridiaceae	**Clostridium**	98.5
92	Thermotogae	**Thermotogae**	Thermotogales	Thermotogaceae	Geotoga	84.3
95	Cloacimonetes	Cloacimonetes	Cloacimonetes	Cloacimonetes	**Cloacimonas**	96.7
96	Firmicutes	Clostridia	Clostridiales	**Clostridiaceae**	Clostridium	92.3
97	Firmicutes	Clostridia	Clostridiales	Ruminococcaceae	**Soleaferrea**	96.0
98	Synergistetes	Synergistia	Synergistales	Synergistaceae	**Synergistes**	99.6

OTU	Phylum (> 77 %)	Class (80 - 85 %)	Order (85 - 90 %)	Family (90 - 95 %)	Genus (> 95 %)	Percent Homology
99	Bacteroidetes	Cytophagia	Cytophagales	Cytophagaceae	**Cytophaga**	97.8
100	Bacteroidetes	Bacteroidia	Bacteroidales	**Marinilabiliaceae**	Anaerophaga	90.5
101	Firmicutes	Bacilli	Lactobacillales	Carnobacteriaceae	**Trichococcus**	99.3
102	Bacteroidetes	Bacteroidia	**Bacteroidales**	Bacteroidaceae	Bacteroides	88.6
103	Chloroflexi	Anaerolineae	Anaerolineales	Anaerolineaceae	**Bellilinea**	98.2
104	Synergistetes	Synergistia	Synergistales	Synergistaceae	**Synergistes**	99.6
105	Bacteroidetes	Bacteroidia	**Bacteroidales**	Bacteroidaceae	Bacteroides	87.2
106	Bacteroidetes	Cytophagia	Cytophagales	Cytophagaceae	**Cytophaga**	97.0
107	Cloacimonetes	Cloacimonetes	Cloacimonetes	Cloacimonetes	**Cloacimonas**	99.3
108	Bacteroidetes	Sphingobacteria	Sphingobacteriales	**Sphingobacteriaceae**	Solitalea	90.1
109	Synergistetes	Synergistia	Synergistales	Synergistaceae	**Synergistes**	98.9
110	Bacteroidetes	Bacteroidia	Bacteroidales	Porphyromonadaceae	**Parabacteroides**	99.3
111	Bacteroidetes	Bacteroidia	Bacteroidales	**Bacteroidaceae**	Bacteroides	94.1
112	Chloroflexi	Anaerolineae	Anaerolineales	Anaerolineaceae	**Longilinea**	96.7
113	Bacteroidetes	Bacteroidia	Bacteroidales	Porphyromonadaceae	**Petrimonas**	97.1
114	Firmicutes	Clostridia	Clostridiales	Clostridiaceae	**Clostridium**	98.5
115	Firmicutes	Clostridia	Clostridiales	Clostridiaceae	**Clostridium**	99.2
116	Chloroflexi	Anaerolineae	Anaerolineales	Anaerolineaceae	**Bellilinea**	95.6
117	Bacteroidetes	Bacteroidia	**Bacteroidales**	Rikenellaceae	Rikenella	89.8
118	Bacteroidetes	Bacteroidia	**Bacteroidales**	Rikenellaceae	Rikenella	88.3
119	Bacteroidetes	Cytophagia	Cytophagales	Cytophagaceae	**Cytophaga**	98.5
120	Bacteroidetes	Bacteroidia	**Bacteroidales**	Rikenellaceae	Rikenella	87.2
121	Synergistetes	Synergistia	Synergistales	Synergistaceae	**Synergistes**	98.8
122	Bacteroidetes	Cytophagia	Cytophagales	Cytophagaceae	**Cytophaga**	98.4
123	Chloroflexi	Anaerolineae	Anaerolineales	Anaerolineaceae	**Bellilinea**	96.7

Figure 7.3. Dual hierarchal clustering of the 50 most abundant bacteria. These OTUs represented 63.1 ± 2.3 % of total microbial community abundance in all the digesters. Taxonomic classification in bold font represent the valid level based on percent homology with the homology percentage ranges in parentheses. Communities on day 45 clustered separately from communities on day 15. On day 45, bacterial communities in the digesters fed catalyzed APL clustered separately from all other communities. *Clostridiaceae* (OTU 96) and *Ruminococcaceae* (OTU 97) were dominant in all digesters on days 15 and 45. In inhibited digesters, *Bacteroidales* (OTU 2), *Enterococcus* (OTU 15), *Erysipelotrichales* (OTU 22), *Campylobacter* (OTU 30), and *Tissierrella* (OTU 36) were dominant, but not in other digesters.

Similar to results observed for archaeal community, the pyrolysis conditions under which APL was produced affected the bacterial communities. On day 15, the bacterial communities in all digesters were similar, as shown by 95%

confidence ellipses in the nMDS plot (Figure S7.2). On day 45, however, the bacterial community in digesters fed inhibitory APL (i.e., catalyzed APL) was significantly different from the other digester communities (Figure S7.2). The difference was also observed among the dominant bacterial OTUs, which were different in digesters fed catalyzed APL for 45 days compared to those in uninhibited digesters (Figure 7.3).

In uninhibited digesters, the dominant bacterial OTUs were Bacteroidales (OTU 54 and 59), *Kosmotoga* (OTU 63), and Thermotogae (OTU 92) (Figure 7.3). *Kosmotoga* and Thermotogae belong to the phylum Thermotogae, which are thermophilic, strict anaerobic bacteria, fermenting a variety of carbohydrates, organic acids, alcohols and proteinaceous substrates (L'Haridon et al. 2014). DESeq2 analysis on control versus digesters fed non-catalyzed APL on day 45 revealed the relative abundance of only three bacterial OTUs (family Ruminococcaceae and genera *Leptospira* and *Pelospora*) decreased by more than 2-fold in digesters fed non-catalyzed APL compared to control digesters, thus indicating the high similarity between the bacterial community in the control digesters and digesters fed non-catalyzed APL.

In the inhibited digesters, the relative abundance of Bacteroidales (OTU 2), *Enterococcus* (OTU 15), Erysipelotrichales (OTU 22), *Campylobacter* (OTU 30) and *Tissierrella* (OTU 36) increased to more than 65%, whereas they remained less than 40% in uninhibited digesters (Figure 7.3). DESeq2 analysis indicated a significant increase ($p < 0.001$) in the relative abundance of these five OTUs in the inhibited digesters fed catalyzed APL as compared to the control digesters (Figure

S7.3). Among the five OTUs that were favored in inhibited digesters, *Enterococcus* is a facultative anaerobic bacterium that requires several amino acids, purine and pyrimidine bases for growth (Vos et al. 2009). Pyrimidines were detected in relatively high concentration in catalyzed APL in a previous study (Seyedi et al. 2019). Bacteroidales, Erysipelotrichales, *Campylobacter* and *Tissierella* are fermenters that can use carbohydrates, proteins or amino acids to produce organic acids (Collins and Shah 1986; Vandamme and De Ley 1991; Bosshard et al. 2002; Verbarg et al. 2004; O'Cuív et al. 2011; Su et al. 2014).

Syntrophomonadaceae and *Synergistaceae* were the dominant families of Syntrophic bacteria during quasi steady state in all digesters. On day 45, *Syntrophomonadaceae* contributed to 2 ± 0.5% and *Synergistaceae* contributed to 8 ± 1.2% of the total microbial relative abundance. *Syntrophomonadaceae* and *Synergistaceae* are known to utilize fatty acids and amino acids, respectively, in syntrophic association with H_2-consuming methanogens (Vartoukian et al. 2007; Sieber et al. 2010). DESeq2 analysis identified two syntrophic bacterial OTUs, *Syntrophomonadaceae* (OTU 11) and *Synergistaceae* (OTU 47), whose relative abundance were statistically higher ($p < 0.001$) in inhibited digesters fed catalyzed APL as compared to the control digesters (Figure S7.3). *Syntrophomonadaceae* (OTU 11) contributed 32% of the total relative abundance of family *Syntrophomonadaceae* in digesters fed catalyzed APL, but only contributed to 0.4% and 1% of the *Syntrophomonadaceae* family in the control digesters and the digesters fed non-catalyzed APL, respectively. *Synergistaceae* (OTU 47), which was also among the first 50 dominant bacterial OTUs observed among all

digesters, contributed to 14% of total relative abundance of the family Synergistaceae in digesters fed catalyzed APL, but only contributed to 4% of the total relative abundance of the family Synergistaceae in uninhibited digesters. Along with the archaeal community structure, the above results indicate that continuous addition of catalyzed APL resulted in a significant shift in the anaerobic digester hydrolytic/fermentative and syntrophic bacteria community.

7.3.4. Long-term semi-continuous anaerobic digestion

During long-term co-digestion (>500 days), the microorganisms were exposed to incremental non-catalyzed APL loadings in order to acclimate to the toxic compounds and show tolerance. At low APL OLRs of 0.06 and 0.1 gCOD/Lr-d, the expected theoretical stoichiometric methane production from APL COD was observed; however, higher OLRs inhibited methane production ostensibly due to APL toxicity that could be attributed to the phenolics, which are well-known toxicants in the APL (Torri and Fabbri 2014; Zhou et al. 2019; Yu et al. 2020; Wen et al. 2020) (Figure 7.4B). Phenolic compounds exert toxicity by disrupting cell membrane proteins and permeability, resulting in inactivation of enzymatic systems and damage to intracellular components (Madigou et al. 2016; Zhou et al. 2019). Corresponding to methane production results, digestate COD, SCOD and VFA concentrations increased in inhibited co-digesters at higher APL OLRs (Figure S7.4).

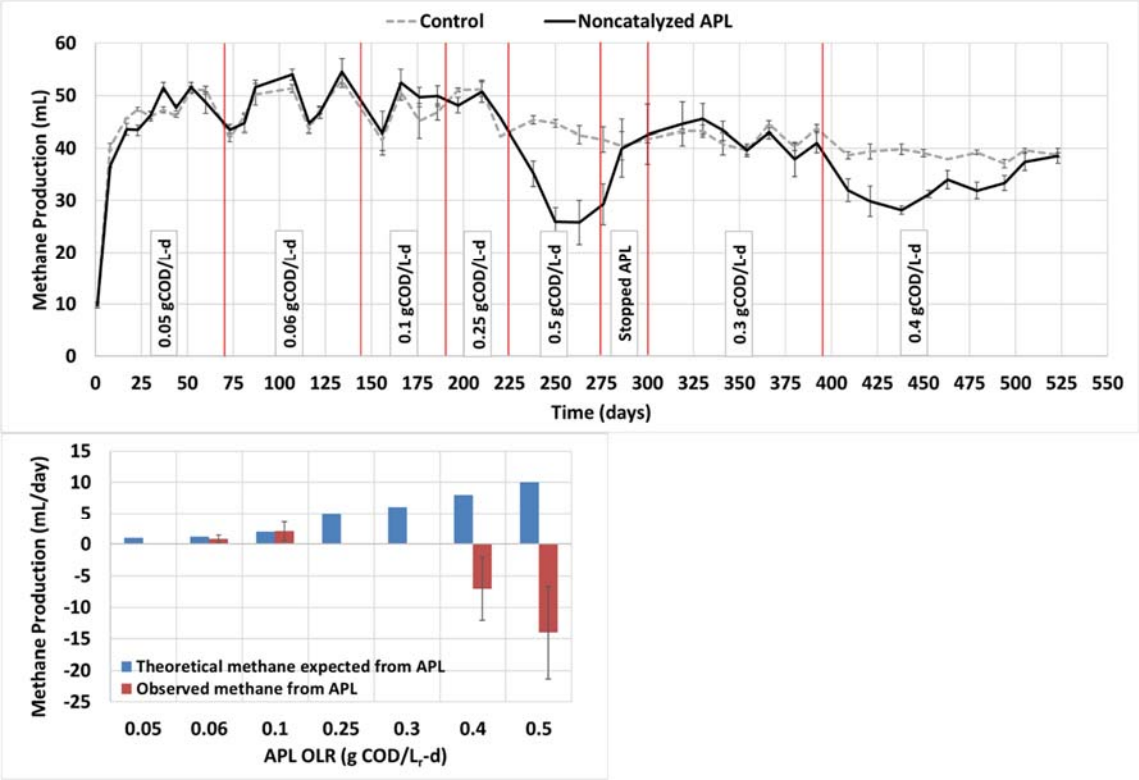

Figure 7.4. Methane production results from the long-term acclimation study. Control digesters received synthetic primary sludge and no APL, whereas non-catalyzed APL digesters were co-fed synthetic primary sludge and non-catalyzed APL. (A) Daily methane volume produced; the red lines show the time at which the APL OLR was changed. (B) Comparison between theoretical stoichiometric maximum daily expected methane from APL COD (blue bars) and the observed methane produced from APL (compared to controls) at each organic loading rate (red bars). Whiskers represent one standard deviation above and below the mean. Some whiskers are small and not visible.

During the first 67 days operating at 0.05 gCOD/L_r-d APL, no statistical difference was observed between control digesters and digesters fed non-catalyzed APL ($p>0.05$, $n=201$) (Figure 7.4A), and no excess methane was observed from APL addition (Figure 7.4B). This is probably due to the very low APL OLR and low associated methane production expected (1 mL/d).

When the APL OLR was increased to 0.06 and 0.1 gCOD/L_r-d, methane

production from APL was observed (Figure 7.4). The average daily methane production from co-digesters receiving non-catalyzed APL was statistically higher than that of the control digesters under both 0.06 and 0.1 gCOD/L_r-d ($p=0.01$, $n=207$ and $p=3\times10^{-12}$, $n=135$, respectively) (Figure 7.4B). Previously, an APL digester loading rate higher than 0.05 gCOD/L_r-d for non-catalyzed APL was reported as not sustainable due to toxicity (Seyedi et al. 2019), but after acclimation, higher sustainable OLR values were observed in the current study.

Increasing the APL OLR to 0.25 and 0.5 gCOD/L_r-d resulted in either no methane production from APL or inhibition of the co-digester methane production (Figure 7.4A, 7.4B). To avoid permanent inhibition, the APL OLR was stopped on day 275 and the co-digester methane production recovered in 25 days. After recovery, co-digesters were fed APL at 0.3 gCOD/L_r-d on day 301 and were continued for 94 days, where no statistical difference was observed between methane production from co-digesters versus control digesters ($p>0.05$, $n=282$). Finally, the APL OLR was raised to 0.4 gCOD/L_r-d, which initially resulted in inhibition of methane production but started to show acclimation, where in the last six days, no statistical difference in methane production was observed between the control digesters and co-digesters fed non-catalyzed APL ($p>0.05$, $n=18$) (Figure 7.4A).

Overall, results from the long-term co-digestion of non-catalyzed APL demonstrate the viability of anaerobic co-digestion of conventional APL and the capability of microorganisms to acclimate to APL. However, acclimation can take

a very long time and may be inefficient in a real wastewater treatment application. One strategy to overcome this is to use seed microorganisms that are already acclimated to similar compounds present in the APL, such as biomass from anerobic digesters treating phenolic wastewater (Fang and Zhou 2000; Madigou et al. 2016).

7.4. Inhibition by APL and future considerations

Similar to the results observed for non-catalyzed APL from biosolids, the presence of phenolic compounds in APL derived from different pyrolysis conditions has previously been reported to inhibit anaerobic digestion. In a recent study on anaerobic digestion of APL generated from birch bark at 500 °C, a high concentration of phenolics (24 g/kg total phenolics) observed in the APL was mentioned to be a major microbial inhibitor (Wen et al. 2020).Yu et al. (2020) employed different dilutions of APL in anaerobic digestion and observed that an elevated concentration of phenolics in less diluted APL resulted in anaerobic digester failure. Zhou et al. (2019) performed anaerobic digestion of APL derived from pyrolysis of corn stover at 500 C, and phenols were reported as potential major toxicants in raw APL.

Co-digestion of non-catalyzed APL produced through the conventional pyrolysis process showed no inhibition during anaerobic co-digestion at loading rates of 0.1 gCOD/L_r-d. Despite detecting fewer phenolic compounds in catalyzed APL, it exerted greater inhibition during co-digestion with synthetic primary sludge.

The catalyzed APL had a COD concentration of 33 g/L; however, the organic compounds identified by GC-FID only contributed a small fraction of this COD (0.74% w/w). Catalytic pyrolysis can be advantageous over conventional pyrolysis to increase py-gas production; however, the remaining organic compounds in the catalytic APL undetected by GC-FID are ostensibly more toxic or recalcitrant to methanogenic processes and, therefore, complicate the management of APL by anaerobic digestion.

Utilizing acclimated biomass to help improve anaerobic digestion of APL is a strategy to reduce the toxic effect of APL (Zhou et al. 2019; Wen et al. 2020). Methanogenic cultures already exposed to similar constituents as in APL, such as biomass in anaerobic digesters treating phenolic wastewater, could be a beneficial seed biomass to reduce the long acclimation period required (Fang and Zhou 2000; Madigou et al. 2016). Additionally, pretreatment of toxic phenolic compounds via partial oxidation using chemical oxidation processes such as ozonation may be another promising strategy to transform recalcitrant APL organics into more easily degradable and less toxic compounds (Alvares et al. 2001). For example, Xu et al. (2011) found that aldehydes and alcohols in bio-oil were oxidized to more easily degradable carboxylic acids after bio-oil was treated with ozone. Recalcitrant organics including nitrogenous aromatics and polyaromatics were also ozonated and organic acids were produced that were more susceptible to biological degradability (Alvares et al. 2001). Ozonation of olive mill waste removed phenolic inhibitors and methane yield increased by more than 16% (Benitez et al. 1997). The feasible application of anaerobic co-digestion of APL for energy recovery and

a better assessment of its environmental and economic impacts require further investigation (Ma and Liu 2019).

7.5. Conclusions

APL derived from wastewater solids pyrolysis has a high COD content which offers potential to be recovered as methane from anaerobic digesters; however, some APL compounds are inhibitory to anaerobic microbes. Results of this study show that, at non-catalytic APL OLRs of 0.06 and 0.1 gCOD/L_r-d, quasi steady state methane production from APL is sustainable in co-digesters also fed synthetic primary sludge. However, at lower APL OLRs, no APL methane production was discernable, and, at higher APL OLRs, methanogenesis was inhibited. Catalyzed APL with lower COD and fewer detectable phenolic compounds inhibited methane production more than non-catalyzed APL. Potential inhibitory compounds present in catalyzed APL undetected by current methods ostensibly caused the observed toxicity. Acetoclastic Methanosaeta was significantly inhibited in digesters fed catalyzed APL but remained dominant in uninhibited digesters. The conditions under which pyrolysis is conducted substantially affect APL biodegradability and the resulting microbial community in anaerobic digesters fed APL. It is apparent that pyrolysis byproduct utilization is an important consideration when selecting biosolids pyrolysis scenarios. In the future, additional strategies such as using specific, acclimated biomass, APL pretreatment or addition of biochar to the digester may improve APL conversion to biogas containing methane for renewable energy.

7.6. Supplementary Materials

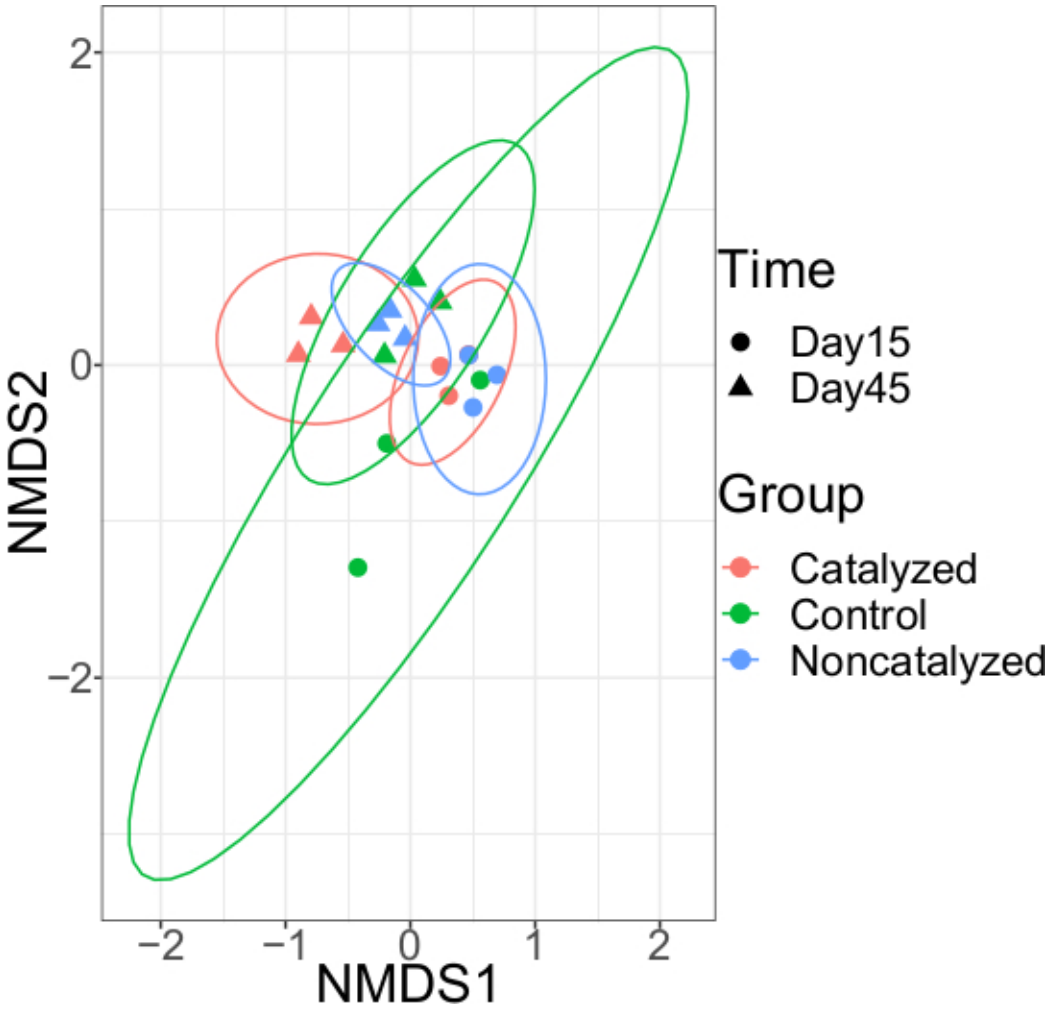

Figure S7.1 Archaea nMDS plot. Ellipses represent 95% confidence intervals for the three points (each group represents the three triplicate digesters). On day 15, all digester Archaeal communities were similar. Exposure to catalyzed APL for 45 days altered the Archaeal community compared to control digester communities, whereas the Archaeal communities in digesters fed non-catalyzed APL were more similar

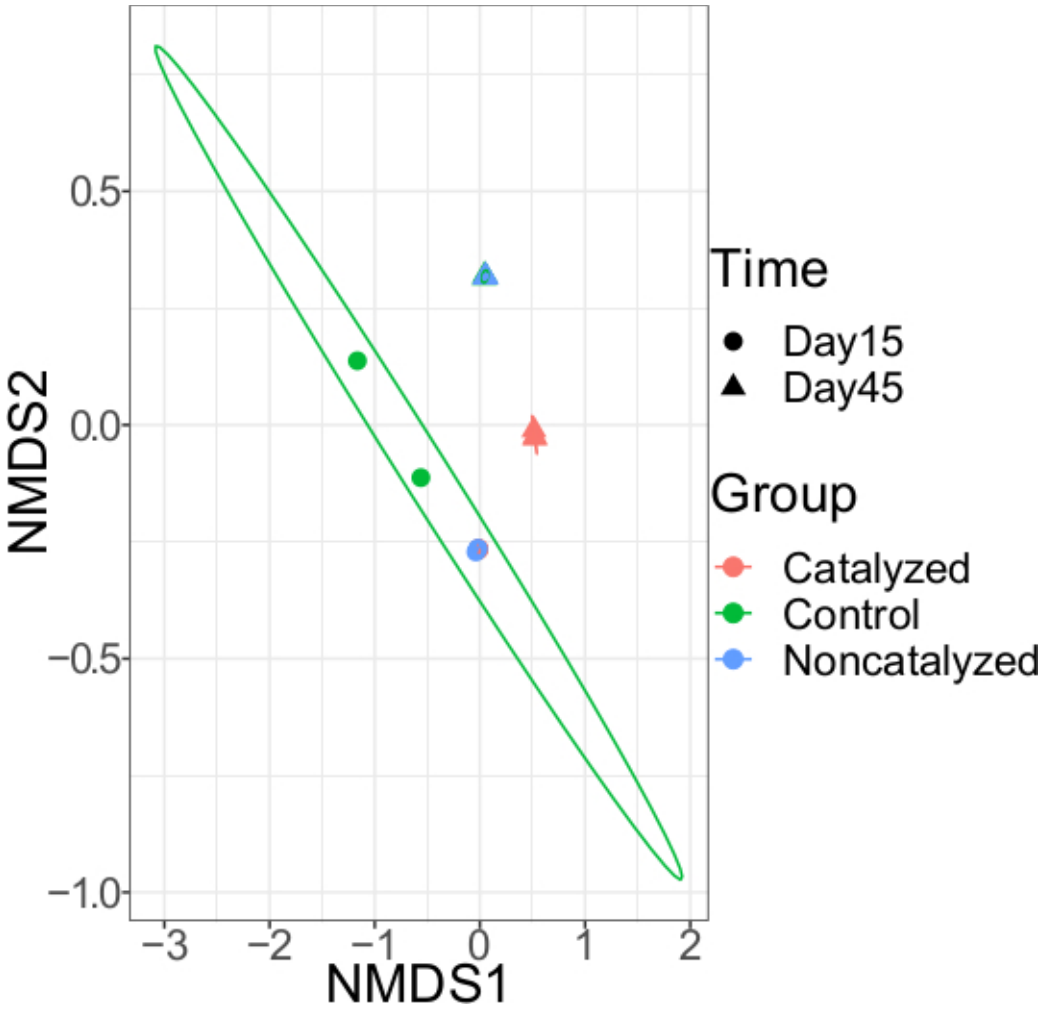

Figure S7.2 Bacteria nMDS plot. Ellipses represent 95% confidence intervals for triplicate digesters (each group represents the three triplicate digesters). Some ellipses are small and not visible. On day 15, all digester bacterial communities were similar. On day 45, Bacterial communities in digesters fed catalyzed APL was significantly different from Bacterial communities control digesters and digesters fed non-catalyzed APL. The points representing catalyzed digesters on day 15 and non-catalyzed digesters on day 15 overlap. Also, the points representing control digesters on day 45 and non-catalyzed digesters on day 45 overlap.

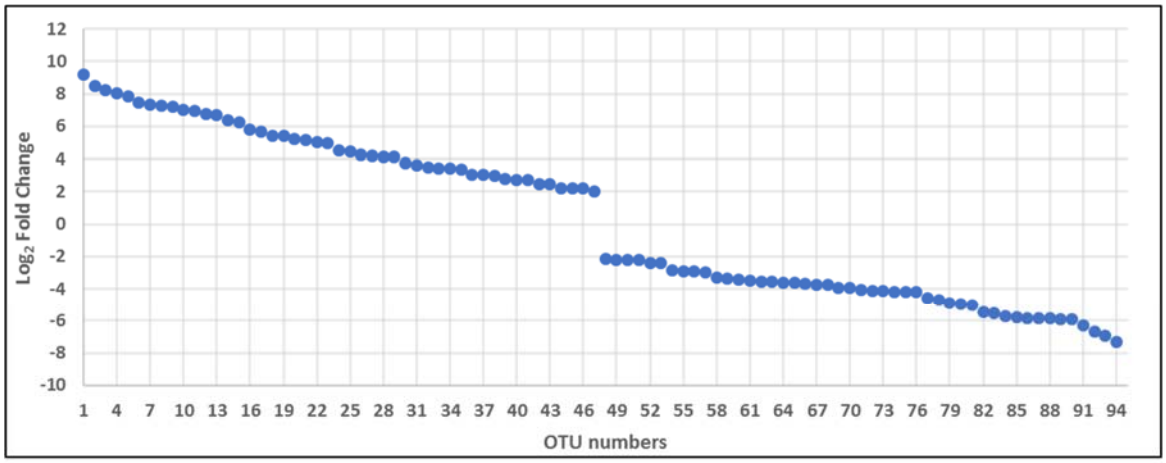

OTU	Family	Genus	Log_2 Fold change
1	Enterococcaceae	Enterococcus	9.2
2	Rikenellaceae	Rikenella	8.5
3	Porphyromonadaceae	Proteiniphilum	8.3
4	Porphyromonadaceae	Proteiniphilum	8.0
5	Ruminococcaceae	Ruminiclostridium	7.8
6	Desulfovibrionaceae	Desulfovibrio	7.5
7	Enterococcaceae	Enterococcus	7.4
8	Porphyromonadaceae	Proteiniphilum	7.3
9	Ruminococcaceae	Acetivibrio	7.2
10	Ruminococcaceae	Sporobacter	7.0
11	Syntrophomonadaceae	Syntrophomonas	7.0
12	Ruminococcaceae	Ruminiclostridium	6.8
13	Ruminococcaceae	Soleaferrea	6.7
14	Ruminococcaceae	Ruminiclostridium	6.4
15	Enterococcaceae	Enterococcus	6.3
16	Eubacteriaceae	Eubacterium	5.8
17	Eubacteriaceae	Eubacterium	5.7
18	Ruminococcaceae	Acetivibrio	5.4
19	Prevotellaceae	Prevotella	5.4
20	Clostridiaceae	Clostridium	5.2
21	Mycoplasmataceae	Mycoplasma	5.2
22	Erysipelotrichaceae	Turicibacter	5.0
23	Ruminococcaceae	Ruminococcus	4.9
24	Clostridiaceae	Proteiniclasticum	4.6
25	Bacillaceae	Terribacillus	4.4
26	Porphyromonadaceae	Parabacteroides	4.2
27	Ruminococcaceae	Acetivibrio	4.2
28	Enterococcaceae	Enterococcus	4.2
29	Synergistaceae	Synergistes	4.1
30	Campylobacteraceae	Campylobacter	3.8
31	Bacteroidaceae	Anaerorhabdus	3.6
32	Peptoniphilaceae	Gallicola	3.5
33	Clostridiaceae	Clostridium	3.5
34	Verrucomicrobiaceae	Verrucomicrobium	3.4
35	Bacteroidaceae	Bacteroides	3.4
36	Clostridiales Family Xi.	Tissierella	3.1
37	Clostridiales Family Xi.	Tissierella	3.0
38	Syntrophomonadaceae	Syntrophomonas	3.0
39	Anaerolineaceae	Leptolinea	2.8
40	Anaerolineaceae	Bellilinea	2.7
41	Synergistaceae	Cloacibacillus	2.7
42	Clostridiales Family Xi.	Sedimentibacter	2.5
43	Clostridiales Family Xi.	Sedimentibacter	2.4
44	Dehalococcoidaceae	Dehalococcoides	2.2
45	Spirochaetaceae	Treponema	2.2
46	Clostridiaceae	Clostridium	2.2
47	Synergistaceae	Synergistes	2.0

OTU	Family	Genus	Log_2 Fold change
48	Rikenellaceae	Rikenella	-2.1
49	Syntrophomonadaceae	Syntrophomonas	-2.2
50	Cloacimonetes	Cloacimonas	-2.2
51	Puniceicoccaceae	Puniceicoccus	-2.2
52	Verrucomicrobiaceae	Verrucomicrobium	-2.4
53	Endomicrobia	Endomicrobium	-2.4
54	Rikenellaceae	Rikenella	-2.9
55	Deferribacteraceae	Deferribacter	-2.9
56	Methanosaetaceae	Methanosaeta	-2.9
57	Deferribacteraceae	Deferribacter	-3.0
58	Eubacteriaceae	Acetobacterium	-3.3
59	Rikenellaceae	Rikenella	-3.3
60	Geobacteraceae	Geobacter	-3.4
61	Syntrophobacteraceae	Syntrophobacter	-3.5
62	Eubacteriaceae	Acetobacterium	-3.5
63	Thermotogaceae	Kosmotoga	-3.5
64	Syntrophorhabdaceae	Syntrophorhabdus	-3.6
65	Eubacteriaceae	Acetobacterium	-3.6
66	Verrucomicrobiaceae	Verrucomicrobium	-3.7
67	Desulfobacteraceae	Desulfofaba	-3.7
68	Syntrophaceae	Syntrophus	-3.8
69	Bacteroidaceae	Bacteroides	-3.9
70	Clostridiaceae	Clostridium	-4.0
71	Methanosaetaceae	Methanosaeta	-4.1
72	Desulfobacteraceae	Desulfofaba	-4.1
73	Leptospiraceae	Leptospira	-4.1
74	Bacteroidaceae	Bacteroides	-4.2
75	Synergistaceae	Synergistes	-4.2
76	Syntrophaceae	Smithella	-4.2
77	Ruminococcaceae	Ruminococcus	-4.6
78	Clostridiaceae	Clostridium	-4.7
79	Rubrobacteraceae	Rubrobacter	-4.9
80	Desulfobacteraceae	Desulfofaba	-4.9
81	Ruminococcaceae	Ruminococcus	-5.0
82	Bacillaceae	Bacillus	-5.5
83	Syntrophaceae	Syntrophus	-5.6
84	Lachnospiraceae	Hespellia	-5.7
85	Ruminococcaceae	Ruminococcus	-5.8
86	Clostridiaceae	Clostridium	-5.9
87	Synergistaceae	Aminomonas	-5.9
88	Holophagaceae	Geothrix	-5.9
89	Ruminococcaceae	Ruminococcus	-5.9
90	Eubacteriaceae	Eubacterium	-5.9
91	Thermotogaceae	Geotoga	-6.3
92	Thermotogaceae	Geotoga	-6.7
93	Clostridiaceae	Clostridium	-6.9
94	Eubacteriaceae	Eubacterium	-7.3

Figure S7.3 DESeq2 results to identify statistically different ($p<0.001$) OTUs between control digesters and digesters fed catalyzed APL. OTUs with greater/less than ±2 fold changes are shown. OTUs greater than 2-fold change are more abundant in digesters fed catalyzed APL compared to control digesters.

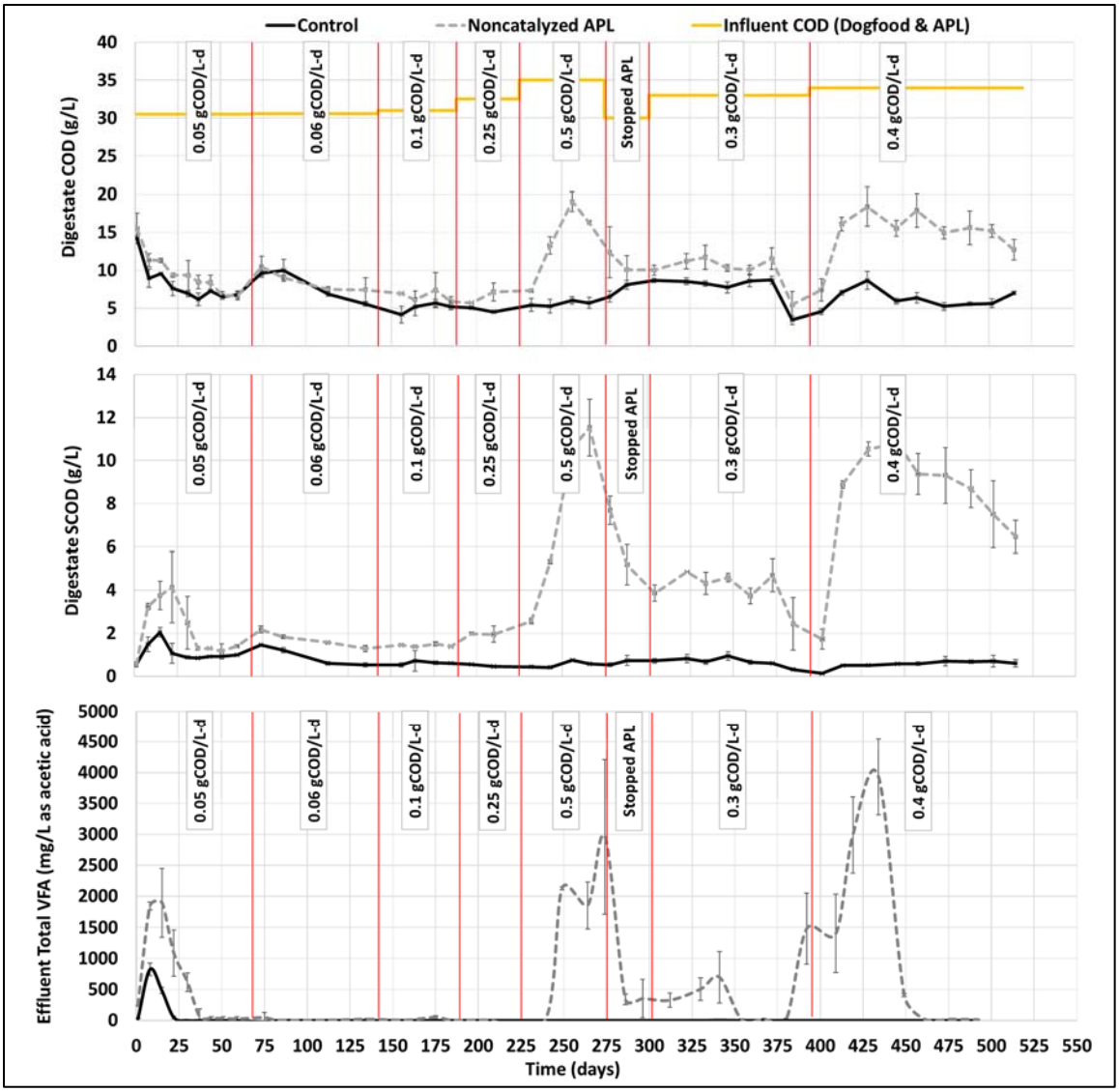

Figure S7.4 Long-term co-digestion functional data. Average and standard deviation values are from triplicate systems. (A) Digestate COD concentration, (B) Digestate SCOD concentration, (C) Digestate total VFA concentration as mg/L acetic acid. Error bars represent one standard deviation above and below the mean. Some whiskers are small and may not be visible.

Table S7.1 Organic compounds observed in catalyzed and non-catalyzed APL with and without air stripping, quantified by GC-FID and IC_{50} values

Compounds quantified by GC-FID (1701 Capillary)		**Non-catalyzed APL**	**Non-catalyzed air-stripped APL**	**Catalyzed APL**	**Catalyzed air-stripped APL**	**IC_{50} value**
Compound	**Molecular weight (g/mol)**	**% w/w (raw basis) [a] (Average ± Standard deviation)**				**mg/L**
phenol	94.1	0.22 ± 0.13	0.21 ± 0.12	-	-	2100[b]
styrene	104	0.06 ± 0.03	-	0.05 ± 0.03	-	150[c]
m-xylene	106	0.21 ± 0.12	0.2 ± 0.12	-	-	250[b]
o-xylene	106	0.19 ± 0.11	0.18 ± 0.1	-	-	-
ethylbenzene	106	0.22 ± 0.12	-	0.2 ± 0.12	-	160[b]
m,p-cresol	108	0.44 ± 0.25	0.43 ± 0.25	-	-	890[b], 91[b]
o-cresol	108	0.19 ± 0.11	-	-	-	-
anisole	108	0.09 ± 0.05	0.08 ± 0.05	-	-	720[b]
4-vinylphenol	120	-	0.75 ± 0.43	-	-	
3-ethylphenol	122	-	0.19 ± 0.11	-	-	
3,4-dimethylphenol	122	-	0.15 ± 0.08	-	-	
3,5-dimethylphenol	122	0.32 ± 0.18	0.3 ± 0.17	-	-	-
2,5-dimethylphenol	122	0.22 ± 0.13	0.21 ± 0.12	-	-	-
2-methylanisole	122	0.16 ± 0.09	0.11 ± 0.06	-	-	-
3-methylanisole	122	0.13 ± 0.08	0.11 ± 0.06	-	-	-
3-methoxy-5-methylphenol	138	0.31 ± 0.18	0.29 ± 0.17	-	-	-
2-methoxy-4-methylphenol	138	0.27 ± 0.16	0.26 ± 0.15	-	-	-
4-ethoxystyrene	148	0.11 ± 0.06	0.1 ± 0.06	-	-	-
4-ethyl-2-methoxyphenol	152	0.12 ± 0.07	0.21 ± 0.12	-	-	-
3,4-dimethoxytoluene	152	0.12 ± 0.07	0.11 ± 0.06	-	-	-
4'-hydroxy-3'-methoxyacetophenone	166	0.33 ± 0.19	0.23 ± 0.13	-	-	-
2-methoxy-4-propylphenol	166	0.11 ± 0.06	0.11 ± 0.07	-	-	-
1,2,3-trimethoxybenzene	168	0.15 ± 0.09	0.16 ± 0.1	-	-	-
2,5-dimethoxybenzylalcohol	168	-	-	0.22 ± 0.13	0.22 ± 0.13	
2',4'-dimethoxyacetophenone	180	0.02 ± 0.01	-	-	-	-
3,5-dimethoxy-4-hydroxybenzaldehyde	182	0.43 ± 0.25	0.25 ± 0.15	0.27 ± 0.15	0.27 ± 0.16	-
3',5'-dimethoxy-4'-hydroxyacetophenone	196	0.54 ± 0.31	0.47 ± 0.27	-	-	-
Total of known compounds	-	4.96	5.11	0.74	0.49	-

[a] (Liu et al. 2017), [b] (Blum and Speece 1991), [c] (Araya et al. 2000)

7.7. References

Alvares ABC, Diaper C, Parsons SA (2001) Partial oxidation by ozone to remove recalcitrance from wastewaters - a review. Environ Technol (United Kingdom) 22:409–427. https://doi.org/10.1080/09593332208618273

American Public Health Association (1998) Standard Methods for the Examination of Water and Wastewater.

Anders S, Huber W (2010) Differential expression analysis for sequence count data. Genome Biol 11:R106. https://doi.org/10.1186/gb-2010-11-10-r106

Benitez FJ, Beltran-Heredia J, Torregrosa J, Acero JL (1997) Improvement of the anaerobic biodegradation of olive mill wastewaters by prior ozonation pretreatment. Bioprocess Eng 17:169–175. https://doi.org/10.1007/s004490050371

Benn N, Zitomer D (2018) Pretreatment and Anaerobic Co-digestion of Selected PHB and PLA Bioplastics. Front Environ Sci 5:1–9. https://doi.org/10.3389/fenvs.2017.00093

Bosshard PP, Zbinden R, Altwegg M (2002) novel anaerobic , Gram-positive bacterium. Int J Syst Evol Microbiol 12:1263–1266. https://doi.org/10.1099/ijs.0.02056-0.A

Carballa M, Regueiro L, Lema JM (2015) Microbial management of anaerobic digestion: Exploiting the microbiome-functionality nexus. Curr Opin Biotechnol 33:103–111. https://doi.org/10.1016/j.copbio.2015.01.008

Carey DE, Zitomer DH, Kappell AD, et al (2016) Chronic exposure to triclosan sustains microbial community shifts and alters antibiotic resistance gene levels in anaerobic digesters. Environ Sci Process Impacts 18:1060–1067. https://doi.org/10.1039/C6EM00282J

Collins MD, Shah HN (1986) Reclassification of Bacteroides praeacutus Tissier (Holdeman and Moore) in a New Genus , Tissierella , as Tissierella praeacuta. Int J Syst Bacteriol 461–463. https://doi.org/10.1099/00207713-36-3-461

Dang Y, Holmes DE, Zhao Z, et al (2016) Enhancing anaerobic digestion of complex organic waste with carbon-based conductive materials. Bioresour Technol 220:516–522. https://doi.org/10.1016/j.biortech.2016.08.114

Falk MW, Song KG, Matiasek MG, Wuertz S (2009) Microbial community dynamics in replicate membrane bioreactors - Natural reproducible fluctuations. Water Res 43:842–852. https://doi.org/10.1016/j.watres.2008.11.021

Fang HH, Zhou GM (2000) Degradation of phenol and p-cresol in reactors. Water Sci Technol 42:237–244

Fonts I, Gea G, Azuara M, et al (2012) Sewage sludge pyrolysis for liquid production: A review. Renew Sustain Energy Rev 16:2781–2805. https://doi.org/10.1016/j.rser.2012.02.070

Hübner T, Mumme J (2015) Integration of pyrolysis and anaerobic digestion – Use of aqueous liquor from digestate pyrolysis for biogas production. Bioresour Technol 183:86–92. https://doi.org/10.1016/j.biortech.2015.02.037

Kappell AD, Kimbell LK, Seib MD, et al (2018) Removal of antibiotic resistance genes in an anaerobic membrane bioreactor treating primary clarifier effluent at 20 °C. Environ Sci Water Res Technol 4:1783–1793. https://doi.org/10.1039/c8ew00270c

Kimbell LK, Kappell AD, McNamara PJ (2018) Effect of pyrolysis on the removal of antibiotic resistance genes and class I integrons from municipal wastewater biosolids. Environ Sci Water Res Technol 4:1807–1818. https://doi.org/10.1039/c8ew00141c

L'Haridon S, Jiang L, Alain K, et al (2014) Kosmotoga pacifica sp. nov., a thermophilic chemoorganoheterotrophic bacterium isolated from an East Pacific hydrothermal sediment. Extremophiles 18:81–88. https://doi.org/10.1007/s00792-013-0596-7

Li H, Xu Q, Xue H, Yan Y (2009) Catalytic reforming of the aqueous phase derived from fast-pyrolysis of biomass. Renew Energy 34:2872–2877. https://doi.org/10.1016/j.renene.2009.04.007

Liu Z, Mayer BK, Venkiteshwaran K, et al (2020) The state of technologies and research for energy recovery from municipal wastewater sludge and biosolids. Curr. Opin. Environ. Sci. Heal. 14:31–36

Liu Z, McNamara P, Zitomer D (2017) Autocatalytic Pyrolysis of Wastewater Biosolids for Product Upgrading. Environ Sci Technol 51:9808–9816. https://doi.org/10.1021/acs.est.7b02913

Liu Z, Singer S, Tong Y, et al (2018) Characteristics and applications of biochars derived from wastewater solids. Renew Sustain Energy Rev 90:650–664. https://doi.org/10.1016/j.rser.2018.02.040

Ma Y, Liu Y (2019) Turning food waste to energy and resources towards a great environmental and economic sustainability: An innovative integrated biological approach. Biotechnol. Adv. 37:107414

Madigou C, Poirier S, Bureau C, Chapleur O (2016) Acclimation strategy to increase phenol tolerance of an anaerobic microbiota. Bioresour Technol 216:77–86. https://doi.org/10.1016/j.biortech.2016.05.045

McNamara PJ, Koch JD, Liu Z, Zitomer DH (2016) Pyrolysis of Dried Wastewater Biosolids Can Be Energy Positive. Water Environ Res 88:804–810. https://doi.org/10.2175/106143016X14609975747441

O'Cuív P, Klaassens ES, Durkin AS, et al (2011) Draft genome sequence of Turicibacter sanguinis PC909, isolated from human feces. J Bacteriol 193:1288–1289. https://doi.org/10.1128/JB.01328-10

Parry DL, Lewis FM, Vandenburgh S, et al (2012) Pyrolysis of Dried Biosolids for Increased Biogas Production. In: Water Environ. Fed. New Orleans, LA

Ross JJ, Zitomer DH, Miller TR, et al (2016) Emerging investigators series: Pyrolysis removes common microconstituents triclocarban, triclosan, and nonylphenol from biosolids. Environ Sci Water Res Technol 2:282–289. https://doi.org/10.1039/c5ew00229j

Seyedi S (2018) Anaerobic Co-digestion of Aqueous Liquid from Biosolids Pyrolysis. Master's Thesis. Marquette University. Milwaukee, WI. USA

Seyedi S, Venkiteshwaran K, Zitomer D (2019) Toxicity of Various Pyrolysis Liquids From Biosolids on Methane Production Yield. Front Energy Res 7:1–12. https://doi.org/10.3389/fenrg.2019.00005

Shkoporov AN, Chaplin A V., Shcherbakova VA, et al (2016) Ruthenibacterium lactatiformans gen. nov., sp. nov., an anaerobic, lactate-producing member of the family Ruminococcaceae isolated from human faeces. Int J Syst Evol Microbiol 66:3041–3049. https://doi.org/10.1099/ijsem.0.001143

Sieber JR, Sims DR, Han C, et al (2010) The genome of Syntrophomonas wolfei: New insights into syntrophic metabolism and biohydrogen production. Environ Microbiol 12:2289–2301. https://doi.org/10.1111/j.1462-2920.2010.02237.x

Speece RE (2008) Anaerobic Biotechnology and Odor/Corrosion Control for Municipalities and Industries. Archae Press, Nashville, TN

Su XL, Tian Q, Zhang J, et al (2014) Acetobacteroides hydrogenigenes gen. nov., Sp. nov., An anaerobic hydrogen-producing bacterium in the family Rikenellaceae isolated from a reed swamp. Int J Syst Evol Microbiol 64:2986–2991. https://doi.org/10.1099/ijs.0.063917-0

Torri C, Fabbri D (2014) Biochar enables anaerobic digestion of aqueous phase from intermediate pyrolysis of biomass. Bioresour Technol 172:335–341. https://doi.org/10.1016/j.biortech.2014.09.021

Tsai WT, Chang JH, Hsien KJ, Chang YM (2009) Production of pyrolytic liquids from industrial sewage sludges in an induction-heating reactor. Bioresour Technol 100:406–412. https://doi.org/10.1016/j.biortech.2008.06.013

Vandamme P, De Ley J (1991) Proposal for a New Family, Campylobacteraceae. Int J Syst Evol Microbiol 41:451–455. https://doi.org/10.1099/00207713-41-3-451

Vartoukian SR, Palmer RM, Wade WG (2007) The division "Synergistes." Anaerobe 13:99–106. https://doi.org/10.1016/j.anaerobe.2007.05.004

Venkiteshwaran K, Benn N, Seyedi S, Zitomer D (2019) Methane yield and lag correlate with bacterial community shift following bioplastic anaerobic co-digestion. Bioresour Technol Reports 7:100198. https://doi.org/10.1016/j.biteb.2019.100198

Venkiteshwaran K, Milferstedt K, Hamelin J, Zitomer DH (2016) Anaerobic digester bioaugmentation influences quasi steady state performance and microbial community. Water Res 104:128–136. https://doi.org/10.1016/j.watres.2016.08.012

Verbarg S, Rheims H, Emus S, et al (2004) Erysipelothrix inopinata sp. nov., isolated in the course of sterile filtration of vegetable peptone broth, and description of Erysipelotrichaceae fam. nov. Int J Syst Evol Microbiol 54:221–225. https://doi.org/10.1099/ijs.0.02898-0

Vos P De, Garrity GM, Jones D, et al (2009) Bergey's manual of systematic bacteriology - Vol 3: The Firmicutes. Springer-Verlag New York

Wen C, Moreira CM, Rehmann L, Berruti F (2020) Feasibility of anaerobic digestion as a treatment for the aqueous pyrolysis condensate (APC) of birch bark. Bioresour Technol 307:123199. https://doi.org/10.1016/j.biortech.2020.123199

Xu J, Jiang J, Dai W, et al (2011) Bio-oil upgrading by means of ozone oxidation and esterification to remove water and to improve fuel characteristics. Energy and Fuels 25:1798–1801. https://doi.org/10.1021/ef101726g

Xu K, Liu H, Chen J (2010) Effect of classic methanogenic inhibitors on the quantity and diversity of archaeal community and the reductive homoacetogenic activity during the process of anaerobic sludge digestion. Bioresour Technol 101:2600–2607. https://doi.org/10.1016/j.biortech.2009.10.059

Yenigün O, Demirel B (2013) Ammonia inhibition in anaerobic digestion: A review. Process Biochem 48:901–911. https://doi.org/10.1016/j.procbio.2013.04.012

Yu X, Zhang C, Qiu L, et al (2020) Anaerobic digestion of swine manure using aqueous pyrolysis liquid as an additive. Renew Energy 147:2484–2493. https://doi.org/10.1016/j.renene.2019.10.096

Zhou H, Brown RC, Wen Z (2019) Anaerobic digestion of aqueous phase from pyrolysis of biomass: Reducing toxicity and improving microbial tolerance. Bioresour Technol 292:. https://doi.org/10.1016/j.biortech.2019.121976

Specifications :: Milorganite. https://www.milorganite.com/professionals/product-information/specifications. Accessed 13 Apr 2020a

Fertilizer Basics | Milorganite. https://www.milorganite.com/lawn-care/fertilizer-basics. Accessed 14 Apr 2020b